ECONOMIC AND ENVIRONMENTAL COSTS, BENEFITS, AND TRADE-OFFS OF LOW-CARBON TECHNOLOGIES IN THE ELECTRIC POWER SECTOR

SUBMITTED IN PARTIAL FULFILLMENT OF THE REQUIREMENTS FOR

THE DEGREE OF

DOCTOR OF PHILOSOPHY

IN

ENGINEERING AND PUBLIC POLICY

MICHAEL T. CRAIG

B.A., ENVIRONMENTAL STUDIES, WASHINGTON UNIVERSITY IN ST. LOUIS
M.S., TECHNOLOGY AND POLICY, MASSACHUSETTS INSTITUTE OF TECHNOLOGY

CARNEGIE MELLON UNIVERSITY
PITTSBURGH, PA

DECEMBER, 2017

ACKNOWLEDGEMENTS

I'm grateful for the many funding sources that made this thesis possible. The National Science Foundation (Grant Number EFRI-1441131), the National Oceanic and Atmospheric Administration (Award Number A14OAR4310249), and the Achievement Rewards for College Scientists (ARCS) Foundation supported all parts of this thesis. Chapters 2 and 3 were also supported by the Steinbrenner Institute for Environmental Education and Research and by the Carnegie Mellon College of Engineering, while Chapter 4 was also supported by the Claire and John Bertucci Fellowship from the Carnegie Mellon College of Engineering. Thanks to Energy Exemplar for providing a free PLEXOS academic license for Chapters 2 and 3, and to the Extreme Science and Engineering Discovery Environment (XSEDE), which is supported by National Science Foundation (Grant Number ACI-1548562), for computing resources for Chapter 4.

I owe a sincere thanks to my mentors over the years. Dr. John Orrock gave me my first taste of research, laying the groundwork for the next eight years of my life. Shortly thereafter, Dr. Itai Sened and Jacqueline Savitz provided me early research and work opportunities on energy. Dr. Mort Webster took me on as an advisee in my Master's program, despite my lack of research in the electric power sector, setting me down the course I remain on to this day. Two years later, Dr. Paulina Jaramillo, my committe chair, brought me on at Carnegie Mellon and has provided me with invaluable support and insight while allowing me to explore my research passions. Drs. Kelly Klima, Haibo Zhai, and Bri-Mathias Hodge have also graciously agreed to serve on my committee and have improved my analytic, writing, and research skills.

Last but not least, I must thank my family: Ethan, Caitlin, Mom, and Dad. I would not be where I am today without your love, patience, and support. I love you all.

ABSTRACT

Motivated by the role of decarbonizing the electric power sector to mitigate climate change, I assess the economic and environmental merits of three key technologies for decarbonizing the electric power sector across four chapters in this thesis. These chapters explore how adding flexibility to power plants equipped with carbon capture and sequestration (CCS) affects system costs and carbon dioxide (CO_2) emissions, how grid-scale electricity storage affects system CO_2 emissions as a power system decarbonizes, and how distributed solar photovoltaic (distributed PV) electricity generation suppresses wholesale electricity prices. In each chapter, I address these questions through a combination of power system optimization, statistics, and techno-economic analysis, and tie my findings to policy implications.

In Chapter 2, I compare the cost-effectiveness of "flexible" CCS retrofits to other compliance strategies with the U.S. Clean Power Plan (CPP) and a hypothetical stronger CPP. Relative to "normal" CCS, "flexible" CCS retrofits include solvent storage that allows the generator to temporarily eliminate the CCS parasitic load and increase the generator's net efficiency, capacity, and ramp rate. Using a unit commitment and economic dispatch (UCED) model, I find that flexible CCS achieves more cost-effective emissions reductions than normal CCS under the CPP and stronger CPP, but that flexible CCS is less cost-effective than other compliance strategies under both reduction targets.

In Chapter 3, I conduct a detailed comparison of how flexible versus normal CCS retrofits affect total system costs and CO_2 emissions under a moderate and strong CO_2 emission limit. Given that a key benefit of flexible CCS relative to normal CCS is increased reserve provision, I break total system costs into generation, reserve, and CCS capital costs. Using a

UCED model, I find that flexible CCS retrofits reduce total system costs relative to normal CCS retrofits under both emission limits. Furthermore, 40-80% of these cost reductions come from reserve cost reductions. Accounting for costs and CO_2 emissions, though, flexible CCS poses a trade-off to policymakers under the moderate emission limit, as flexible CCS increases system CO_2 emissions relative to normal CCS. No such trade-off exists under the stronger emission limit, as flexible CCS reduces system CO_2 emissions and costs relative to normal CCS.

In Chapter 4, I quantify how storage affects operational CO_2 emissions as a power system decarbonizes under a moderate and strong CO_2 emission limit through 2045. In so doing, I aim to better understand how storage transitions from increasing CO_2 emissions in historic U.S. systems to enabling deeply decarbonized systems. Additionally, under each target I compare how storage affects CO_2 emissions when participating in only energy, only reserve, and energy and reserve markets. Using a capacity expansion (CE) model to forecast fleet changes through 2045 and a UCED model to quantify how storage affects system CO_2 emissions, I find that storage quickly transitions from increasing to decreasing CO_2 emissions under the moderate and strong emission limits. Whether storage provides only energy, only reserves, or energy and reserves drives large differences in the magnitude, but not the direction, of the effect of storage on CO_2 emissions.

In Chapter 5, I quantify a benefit of distributed photovoltaic (PV) generation often overlooked by value of solar studies, namely the market price response. By displacing high-cost marginal generators, distributed PV generation reduces wholesale electricity prices, which in turn reduces utilities' energy procurement costs. Using 2013 through 2015 data from California including a database of all distributed PV systems in the three California investor owned utilities, we estimate historic hourly distributed PV generation in California, then link that generation to reduced wholesale electricity prices via linear regression. From 2013 through 2015, we find that

distributed PV suppressed historic median hourly LMPs by up to $2.7-3.1/MWh, yielding avoided costs of up to $650-730 million. These avoided costs are smaller than but on the order of other avoided costs commonly included in value of solar studies, so merit inclusion in future studies to properly value distributed PV.

TABLE OF CONTENTS

Chapter 1: Introduction 1
Chapter 2: The Economic Merits of Flexible Carbon Capture and Sequestration as a Compliance Strategy with the Clean Power Plan 8
2.1 Abstract 8
2.2 Introduction 9
2.3 Methods 11
2.3.1 Unit Commitment and Economic Dispatch Model 12
2.3.2 Base Generator Fleet 13
2.3.3 CPP Compliance Scenarios 15
2.3.4 Normal and Flexible CCS Models 17
2.3.5 Cost-Effectiveness and Equivalent Capital Cost Calculations 18
2.4 Results 20
2.4.1 CO_2 Emissions Reductions in Compliance Scenarios 20
2.4.2 Total Costs 22
2.4.3 Cost-Effectiveness of CO_2 Emissions Reductions 23
2.4.4 Flexible CCS ECCs 27
2.5 Discussion 27
2.6 Conclusion 29
2.7 References 30
Chapter 3: Trade-offs in Cost and Emission Reductions between Flexible and Normal Carbon Capture and Sequestration under Carbon Dioxide Emission Constraints 33
3.1 Abstract 33
3.2 Introduction 34
3.3 Methods 36
3.3.1 Overview of Flexible CCS Operations 36
3.3.2 Flexible CCS Generator Model 40
3.3.3 Power System Modeling 44
3.3.4 Capital Costs of Solvent Storage 46
3.4 Results 47
3.4.1 Flexible CCS Operations 49
3.4.2 System Costs and Emissions with Normal and Flexible CCS 54
3.4.3 Net System Value of Flexible Versus Normal CCS 59
3.4.4 Sensitivity to High Natural Gas Prices 62
3.5 Discussion 63
3.6 Conclusion 65
3.7 References 66
Chapter 4: Carbon Dioxide Emissions Effects of Grid-Scale Electricity Storage in a Decarbonizing Power System 69
4.1 Abstract 69
4.2 Introduction 70
4.3 Methods 72
4.3.1 CE Model 73
4.3.2 UCED Model 74

4.3.3 Storage Model 75
4.3.4 Scenarios 76
4.4 Results 77
4.4.1 Annual Generation and Reserve Provision by Fuel Type without Storage 77
4.4.2 Storage Operations 79
4.4.3 Effect of Storage on Generation by Fuel Type 82
4.4.4 Change in System CO_2 Emissions 85
4.4.5 Sensitivity Analysis 88
4.5 Discussion 90
4.6 Conclusion 92
4.7 References 93
Chapter 5: A Retrospective Analysis of the Market Price Response to Distributed Photovoltaic Generation in California 97
5.1 Abstract 97
5.2 Introduction 98
5.3 Methods 101
5.3.1 Estimating Distributed PV Generation 101
5.3.2 Estimating the Response of Day-Ahead Wholesale Electricity Prices to Distributed PV Generation 106
5.4 Results 109
5.4.1 Validation of Methods for Estimating Historic Distributed PV Generation 109
5.4.2 Generation by All Distributed PV Systems in Each IOU 113
5.4.3 Wholesale Electricity Price Response to Distributed PV Generation 115
5.4.4 Sensitivity Analysis 117
5.5 Discussion 118
5.6 Conclusion 120
5.7 References 121
Chapter 6: Conclusion 126
Appendix A: Supplemental Information for Chapter 2 130
A.1: Unit Commitment and Economic Dispatch Formulation 130
A.2: Modifications to IPM Fleet 136
A.3: Parameters Added to IPM Fleet 137
A.4: Generation Profiles for Hydropower, Wind, and Solar Plants 139
A.5: Base Fleet Simplifications for Computational Efficiency 140
A.6: Hourly Demand Profile in 2030 141
A.7: Determining Affected EGUs for Application of Shadow CO_2 Price 142
A.8: Economic Dispatch Model to Determine Shadow CO_2 Price 144
A.9: Capital Recovery Factor and Total Operational Cost in Cost-Effectiveness Calculation 145
A.10: Capital Costs Used in Cost-Effectiveness and Break-Even Calculations 145
A.11: Shadow CO_2 Prices Necessary to Achieve Compliance with the Clean Power Plan or Stronger Clean Power Plan 146
A.12: Generation Mix of Clean Power Plan and Stronger Clean Power Plan Scenarios 147
A.13: Flexible CCS Equivalent Capital Costs 148
A.14: References 149
Appendix B: Supplemental Information for Chapter 3 152
B.1: Description of Venting Components of Flexible CCS Model 152

B.2: Justification of Flexible CCS Design Parameters 156
B.3: Regressions Based on Data from the Integrated Environmental Control Model 158
B.4: Mathematical Formulation of Flexible CCS Model 168
B.5: Generator Fleet Characteristics 181
B.6: CO_2 Prices Used to Achieve Compliance with the Moderate and Strong CO_2 Emission Limits 182
B.7: Flexible CCS Operations with Solvent Storage and Venting 183
B.8: Capacity Factors of CCS Generators 183
B.9: Sensitivity to High Natural Gas Prices 185
B.10: References 190
Appendix C: Supplemental Information for Chapter 4 191
C.1: Initial Generator Fleet 191
C.2: Fuel Prices 194
C.3: Analysis of Representativeness of 2015 Demand Profile 195
C.4: Capacity Expansion (CE) Model Formulation 197
C.5: Parameters of Generators that Can Be Added in CE Model 206
C.6: Generator Retirements in the CE Model 208
C.7: Solar and Wind Electricity Generation 209
C.8: Calculating Reserve Requirements 212
C.9: Selection of Representative Days per Season Included in CE Model 220
C.10: Unit Commitment and Economic Dispatch (UCED) Formulation 221
C.11: Economic Dispatch Model for Converting CO_2 Cap to CO_2 Price 228
C.12: Scenario Details 229
C.13: Shadow CO_2 Prices Enforced in and Annual CO_2 Emissions Output by UCED Model 230
C.14: Generator Fleet Composition over Time 231
C.15: Reserve Provision by Generator Type without Storage 232
C.16: Equation Used to Calculate Effect of Storage on System CO_2 Emissions 235
C.17: Re-dispatching Among Gas-fired Generators Due to Storage 235
C.18: Estimating System CO_2 Emissions Due to Dispatching of Regulation Reserves Provided by Storage 237
C.19: Sensitivity Analysis Results 239
C.20: References 242
Appendix D: Supplemental Information for Chapter 5 245
D.1: Histograms of PV System Azimuths and Tilts in NEM Dataset 245
D.2: Supplemental Description of Metered Generation and PV Systems in the CSI Dataset 246
D.3: Details and Sensitivity Analysis on Scale Up Metered Generation Method 249
D.4: Summary Statistics of Meteorology and Solar Irradiance Data from the NSRDB 253
D.5: Cross-Validation of Hour-of-Day Correction Factors for Adjusted Generic Configuration Method 254
D.6: Supplemental Regression Information 255
D.7: Comparison of Actual and Estimated Max Hourly and Total Generation by PV Systems During Validation 265
D.8: Supplemental Results for Estimates of Distributed PV Generation 266
D.9: Supplemental Results for Market Price Response to Distributed PV Generation 273
D.10: Estimating Avoided Costs on Per-Generation and Per-Capacity Bases 277

D.11: Results for Sensitivity Analysis on Efficiency Degradation and Higher Inverter Load 278
D.12 References 279

LIST OF TABLES

Table 2.1: Incremental total annualized costs of each compliance scenario under the CPP and stronger CPP relative to the base scenario assuming best guess capital cost values. 23
Table 3.1: Terms used to describe normal and flexible CCS operations. 38
Table 3.2: Summary of major differences in CCS operations and system costs and emissions between normal and flexible CCS scenarios under the moderate and strong CO_2 emission limits. 48
Table 4.1: Reserve types, response timeframes, and hourly requirements in the CE and UCED models. 74
Table 4.2: Storage parameters given the market in which it participates, and which storage technology each set of parameters is based on given real-world applications of each technology. 76
Table 5.1: Summary statistics for distributed PV systems in the NEM and CSI datasets interconnected through 2015, the end of our period of analysis. 102
Table 5.2: Summary of methods we use to estimate distributed PV generation. 102
Table 5.3: PV system configuration used in the generic and adjusted generic configuration methods. 106
Table 5.4: Coefficients and standard errors for Regressions 1 and 2 using Newey-West standard errors. 109
Table 5.5: Means and standard deviations for root mean square errors (RMSEs) and normalized RMSEs (NRMSEs) during daytime hours between hourly metered and estimated generation across individual PV systems by method used to estimate generation. 110
Table 5.6: Normalized root mean square errors (NRMSE) and mean bias errors (MBE) during daytime hours between hourly metered and estimated generation at the IOU level by method used to estimate generation. 111
Table 5.7: Total distributed PV generation from 2013 through 2015 in PGE, SCE, and SDGE by method used to estimate generation. 113
Table 5.8: Avoided costs from 2013 through 2015 by zone due to LMP reductions from, i.e. the market price response to, distributed PV generation. 117
Table A.1: Variables, parameters and sets used in the UCED formulation. 130
Table A.2: Capacity by fuel type of the base fleet. 136
Table A.3: Unit commitment parameter values by plant and fuel type and plant size, if applicable, used in our model. 137
Table A.4: Capacity-weighted fuel prices for the base fleet. 139
Table A.5: Heat rate intervals (Btu/kWh) for each type of unit aggregated in the base fleet. 141
Table A.6: Combined annual demand from 2004 to 2013 of the states included in our study system. 142
Table A.7: Range of capital costs included in cost-effectiveness calculations 146
Table A.8: CO_2 price necessary for each compliance scenario to comply with the CPP or stronger CPP. 146
Table A.9: ECCs for flexible CCS to achieve as cost-effective emissions reductions as additional wind or normal CCS retrofits under the CPP 149
Table A.10: ECCs for flexible CCS to achieve as cost-effective emissions reductions as additional wind or normal CCS retrofits under the stronger CPP. 149

Table B.1: Flexible and, in some cases, normal CCS operational parameters estimated using regressions based on data from the IECM. 158
Table B.2: Amine scrubber power requirement and CO_2 unit compression energy values used to model flexible CCS generators during full discharging of stored lean solvent in the IECM. 160
Table B.3: Definitions of variables and parameters used in flexible CCS model formulation. . 168
Table B.4: Key parameters for flexible CCS proxy units and coal-fired generator pre-CCS retrofit. 172
Table B.5: Number of generators, average capacity, and capacity-weighted heat rate and CO_2 emission rate for each non-renewable generator type in the base fleet after generator aggregation. 181
Table B.6: Total installed average fuel price and capacity by fuel type of the base fleet. 182
Table B.7: CO_2 price necessary to comply with the moderate or strong CO_2 emission limit via re-dispatching at each de-rated installed capacity of flexible or normal CCS. 182
Table C.1: Unit commitment parameter values by plant and fuel type and plant size, if applicable, used in our model. 191
Table C.2: VOM costs by plant type. 193
Table C.3: Key summary statistics for initial generator fleet after compression..... 194
Table C.4: Fuel prices by year used in our analysis. 195
Table C.5: Annual total and hourly peak electricity demand in ERCOT in 2013, 2014, and 2015. 196
Table C.6: Variables, parameters, and sets used in CE formulation..... 197
Table C.7: Key parameters of new technologies that can be added to the generator fleet by the CE model. 207
Table C.8: Additional key parameters of new technologies that can be added to the generator fleet by the CE model. 208
Table C.9: Lifetimes of new and existing generators by plant type. 209
Table C.10: Formula and time scale of data used to calculate hourly reserve requirement for each reserve type included in the CE and UCED models. 213
Table C.11: Variables, parameters, and sets used in UCED formulation. 221
Table C.12: Annual CO_2 emission limit (in million tons) imposed under each decarbonization target by year in the CE model. 229
Table C.13: Natural gas prices in the low natural gas price scenario. 229
Table C.14: Shadow CO_2 price (in $/ton) enforced in the UCED model in each year and decarbonization target in order to comply with the annual CO_2 emission limit. 230
Table C.15: Annual CO_2 emissions (in million tons) output by the UCED model without storage in each year and decarbonization target. 231
Table D.1: Summary statistics for meteorology and solar irradiance variables obtained from the National Solar Radiation Database across zip codes from 2013 through 2015. 254
Table D.2: Root mean square errors (RMSEs) between hourly metered generation and estimated generation using the generic configuration method without and with correction factors..... 255
Table D.3: Coefficients and standard errors for Regressions 1 and 2 without year fixed effects using Newey-West standard error. 256
Table D.4: Descriptive statistics for non-dummy variables used in Regressions 1 and 2, where t indexes hour and SP15 and NP15 index CAISO zones. 258
Table D.5: Coefficients and 3-day block bootstrapped (N=250) standard errors for Regressions 1 and 2. 260

Table D.6: Coefficients and standard errors for intercepts and time dummy variables in Regressions 1 and 2 using Newey-West standard errors. 261
Table D.7: Avoided costs per distributed PV generation from 2013 through 2015 for each method used to estimate distributed PV generation. 277
Table D.8: Total distributed PV generation from 2013 through 2015 in PGE, SCE, and SDGE by method used to estimate generation. 279
Table D.9: Avoided costs from 2013 through 2015 by zone due to LMP reductions from, i.e. the market price response to, distributed PV generation. 279

LIST OF FIGURES

Figure 2.1: Total emissions from affected EGUs under the CPP (left) and stronger CPP (right) from our UCED model, plus each emissions mass limit (black line). 21
Figure 2.2: Cost per ton of CO_2 emission reductions versus CO_2 emissions reductions for each compliance scenario relative to the base scenario under the CPP (left) and stronger CPP (right). 26
Figure 3.1: Schematic of a flexible CCS generator with solvent storage. 39
Figure 3.2: Tree showing which proxy units are on or off given the operations of a flexible CCS generator at any given time. 42
Figure 3.3: Annual net electricity output and reserve provision by operational mode for 1.5 and 3 GW of normal and flexible CCS generators under the (a) moderate and (b) strong emission limits. 52
Figure 3.4: Sum of energy used to charge stored lean solvent (a) and net electricity output while discharging stored lean solvent (b) for each hour of the day in 2030 by all flexible CCS generators combined in the 1.5 GW scenario under the moderate emission limit. 53
Figure 3.5: Change in electricity generation, start-up, and reserve costs, best guess annualized solvent storage capital costs, and the sum of all four (total annual system costs), with 1.5 or 3 GW of flexible CCS instead of normal CCS under the (a) moderate and (b) strong emission limits. 58
Figure 3.6: Annual change in total operational plus capital costs versus annual change in system CO_2 emissions with an equal installed capacity of flexible CCS relative to normal CCS for solvent storage tank sizes under the (a) moderate and (b) strong emission limits. 61
Figure 4.1: Electricity generation by fuel type in each analyzed year under the moderate (left) and strong (right) decarbonization target. 78
Figure 4.2: Storage electricity generation or flexibility, contingency, or regulation reserve provision under the moderate (left) and strong (right) decarbonization targets when storage participates in only energy (top row), only reserve (middle row), or energy and reserve (bottom row) markets. 80
Figure 4.3: Discharging (positive values) and charging (negative values) by storage for each hour of the day summed across all days in each year from 2015 through 2045 under the moderate decarbonization target when only participating in the energy market (top) and when participating in both energy and reserve markets (bottom). 81
Figure 4.4: Change in generation by fuel type with storage versus without storage under the moderate (left) and strong (right) decarbonization targets when storage participates in only energy (top row), only reserve (middle row), or energy and reserve (bottom row) markets. 84
Figure 4.5: Change in system CO_2 emissions with storage versus without storage under the moderate (left) and strong (right) decarbonization targets when storage participates in only energy (top row), only reserve (middle row), or energy and reserve (bottom row) markets. 87
Figure 5.1: Box plots of metered generation (unshaded boxes) and the error in estimated generation (defined as estimated minus metered generation) (shaded boxes) by hour of day and IOU for the specific configuration (first row), generic configuration (second row), adjusted generic configuration (third row), and scale up method (fourth row). 112

Figure 5.2: Median electricity generation (dark lines) +/- 1 standard deviation (faded lines) for all distributed PV systems in PGE, SCE, and SDGE by hour of day and method used to estimate generation from 2013 through 2015. 114
Figure 5.3: Median change in NP15 and SP15 LMPs (dark lines) +/- 1 standard deviation (faded lines) due to distributed PV generation by hour of day and method used to estimate generation from 2013 through 2015. 116
Figure A.1: Generation mix for base and compliance scenarios with the Clean Power Plan (top) and stronger Clean Power Plan (bottom) for 2030. 148
Figure B.1: A full schematic of a flexible CCS generator equipped with a flue gas bypass and solvent storage system. 154
Figure B.2: Tree showing which venting and solvent storage proxy units are on or off given the operations of a flexible CCS generator equipped with a flue gas bypass and solvent storage system at any given time. 155
Figure B.3: Regressions of various CCS operational and design parameters estimated using data from the IECM. 167
Figure B.4: Net heat rates pre-CCS retrofit of coal-fired generators eligible for CCS retrofits in our fleet (blue dots) and of coal-fired generators modeled in IECM to derive our CCS parameters (orange dots). 168
Figure B.5: Capacity factors for each coal-fired generator retrofit with normal and flexible CCS at 1.5 or 3 GW of total installed CCS under the moderate CO_2 emission limit (top) and strong CO_2 emission limit (bottom). 184
Figure B.6: Capacity factors for each coal-fired generator retrofit with normal and flexible CCS at 1.5 or 3 GW of total installed CCS under moderate emission limit and high natural gas price. 188
Figure B.7: Annual net electricity output and reserve provision by operational mode for 1.5 and 3 GW of normal and flexible CCS generators under the moderate emission limit and high natural gas price. 188
Figure B.8: Change in electricity generation, start-up, and reserve costs, best guess annualized solvent storage capital costs, and the sum of all four (annual total system costs), with 1.5 or 3 GW of flexible CCS instead of normal CCS under the moderate emission limit and high natural gas prices. 189
Figure B.9: Annual change in total operational plus capital costs versus annual change in CO_2 emissions with an equal installed capacity of flexible CCS relative to normal CCS for solvent storage tank sizes under the moderate emission limit and high natural gas prices. 189
Figure C.1: Total electricity demand by month in 2013, 2014, and 2015 in ERCOT. 196
Figure C.2: Average demand by hour of day for the entire year in 2013, 2014, and 2015. 197
Figure C.3: Wind power output forecast errors for a year of 10-minute wind power output data for 13.8 GW of wind capacity. 215
Figure C.4: Solar power output forecast errors for 326 MW solar for a year of 5-minute solar power output data by hour of day and grouped in pairs of months. 217
Figure C.5: Time series of wind component of regulation reserve requirement (top), wind generation (second from top), solar component of regulation reserve requirement (second from bottom), and solar generation (bottom). 218
Figure C.6: Time series of wind component of flexibility reserve requirement (top), wind generation (second from top), solar component of flexibility reserve requirement (second from bottom), and solar generation (bottom). 219

Figure C.7: Time series of hourly regulation, flexibility, contingency, and total reserve requirements (top); hourly electricity demand (2nd from top); hourly wind generation (3rd from top); and hourly solar generation (bottom). 220
Figure C.8: Installed capacity by generator type output by our CE model each decade under the moderate (left) and strong (right) decarbonization targets. 232
Figure C.9: Provided regulation, flexibility, and contingency reserves by fuel type and year under the moderate decarbonization target without storage in the generator fleet. 233
Figure C.10: Provided regulation, flexibility, and contingency reserves by fuel type and year under the strong decarbonization target without storage in the generator fleet. 234
Figure C.11: Change in cumulative generation by NGCC generators with versus without storage against each generator's CO_2 emission rate under the strong decarbonization target in 2045 when storage participates in only energy (top), only reserve (middle), or energy and reserve (bottom) markets. 237
Figure C.12: Change in system CO_2 emissions with storage versus without storage when storage participates in only energy (top left), only reserve (top right), and energy and reserve (bottom) markets for each sensitivity analysis under the moderate decarbonization target. 240
Figure C.13: Change in system CO_2 emissions with storage versus without storage when storage participates in only energy (top left), only reserve (top right), and energy and reserve (bottom) markets for each sensitivity analysis under the strong decarbonization target. 241
Figure D.1: Histograms of azimuths (top) and tilts (bottom) for fixed array PV systems interconnected through 2015 in the NEM dataset by IOU. 246
Figure D.2: Histograms of azimuths (top) and tilts (bottom) for PV systems in the CSI dataset with metered generation by IOU. 247
Figure D.3: Time series indicating availability of metered generation for each PV system in the CSI dataset from 2013 through 2015. Each line indicates data availability for one PV system. 248
Figure D.4: Schematic for estimating hourly generation by each PV system in the NEM dataset from 2013 through 2015 by scaling up metered generation in the CSI dataset. 249
Figure D.5: Histogram of distance between PV systems in the NEM dataset and the zip code from which we obtain metered generation for each PV system in the scale up method. 251
Figure D.6: Histograms of distances between PV systems and zip codes from which we obtain CFs in PGE (top), SCE (middle), and SDGE (bottom) when using CFs from the 1st, 2nd, 3rd, 6th, and 10th nearest zip code to each PV system (excluding each PV system's own zip code). 252
Figure D.7: NRMSEs in PGE, SCE, and SDGE when using CFs from the 1st, 2nd, 3rd, 6th, and 10th nearest zip codes to each PV system. 253
Figure D.8: Autocorrelation (top) and partial autocorrelation (bottom) function plots of residuals from Regressions 1 (left) and 2 (right). 259
Figure D.9: Time series of actual (solid line) and predicted (red dashed line) LMPs in NP15 using Regression 1. 263
Figure D.10: Time series of actual (solid line) and predicted (red dashed line) LMPs in SP15 using Regression 2. 264
Figure D.11: Maximum hourly (top row) and total (bottom row) estimated versus metered generation for all PV systems in our validation analysis by method for estimating PV generation. 266
Figure D.12: Distributed PV generation in June of 2013, 2014, and 2015 by hour of day in PGE, SCE, and SDGE by method used to estimate generation. 268

Figure D.13: Distributed PV generation in December of 2013, 2014, and 2015 by hour of day in PGE, SCE, and SDGE by method used to estimate generation. 269
Figure D.14: Four 10-day time series in each season of net demand (solid line with star markers) and distributed PV generation in NP15 by method used to estimate generation. 271
Figure D.15: Four 10-day time series in each season of net demand (solid line with star markers) and distributed PV generation in SP15 by method used to estimate generation. 272
Figure D.16: Boxplots of historic LMPs ($$_{2015}$/MWh) from 2013 through 2015 in NP15 (left) and SP15 (right) by hour of day. 273
Figure D.17: Boxplots of changes in LMPs ($$_{2015}$/MWh) with versus without distributed generation by hour of day in June 2013, 2014, and 2015 in NP15 (left) and SP15 (right) by method used to estimate distributed PV generation. 275
Figure D.18: Boxplots of changes in LMPs ($$_{2015}$/MWh) with versus without distributed generation by hour of day in December 2013, 2014, and 2015 in NP15 (left) and SP15 (right) by method used to estimate distributed PV generation. 276

CHAPTER 1: INTRODUCTION

Climate change poses a serious threat to humans and natural systems [1], and already affects the U.S. [2]. International efforts to reduce greenhouse gas (GHG) emissions, the primary drivers of climate change [3], recently culminated in the 2015 Paris Agreement, under which nations submit self-determined GHG emission reduction targets for 2030 [4], [5]. However, even if all countries meet their targets, global energy- and industry-related GHG emissions will likely rise through 2030 and beyond [4], [6]. In comparison, limiting the global average temperature increase to 2 degrees Celsius as espoused by the Paris Agreement [7] would require reducing global GHG emissions by 40-70% from 2010 levels by 2050 and by 100% by 2100 [8].

In the U.S., the electric power sector has historically emitted more GHGs than any other sector [9], although CO_2 emissions from transportation surpassed those from the electric power sector in 2016 [10]. In 2015, the electric power sector accounted for 38% of total GHG emissions [9]. Consequently, decarbonizing the U.S. economy in line with global climate targets will require significant reductions in GHG emissions from the electric power sector [11]. To that end, in 2015 the U.S. Environmental Protection Agency promulgated the first federal regulations on CO_2 emissions from new and existing fossil-fired power plants in New Source Performance Standards [12] and the Clean Power Plan [13], respectively, although the Trump administration published its plan to repeal the latter in October 2017 [14].

Environmental policies and regulations, such as Renewable Portfolio Standards and the Mercury and Air Toxics Standards, and market forces, particularly low natural gas prices and rapid growth in wind and solar energy, are transforming the U.S. electric power system. Natural gas prices fell from $8 to $3 per thousand cubic feet from 2005 to 2016 [15], driving an increase

in gas-fired generation, such that gas-fired generation surpassed coal-fired generation in 2017 for the first time in decades [10]. Coal-fired power plant retirements have surged in recent years: 14 GW retired in 2015 alone [16] and another 51 GW have announced retirement or a switch to natural gas through 2030 [17]. Nuclear plants have also struggled economically, resulting in early retirements of at least five plants in recent years [18], [19]. At the same time, new technologies have gained momentum over the last decade. As of 2016, installed wind and solar capacity reached 82 [20] and 47 GW [21], respectively. Additionally, the first U.S. utility-scale power plant equipped with carbon capture and sequestration began operations in 2017 [22] and the first Generation 3+ nuclear reactors in the U.S. are under construction [23]. Overall, these changes contributed to a 20% reduction in GHG emissions from the electric power sector from 2005 levels by 2015 [9]. While this reduction is significant, reductions on the order of 80-100% will likely be necessary to aggressively mitigate climate change [4], [11], [24].

To that end, this thesis presents four research papers I wrote while at Carnegie Mellon University that focus on three key technologies for deep decarbonization of the electric power sector: carbon capture and sequestration (CCS), grid-scale electricity storage (simply referred to here as storage), and distributed solar photovoltaic (distributed PV). In recent years, concerns around all three technologies have arisen. High costs have plagued CCS, limiting its deployment and leading some experts to question its viability as a major decarbonization technology [25], [26]. Unlike for CCS, storage costs have fallen precipitously in recent years [27], but recent studies indicate storage may increase net system CO_2 emissions in current U.S. power systems [28]–[30]. Finally, while distributed PV capacity has grown rapidly in recent years, debates around the value of distributed PV [31] could lead to policies that inhibit future growth. Through power system optimization, statistics, and techno-economic analysis, the research presented in

this thesis addresses each of these challenges facing CCS, storage, and distributed PV. Each chapter also leverages sensitivity analysis to test the robustness of results to key uncertainties, and links key results to specific policy implications or recommendations.

In Chapters 2 and 3, I explore the system cost and emission implications in the upper Midwest of adding flexibility to CCS-equipped generators through on-site solvent storage. Added flexibility could allow a CCS-equipped generator to provide more grid services, e.g. reserves, increasing the system value of CCS and potentially making it an economic CO_2 reduction strategy. In both chapters, I compare system costs and emissions with flexible CCS versus other CO_2 reduction strategies using a unit commitment and economic dispatch (UCED) model, a power system optimization model that enforces system- and unit-level constraints while minimizing operating costs. To capture the dynamic operations of flexible CCS, I develop a model of a flexible CCS generator and embed it in the UCED model.

In Chapter 2, I compare the cost-effectiveness of reducing CO_2 emissions with flexible CCS relative to wind, re-dispatching, and normal CCS under the U.S. Clean Power Plan (CPP) and a hypothetical stronger CPP. Using the UCED model, I find that flexible CCS tends to offer more cost-effective emission reductions than normal CCS. However, I also find that other CO_2 emission reduction technologies are more cost-effective than flexible CCS, suggesting CCS will play a minor role in complying with the CPP. Chapter 3 builds on Chapter 2 by providing a detailed accounting of system CO_2 emissions and costs, including regulation reserve, generation, and start-up costs, with flexible versus normal CCS. In so doing, I find two key trade-offs between flexible and normal CCS. First, under a moderate emission limit similar to that of the CPP, flexible CCS reduces costs but increases emissions relative to normal CCS, posing a trade-off between costs and emissions to policymakers. However, under a stronger emission limit,

flexible CCS reduces costs and CO_2 emissions relative to normal CCS, thereby posing a trade-off between near-term and long-term priorities. Taken together, Chapters 2 and 3 indicate that while flexible CCS offers several advantages relative to normal CCS, it may also pose trade-offs between economic and environmental objectives. Furthermore, Chapters 2 and 3 indicate that flexible CCS does not fully resolve cost issues that have hindered CCS deployment thus far.

In Chapter 4, I quantify how storage affects system CO_2 emissions as the Texas power system decarbonizes over time. This research begins to fill the gap between two groups of papers: those that find storage would increase emissions in current U.S. power systems and those that find storage will be a key to deep decarbonization. I specifically quantify how storage affects CO_2 emissions under a moderate and strong decarbonization target when participating in only energy, only reserve, and energy and reserve markets. To forecast generator fleet changes, I use a capacity expansion (CE) model, which determines generator additions and operations that minimize fixed and variable costs while meeting system- and unit-level constraints. I then use a UCED model to estimate how storage affects system CO_2 emissions. I find that storage can contribute to CO_2 emission reductions well before deep decarbonization, as early as 2025. Whether storage provides only energy, only reserves, or energy and reserves significantly affects the magnitude, but not direction, of the effect of storage on system CO_2 emissions. Thus, policymakers have a key lever over how storage affects emissions through incentivizing storage to participate in certain markets.

In Chapter 5, in order to improve the valuation of distributed PV generation in value of solar studies, I quantify an often overlooked benefit of distributed PV, namely the market price response. By offsetting some energy demand on-site, distributed PV generation reduces the need for electricity from marginal high-cost generators, which suppresses wholesale electricity prices

and reduces utility expenditures in wholesale energy markets. To quantify wholesale price reductions by distributed PV generation, we use 2013 through 2015 data from California, the state with the highest distributed PV capacity in the U.S. Using a database of all distributed PV systems in the three investor owned utilities (IOUs) in CA, we estimate hourly distributed PV generation from 2013 through 2015 using four methods, thereby hedging against potential biases associated with each and capturing heterogeneity in location and configuration among distributed PV systems. We then estimate wholesale price reductions due to our estimated distributed PV generation using linear regression. From 2013 through 2015, we find that distributed PV suppressed historic median hourly wholesale prices by up to $2.7-3.1/MWh, or by 7-8%, during peak daily PV generation (12-1 p.m. PST). Lower wholesale prices, in turn, reduced utility expenditures in wholesale markets by up to $650-730 million. These avoided costs are smaller than but on the order of other avoided costs commonly included in value of solar studies, so merit inclusion in future studies to properly value distributed PV.

Mitigating climate change is one of the grand challenges of our time. Policy will likely play a fundamental role in this effort, but to do so, it must be grounded in sound, relevant analysis [32]. In each chapter in this thesis, I have taken a key decarbonization technology, identified a policy-relevant challenge or uncertainty associated with it, and addressed that uncertainty or challenge through rigorous, transparent analysis. In so doing, I hope to have helped inform effective policy for mitigating climate change and, in turn, contributed to the fight against climate change.

References

[1] IPCC, *Impacts, Adaptation and Vulnerability. Part A: Global and Sectoral Aspects. Working Group II Contribution to the Fifth Assessment Report of the Intergovernmental*

Panel on Climate Change. Cambridge, UK: Cambridge University Press, 2014.

[2] U.S. National Climate Assessment, *Climate Change Impacts in the United States Climate Change Impacts in the United States*. 2014.

[3] IPCC, "Climate Change 2013 The Physical Science Basis. Working Group I Contribution to the Fifth Assessment Report of the Intergovernmental Panel on Climate Change," 2013.

[4] A. A. Fawcett, G. C. Iyer, L. E. Clarke, J. A. Edmonds, N. E. Hultman, H. C. McJeon, J. Rogelj, R. Schuler, J. Alsalam, G. R. Asrar, J. Creason, M. Jeong, J. McFarland, A. Mundra, and W. Shi, "Can Paris pledges avert severe climate change?," *Science*, vol. 350, no. 6265, pp. 1168–1169, 2015.

[5] UNFCCC, "INDCs as Communicated by Parties," 2016. [Online]. Available: http://www4.unfccc.int/submissions/INDC/Submission Pages/submissions.aspx.

[6] United Nations Environment Programme (UNEP), "The Emissions Gap Report 2017: A UN Environment Synthesis Report," 2017.

[7] United Nations Framework Convention on Climate Change, "Paris Agreement," 2015.

[8] IPCC, "Climate Change 2014 Mitigation of Climate Change. Working Group III Contribution to the Fifth Assessment Report of the Intergovernmental Panel on Climate Change," 2014.

[9] U.S. Environmental Protection Agency, "Inventory of U.S. Greenhouse Gas Emissions and Sinks: 1990-2015," 2017.

[10] U.S. Energy Information Administration, "Monthly Energy Review," 2017.

[11] Deep Decarbonization Pathways Project, "Pathways to Deep Decarbonization," 2015.

[12] U.S. Environmental Protection Agency, "Standards of performance for greenhouse gas emissions from new, modified, and reconstructed stationary sources: Electric utility generating units. Federal Register Vol. 80: 64510-64660," 2015.

[13] U.S. Environmental Protection Agency, "Carbon pollution emission guidelines for existing stationary sources: Electric utility generating units. Federal Register Vol. 80: 64661-65120," 2015.

[14] U.S. Environmental Protection Agency, "Repeal of carbon pollution emission guidelines for existing stationary sources: Electric utility generating Units. Federal Register Vol. 82: 48035-48049," 2017.

[15] U.S. Energy Information Administration, "Natural gas prices: Electric power price," *EIA.gov*, 2017. [Online]. Available: http://www.eia.gov/dnav/ng/NG_PRI_SUM_A_EPG0_PEU_DMCF_M.htm.

[16] U.S. Energy Information Administration, "Coal made up more than 80% of retired electricity generating capacity in 2015," *Today in Energy*, 2016. [Online]. Available: http://www.eia.gov/todayinenergy/detail.cfm?id=25272.

[17] Union of Concerned Scientists, "A Dwindling Role for Coal," 2017.

[18] U.S. Energy Information Administration, "Fort Calhoun becomes fifth U.S. nuclear plant to retire in past five years," *Today in Energy*, 2016. [Online]. Available: https://www.eia.gov/todayinenergy/detail.php?id=28572.

[19] M. B. Roth and P. Jaramillo, "Going nuclear for climate mitigation: An analysis of the cost effectiveness of preserving existing U.S. nuclear power plants as a carbon avoidance strategy," *Energy*, vol. 131, pp. 67–77, 2017.

[20] U.S. Department of Energy, "U.S. installed and potential wind power capacity and generation," *WINDExchange*, 2017. [Online]. Available: https://windexchange.energy.gov/maps-data/321.

[21] Solar Energy Industries Association, "U.S. Solar Market Insight: In second largest Q2 in history, U.S. solar industry adds 2.4 GW of capacity," *SEIA.org*, 2017. [Online]. Available: https://www.seia.org/us-solar-market-insight.

[22] Global CCS Institute, "Petra Nova Carbon Capture," *Projects Database*, 2017. [Online]. Available: https://www.globalccsinstitute.com/projects/petra-nova-carbon-capture-project.

[23] Georgia Power, "Vogtle 3 & 4 project overview," *GeorgiaPower.com*, 2016. [Online]. Available: https://www.georgiapower.com/about-energy/energy-sources/nuclear/overview.cshtml.

[24] The White House, "United States Mid-Century Strategy for Deep Decarbonization," 2016.

[25] V. Scott, S. Gilfillan, N. Markusson, H. Chalmers, and R. S. Haszeldine, "Last chance for carbon capture and storage," *Nat. Clim. Chang.*, vol. 3, no. 2, pp. 105–111, 2012.

[26] V. Maddali, G. A. Tularam, and P. Glynn, "Economic and Time-Sensitive Issues Surrounding CCS: A Policy Analysis," *Environ. Sci. Technol.*, vol. 49, pp. 8959–8968, 2015.

[27] N. Kittner, F. Lill, and D. M. Kammen, "Energy storage deployment and innovation for the clean energy transition," *Nat. Energy*, vol. 2, no. July, p. 17125, 2017.

[28] E. S. Hittinger and I. M. L. Azevedo, "Bulk energy storage increases United States electricity system emissions," *Environ. Sci. Technol.*, vol. 49, pp. 3203–3210, 2015.

[29] R. T. Carson and K. Novan, "The private and social economics of bulk electricity storage," *J. Environ. Econ. Manage.*, vol. 66, no. 3, pp. 404–423, 2013.

[30] M. J. Fisher and J. Apt, "Emissions and economics of behind-the-meter electricity storage," *Environ. Sci. Technol.*, vol. 51, no. 3, pp. 1094–1101, 2017.

[31] L. Hansen, V. Lacy, and D. Glick, "A review of solar PV benefit and cost studies," *Rocky Mountain Institute Electricity Innovation Lab*. p. 59, 2013.

[32] M. G. Morgan, *Theory and Practice in Policy Analysis*. Cambridge, UK: Cambridge University Press, 2017.

CHAPTER 2:
THE ECONOMIC MERITS OF FLEXIBLE CARBON CAPTURE AND SEQUESTRATION AS A COMPLIANCE STRATEGY WITH THE CLEAN POWER PLAN

2.1 ABSTRACT

Many studies indicate that carbon capture and sequestration (CCS) will be a key technology for achieving large CO_2 emissions reductions. Relative to "normal" CCS, "flexible" CCS retrofits include solvent storage that allows the generator to temporarily eliminate the CCS parasitic load and increase the generator's net efficiency, capacity, and ramp rate. Due to this flexibility, flexible CCS generators provide system benefits that normal CCS generators do not, which could make flexible CCS an economic CO_2 emissions reduction strategy. Here, we estimate the system-level cost-effectiveness of reducing CO_2 emissions with flexible CCS compared to re-dispatching, wind, and normal CCS under the Clean Power Plan (CPP) and a hypothetical "stronger CPP." We rely on a unit commitment and economic dispatch (UCED) model, and find that flexible CCS achieves more cost-effective emissions reductions than normal CCS under the CPP and stronger CPP, indicating that policies that promote CCS should encourage flexible CCS. However, we find that flexible CCS is less cost-effective than wind under both reduction targets, and less and more cost-effective than re-dispatching under the CPP and stronger CPP, respectively. Thus, CCS will likely be a minor CPP compliance strategy, but may play a larger role under a stronger emission reduction target.

This chapter is published as Craig, M.T., P. Jaramillo, H. Zhai, and K. Klima. (2017). The economic merits of flexible carbon capture and sequestration as a compliance strategy with the Clean Power Plan. *Environmental Science & Technology*, 51, 1102-1109. doi:10.1021/acs.est.6b03652.

2.2 INTRODUCTION

Climate change poses a serious threat to humans and natural systems [1]. In order to avert large temperature increases under climate change, carbon dioxide (CO_2) emissions from the electric power sector must decrease significantly [2]. Many studies suggest that large (>50%) CO_2 emissions reductions will not be possible without carbon capture and sequestration (CCS) [3], [4]. Yet, only one utility-scale power plant equipped with CCS – the Boundary Dam plant – is currently operational in the world [5]. The Boundary Dam plant is equipped with amine-based post-combustion CCS, the most commercially-developed CCS system, which uses liquid amine to absorb and remove CO_2 from the flue gas of a coal-fired electric generating unit (EGU). "Normal" CCS retrofits like the one at the Boundary Dam plant can reduce CO_2 emissions, but consume significant amounts of energy due to large parasitic loads of the CO_2 capture process, which in turn significantly reduces the net power capacity of the retrofitted EGU. Large capital costs of the retrofits and the increased operation costs associated with the large parasitic loads have hindered large-scale CCS deployment [6].

Relative to a normal CCS retrofit, a "flexible" CCS retrofit includes an additional feature – solvent storage – that allows the generator to temporarily eliminate most of the large parasitic loads of the CO_2 capture process while maintaining a constant CO_2 capture rate [7], [8]. This temporary reduction in the large parasitic loads allows a flexible CCS generator to temporarily increase its net capacity, net efficiency, and ramping capability [7], [9], which in turn yields system benefits that are not available in a normal CCS generator. Furthermore, this flexibility may be increasingly valuable as the penetration of renewables and other technologies increases [10]. Because of these system benefits, flexible CCS may be an economic strategy to reduce CO_2 emissions.

Prior research on flexible CCS with solvent storage can largely be divided into two groups. One group used profit-maximizing optimization models with exogenous electricity prices to determine the optimal operations and profitability of flexible CCS generators [7], [8], [11]. These papers demonstrated that flexible CCS units could use solvent storage to arbitrage electricity price variability throughout the day. However, this arbitrage only marginally increased profits in systems with very large intra-day price differentials [11]. Furthermore, adding amine solvent storage to a normal CCS generator tended to only increase the profitability of a CCS plant at low carbon prices, when construction of a CCS generator would not be justified [7], [8], [12].

Other research used cost-minimizing dispatch models that demonstrated system-wide benefits of flexible CCS generators. Van der Wijk et al. [9], for instance, found that solvent storage-equipped flexible CCS generators could provide four to ten times greater amounts of raise reserves than normal CCS generators, which would reduce reserve provision costs. They also demonstrated that flexible CCS could provide slight reductions in system emissions and wind curtailment compared to normal CCS. Conversely, Cohen et al. [13] demonstrated benefits from increased reserve provision by venting-equipped flexible CCS generators but not from adding solvent storage to those generators.

Taken together, past research suggests that a weak case exists for private investment in flexible CCS, but system benefits of flexible CCS may make it an economic CO_2 emissions reduction strategy. Yet, past papers did not compare flexible CCS to common CO_2 emissions reductions strategies like re-dispatching (decreasing the capacity factors of coal-fired EGUs by increasing the capacity factors of less carbon-intensive EGUs, mainly natural gas) and building new wind capacity. Furthermore, neither Cohen et al. [13] nor Van der Wijk et al. [9] included

reserve provision costs in the optimization problem, which is necessary to fully value solvent storage. Thus, little information exists on the trade-offs between using flexible CCS and other strategies for reducing CO_2 emissions.

Here, we begin to fill these knowledge gaps by considering flexible CCS as an emissions reduction technology in the context of the Clean Power Plan (CPP) and a hypothetical "stronger CPP". The CPP set the first federal limits on CO_2 emissions from existing EGUs in the U.S. and aims to reduce CO_2 emissions in 2030 by 870 million short tons, or 32% from 2005 levels [14]. While these targets are significant, they are likely insufficient to meet climate stabilization goals [15]. Thus, in this paper we also consider a hypothetical stronger CPP that would require a 50% reduction in existing EGU emissions (relative to 2005 levels) by 2030, using the same emissions reduction framework as the CPP.

We assess the merits of flexible CCS as a CPP or stronger CPP compliance strategy with two metrics. First, we compare the cost-effectiveness of CO_2 emissions reductions of flexible CCS retrofits to other CPP compliance strategies, namely re-dispatching, additional wind, and normal CCS retrofits. In this context, we define cost effectiveness as the total operational and capital costs per ton of CO_2 emissions reduced. Second, we calculate the equivalent capital cost (ECC) for flexible CCS retrofits relative to each other compliance strategy, which indicates the capital cost of flexible CCS at which it would reach the same cost-effectiveness and quantity of CO_2 emissions reductions as an alternative compliance strategy.

2.3 METHODS

The upper Midwest area of the Midcontinent Independent System Operator (MISO), which oversees a competitive wholesale market place, will likely face a large capacity of coal-

fired plant retirements [16] and has good wind resources [17], making it an ideal study system for changes under the CPP. As such, we conduct our study in this region, which includes North Dakota, South Dakota, Minnesota, Iowa, Wisconsin, Michigan, Missouri, Illinois, and Indiana.

2.3.1 Unit Commitment and Economic Dispatch Model

We determine operational costs and emissions of each power plant fleet using a unit commitment and economic dispatch (UCED) model that minimizes total system electricity, reserve, start-up, and non-served energy costs subject to various system- and unit-level constraints. By including reserve costs in the objective function of our UCED, we capture the changes in operating costs that result from flexible CCS generators being able to provide system reserves. We constructed the UCED model in PLEXOS Version 7.2 [18], a commercially-available software package commonly used in power system analyses [19], and solved it using CPLEX Version 12.6.1 [20]. We ignore transmission constraints within MISO and imports and exports to and from MISO to limit problem size [21]. Appendix A provides the complete UCED formulation and the 2030 demand profile used in the UCED. In order to allow curtailment of renewable resources, the UCED includes wind and solar generators as dispatchable resources with hourly capacity factors from the National Renewable Energy Laboratory (Appendix A) [22], [23].

Like MISO's day-ahead market [24], we run the UCED model at hourly intervals for a 24-hour period. Additionally, the optimization includes a 24-hour look-ahead period (in 6-hour intervals), which allows us to optimize dispatch decisions over a longer time horizon for a relatively light computational penalty. The solution for one 24-hour horizon serves as the initial conditions for the next day's optimization.

Our UCED model includes reserve requirements and reserve costs. Given the large penetration of wind power in all of our scenarios, we set hourly spinning reserve requirements equal to 3% of maximum daily load plus 5% of hourly wind generation [21], [25]. In order to include reserve costs in the UCED objective function, a cost coefficient, or reserve offer price, must be included with each generator's reserve offers. To determine this coefficient, we assume that reserve offer prices are proportional to the generator's operating cost, or marginal cost of energy [26], [27]. Based on 2015 MISO energy [28] and spinning reserve offer prices [29], the capacity-weighted average proportion of spinning reserve to energy offer prices is approximately 26%. As a result, we set spinning reserve offer prices to 26% of each generator's operating cost.

2.3.2 Base Generator Fleet

We construct a base generator fleet for 2030 for the upper Midwest portion of MISO. The base fleet accounts for fleet changes through 2030, such as generator additions and retirements, expected under the CPP. However, generator additions and retirements characterized in this base fleet are not sufficient to comply with the CPP, as CPP compliance will be largely driven by re-dispatching, i.e. scheduling lower-emitting plants to generate more electricity than they would in the absence of the CPP. As a result, while our base fleet accounts for power plant additions and retirements (some of which may be driven by the CPP), we define our compliance scenarios as the additional strategies that would enable the base fleet to comply with the CPP. Such strategies include re-dispatching, adding wind capacity, and/or adding normal or flexible CCS retrofits to this 2030 base fleet.

It could be argued that adding our compliance strategies to a 2030 base fleet instead of a 2015 fleet may underestimate the cost-effectiveness of these strategies because CCS could

replace some of the fleet changes we assume will occur between now and 2030 as states comply with the CPP. We suggest, however, that many of these fleet changes through 2030, particularly coal plant retirements and renewable capacity additions, would likely occur even without the CPP due to existing environmental regulations and state-level policies such as Renewable Portfolio Standards [30]. Furthermore, since the Clean Energy Incentive Program [14] under the CPP incentivizes early deployment of energy efficiency and renewables, these technologies will likely be deployed prior to CCS. Thus, our analysis considers CCS as a post-2030 CPP compliance strategy, which provides sufficient time to plan for CCS deployment. Finally, by also analyzing larger emissions reductions under a hypothetical stronger CPP with the same 2030 base fleet, we capture the effect on costs and emissions from each compliance strategy in a generator fleet that has not already changed in response to an emissions reduction target, thereby eliminating any bias that may occur in our CPP analysis.

To build our base fleet, we rely on a 2030 generator fleet [31] from the Environmental Protection Agency's Integrated Planning Model (IPM), a cost-minimizing dispatch and capacity expansion optimization model for the U.S. electric power system that forecasts generator additions, retirements, control technology retrofits, and other changes in the power plant fleet in response to regulations [32]. We then alter the IPM fleet in several ways, including changing power plant heat rates and adding necessary unit commitment parameters like ramp rates, as further described in Appendix A. Our final base fleet consists of 1,232 generators with a total capacity of 164 GW. Appendix A includes a summary of installed capacity by fuel type, as well as fuel prices.

2.3.3 CPP Compliance Scenarios

States can comply jointly with the CPP under a single rate- or mass-based target [14]. Given that states have extensive experience with the SO_2 cap-and-trade program [33], we assume that states in our study region will comply jointly with the CPP or stronger CPP under a single regional mass-based limit that equals the sum of each state's mass limit. Under the CPP, the regional CO_2 emissions mass limit equals 346 million tons in 2030, or 32% below 2005 emissions [34]. To test the sensitivity of our results to larger emissions reductions, we also assess a hypothetical "stronger CPP", under which the regional CO_2 emissions mass limit equals 249 million tons in 2030, or 50% below 2005 emissions. Since the EPA projects that re-dispatching among affected EGUs in combination with building additional wind power capacity will account for the bulk of emissions reductions under the CPP [16], we include these as our first two strategies. Additionally, we include normal and flexible CCS retrofits.

2.3.3.1 Re-dispatching among Affected EGUs

Enforcing compliance with the CPP through a mass limit in our UCED model would be intractable, as it would require running the UCED for an entire year at once. Instead, we enforce re-dispatching among affected EGUs by including a shadow CO_2 price on emissions from all affected EGUs as described in Oates and Jaramillo [35]. Appendix A describes our selection of affected EGUs. To calculate this shadow CO_2 price we use a simple economic dispatch (ED) model. The ED model minimizes total energy costs subject to the constraints that supply equals demand and each generator's electricity generation varies between zero and its maximum capacity, as described in Appendix A. To determine the shadow CO_2 price, we increment a CO_2 price upwards from \$0/ton in \$1/ton increments until CO_2 emissions from affected EGUs meet

the regional mass limit in the simple ED. We then include these shadow CO_2 prices in the operating cost and reserve offer prices of affected EGUs in the full UCED.

2.3.3.2 Normal and Flexible CCS Retrofits

To evaluate CCS as a compliance mechanism, we model CCS systems with a 90% CO_2 capture rate, which maximizes the efficiency of the CO_2 removal process in a cost-effective manner [36]. We select coal-fired generators for CCS retrofits based on four common attributes of coal-fired generators for which CCS retrofits are most economic: generators 1) younger than 40 years old (as of 2020), 2) with net thermal efficiencies greater than 30%, 3) with net capacities greater than 300 MW, and 4) with SO_2 scrubbers and selective catalytic reduction (SCR) for post-combustion NO_x control [37]. From this group of eligible generators, we retrofit CCS on generators in order of decreasing net efficiency prior to the CCS retrofit because more efficient generators are more likely to be economically viable to operate, and therefore profitable, post-CCS retrofit.

In order to examine how the cost-effectiveness of CO_2 emissions reductions changes with increasing CCS deployment, we construct three normal and three flexible CCS compliance scenarios for the CPP and stronger CPP each (for a total of 12 CCS scenarios) by modeling CCS retrofits on coal-fired generators. The combined net CCS capacities in these scenarios are 2, 4.5, and 8.5 GW. After accounting for the net capacity penalty of CCS retrofits, the de-rated CCS-equipped coal-fired capacities in these scenarios are 1.6, 3.9, and 6.2 GW, respectively, or up to 4% of the total installed capacity of the base fleet. With 6.2 GW of CCS-equipped generators, the scenario complies with the CPP without a shadow CO_2 price, so we do not test higher retrofit capacities. However, the other two scenarios require some re-dispatching in addition to the CCS

retrofits to comply with the CPP, so we also enforce re-dispatching via a shadow CO_2 price in those scenarios. The same CCS installed capacities are also used in compliance scenarios with our hypothetical stronger CPP, as 8.5 GW entails retrofitting CCS at all eligible coal-fired generators per the four above criteria.

2.3.3.3 Additional Wind Capacity

In order to model compliance using wind power instead of CCS, we create three wind compliance scenarios under the CPP and stronger CPP each. To create each wind scenario, we add wind capacity to the 2030 base fleet until the scenario's shadow CO_2 price necessary to comply with the CPP equals that of a CCS scenario. By controlling for CO_2 price between the CCS and wind compliance scenarios, we hold constant the effects of re-dispatching on emissions and costs, which allows for a direct comparison between additional wind and normal and flexible CCS retrofits as compliance strategies. Relative to the base fleet, which already includes 33 GW of installed wind capacity, this results in 2.5, 5.5, and 6.5 GW of additional wind power capacity under the CPP and 3, 9, and 14 GW of additional wind power capacity under the hypothetical stronger CPP. Appendix A provides the shadow CO_2 price included in each compliance scenario.

2.3.4 Normal and Flexible CCS Models

In order to include CCS in our UCED model, we need operating parameters for retrofitted coal power plants. For this analysis, we assume the maximum fuel input to the boiler at a coal-fired generator remains constant before and after the CCS retrofit, and that no auxiliary boilers are installed. As such, the coal-fired generator must provide the entire parasitic load of the CCS system, meaning its net efficiency and capacity, and therefore ramp rate, decrease upon

CCS retrofit. Given elevated SO_2 removal requirements of CCS, we also zero out SO_2 emissions upon CCS retrofit. To estimate plant-specific CCS retrofit parameters, e.g. net capacity and heat rate penalties, we relied on linear regressions based on data from the Integrated Environmental Control Model (IECM), a power plant modeling tool [38], as detailed in Craig et al. [39] We used net heat rate as the independent parameter for these regressions and developed separate regression models for bituminous and sub-bituminous coal.

A coal plant with flexible CCS has additional specific operating constraints compared to normal CCS. To account for these operating constraints, we develop a flexible CCS operational model that provides constraints that can be included in the UCED model and estimates operational costs and emissions across flexible CCS operations. This flexible CCS model disaggregates a single flexible CCS generator into eight separate proxy units that account for net electricity generation, costs, and emissions of the flexible CCS generator in different operational modes, e.g. while discharging stored lean solvent. Proxy unit operations are linked through numerous constraints. To estimate the values for flexible CCS design and operational parameters we relied on data in existing literature and regressions based on IECM data. Craig et al. [39] provide a detailed description of our flexible CCS model.

2.3.5 Cost-Effectiveness and Equivalent Capital Cost Calculations

The results of the UCED model provide the basis for comparing operational costs and benefits of our compliance scenarios. However, that model does not account for capital costs of new wind installations or CCS retrofits. In order to compare the effectiveness of our compliance scenarios, a consistent metric must be used that accounts for all costs and CO_2 emissions

benefits. We therefore calculate the cost-effectiveness (*CE*) of reducing CO_2 emissions for each compliance scenario (*c)* as:

$$CE_c = \frac{(TOC_c + TCC_c) - TOC_{Base}}{ACE_c - ACE_{Base}} \qquad \text{(Equation 2.1)}$$

where *Base* refers to the base fleet; *TOC* = total operational costs, or the sum of electricity generation, start-up, and reserve costs [$\$_{2011}$]*; TCC* = total annualized capital costs of additional wind capacity or CCS retrofits added in our compliance scenarios [$\$_{2011}$]; and *ACE* = total CO_2 emissions from affected EGUs [tons]. Appendix A specifies how we calculate *TOC* and the capital recovery factor (*CRF*) we use to annualize capital costs. We assume revenues collected through a carbon market are recycled into the economy, so do not constitute real economic costs. To account for uncertainty in capital costs of wind and CCS retrofits, we calculate cost-effectiveness over a range of capital costs (Appendix A).

With these cost-effectiveness estimates, we calculate a per-kW equivalent capital cost (ECC) for flexible CCS relative to each compliance strategy. Each ECC indicates the capital cost of flexible CCS retrofits at which such retrofits would reach the same cost-effectiveness and quantity of CO_2 emissions reductions as an alternative compliance strategy. We calculate the ECC as:

$$ECC_f = \frac{(CE_a * ACE_a) - TOC_f}{FCC_f} * \frac{1}{CRF_f} \qquad \text{(Equation 2.2)}$$

where *f* and *a* indicate flexible CCS and alternative compliance strategies, respectively, and *FCC* is the installed de-rated capacity of flexible CCS [MW]. We use the same *CRF* used to annualize capital costs for Equation 2.1.

2.4 RESULTS

2.4.1 CO_2 Emissions Reductions in Compliance Scenarios

Figure 2.1 shows affected EGU CO_2 emissions in each scenario under the CPP and stronger CPP in addition to both mass limits. This figure highlights that the base 2030 fleet does not, on its own, comply with either policy. However, since CO_2 emissions under the base scenario are much closer to the CPP than stronger CPP mass limit, CO_2 emissions reductions under the stronger CPP compliance scenarios are roughly five to seven times greater than those under the CPP compliance scenarios.

Since we set the shadow CO_2 price for each compliance scenario using a simple ED model that does not account for all system constraints, that price does not guarantee emissions reductions in the full UCED model. In fact, Figure 2.1 indicates that the scenario that reduces emissions solely through re-dispatching does not comply with the CPP, whereas the compliance scenarios that reduce emissions partly through additional wind or CCS retrofits do not comply with the stronger CPP. However, these instances of non-compliance are a construct of using a shadow CO_2 price determined by a simplified ED model to comply with the relevant emission mass limits, not an indication that the strategy could not be used to comply with the mass limit. Indeed, affected EGU CO_2 emissions under these scenarios only exceed the relevant mass limit by less than 2.5%. Thus, we subsequently analyze these scenarios in the same way as scenarios that comply with the relevant mass limit.

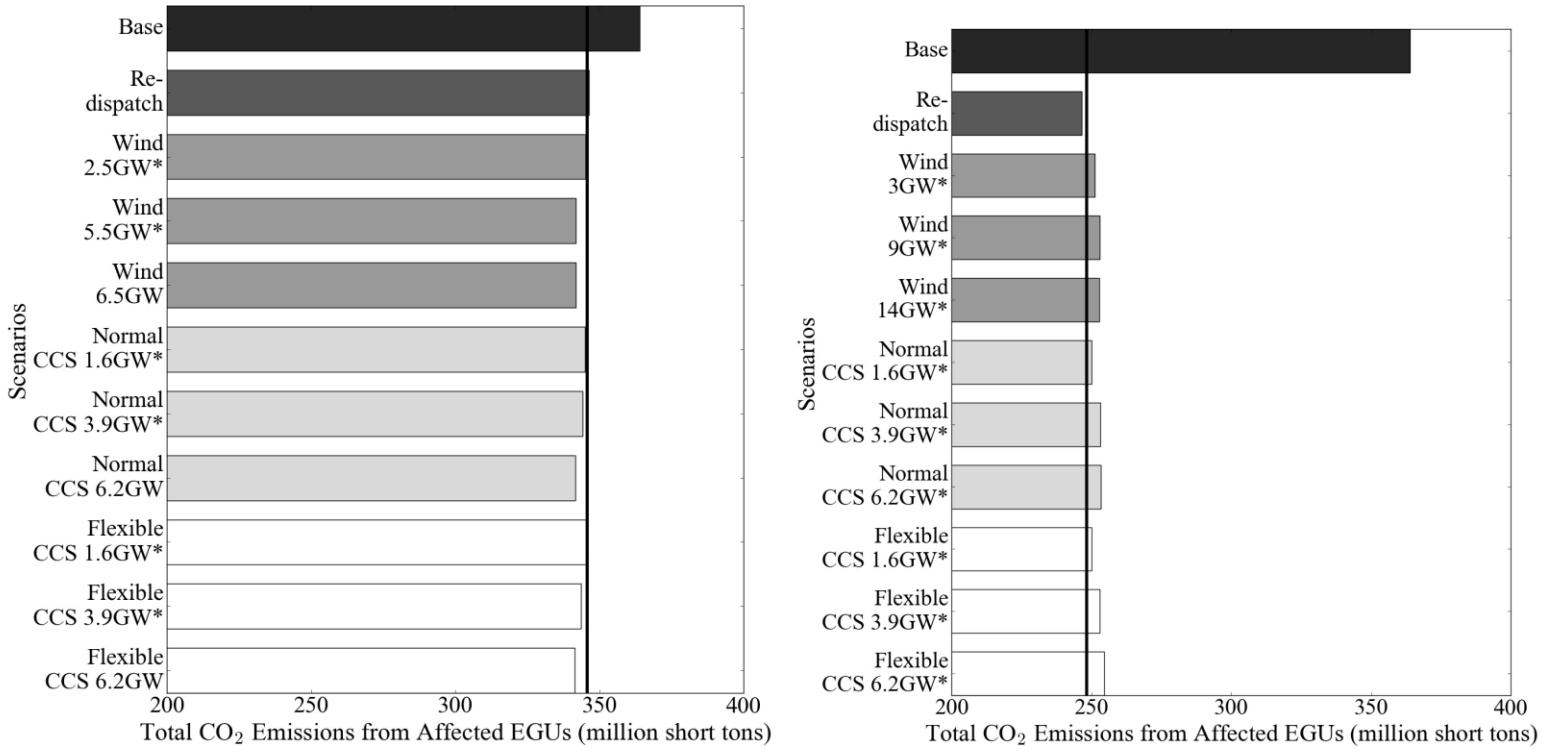

Figure 2.1: Total emissions from affected EGUs under the CPP (left) and stronger CPP (right) from our UCED model, plus each emissions mass limit (black line). * indicates wind and CCS compliance scenarios that include some re-dispatching.

2.4.2 Total Costs

This section discusses the total annualized costs included in the cost-effectiveness calculation for each compliance scenario (see numerator of Equation 2.1). Electricity generation costs dominate total annualized costs under the CPP and stronger CPP. In the re-dispatch CPP compliance scenario, for instance, annual electricity generation costs equal $13.2 billion ($_{2011}$), whereas start-up and reserve costs equal $0.1 and $0.3 billion, respectively. Total annualized costs also include annualized capital costs of new wind or CCS added in the compliance scenarios, which account for 1% to 10% of total costs, depending on the scenario.

Table 2.1 provides total annualized cost increases relative to the base scenario for each CPP and stronger CPP compliance scenario assuming best guess capital cost values. Among our CPP compliance scenarios, total annualized costs relative to the base scenario increase between $100 million in the re-dispatch scenario and $1.28 billion in the 6.2 GW normal CCS scenario. Given that re-dispatching increases costs the least, substituting re-dispatching with additional wind or CCS increases total annualized costs. Total costs increase less under wind, which provides zero marginal cost electricity, than flexible CCS. Flexible CCS, in turn, provides significantly more reserves than normal CCS and therefore further reduce reserve costs [39], resulting in lower total annualized costs than normal CCS. However, since reserve costs account for only a small fraction of total annualized costs, the latter costs are not significantly lower with flexible than normal CCS.

Under the stronger CPP, re-dispatch costs increase relative to the CPP as electricity generation increasingly shifts to units with lower CO_2 emissions rates but higher operational costs. Unlike under the CPP, costs increase the most under re-dispatching, and substituting re-dispatching with wind or normal or flexible CCS reduces total annualized costs. For the same

reasons as under the CPP, additional wind incurs the lowest cost increases, and flexible CCS increases costs less than normal CCS.

Table 2.1: Incremental total annualized costs of each compliance scenario under the CPP and stronger CPP relative to the base scenario assuming best guess capital cost values.

	Total Annualized Compliance Cost (million $$_{2011}$)	
Compliance Scenario	**CPP**	**Stronger CPP**
Re-dispatch	100	2,770
Normal CCS retrofits, 1.6 GW†*	350	2,580
Flexible CCS retrofits, 1.6 GW†*	330	2,560
Wind, 2.5 GW†	140	N/A
Wind, 3 GW*	N/A	2,320
Normal CCS retrofits, 3.9 GW†*	840	2,450
Flexible CCS retrofits, 3.9 GW†*	780	2,410
Wind, 5.5 GW†	230	N/A
Wind, 9 GW*	N/A	1,840
Normal CCS retrofits, 6.2 GW*	1,280	2,490
Flexible CCS retrofits, 6.2 GW*	1,180	2,400
Wind, 6.5 GW	270	N/A
Wind, 14 GW*	N/A	1,580

† and * indicate wind and CCS compliance scenarios that include some re-dispatching under the CPP and stronger CPP, respectively.

2.4.3 Cost-Effectiveness of CO_2 Emissions Reductions

2.4.3.1 CPP

Our results indicate that the cost of complying with the CPP varies significantly among compliance strategies from $0 to $60 per ton of avoided CO_2 (Figure 2.2). Depending on wind capital costs, re-dispatching or wind achieves the most cost-effective CO_2 emissions reductions, whereas normal CCS achieves the least cost-effective reductions. Additionally, replacing re-dispatching with wind or CCS increases the quantity of emissions reductions. Consequently, a trade-off exists between cost-effectiveness and quantity of emission reductions when substituting CCS or wind for re-dispatching, except at low wind capital costs (less than $1,650/kW). Among

CCS technologies, flexible CCS tends to achieve greater emissions reductions more cost-effectively than normal CCS, with the exception of the 1.6 GW CCS scenarios, which have low utilization rates at one retrofit CCS plant [39].

At each capacity of normal or flexible CCS retrofits, similar or greater reductions can be obtained more cost-effectively with additional wind capacity. For instance, the 5.5 and 6.5 GW wind scenarios achieve similar emissions reductions as the 6.2 GW CCS scenarios, but at roughly a fifth of the cost. Additionally, while the 1.6 GW CCS scenarios can achieve as cost-effective emissions reductions as the 5.5 or 6.5 GW wind scenarios, the emissions reductions they achieve are roughly 13% lower.

2.4.3.2 Stronger CPP

Costs of compliance with the stronger CPP range from $7 to $23 per ton (Figure 2.2). Re-dispatching achieves the most emissions reductions but is the least cost-effective, as the addition of wind or CCS increases cost-effectiveness (by up to 40%) and decreases emission reductions (by up to 7%). This trend opposes that under the CPP, indicating the increasing cost-effectiveness of CCS and wind relative to re-dispatching under a stronger emission reduction target. Two factors mostly account for these opposing trends: higher re-dispatch costs and higher capacity factors of CCS-equipped generators under the stronger CPP [39]. Higher CCS capacity factors yield greater system benefits for the same capital cost, thereby increasing the cost-effectiveness of CCS.

Additional wind capacity tends to be a more economic compliance strategy than flexible and normal CCS, as under the CPP. The 9 and 14 GW wind scenarios provide similar emissions reductions at greater cost-effectiveness (by 20-35%) than the 3.9 and 6.2 GW normal and

flexible CCS scenarios. All wind scenarios also achieve more cost-effective emissions reductions than the 1.6 GW CCS scenarios, but the 1.6 GW CCS scenarios achieve more emissions reductions.

Flexible CCS tends to be a more economic compliance strategy than normal CCS, as under the CPP. At all tested capacities, flexible CCS achieves more cost-effective emission reductions than normal CCS. Furthermore, at 1.6 and 3.9 GW of CCS retrofits, flexible CCS achieves greater emissions reductions than normal CCS. However, at 6.2 GW, flexible CCS achieves less emissions reductions due to less electricity generation by CCS-equipped generators [39].

The cost-effectiveness values of individual compliance scenarios differ significantly under the two emission reduction targets. The re-dispatch compliance scenario is four times more cost-effective under the CPP than under the stronger CPP, whereas the wind and CCS compliance scenarios are less and more cost-effective, respectively, under the stronger CPP than under the CPP. Wind and CCS scenarios include more re-dispatching under the stronger CPP than CPP, so re-dispatch costs account for a larger proportion of total costs in those scenarios under the stronger CPP than CPP. Indeed, under the CPP, no re-dispatching occurs in the 6.5 GW wind or 6.2 GW CCS scenarios. Due to greater re-dispatch costs, the wind scenarios are less cost-effective under the stronger CPP. Conversely, in the CCS scenarios, a mix of re-dispatch and CCS under the stronger CPP achieve more cost-effective emissions reductions than large or absolute reliance on CCS under the CPP, indicating CCS is more cost-effective when accompanied by other carbon mitigation strategies.

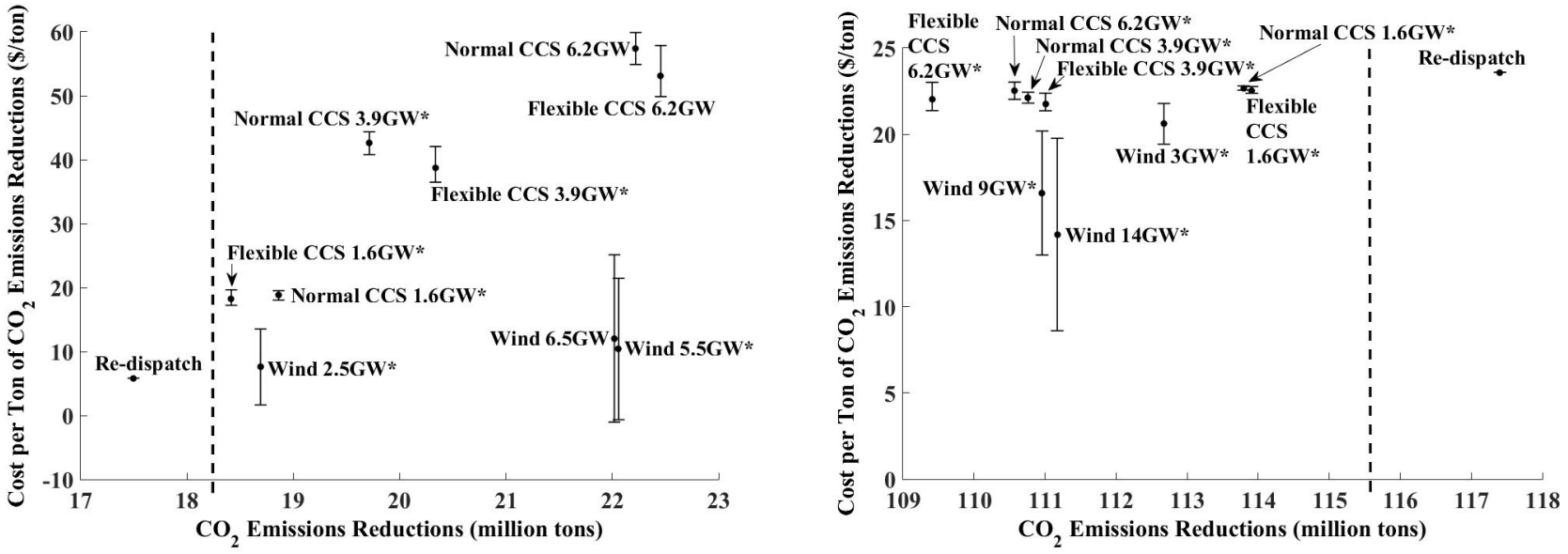

Figure 2.2: Cost per ton of CO_2 emission reductions versus CO_2 emissions reductions for each compliance scenario relative to the base scenario under the CPP (left) and stronger CPP (right). Error bars indicate cost per ton at low and high capital cost values, dashed vertical lines indicate the emissions reductions necessary to achieve each mass limit, and * indicates wind and CCS compliance scenarios that include some re-dispatching.

2.4.4 Flexible CCS ECCs

The ECCs for flexible CCS with respect to each installed capacity of wind tested are negative or below the lowest flexible CCS capital cost estimate used in the cost-effectiveness analysis, or $1,160/kW, under the CPP and stronger CPP (Appendix A). Negative ECCs indicate that even if the capital cost of flexible CCS was zero, flexible CCS would still be more expensive than the alternative compliance strategy due to the energy penalty and consequently high operating cost of CCS. ECCs relative to re-dispatching are also negative under the CPP, but range from $2,000-$2,900/kW under the stronger CPP, well above the current estimates of the capital costs of flexible CCS (1,200 to 1,500 $\$_{2011}$ per net kW), indicating that flexible CCS would likely be a more cost-effective carbon mitigation strategy than re-dispatching under the stronger CPP. Across installed CCS capacities under the CPP and stronger CPP, ECCs relative to normal CCS range from $1,300-$1,600, some of which exceed the upper flexible CCS capital cost estimate of $1,490/kW, also indicating that flexible CCS would likely be a more cost-effective carbon mitigation strategy than normal CCS given best guess flexible CCS capital cost estimates.

2.5 DISCUSSION

In order to better understand whether flexible CCS would be an economic strategy to reduce CO_2 emissions, we compared the cost-effectiveness of CO_2 emissions reductions with flexible CCS to that of three alternative emissions reduction strategies – re-dispatching, additional wind capacity, and normal CCS retrofits – under the CPP and a hypothetical stronger CPP. Under the CPP and stronger CPP, flexible CCS mostly achieved greater and more cost-effective emissions reductions than normal CCS. Additionally, in many scenarios, flexible CCS

ECCs relative to normal CCS exceeded high capital cost estimates currently available for flexible CCS. This finding in conjunction with the cost-effectiveness results indicate that flexible CCS, due to its system benefits, would be a more economic CO_2 reduction strategy than normal CCS from the perspective of the power system. Thus, public policies aimed at encouraging CCS deployment should prioritize support for flexible rather than normal CCS deployment.

However, under the CPP and stronger CPP we found that flexible CCS was a less economic compliance strategy than wind, which achieved larger and more cost-effective CO_2 emissions reductions in most cases. Thus, under both reduction targets, wind would likely be a more common compliance strategy than CCS. The comparison between re-dispatching and flexible CCS is less clear. Under the CPP, re-dispatching achieved more cost-effective but less emissions reductions than flexible CCS, whereas the opposite was true under the stronger CPP. As such, CCS and re-dispatching pose a trade-off between the cost and quantity of emissions reductions under both targets. However, the fact that CCS proved more cost-effective than re-dispatching only under the stronger CPP suggests CCS would be a more viable compliance strategy at higher emission reduction targets than those set forth under the CPP. Higher natural gas prices would improve the merits of CCS relative to re-dispatching.

Nonetheless, given the existence of the CPP, our results indicate that deployment of CCS in the mid-term in our study system, the upper Midwest, will likely be limited, since at least one dominant emissions reduction strategy (wind) exists. ECCs of flexible CCS with respect to wind and re-dispatching reinforce this point, as they are either negative or well below low capital cost estimates for flexible CCS.

This research could be expanded in several ways. First, our UCED model runs in hourly time steps, but shorter time steps may capture additional value from the flexibility of flexible

CCS generators and thereby increase the value of flexible CCS relative to other compliance strategies. Additionally, we ignore transmission costs associated with wind deployment, which could increase wind capital costs, or transportation and storage costs and enhanced oil recovery revenues associated with CCS, which could increase or decrease CCS costs. We also do not consider space limitations at coal-fired generators that could preclude normal or, given larger space requirements for solvent storage tanks, flexible CCS retrofits. Finally, flexible CCS may be more economic in systems with higher renewable penetration. Whereas wind generates 18% of annual electricity in our test system (Appendix A), California, for instance, has a mandate for 33% electricity generation by 2020 [40]. Assessments of the value of flexible CCS in such high renewable systems would indicate whether those systems would be suitable early markets for flexible CCS deployment in the U.S.

2.6 CONCLUSION

The CPP is one of the main components of the U.S.'s Intended Nationally Determined Contribution (INDC) submitted at the 2015 Conference of Parties 21 in Paris [41], but meeting the targets set forth in the INDC will likely require further emissions reductions than those that would be achieved under the CPP [15] or stronger CPP. If the CPP is not strengthened, our analysis indicates that CCS will play little role in meeting the U.S. INDC. Even under a stronger CPP, though, our analysis indicates CCS would be more competitive but still likely play only a modest role. Yet, in the long-term, meeting a 2°C temperature increase limit would require more aggressive emissions reductions than those put forth by the INDCs submitted in Paris [42], and such reductions are likely not possible without CCS [3], [4]. Reconciling the poor mid-term deployment prospects of CCS that we found with long-term deployment needs to mitigate

climate change will likely require public funding or other support for CCS beyond the CPP in the upper Midwest, and potentially in the U.S. more broadly.

2.7 REFERENCES

[1] IPCC, *Impacts, Adaptation and Vulnerability. Part A: Global and Sectoral Aspects. Working Group II Contribution to the Fifth Assessment Report of the Intergovernmental Panel on Climate Change*. Cambridge, UK: Cambridge University Press, 2014.

[2] R. W. Fri, M. A. Brown, D. Arent, A. Carlson, M. Carter, L. Clarke, F. de la Chesnaye, G. C. Eads, G. Giuliano, A. Hoffman, R. O. Keohane, L. Lutzenhiser, B. McCarl, M. McFarland, M. D. Nichols, E. S. Rubin, T. H. Tietenberg, J. A. Trainham, L. Geller, A. Crane, T. Menzies, K. Weller, and S. Freeland, "Limiting the Magnitude of Future Climate Change," 2010.

[3] P. J. Loftus, A. M. Cohen, J. C. S. Long, and J. D. Jenkins, "A critical review of global decarbonization scenarios: what do they tell us about feasibility?," *WIREs Clim. Chang.*, vol. 6, pp. 93–112, 2015.

[4] Deep Decarbonization Pathways Project, "Pathways to Deep Decarbonization," 2015.

[5] Massaschusetts Institute of Technology, "Carbon Capture and Sequestration Technologies Program," 2016. [Online]. Available: https://sequestration.mit.edu/. [Accessed: 01-Jun-2016].

[6] E. S. Rubin, J. E. Davison, and H. J. Herzog, "The cost of CO2 capture and storage," *Int. J. Greenh. Gas Control*, vol. 40, pp. 378–400, 2015.

[7] D. L. Oates, P. Versteeg, E. Hittinger, and P. Jaramillo, "Profitability of CCS with flue gas bypass and solvent storage," *Int. J. Greenh. Gas Control*, vol. 27, pp. 279–288, 2014.

[8] S. M. Cohen, G. T. Rochelle, and M. E. Webber, "Optimizing post-combustion CO2 capture in response to volatile electricity prices," *Int. J. Greenh. Gas Control*, vol. 8, pp. 180–195, 2012.

[9] P. C. Van der Wijk, A. S. Brouwer, M. Van den Broek, T. Slot, G. Stienstra, W. Van der Veen, and A. P. C. Faaij, "Benefits of coal-fired power generation with flexible CCS in a future northwest European power system with large scale wind power," *Int. J. Greenh. Gas Control*, vol. 28, pp. 216–233, 2014.

[10] J. Cochran, P. Denholm, B. Speer, and M. Miller, "Grid Integration and the Carrying Capacity of the U.S . Grid to Incorporate Variable Renewable Energy Renewable Energy," 2015.

[11] D. Patiño-Echeverri and D. C. Hoppock, "Reducing the energy penalty costs of postcombustion CCS systems with amine-storage," *Environ. Sci. Technol.*, vol. 46, pp. 1243–1252, 2012.

[12] P. Versteeg, D. L. Oates, E. Hittinger, and E. S. Rubin, “Cycling coal and natural gas-fired power plants with CCS,” *Energy Procedia*, vol. 37, pp. 2676–2683, 2013.

[13] S. M. Cohen, G. T. Rochelle, and M. E. Webber, “Optimal CO2 capture operation in an advanced electric grid,” *Energy Procedia*, vol. 37, pp. 2585–2594, 2013.

[14] U.S. Environmental Protection Agency, “Carbon pollution emission guidelines for existing stationary sources: Electric utility generating units. Federal Register Vol. 80: 64661-65120,” 2015.

[15] J. Larsen, K. Larsen, W. Herndon, and S. Mohan, “Taking Stock: Progress Toward Meeting US Climate Goals,” 2016.

[16] U.S. Environmental Protection Agency, “Regulatory Impact Analysis for the Clean Power Plan Final Rule,” 2015.

[17] U.S. National Renewable Energy Laboratory, “Wind Research: Wind Resource Assessment,” 2015. [Online]. Available: http://www.nrel.gov/wind/resource_assessment.html. [Accessed: 08-Oct-2015].

[18] Energy Exemplar, “PLEXOS Integrated Energy Model. Version 7.2,” 2015.

[19] J. King, B. Kirby, and M. Milligan, “Operating Reserve Reductions From a Proposed Energy Imbalance Market With Wind and Solar Generation in the Western Interconnection,” 2012.

[20] IBM, “IBM ILOG CPLEX Optimization Studio: CPLEX User’s Manual. Version 12 Release 6.,” 2014.

[21] D. L. Oates and P. Jaramillo, “Production cost and air emissions impacts of coal cycling in power systems with large-scale wind penetration,” *Environ. Res. Lett.*, vol. 8, no. 2, p. 24022, Jun. 2013.

[22] U.S. National Renewable Energy Laboratory, “Transmission Grid Integration: Eastern Wind Dataset,” 2012.

[23] U.S. National Renewable Energy Laboratory, “Transmission Grid Integration: Solar Power Data for Integration Studies Dataset,” 2010.

[24] M. Kessler, “Re: Midcontinent Independent System Operator, Inc. Amendment filing Docket No. ER14-1940-000. Filing to U.S. Federal Energy Regulatory Commission.” 2014.

[25] D. Lew, “Western Wind and Solar Integration Study,” 2010.

[26] E. Denny and M. O’Malley, “Wind generation, power system operation and emissions reduction,” *IEEE Trans. Power Syst.*, vol. 21, no. 1, pp. 341–347, 2006.

[27] A. Cornelius, “Assessing the impact of flexible ramp capability products in the Midcontinent ISO,” Duke University, 2014.

[28] Midcontinent Independent System Operator, “Offers: Day-Ahead Cleared Offers,” 2015. [Online]. Available:

https://www.misoenergy.org/Library/MarketReports/Pages/MarketReports.aspx.

[29] Midcontinent Independent System Operator, "Offers: ASM Day-Ahead Cleared Offers," 2015. [Online]. Available: https://www.misoenergy.org/Library/MarketReports/Pages/MarketReports.aspx.

[30] U.S. Department of Energy, NC Clean Energy Technology Center, and North Carolina State University, "Database of state incentives for renewables and efficiency," 2017. [Online]. Available: http://www.dsireusa.org/. [Accessed: 06-Dec-2015].

[31] U.S. Environmental Protection Agency, "Parsed File: Mass-Based, 2030. Docket No. EPA-HQ-OAR-2013-0602," 2015.

[32] U.S. Environmental Protection Agency, "Documentation for EPA Base Case v.5.13 Using the Integrated Planning Model," 2013.

[33] R. Schmalensee and R. Stavins, "The SO2 Allowance Trading System: The Ironic History of a Grand Policy Experiment," Aug. 2012.

[34] U.S. Environmental Protection Agency, "Data File: Goal Computation Appendix 1-5." 2015.

[35] D. L. Oates and P. Jaramillo, "State cooperation under the EPA's proposed clean power plan," *Electr. J.*, vol. 28, no. 3, pp. 26–40, 2015.

[36] A. B. Rao and E. S. Rubin, "Identifying cost-effective CO 2 control levels for amine-based CO 2 capture systems," *Ind. Eng. Chem. Res.*, vol. 45, no. 8, pp. 2421–2429, 2006.

[37] H. Zhai, Y. Ou, and E. S. Rubin, "Opportunities for decarbonizing existing U.S. coal-fired power plants via CO2 capture, utilization and storage," *Environ. Sci. Technol.*, vol. 49, no. 13, pp. 7571–9, 2015.

[38] Carnegie Mellon University, "Integrated Environmental Control Model. Version 8.0.2." 2015.

[39] M. Craig, P. Jaramillo, H. Zhai, and K. Klima, "The economic merits of flexible carbon capture and sequestration as a compliance strategy with the Clean Power Plan," *Environ. Sci. Technol.*, vol. 51, pp. 1102–1109, 2017.

[40] California Public Utilities Commission, "California Renewables Portfolio Standard (RPS)," *CA.gov*, 2016. [Online]. Available: http://www.cpuc.ca.gov/RPS_Homepage/.

[41] United States of America, "U.S. Cover Note, INDC and Accompanying Information," 2015. [Online]. Available: http://www4.unfccc.int/submissions/INDC/Submission Pages/submissions.aspx. [Accessed: 12-Feb-2016].

[42] A. A. Fawcett, G. C. Iyer, L. E. Clarke, J. A. Edmonds, N. E. Hultman, H. C. McJeon, J. Rogelj, R. Schuler, J. Alsalam, G. R. Asrar, J. Creason, M. Jeong, J. McFarland, A. Mundra, and W. Shi, "Can Paris pledges avert severe climate change?," *Science*, vol. 350, no. 6265, pp. 1168–1169, 2015.

CHAPTER 3:
TRADE-OFFS IN COST AND EMISSION REDUCTIONS BETWEEN FLEXIBLE AND NORMAL CARBON CAPTURE AND SEQUESTRATION UNDER CARBON DIOXIDE EMISSION CONSTRAINTS

3.1 ABSTRACT

Relative to "normal" amine-based post-combustion capture carbon and sequestration (CCS), flexible CCS adds a flue gas bypass and/or solvent storage system. Here, we focus on flexible CCS equipped with a solvent storage system. A primary advantage of flexible over normal CCS is increased reserve provision. However, no studies have quantified system-level cost savings from those reserves, which could drive the public benefits and rationale for policy support of flexible over normal CCS. Here, we quantify total power system costs, including generation, reserve, and capital costs, as well as carbon dioxide (CO_2) emissions of generator fleets with flexible versus normal CCS. We do so under a moderate and strong CO_2 emission limit. Relative to normal CCS, solvent storage-equipped flexible CCS reduces system-wide operational plus annualized CCS capital costs but increases system-wide CO_2 emissions under the moderate limit, whereas it reduces system-wide costs and emissions under the strong limit. Under both limits, we find that reductions in reserve costs constitute 40-80% of the reductions in total operational costs with flexible CCS rather than normal CCS. Thus, flexible versus normal CCS deployment decisions pose cost and emissions tradeoffs to policymakers under a moderate emission limit as well as tradeoffs between near- and long-term policy objectives.

This chapter is published as Craig, M.T., H. Zhai, P. Jaramillo, and K. Klima. (2017). Trade-offs in cost and emission reductions between flexible and normal carbon capture and sequestration under carbon dioxide emission constraints. *International Journal of Greenhouse Gas Control*, 66, 25-34. doi:10.1016/j.ijggc.2017.09.003.

3.2 INTRODUCTION

Climate change could significantly affect human and natural systems [1]. To avert those effects, carbon dioxide (CO_2) emissions from the electric power sector must decrease significantly [2]. Many studies indicate that achieving such large reductions will require widespread deployment of carbon capture and sequestration [3], yet high capital costs have largely hindered deployment of the technology [4]. In addition, operational costs in amine-based post-combustion carbon capture and sequestration (hereafter "CCS") increase due to the large parasitic loads of the CO_2 capture process that reduce the net power capacity and efficiency of CCS-equipped generators, and thus increase fuel costs.

To address the cost barrier to CCS deployment, several papers have considered the merits of "flexible" CCS [5]–[8]. Flexible CCS differs from "normal" CCS in that it includes two additional features that allow the power plant to temporarily eliminate most of the large parasitic loads of the CO_2 capture process: it can vent flue gas, which temporarily increases the generator's CO_2 emissions rate; or it can use stored solvent from a reservoir, which does not change the generator's CO_2 emissions rate [6], [9]. By mostly eliminating the large parasitic loads of the CO_2 capture process, these two features allow a flexible CCS generator to temporarily increase its net capacity, net efficiency, and ramping capability relative to a normal CCS generator [6], [5].

Past analyses of flexible CCS examined the private or system benefits of flexible CCS relative to normal CCS. To quantify private benefits, most papers used profit-maximizing optimization models with exogenous electricity prices to determine the profitability of generating electricity at flexible versus normal CCS generators across a range of CO_2 prices [6], [9]–[11]. These papers found that adding amine solvent storage and/or venting to a normal CCS generator

tended to increase the profitability of a CCS plant at low carbon prices, but not at high carbon prices when construction of a CCS generator would be justified. Thus, these papers indicate that little private case exists for installing flexible rather than normal CCS based on profits from electricity generation.

Other research used cost-minimizing dispatch models to determine how flexible CCS generators would operate in the context of a competitive wholesale electricity market. In general, these papers found that flexible CCS provides some system-wide benefits relative to normal CCS primarily through increased provision of system reserves. Van der Wijk et al. [5] found that solvent storage-equipped flexible CCS generators provided four to ten times more up reserves than normal CCS generators in the Dutch power system in 2020 and 2030 under high wind penetration. Cohen et al. [12] similarly documented a 10% to 30% increase in reserve provision by flexible CCS generators relative to normal CCS generators in a 2020 high-wind system, although adding solvent storage to venting-enabled flexible CCS units yielded little additional benefit. Although these system-level analyses [5], [12] found the primary benefit of flexible CCS to be through increased reserve provision, they did not capture the potential cost reductions from increased flexible CCS reserves. Quantifying these cost reductions is crucial to determining the net system value of flexible CCS, which in turn has important implications for public policy as well as for the prospects of near-term CCS deployment given ongoing cost constraints on CCS deployment. Craig et al. [13] aimed to fill this gap in the literature. Using a cost-minimizing dispatch model that included reserve costs, the authors compared the cost-effectiveness of flexible CCS to that of other CO_2 mitigation strategies in meeting a moderate or aggressive CO_2 emission reduction target. They found that flexible CCS retrofits could achieve more cost-effective emission reductions than normal CCS retrofits and re-dispatching from coal- to gas-

fired generators in some cases, but achieve less cost-effective emission reductions than additional wind capacity in all cases. That work, however, did not include a detailed comparison of normal versus flexible CCS. Additionally, the authors did not consider the effect of solvent storage tank size, a key flexible CCS parameter, on the relative merits of flexible CCS. This paper aims to better understand the trade-offs between normal and flexible CCS.

In this paper, we quantify the difference in total system CO_2 emissions and costs of flexible versus normal CCS retrofits accounting for reserve procurement costs as well as electricity generation, start-up, and CCS retrofit capital costs. Using system costs and CO_2 emissions, we compare the net system value of flexible to normal CCS retrofits under two CO_2 emission constraints: a "moderate" emission limit that aims to reduce CO_2 emissions from the U.S. electric power sector by 32% from 2005 levels by 2030; and a "strong" emission limit that increases the reduction target to 50%. Given our focus on the system value of flexible CCS under CO_2 emission constraints, we focus on flexible CCS equipped with solvent storage in this paper, although our flexible CCS model also accommodates venting. We evaluate the sensitivity of our results to solvent storage tank size and natural gas price.

3.3 METHODS

3.3.1 Overview of Flexible CCS Operations

Figure 3.1 provides a high-level overview of the operations of a flexible CCS generator equipped with solvent storage. A solvent-storage-equipped flexible CCS generator has three operational modes as described in Table 3.1. During "normal CCS operations," a flexible CCS generator operates like a normal CCS generator. Specifically, it delivers electricity to the grid while simultaneously capturing CO_2 with "continuous lean solvent," which is continuously

regenerated from rich solvent, i.e. solvent bound to CO_2. For a given fuel input quantity, continuously regenerating solvent imposes a significant net heat rate and net capacity penalty of roughly 30-45% and 25-30%, respectively, on the generator. A flexible CCS generator can also engage in "charging stored lean solvent" operations by delivering electricity to the grid while simultaneously capturing CO_2 and regenerating some controllable mix of continuous lean and "stored" lean solvent. Stored lean solvent is regenerated from stored rich solvent. Per assumptions detailed below, regenerating stored solvent imposes the same net heat rate penalty and a slightly higher net capacity penalty on the generator as regenerating continuous solvent. A flexible CCS generator can also engage in "discharging stored lean solvent" operations, during which the generator delivers electricity to the grid while capturing CO_2 with some controllable mix of continuous and stored lean solvent. The generator stores resulting rich solvent from the stored lean solvent stream for regeneration at some later time during "charging" operations. In deferring regeneration of the stored solvent, the generator reduces the CCS system's net heat rate and net capacity penalties by up to 90% depending on the amount of stored solvent discharged, thereby allowing the generator to operate more efficiently and at a higher net capacity for a brief period of time. This flexibility can lead to greater profitability, e.g. by increasing net electricity output during peak price periods, or to increase system efficiency, e.g. by reducing curtailment of renewables. The maximum duration of the "charge" and "discharge" operational modes depends on the solvent storage tank size.

Table 3.1: Terms used to describe normal and flexible CCS operations.

Term	Description
Normal CCS operational mode	Net electricity output to the grid and CO_2 capture operations, including solvent regeneration, that occur at a normal or flexible CCS generator during steady-state operations.
Continuous solvent	Rich and lean solvent that is continuously regenerated at a normal or flexible CCS generator in order to capture CO_2 during normal operations.
Stored solvent	Rich or lean solvent stored in storage tanks at a flexible CCS generator.
Charging stored lean solvent operational mode	Passing stored CO_2-rich solvent through the regenerator at a flexible CCS generator, and storing the regenerated CO_2-lean solvent that can be used to absorb CO_2 at some later time. Depending on the regenerator size, stored solvent passed through the regenerator may displace continuously regenerated solvent.
Discharging stored lean solvent operational mode	Passing stored CO_2-lean solvent to the absorber in order to absorb CO_2 at a flexible CCS generator, then storing the resulting CO_2-rich solvent in order to defer regeneration to some later time. Stored lean solvent passed to the absorber displaces some or all continuously regenerated solvent during “partial” or “full” discharging, respectively.

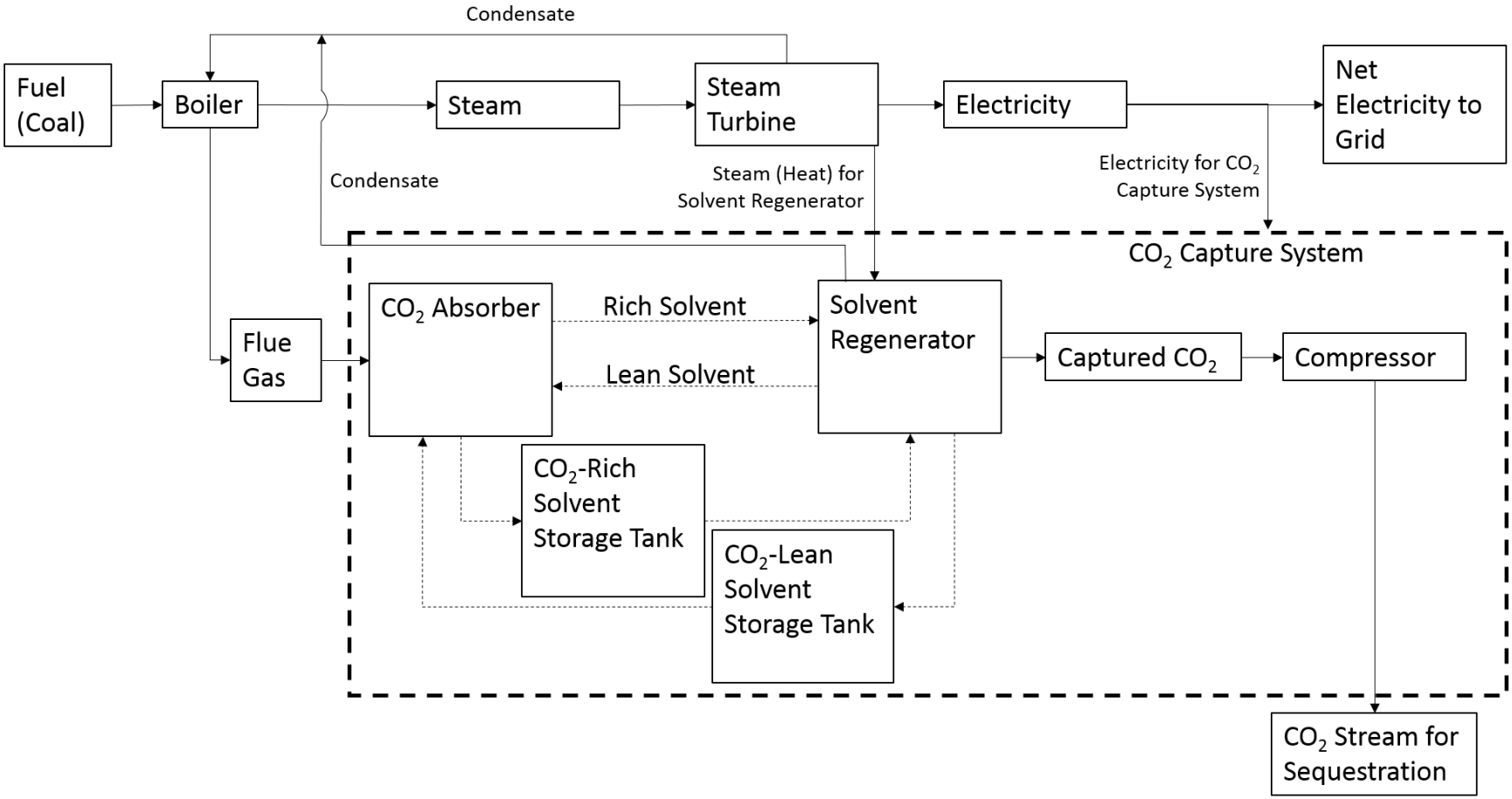

Figure 3.1: Schematic of a flexible CCS generator with solvent storage. The dashed box indicates the CO_2 capture system. Dashed lines indicate the operational choice of using stored solvent in place of continuously-regenerated solvent.

3.3.2 Flexible CCS Generator Model

For our previous work [13], we developed a model of a flexible CCS generator equipped with solvent storage and/or venting. However, given our focus on solvent-storage-equipped flexible CCS, this section describes our model for a flexible CCS generator equipped only with solvent storage. Appendix B provides a description of the venting components of our model. In modeling a solvent-storage-equipped flexible CCS generator, we make four design assumptions. (1) Versteeg et al. [10] found 1 hour of storage capacity to be optimal for amine-based CCS, while other work has shown some flexibility benefits with similar tank sizes [5], [12]. For this analysis, we thus assume that the solvent storage tanks can store sufficient lean solvent to enable maximum net electricity output while discharging stored lean solvent for either 1 or 2 hours. (2) We assume that the regenerator solvent throughput capacity of a flexible CCS generator equals that of a regenerator at a normal CCS generator of equal net power output capacity during normal operations [5], [6], [10], [12]. (3) We assume that discharging stored solvent can reduce the CCS system's parasitic load by up to 90%, which corresponds to eliminating the parasitic load of the solvent regenerator and CO_2 compressor [11]. (4) We assume that the coal-fired generator's steam turbine and fuel input capacity are not modified when the generator is retrofit with CCS. Consequently, the steam turbine can provide the unit's maximum net power capacity achievable while discharging stored lean solvent or venting. Appendix B includes further justification for each design assumption.

Several operational features result from these assumptions. Per assumption (2), charging stored lean solvent necessarily reduces regeneration of continuous solvent. Consequently, in order to maintain a constant CO_2 capture rate (i.e., to capture 90% of CO_2 emissions) while charging, both fuel input and net electricity output to the grid must decrease. Additionally, per

assumption (3) and (4), discharging stored solvent enables greater net electricity output at greater efficiency than during normal CCS operations. Since discharging stored solvent increases net electricity generation by increasing the steam turbine load rather than fuel input, discharging stored solvent also allows for faster ramping than normal CCS operations.

In order to incorporate all of these operational features in a unit commitment and economic dispatch (UCED) model of a power system, we develop a model of flexible CCS operations that simulates the dynamic nature of the net heat rate, net capacity, and emissions and ramp rates of a flexible CCS generator. This model disaggregates a single flexible CCS generator into proxy units and links their operations with a series of constraints. Each proxy unit accounts for net electricity output, reserve provision, costs, and emissions of the flexible CCS generator in a particular operational mode, e.g. while discharging stored lean solvent. As such, we parametrize each proxy unit according to the operational mode it represents. Furthermore, proxy units substitute for one another such that net electricity output, reserve provision, and emissions for a given time period are divided among the proxy units based on the operational mode of the flexible CCS generator (Figure 3.2). For instance, when discharging stored solvent, the discharge stored solvent proxy unit accounts for some or all net electricity output, costs, and emissions from the flexible CCS generator in that period. Finally, UCED models typically use generator-specific net heat rates that are constant, i.e. they assume the ratio between fuel input and net electricity output does not change. However, this ratio varies significantly at a flexible CCS unit due to variability in CO_2 capture operations. Consequently, we use gross instead of net heat rates for most flexible CCS proxy units. This requires separately accounting for energy used to capture CO_2, which we do using specific proxy units.

We disaggregate a flexible CCS generator into five types of proxy units. Figure 3.2 indicates which proxy units are on or off given the operational mode of the flexible CCS generator at any time. Two types of proxy units account for net electricity output and reserve provision: the base and discharge stored lean solvent units. The base proxy unit represents normal CCS operations in conjunction with the continuous solvent proxy unit, which accounts for the parasitic load of the CCS system during normal operations. The discharge stored lean solvent unit accounts for increased net electricity output and efficiency relative to normal CCS operations when discharging stored lean solvent. Like the continuous solvent proxy unit, the charge stored lean solvent proxy unit accounts for energy consumed by the CCS system to regenerate solvent. Finally, the stored solvent tank proxy unit tracks the mass balance of stored rich and lean solvent over time. The continuous solvent, charge stored lean solvent, and stored solvent tank proxy units do not generate electricity or provide reserves.

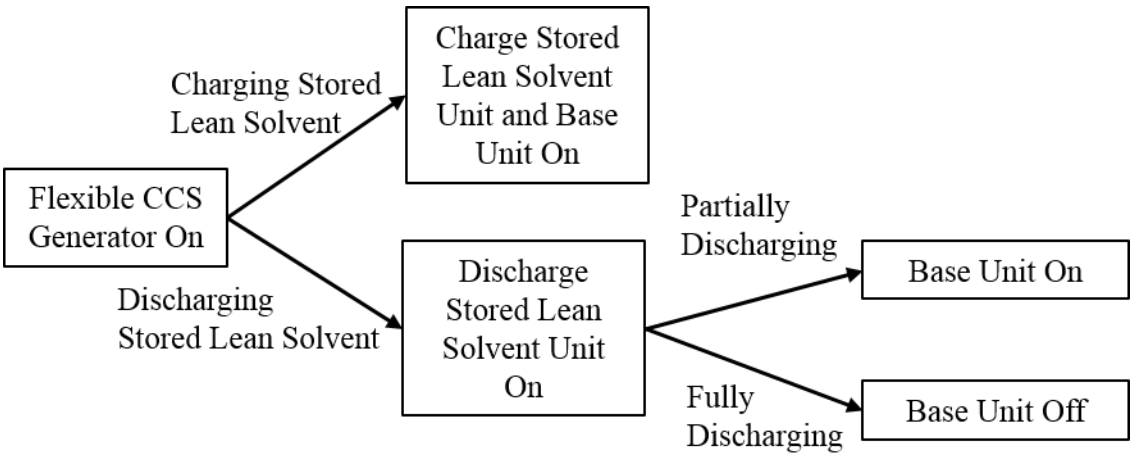

Figure 3.2: Tree showing which proxy units are on or off given the operations of a flexible CCS generator at any given time. When the base proxy unit is on, the continuous solvent proxy unit is also on.

Continuous and stored solvent flows are represented in units of energy. For instance, the amount of energy used to capture CO_2 and regenerate continuous lean solvent represent the continuous solvent flows in the model. Additionally, since proxy units in the model displace net electricity output from one another, the maximum capacity of the discharge proxy unit equals that of the flexible CCS generator while discharging stored lean solvent. To accomplish this, we determine the ratio of net electricity output while discharging stored lean solvent per unit of energy used to charge stored lean solvent using data from the Integrated Environmental Control Model (IECM) Version 8.0.2, a power plant modeling tool [14], as detailed in Appendix B. This ratio, which ranges from three to four depending on coal and plant type, roughly equals the ratio of net electricity output per unit of energy consumed by the CCS system's parasitic load during normal CCS operations plus the fraction of the CCS system's parasitic load transferred to net electricity output while discharging stored solvent (see assumption (3) above). The first component of the ratio allows the discharge proxy unit to displace net electricity output by the base proxy unit, and the second component of the ratio captures the incremental net electricity output of the flexible CCS generator while discharging stored solvent. Consequently, multiplying this ratio by the amount of stored lean solvent yields the net electricity output achievable by the discharge proxy unit when discharging that stored lean solvent.

To parameterize our proxy units, we obtain generator-specific estimates of seven flexible CCS operational parameters by deriving linear regressions with data from the IECM. We use the same approach to estimate two normal CCS operational parameters. Each parameter is regressed against heat rate for bituminous and sub-bituminous coal separately, which allows us to obtain fitted parameter values for each coal-fired generator retrofit with normal or flexible CCS based on the generator's heat rate and coal type. To generate each regression, we begin with a sub-,

super-, or ultra super-critical plant type, then model three plant configurations: no CCS, normal CCS, and flexible CCS. Per assumption (4) above, we maintain a constant fuel input among all three plant configurations. Appendix B details all operational parameters and regressions estimated through this process, and provides the full mathematical formulation of our flexible CCS model.

3.3.3 Power System Modeling

To understand flexible CCS operations in the context of a competitive wholesale electricity market, we embed our flexible CCS model in a UCED model. The UCED model dispatches generators under "moderate" and "strong" CO_2 emission limits that would reduce CO_2 emissions by 32% and 50% from 2005 levels by 2030, respectively. The "moderate" emission limit mirrors the U.S. Clean Power Plan [15]. Like Craig et al. [13], we use the upper Midwest portion of the Midcontinent Independent System Operator (MISO) as our study system because of its large wind resources and expected coal-fired plant retirements in the near-term [16], [17]. Specifically, our study system includes North Dakota, South Dakota, Minnesota, Iowa, Wisconsin, Michigan, Missouri, Illinois, and Indiana.

Our UCED model minimizes total system electricity, reserve, start-up, and non-served energy costs subject to various system- and unit-level constraints. The UCED runs at hourly time intervals for a 24-hour optimization window, like the day-ahead MISO market [18], plus a 24-hour look-ahead period. Including the 24-hour look-ahead period allows us to optimize dispatch decisions over a longer timeframe, which is particularly important for accurately modeling day-to-day storage of solvent. Hourly spinning reserve requirements equal 3% of maximum daily load plus 5% of hourly wind generation [19], [20]. In order to fully capture the benefits of any

increased reserve provision from flexible CCS generators, we include reserve costs in the objective function of our UCED using a reserve cost coefficient. Based on the ratio of energy to spinning reserve offer prices in MISO in 2015 [21], [22], we set this reserve cost coefficient to 26% of each generator's operating cost. The UCED model is constructed in PLEXOS Version 7.2 [23] and solved using CPLEX Version 12.6.1 [24]. Additional information on the UCED, including its full formulation, is available in Craig et al. [13].

Since the goal of this paper is to evaluate a future power plant fleet under carbon constraints, we insert normal or flexible CCS with a 90% CO_2 capture rate into a "base" 2030 generator fleet, and then run that fleet in our UCED model. Craig et al. [13] detail how we construct the base generator fleet, and Appendix B details the composition and fuel prices of the base fleet. To test the sensitivity of our results under the moderate emission limit to natural gas price, we consider a higher natural gas price scenario by increasing the generator fleet's capacity-weighted natural gas price from $5.4 per MMBtu to $6.5 per MMBtu. Finally, to examine how CCS operations change with increasing capacity, we retrofit normal and flexible CCS on 2 and 4 GW of coal-fired generators, yielding 1.5 and 3 GW of de-rated CCS capacity. We retrofit CCS in order of decreasing efficiency on young (less than 40 years old), large (net capacities greater than 300 MW), and efficient (net thermal efficiency greater than 30%) coal-fired generators with SO_2 scrubbers and Selective Catalytic Reduction (SCR). Generators with these attributes typically provide the most economic CCS retrofit opportunities [25].

For each generator fleet, we model compliance separately under a "moderate" and "strong" CO_2 emission reduction target. In each case, we assume that states in our study region will comply jointly under a single regional mass-based limit. To ensure each generator fleet complies with a given emissions reduction target, we use a simple economic dispatch model to

determine a unique CO_2 price that applies to fossil steam, integrated gasification combined cycle, and natural gas combined cycle units greater than 25 MW in capacity [13]. The resulting shadow CO_2 prices, which are available in Appendix B, are included in the electricity generation and reserve provision costs of affected generators in the full UCED, and lead to re-dispatching from high- to low-CO_2-emitting generators. These shadow CO_2 prices serve as a mechanism to ensure compliance with the policies using a UCED model [26]. The shadow prices themselves are not the focus of this work and their meaning should not be overstated. Furthermore, shadow prices do not imply an actual financial transaction so we exclude shadow carbon costs from our cost calculations.

3.3.4 Capital Costs of Solvent Storage

To determine whether system-wide benefits of flexible versus normal CCS justify the additional capital costs of flexible CCS, we aggregate solvent storage capital cost estimates from a variety of sources [5], [6], [10], [11]. We annualize capital costs using a capital recovery factor (CRF):

$$CRF = \frac{i*(1+i)^n}{(1+i)^n-1} \qquad \text{(Equation 3.1)}$$

assuming a discount rate (i) of 7% [27] and that solvent storage lifetimes (n) are comparable to CCS retrofit lifetimes, or 30 years [25]. Ultimately, we estimate minimum, best guess, and maximum annualized solvent storage capital costs per hour of peak power output to equal \$0.5, \$1.5, and \$4.5 per net kW per year.

3.4 RESULTS

We provide results for normal and solvent-storage-equipped flexible CCS generators while varying three key parameters: installed CCS capacity (1.5 and 3 GW), solvent storage tank size (1 and 2 hours), and CO_2 emission limit (moderate and strong). Table 3.2 summarizes our results, which are further discussed in the rest of the paper. In each subsection below, we first compare results with flexible versus normal CCS, then present the effect of shifting from the smaller to larger solvent storage tank. In order to demonstrate the capabilities of our flexible CCS model to capture venting operations, we assess operations of flexible CCS equipped with solvent storage and venting under both CO_2 emission limits in Appendix B.

Table 3.2: Summary of major differences in CCS operations and system costs and emissions between normal and flexible CCS scenarios under the moderate and strong CO_2 emission limits. Note that each cell provides the difference in the relevant result with flexible CCS relative to normal CCS. To contextualize these results, shadow CO_2 prices range from $4-7 per ton under the moderate CO_2 emission limit and $33-36 per ton under the strong CO_2 emission limit with 1.5-3 GW of retrofit CCS, respectively.

Result with Flexible CCS Relative to Normal CCS	**Moderate CO_2 Emission Limit**	**Strong CO_2 Emission Limit**	**Change from Moderate to Strong CO_2 Emission Limit**
Total net electricity output by CCS generators	Smaller by 1% to greater than 4%.	Smaller by 1%.	Normal and flexible CCS net electricity output increase by 30% to 40% due to stronger CO_2 emission constraint.
Net electricity output while discharging stored solvent	Accounts for roughly 2% to 5% of total net electricity output by flexible CCS generators.	Accounts for roughly 0.1% to 0.5% of total net electricity output by flexible CCS generators.	As net electricity output while discharging stored lean solvent increases, total net electricity output by flexible CCS generators decreases. At higher CO_2 emission reduction targets, the system cost necessary to replace reduced net electricity output at flexible CCS generators increases.
Total reserve provision by CCS generators	Greater by 10 to 40 times.	Greater by 500 to 700 times.	The amount of reserves provided by flexible CCS does not significantly change, but reserves provided by normal CCS decline.
System costs	Smaller by $20-50 million due to roughly equal reductions in electricity and reserve costs.	Smaller by $12-40 million due mostly to reduced reserve costs.	System costs decrease less under the moderate than strong limit due to lower electricity cost reductions under the latter that are only partially offset by greater reserve cost reductions.
System CO_2 emissions	Larger by 0.3-0.6 million tons due to greater reserve provision by flexible relative to normal CCS generators, which increases net electricity output by high-CO_2-emitting generators.	Smaller by 0.1-0.2 million tons due to greater reserve provision by flexible relative to normal CCS generators, which increases net electricity output by low-CO_2-emitting generators.	Under both CO_2 emission reduction targets, the change in emissions occurs as non-CCS generators shift from providing reserves to generating electricity. Under the moderate limit this shift occurs at high-CO_2-emitting generators, but under the strong limit it occurs at low-CO_2-emitting generators.

3.4.1 Flexible CCS Operations

3.4.1.1 Flexible Versus Normal CCS

For flexible CCS generators equipped only with solvent storage under the moderate and strong emission limits, solvent storage is used almost exclusively for reserve provision across installed capacities of flexible CCS, as shown in Figure 3.3. Reserves enabled by solvent storage exceed reserves provided by normal CCS generators by roughly 10-40 times under the moderate emission limit and by 530-740 times under the strong emission limit across both solvent storage tank sizes. As a result, flexible CCS generators provide a significant share of system reserves under the moderate (14-37%) and strong (17-35%) emission limits, whereas normal CCS generators provide roughly 0.3-3.7% (moderate limit) and less than 0.1% (strong limit) of system reserves.

Figure 3.3 also shows that total net electricity output by flexible CCS generators is slightly less than the output by normal CCS generators in most scenarios under the moderate and strong emission limits. Specifically, total net electricity output by flexible relative to normal CCS generators differs by -1-4% under the moderate limit and by -1% under the strong limit. Net electricity output by flexible CCS generators exceeds the output by normal CCS generators only with 3 GW of CCS under the moderate limit, when normal CCS shifts towards providing reserves at the expense of net electricity output. Both normal and flexible CCS generators meet roughly 1.5-3% and 2-4% of system electricity demand under the moderate and strong emission limits, respectively, while accounting for 1-2% of the generator fleet by capacity. Due mainly to the stronger CO_2 emission constraint under the strong emission limit, total net electricity output by normal and flexible CCS generators increases from the moderate to strong limit by roughly 32-45%. Like total net electricity output by normal and flexible CCS generators, the capacity

factor of each CCS-equipped generator increases from the moderate to strong limit, as described in Appendix B.

Net electricity output while discharging stored lean solvent decreases from the moderate emission limit, when it accounts for roughly 2-5% of total CCS generation, to the strong emission limit, when it accounts for roughly 0.1-0.5% of total CCS generation. The physical intuition for this decrease is as follows. As discharging and subsequent charging decrease, total net electricity output by flexible CCS generators increases for two reasons. First, due to a limited regenerator size, a flexible CCS generator must reduce its net electricity output while charging. Second, since discharging does not fully eliminate the CCS system's parasitic load, the round-trip efficiency of charging and discharging is less than one. As CO_2 emission reduction targets increase, electricity generation shifts from cheap, high-CO_2-emitting generators to more expensive, lower-CO_2-emitting generators, increasing the system cost to replace lower net electricity output from flexible CCS generators that charge and discharge stored solvent for electricity generation. Thus, in order to minimize system operational costs, flexible CCS generators maximize total net electricity output and therefore use stored solvent less for electricity generation at higher emission reduction targets.

Unlike net electricity output, provision of reserves does not significantly increase from the moderate to strong emission limit for normal or flexible CCS. In the case of normal CCS, providing reserves requires spare generation capacity, so provided reserves decrease as net electricity output increases from the moderate to strong limit. Flexible CCS, though, provides significant and similar amounts of reserves under the moderate and strong limits for two reasons. First, nearly all flexible CCS reserves are provided with spare generating capacity achievable by discharging stored lean solvent, which is incremental to flexible CCS's generating capacity

during normal operations. Furthermore, stored-solvent-enabled reserves have a lower marginal cost than electricity generation during normal operations, since the former reflect a reduced heat rate while discharging stored lean solvent.

3.4.1.2 Effect of Solvent Storage Tank Size

Under the moderate emission limit, net electricity output by flexible CCS generators while discharging stored lean solvent increases by 70-100% when the configuration moves from the smaller to larger solvent storage tank. However, since net electricity output while discharging stored solvent makes up less than 5% of total flexible CCS net electricity output for either storage tank size (Figure 3.3a), overall flexible CCS net electricity output differs by less than 2% between the smaller and larger tank size. Reserve provision by flexible CCS generators also differs little (<3%) between tank sizes. As shown in Figure 3.3b, under the strong emission limit, similar but smaller trends take place: electricity generation while discharging stored lean solvent increases by 10-25% from the smaller to larger solvent storage tank, but overall flexible CCS electricity generation and reserve provision differ by less than 1% between tank sizes. Thus, while solvent storage tank size strongly affects the use of stored solvent for electricity generation, it does not significantly affect overall flexible CCS operations.

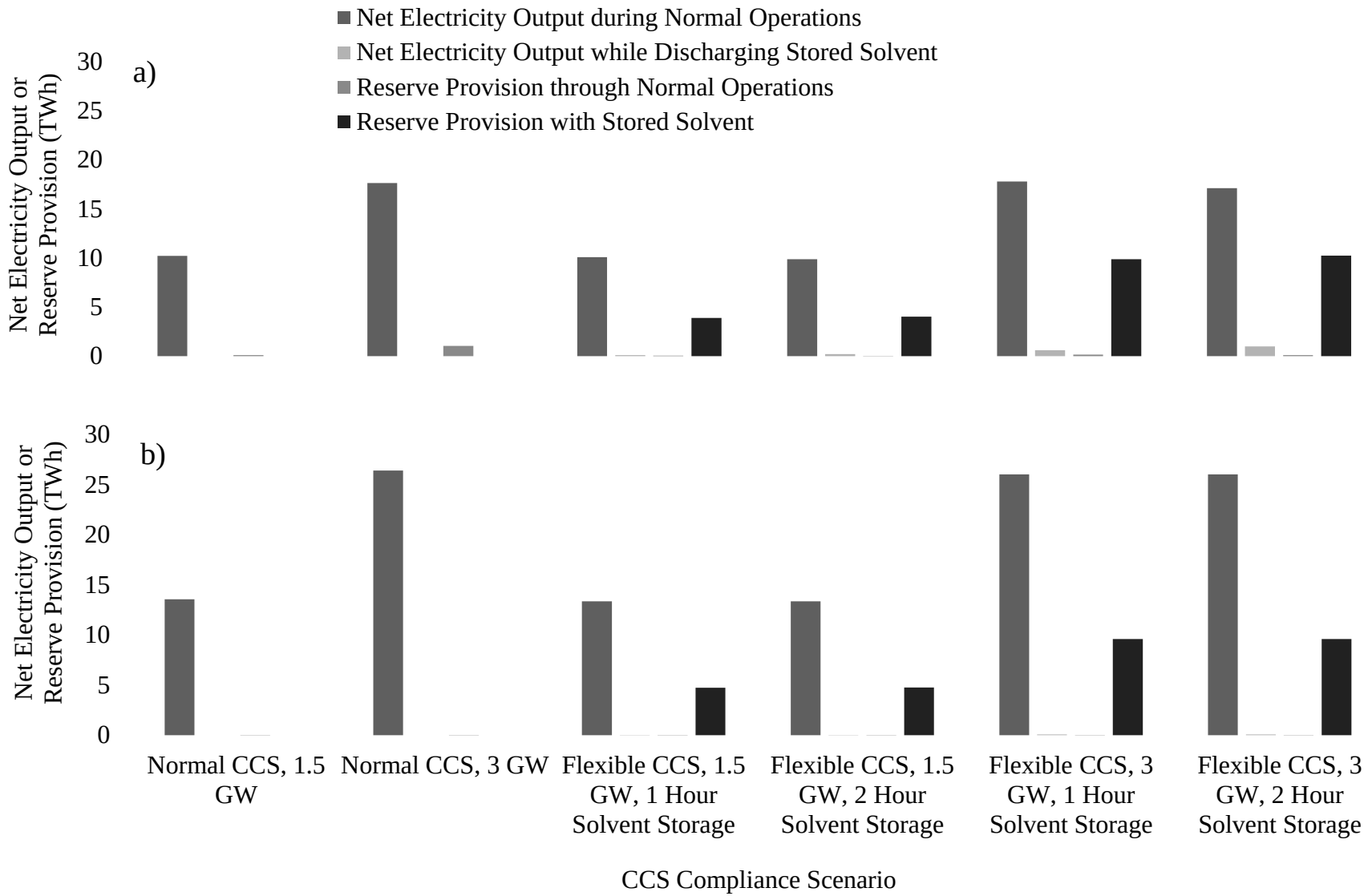

Figure 3.3: Annual net electricity output and reserve provision by operational mode for 1.5 and 3 GW of normal and flexible CCS generators under the (a) moderate and (b) strong emission limits. Flexible CCS generators have 1 or 2 hour solvent storage tank sizes.

3.4.1.3 Daily Profile of Stored Solvent Use

Figure 3.4 depicts the timing of charging and discharging stored solvent summed for all days in 2030 for all flexible CCS generators in the 1.5 GW scenario under the moderate emission limit. Charging tends to occur in the early morning, whereas discharging tends to occur at peak price and demand periods in the late afternoon. Thus, when stored solvent is discharged to enable greater net electricity output, it acts like an energy storage device by shifting energy from the early morning to late afternoon. Similar operational patterns occur under the strong limit.

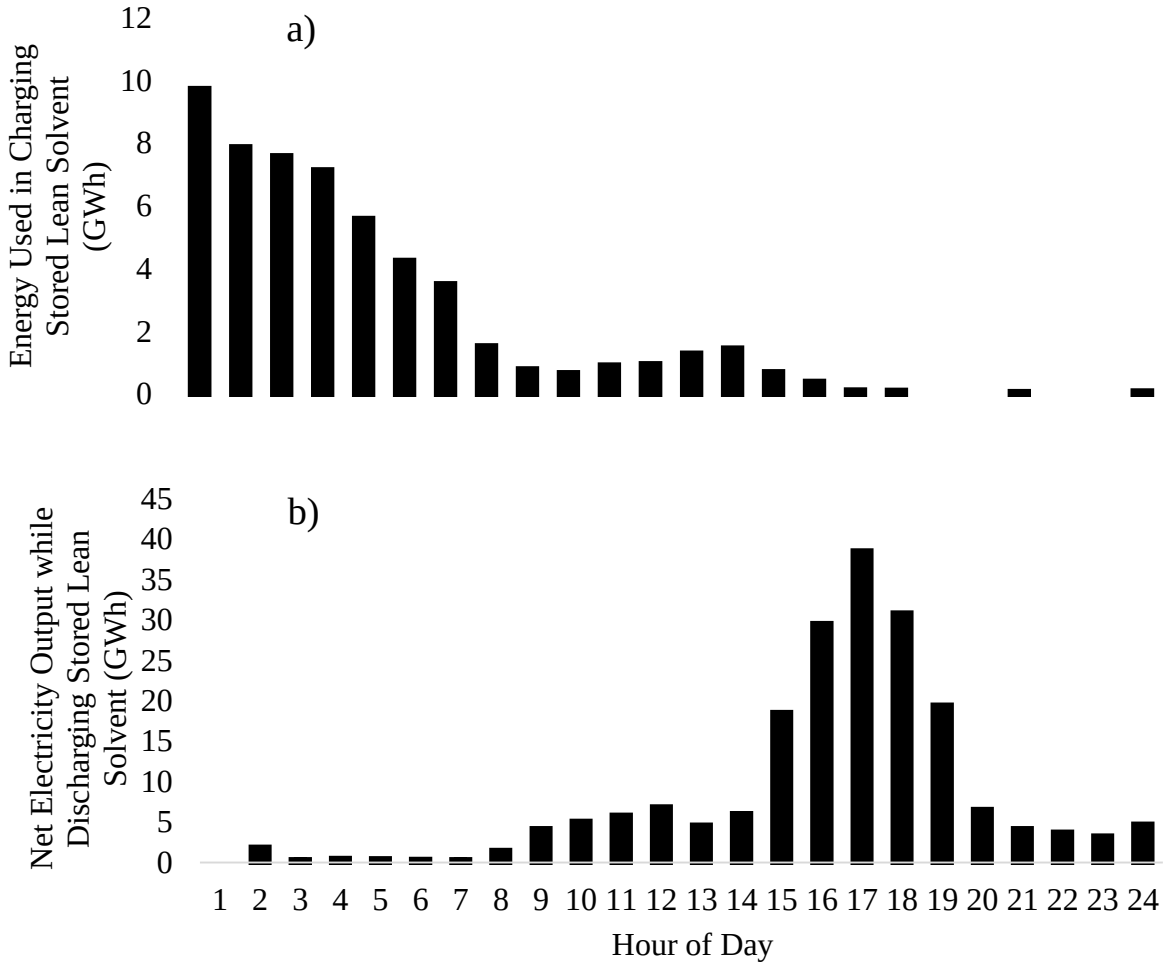

Figure 3.4: Sum of energy used to charge stored lean solvent (a) and net electricity output while discharging stored lean solvent (b) for each hour of the day in 2030 by all flexible CCS generators combined in the 1.5 GW scenario under the moderate emission limit.

3.4.2 System Costs and Emissions with Normal and Flexible CCS

With 1.5 and 3 GW of flexible CCS capacity equipped with a 1 hour solvent storage tank, annualized solvent storage capital costs range from $1 to $7 million and $1.5 to $13.5 million, respectively, with best guess estimates of $2.3 and $4.5 million, respectively. We assume that using a 2-hour solvent storage tank doubles those capital costs, but discuss how economies of scale could affect our results below.

3.4.2.1 Normal Versus Flexible CCS

3.4.2.1.1 Moderate CO_2 Emission Limit

All CCS-equipped fleets comply with the moderate emission limit. However, system CO_2 emissions with flexible CCS exceed those with normal CCS by 0.31 to 0.56 million tons. From normal to flexible CCS, CCS-equipped generators emit more CO_2 due to changes in net electricity output among CCS-equipped generators (Appendix B), but most (66-90%) of the increase in system CO_2 emissions occurs at non-CCS-equipped generators, which generate electricity with additional capacity that is freed-up by the availability of flexible CCS as a reserve asset. Because installed CCS capacity accounts for a small (2%) part of the total generating fleet capacity, these differences in system CO_2 emissions represent a small (<1%) fraction of total system CO_2 emissions. However, in the context of meeting CO_2 emission constraints, these differences in emissions matter, as they are similar to annual expected CO_2 emissions from a 75 MW natural gas combined cycle unit.

Total annual system costs, which equal operational plus annualized solvent storage capital costs, decrease from normal to flexible CCS retrofits by roughly $20-47 million assuming best guess solvent storage capital costs, as shown in Figure 3.5a. Given the small installed CCS

capacity relative to the total fleet installed capacity, total annual system cost reductions from normal to flexible CCS account for less than 1% of total annual system costs. Operational cost reductions from normal to flexible CCS exceed solvent storage capital costs, reducing total system costs. Specifically, operational costs, which include electricity generation, reserve, and start-up costs, decline by $24-53 million from normal to flexible CCS. Electricity generation and reserve cost reductions contribute roughly equally to operational cost reductions. Greater reserve provision by flexible than normal CCS generators drive reserve cost reductions, whereas two factors drive electricity generation cost reductions: (1) greater net electricity output enabled by discharged stored lean solvent during peak demand hours, which displaces generation by high marginal cost units; and (2) greater reserve provision by flexible CCS generators, which frees capacity for electricity generation at non-CCS units that provided those reserves in the normal CCS scenarios. Note that we do not consider the shadow CO_2 prices to be a true economic cost, so we do not include emission costs in system operational costs presented here. As previously described in the Methods, these shadow CO_2 prices just serve as a mechanism to constrain the optimization model to meet the emission targets.

3.4.2.1.2 Strong CO_2 Emission Limit

Unlike under the moderate limit, all CCS fleets (normal and flexible) slightly exceed the strong emission limit by 1-2%, indicating that more re-dispatch or greater installed capacity of CCS would be necessary to comply with the strong limit in our model. Furthermore, unlike the moderate limit results, annual system CO_2 emissions decrease from normal to flexible CCS by 0.09-0.18 million tons under the strong limit. Due to the low installed CCS capacity, this decrease accounts for less than 1% of system CO_2 emissions, but indicates a shift in the value of flexible versus normal CCS under stronger emission constraints. Some (8-50%) of those system

CO_2 emission reductions occur at CCS-equipped generators as net electricity output shifts among CCS-equipped generators from normal to flexible CCS, as described in Appendix B. However, most (50-92%) of those system CO_2 emission reductions come from non-flexible-CCS generators. Due to greater reserve provision by flexible than normal CCS generators, non-CCS generators shift from reserve provision to net electricity output. Greater net electricity output from some non-CCS generators, in turn, reduces electricity output at other non-CCS generators. Since a modest shadow CO_2 price is necessary to comply with the moderate limit, cheap high-CO_2-emitting sources that shift from reserve provision to net electricity output displace net electricity output from more costly lower-CO_2-emitting sources, increasing overall system CO_2 emissions under the moderate limit. Conversely, a high shadow CO_2 price is necessary to comply with the strong limit, increasing the cost of previously-cheap high-CO_2-emitting sources. Consequently, these now-expensive high-CO_2 emitting sources are displaced by now-cheaper low-CO_2-emitting sources that shift from reserve provision to net electricity output, reducing overall system CO_2 emissions under the strong limit.

Assuming best guess solvent storage capital costs, Figure 3.5b shows that total annual system costs decrease from normal to flexible CCS by $12-39 million under the strong limit, as under the moderate limit. Due to the small installed CCS capacity, this cost reduction represents less than 1% of total annual system costs. Electricity generation cost reductions from normal to flexible CCS are lower under the strong limit ($3-11 million) than under the moderate limit ($14-24 million) due to less net electricity output while discharging stored lean solvent under the strong limit. Conversely, reserve cost reductions from normal to flexible CCS are slightly greater under the strong limit ($13-32 million) than under the moderate limit ($11-27 million) because

flexible CCS displaces reserves from more expensive units. Consequently, reserve cost reductions exceed electricity cost reductions by a factor of 3-5 under the strong limit.

3.4.2.2 Effect of Solvent Storage Tank Size

Shifting from the smaller to larger solvent storage tank has a secondary but non-negligible effect on system costs and CO_2 emissions relative to shifting from normal to flexible CCS. With respect to system CO_2 emissions, under the moderate limit, shifting from the smaller to larger solvent storage tank increases system CO_2 emissions by 0.12-0.25 million tons. Under the strong limit, shifting from the smaller to larger solvent storage tank reduces system CO_2 emissions by 0.02-0.04 million tons.

With respect to system costs under the moderate emission limit, operational costs decrease from the smaller to larger tank by $1-2 million (*Figure 3.5*a). However, accounting for stored solvent capital costs and assuming capital costs double when shifting from the smaller to larger tank, total system costs increase from the smaller to larger tank by $1-3 million. In order for total system costs to decrease from the smaller to larger tank, then economies of scale would need to reduce capital costs per unit of storage from the smaller to larger tank. Specifically, capital costs per unit of storage would need to decrease by roughly 33% from the smaller to larger tank in order for total system costs to decrease from the smaller to larger tank. Under the strong emission limit, operational and total system costs both increase from the smaller to larger tank by $1 and $3-6 million, respectively (*Figure 3.5*b). Because operational costs increase from the smaller to larger tank, economies of scale could not lead to total system cost reductions when shifting from the smaller to larger tank.

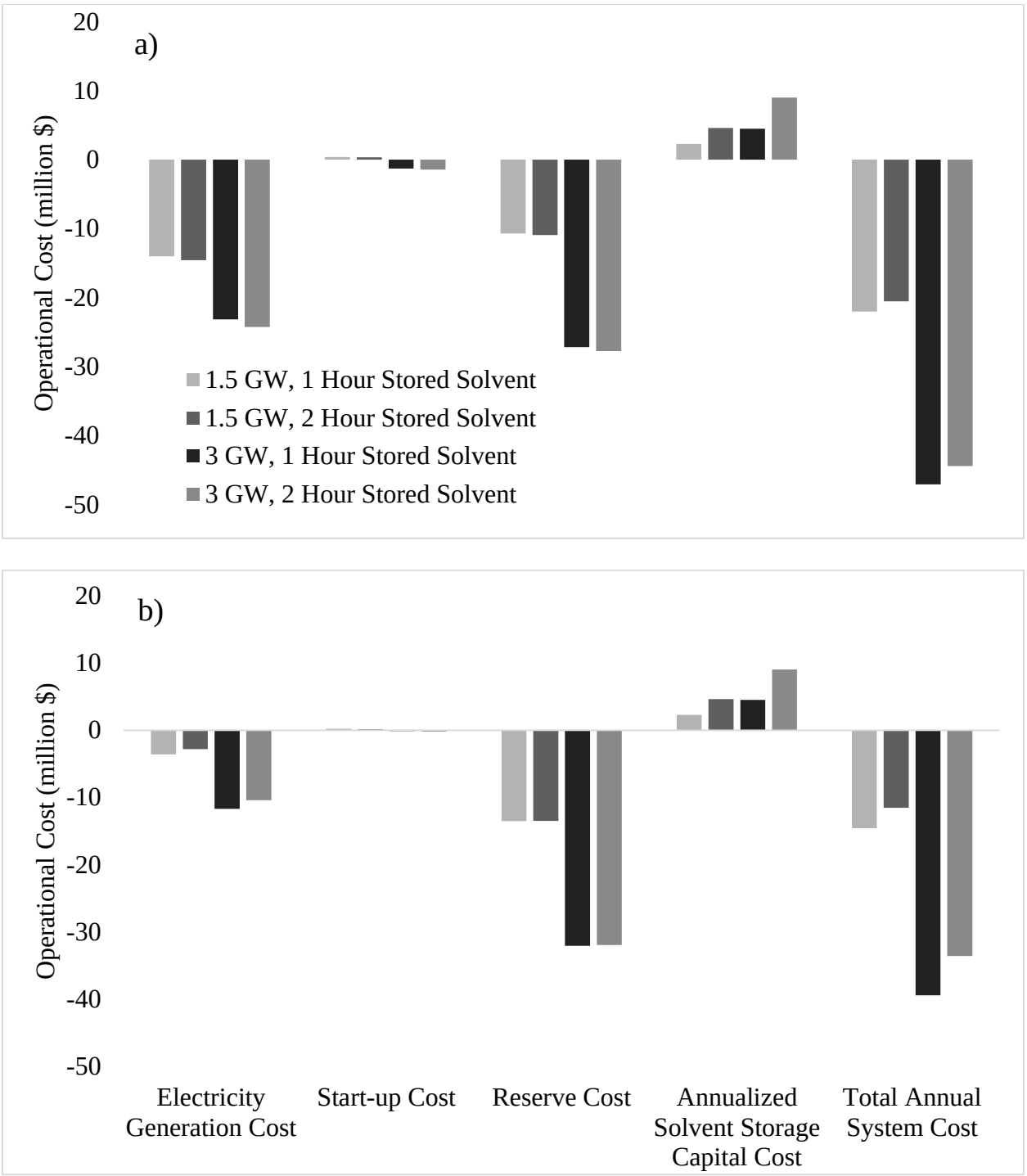

Figure 3.5: Change in electricity generation, start-up, and reserve costs, best guess annualized solvent storage capital costs, and the sum of all four (total annual system costs), with 1.5 or 3 GW of flexible CCS instead of normal CCS under the (a) moderate and (b) strong emission limits. Flexible CCS generators are equipped with a 1 or 2 hour solvent storage tank size.

3.4.3 Net System Value of Flexible Versus Normal CCS

3.4.3.1 Normal Versus Flexible CCS

Figure 3.6 plots the change in total annual system costs, accounting for a range of annualized solvent storage capital costs, against the change in annual system CO_2 emissions from normal to flexible CCS of equal installed capacities. Under the moderate CO_2 emission limit (Figure 3.6a), total system costs from normal to flexible CCS decrease by $7-51 million depending on stored solvent capital costs, but system CO_2 emissions increase by 0.31-0.56 million tons. Thus, normal versus flexible CCS poses a trade-off under moderate emission limits between cost and CO_2 emission reductions. Under the strong CO_2 emission limit (Figure 3.6b), total system costs largely decrease from normal to flexible CCS. At high stored solvent capital costs, total costs increase by up to $2 million from normal to flexible CCS with 1.5 GW CCS installed and with the larger solvent storage tank size. Otherwise, total system costs decrease by $7-43 million across stored solvent capital costs from normal to flexible CCS. Additionally, whereas emissions increase from normal to flexible CCS under the moderate limit, emissions decrease from normal to flexible CCS under the strong limit by 0.09-0.18 million tons. Thus, the value of flexible CCS relative to normal CCS changes with increasing emission reduction targets: whereas flexible CCS reduces system costs less under the strong limit than moderate limit, flexible CCS shifts from increasing to reducing system CO_2 emissions from the moderate to strong limit.

3.4.3.2 Effect of Solvent Storage Tank Size

As with shifting from normal to flexible CCS, the value of shifting from the smaller to larger solvent storage tank changes with CO_2 emission limit. From the smaller to larger tank

under the moderate limit, annual system CO_2 emissions increase by 0.12-0.25 million tons and total annual system costs increase by up to $16 million at all but the lowest stored solvent capital costs, as shown in Figure 3.6a. Thus, under the moderate limit, the smaller tank size yields better system results than the larger tank size. Under the stronger limit, though, system costs increase by $1.3-19 million and system CO_2 emissions decrease by 0.02-0.04 million tons from the smaller to larger tank across stored solvent capital costs. Consequently, under the stronger limit, a tradeoff exists between system costs and CO_2 emissions between solvent storage tank sizes. Additionally, the value of the larger solvent storage tank shifts from increasing to decreasing system CO_2 emissions at stronger emission limits.

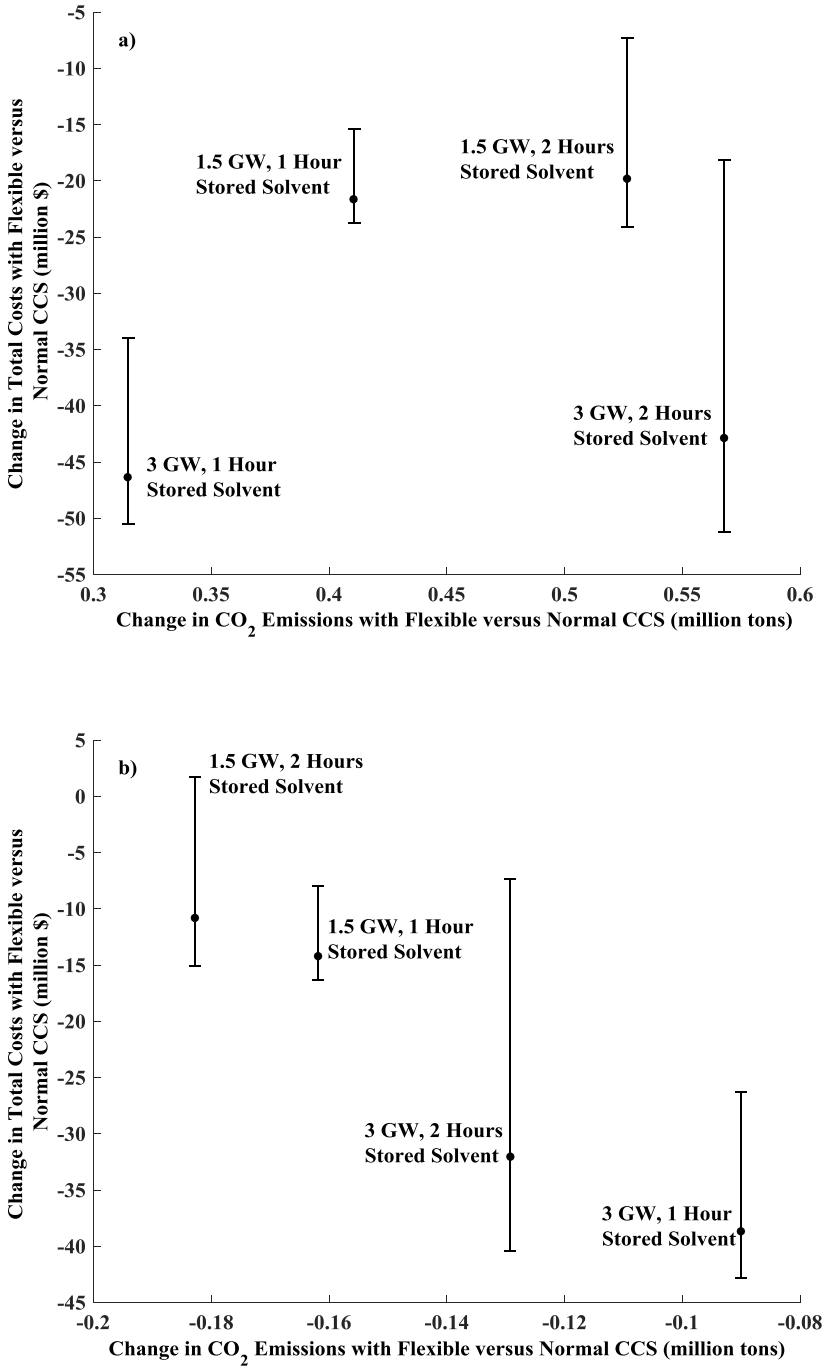

Figure 3.6: Annual change in total operational plus capital costs versus annual change in system CO_2 emissions with an equal installed capacity of flexible CCS relative to normal CCS for solvent storage tank sizes under the (a) moderate and (b) strong emission limits. Negative values indicate reductions with flexible CCS relative to normal CCS. Error bars indicate uncertainty in solvent storage capital costs. Flexible CCS generators are equipped with 1 or 2 hour solvent storage tank sizes.

3.4.4 Sensitivity to High Natural Gas Prices

By increasing the operational costs of natural gas-fired generators, higher natural gas prices generally improve the economics of normal and flexible CCS retrofits, particularly under CO_2 emission constraints. Of interest here, though, is how higher natural gas prices affect the trade-offs between normal and flexible CCS. Given that we find a clear trade-off between normal and flexible CCS under the moderate emission limit (Figure 3.6), we test the sensitivity of our results to higher natural gas prices under the moderate emission limit by increasing the generator fleet's capacity-weighted natural gas price from $5.4 per MMBtu to $6.5 per MMBtu. Since we focus here on comparing normal to flexible CCS, we only consider flexible CCS equipped with a 2 hour solvent storage tank size.

Appendix B provides a full analysis of the high natural gas price results. The shadow CO_2 prices necessary to comply with the moderate emission limit increase with natural gas price. Results in the high natural gas price scenarios largely confirm our prior results. Flexible CCS primarily uses stored solvent for reserve provision, such that reserve provision by CCS generators increases by 9-80 times from normal to flexible CCS. Greater reserve provision reduces reserve costs ($9-25 million) and largely reduces electricity generation costs ($13-40 million) from normal to flexible CCS. Total annual system costs decrease from normal to flexible CCS by $5-65 million across stored solvent capital costs.

At 3 GW CCS installed and high natural gas prices, system CO_2 emissions increase by 1 million tons from normal to flexible CCS, more than that observed under the lower natural gas price and moderate emission limit scenarios. As natural gas prices rise, coal-fired generators become more economic relative to gas-fired generators, so reserves provided by flexible CCS allow for greater coal-fired generation, increasing system CO_2 emissions. At 1.5 GW CCS and

high natural gas prices, though, system CO_2 emissions do not change from normal to flexible CCS. In this scenario, greater CCS utilization from normal to flexible CCS offsets the effect of greater natural gas prices on CO_2 emissions. Overall, relative to lower natural gas prices, the shift from normal to flexible CCS produces similar results under high natural gas prices: total system costs decrease due to reductions in electricity generation and reserve costs, but system CO_2 emissions do not decrease, posing a trade-off between cost and CO_2 emission reductions. Thus, higher natural gas prices do not change the trade-offs posed between normal and flexible CCS retrofits under the moderate emission limit.

3.5 DISCUSSION

To better understand the system value of flexible versus normal CCS under CO_2 emission reduction targets, we quantified system operational costs and CO_2 emissions of a generator fleet with flexible or normal CCS retrofits under a moderate and strong CO_2 emission limit. For flexible CCS retrofits equipped only with solvent storage (excluding the option of CO_2 venting), stored solvent was used primarily to provide reserves under the moderate and strong limits, as found in past studies [5], [12], resulting in significantly greater reserve provision by flexible than normal CCS generators. Unlike past studies, we further quantified system reserve costs, and found that greater reserve provision by flexible than normal CCS generators reduced reserve costs by tens of millions of dollars per year. Under the moderate limit, these system reserve cost reductions were comparable to electricity generation cost reductions that occur when shifting from normal to flexible CCS. Thus, while stored solvent is used primarily to provide reserves, cost reductions from net electricity output while discharging stored lean solvent can be a key contributor to total system cost savings with flexible CCS relative to normal CCS, especially at

high natural gas prices. However, under the strong limit, reserve cost reductions significantly exceeded electricity generation cost reductions when shifting from normal to flexible CCS due to decreased net electricity output with stored solvent.

Effects of solvent storage tank size on system emissions and costs, while secondary to those of using flexible versus normal CCS, differed depending on the emissions reduction target. When moving from the smaller to larger tank, system costs and emissions increased under the moderate limit, mirroring studies that have found electric vehicles with larger batteries result in higher costs and emissions [28], [29]. Under the strong limit, though, costs increased and emissions decreased when shifting from the smaller to larger tank. Thus, a trade-off exists in choosing solvent storage tank size to meet near- versus long-term deployment targets. Given that past studies have found a stronger private case for deployment of smaller solvent storage tanks [6], [10], public policies may be necessary to encourage larger tank size installation in order to accrue greater long-term public benefits.

While we modeled reserve procurement here, we did not model the dispatch of those reserves. Dispatch of reserves offered by a flexible CCS generator would require discharging stored lean solvent, which would later need to be regenerated to return to the initial level of stored lean solvent. Regenerating discharged stored lean solvent would incur costs and therefore reduce the overall benefit of flexible CCS relative to normal CCS. Future research should simulate to what extent reserve dispatch would decrease the relative benefits of flexible CCS compared to normal CCS. Doing so would require an electricity and reserve dispatch model that simulates frequency and contingency events. Our model also does not include frequency regulation and other rapid response reserves, which can have high and volatile prices. Modeling

these reserves would likely improve the system value of flexible CCS relative to normal CCS and should also be a target of future research.

In optimizing our UCED over a 48-hour window, we assume a perfect net-load forecast. In reality, though, most power system operators, including MISO, only clear markets 24 hours in advance. Optimizing flexible CCS operations over shorter time horizons would likely decrease the system value of flexible CCS. Our research also assumed sufficient space is available for CCS retrofits plus the deployment of solvent storage facilities at existing coal-fired generators, such that CCS retrofits can occur at the most economic generators. Future research should examine to what extent flexible CCS retrofits are precluded by space limitations, and how the relative merits of flexible to normal CCS may change for retrofits on less economic generators. Finally, the relative value of flexible CCS compared to normal CCS may vary across power systems, e.g. with differing renewables penetration and fast-ramping resources. High wind penetration, for instance, would likely increase the value of reserves provided by flexible CCS. Our model could be used to examine how high renewable penetration and other factors may affect the relative merits of shifting from normal to flexible CCS.

3.6 CONCLUSION

We found that retrofitting flexible instead of normal CCS reduced total system-wide costs but slightly increased system-wide CO_2 emissions under a moderate CO_2 emission limit in MISO, posing a tradeoff to policymakers. Under a strong CO_2 emission limit, flexible CCS reduced total system-wide costs in nearly all scenarios and decreased system-wide CO_2 emissions in all scenarios. Consequently, while policies designed to meet near-term emission reduction targets may incentivize normal over flexible CCS deployment, such policies could lock

in sub-optimal investments for meeting long-term policy objectives. Policymakers should therefore carefully weigh near- and long-term policy objectives when designing policies that specifically incentivize CCS.

3.7 REFERENCES

[1] IPCC, *Impacts, Adaptation and Vulnerability. Part A: Global and Sectoral Aspects. Working Group II Contribution to the Fifth Assessment Report of the Intergovernmental Panel on Climate Change*. Cambridge, UK: Cambridge University Press, 2014.

[2] R. W. Fri, M. A. Brown, D. Arent, A. Carlson, M. Carter, L. Clarke, F. de la Chesnaye, G. C. Eads, G. Giuliano, A. Hoffman, R. O. Keohane, L. Lutzenhiser, B. McCarl, M. McFarland, M. D. Nichols, E. S. Rubin, T. H. Tietenberg, J. A. Trainham, L. Geller, A. Crane, T. Menzies, K. Weller, and S. Freeland, "Limiting the Magnitude of Future Climate Change," 2010.

[3] P. J. Loftus, A. M. Cohen, J. C. S. Long, and J. D. Jenkins, "A critical review of global decarbonization scenarios: what do they tell us about feasibility?," *WIREs Clim. Chang.*, vol. 6, pp. 93–112, 2015.

[4] E. S. Rubin, J. E. Davison, and H. J. Herzog, "The cost of CO2 capture and storage," *Int. J. Greenh. Gas Control*, vol. 40, pp. 378–400, 2015.

[5] P. C. Van der Wijk, A. S. Brouwer, M. Van den Broek, T. Slot, G. Stienstra, W. Van der Veen, and A. P. C. Faaij, "Benefits of coal-fired power generation with flexible CCS in a future northwest European power system with large scale wind power," *Int. J. Greenh. Gas Control*, vol. 28, pp. 216–233, 2014.

[6] D. L. Oates, P. Versteeg, E. Hittinger, and P. Jaramillo, "Profitability of CCS with flue gas bypass and solvent storage," *Int. J. Greenh. Gas Control*, vol. 27, pp. 279–288, 2014.

[7] M. R. Haines and J. E. Davison, "Designing carbon capture power plants to assist in meeting peak power demand," *Energy Procedia*, vol. 1, no. 1, pp. 1457–1464, 2009.

[8] H. Chalmers and J. Gibbins, "Initial evaluation of the impact of post-combustion capture of carbon dioxide on supercritical pulverised coal power plant part load performance," *Fuel*, vol. 86, no. 14 SPEC. ISS., pp. 2109–2123, 2007.

[9] S. M. Cohen, G. T. Rochelle, and M. E. Webber, "Optimizing post-combustion CO2 capture in response to volatile electricity prices," *Int. J. Greenh. Gas Control*, vol. 8, pp. 180–195, 2012.

[10] P. Versteeg, D. L. Oates, E. Hittinger, and E. S. Rubin, "Cycling coal and natural gas-fired power plants with CCS," *Energy Procedia*, vol. 37, pp. 2676–2683, 2013.

[11] D. Patiño-Echeverri and D. C. Hoppock, "Reducing the energy penalty costs of postcombustion CCS systems with amine-storage," *Environ. Sci. Technol.*, vol. 46, pp.

1243–1252, 2012.

[12] S. M. Cohen, G. T. Rochelle, and M. E. Webber, “Optimal CO2 capture operation in an advanced electric grid,” *Energy Procedia*, vol. 37, pp. 2585–2594, 2013.

[13] M. Craig, P. Jaramillo, H. Zhai, and K. Klima, “The economic merits of flexible carbon capture and sequestration as a compliance strategy with the Clean Power Plan,” *Environ. Sci. Technol.*, vol. 51, pp. 1102–1109, 2017.

[14] Carnegie Mellon University, “Integrated Environmental Control Model. Version 8.0.2.” 2015.

[15] U.S. Environmental Protection Agency, “Carbon pollution emission guidelines for existing stationary sources: Electric utility generating units. Federal Register Vol. 80: 64661-65120,” 2015.

[16] U.S. Environmental Protection Agency, “Regulatory Impact Analysis for the Clean Power Plan Final Rule,” 2015.

[17] U.S. National Renewable Energy Laboratory, “Wind Research: Wind Resource Assessment,” 2015. [Online]. Available: http://www.nrel.gov/wind/resource_assessment.html. [Accessed: 08-Oct-2015].

[18] M. Kessler, “Re: Midcontinent Independent System Operator, Inc. Amendment filing Docket No. ER14-1940-000. Filing to U.S. Federal Energy Regulatory Commission.” 2014.

[19] D. L. Oates and P. Jaramillo, “Production cost and air emissions impacts of coal cycling in power systems with large-scale wind penetration,” *Environ. Res. Lett.*, vol. 8, no. 2, p. 24022, Jun. 2013.

[20] D. Lew, “Western Wind and Solar Integration Study,” 2010.

[21] Midcontinent Independent System Operator, “Offers: Day-Ahead Cleared Offers,” 2015. [Online]. Available: https://www.misoenergy.org/Library/MarketReports/Pages/MarketReports.aspx.

[22] Midcontinent Independent System Operator, “Offers: ASM Day-Ahead Cleared Offers,” 2015. [Online]. Available: https://www.misoenergy.org/Library/MarketReports/Pages/MarketReports.aspx.

[23] Energy Exemplar, “PLEXOS Integrated Energy Model. Version 7.2,” 2015.

[24] IBM, “IBM ILOG CPLEX Optimization Studio: CPLEX User’s Manual. Version 12 Release 6.,” 2014.

[25] H. Zhai, Y. Ou, and E. S. Rubin, “Opportunities for decarbonizing existing U.S. coal-fired power plants via CO2 capture, utilization and storage,” *Environ. Sci. Technol.*, vol. 49, no. 13, pp. 7571–9, 2015.

[26] D. L. Oates and P. Jaramillo, “State cooperation under the EPA’s proposed clean power plan,” *Electr. J.*, vol. 28, no. 3, pp. 26–40, 2015.

[27] The White House Office of Management and Budget, “Guidelines and discount rates for benefit-cost analysis of federal programs. Circular No. A-94 Revised.,” 1992.

[28] J. J. Michalek, M. Chester, P. Jaramillo, and C. Samaras, “Valuation of plug-in vehicle life-cycle air emissions and oil displacement benefits,” *Proc. Natl. Acad. Sci.*, vol. 108, no. 40, pp. 16554–16558, 2011.

[29] N. C. Onat, M. Kucukvar, and O. Tatri, “Conventional, hybrid, plug-in hybrid or electric vehicles? State-based comparative carbon and energy footprint analysis in the United States,” *Appl. Energy*, vol. 150, pp. 36–49, 2015.

CHAPTER 4:
CARBON DIOXIDE EMISSIONS EFFECTS OF GRID-SCALE ELECTRICITY STORAGE IN A DECARBONIZING POWER SYSTEM

4.1 ABSTRACT

While grid-scale electricity storage (hereafter "storage") could be crucial for deeply decarbonizing the electric power system, it would increase carbon dioxide (CO_2) emissions in current systems across the United States. To better understand how storage transitions from increasing to decreasing system CO_2 emissions, we quantify the effect of storage on operational CO_2 emissions as a power system decarbonizes under a moderate and strong CO_2 emission reduction target through 2045. Under each target, we compare the effect of storage on CO_2 emissions when storage participates in only energy, only reserve, and energy and reserve markets. We conduct our study in Texas and use a capacity expansion model to forecast generator fleet changes and a unit commitment and economic dispatch model to quantify system CO_2 emissions with and without storage. We find that storage would increase CO_2 emissions in the current Texas system, but would decrease CO_2 emissions in 2025 through 2045 under both decarbonization targets. Storage reduces CO_2 emissions primarily by enabling gas-fired generation to displace coal-fired generation, but also by reducing wind and solar curtailment. We further find that the market in which storage participates drives large differences in the magnitude, but not the direction, of the effect of storage on CO_2 emissions.

This paper is in review as Craig, M.T., P. Jaramillo, and B.-M. Hodge. (In review.) Carbon dioxide emissions effects of grid-scale electricity storage in a decarbonizing power system. *Environmental Research Letters*.

4.2 INTRODUCTION

In order to avert severe impacts of climate change on humans and natural systems, carbon dioxide (CO_2) emissions from the electric power sector must rapidly decrease [1]. Grid-scale electricity storage (hereafter "storage") could be a key technology for decarbonizing the electric power system [2]–[5]. At high penetrations of wind and solar, storage can reduce wind and solar curtailment by shifting generated electricity across time to meet demand [2]. Furthermore, due to its flexibility, storage can help maintain grid reliability by providing ancillary services, such as regulation reserves [4], [6]. In both cases, storage operations enable greater electricity generation by low-carbon technologies and, in turn, lower system CO_2 emissions. Storage investment can also stimulate greater investment in low-carbon technologies [3], [7].

Conversely, several recent studies suggest that grid-scale and behind-the-meter storage would increase CO_2 emissions in historic power systems [8]–[10]. Using 2009 to 2011 data, Hittinger and Azevedo [8] find that 90% efficient storage engaging in energy arbitrage would have increased CO_2 emissions in wholesale power markets across the U.S. To determine how storage affects system emissions, these studies use marginal emissions factors (MEFs), which predict the emissions associated with a marginal increase in electricity demand [11]. Because MEFs are calculated using historic data, the findings of these studies pertain to a specific set of generation mixes and fuel prices. As such, these studies yield little insight into how storage will affect CO_2 emissions as decarbonization efforts transform power systems. In light of this shortcoming, other papers have used dispatch models to quantify how storage affects emissions. For instance, Tuohy and O'Malley [12] find that storage would increase CO_2 emissions while engaging in energy arbitrage in the Irish power system at high wind penetrations.

When engaging in energy arbitrage, storage's effect on CO_2 emissions depends on which power plants charge storage and which power plants storage displaces when discharging [13]. In historic and current systems, storage would typically charge at night and discharge during the day, when coal and natural gas are the respective marginal fuels [8]. By enabling a shift from gas-fired to coal-fired generation, storage would increase CO_2 emissions [13]. However, as power systems decarbonize, the generation mix, marginal fuel types, and intra-day price differentials will change. These changes, in turn, may shift storage operations and their effects on system emissions, but the speed and extent to which such changes may occur remains unclear. Better understanding these dynamics would not only inform the long-term utility of storage in decarbonization efforts, but also have direct near-term relevance to policies promoting storage.

Although most studies examine how storage affects emissions via energy arbitrage, storage often instead provides ancillary services [14], [15]. Given growing flexibility needs of decarbonizing power systems [16], this trend will likely continue. Prior research on storage's effect on CO_2 emissions when providing ancillary services has limited applicability to current or decarbonized systems, as it has been done on a 30-bus test system [17] or electric vehicles [18].

In this paper, we quantify the operational effects of storage on system CO_2 emissions through 2045 as a power system decarbonizes. We consider two decarbonization targets of reducing CO_2 emissions from electricity generation by 50% and 70% below 2015 levels by 2050. Under each target, we compare the effect of storage on operational system CO_2 emissions when storage participates in only energy, only reserve, and energy and reserve markets. Using scenario analysis, we test the sensitivity of our results to the type of decarbonization policy, natural gas price, coal-fired generator retirements, and storage capacity and efficiency.

4.3 METHODS

In order to capture detailed fleet composition and operational changes, we leverage two power system optimization models in sequence. First, we forecast changes in the generator fleet every 5 years from 2020 through 2045 using a capacity expansion (CE) model and accompanying heuristics. Second, using generator fleets output by the CE model, we quantify operational system CO_2 emissions with and without storage with a unit commitment and economic dispatch (UCED) model. Given its high computational requirements, we run the UCED model every 10 years from 2025 through 2045. To ground our analysis, we also run the UCED with our initial generator fleet with and without storage in 2015. We construct the CE and UCED models in the General Algebraic Modeling System Version 24.4 [19] and solve them using CPLEX Version 12 [20].

We conduct our analysis in the Electricity Reliability Council of Texas (ERCOT) power system due to its plentiful wind and solar resources [21], diverse fuel mix [22], and negligible power flows with neighboring systems [22]. To construct our initial generator fleet, we modify the 2015 ERCOT generator fleet in the National Electric Energy Data System [23] (see Appendix C for full details). We obtain future fuel prices from the U.S. Energy Information Administration [24], [25] and Environmental Protection Agency [26] (Appendix C).

The CE and UCED models share several features. First, given recent transmission buildouts in ERCOT to accommodate wind generation [27], we assume transmission will keep pace with generator additions, so ignore transmission in our analysis [28]. Second, since ERCOT has limited interconnections with neighboring systems [22], we ignore power imports and exports. Third, to capture spatial and temporal variability in wind and solar generation, we match

wind and solar plants to hourly simulated wind and solar generation profiles [29], [30] and include them as dispatchable resources (Appendix C).

4.3.1 CE Model

The CE model optimizes generator additions and electricity generation and reserve provision by added and existing generators in order to minimize costs under system- and generator-level unit commitment constraints (Appendix C). System constraints ensure hourly electricity generation and reserve provision meet electricity demand and reserve requirements, total installed capacity meets the current ERCOT planning margin target (13.75% above peak net demand) [31], and total annual CO_2 emissions comply with a CO_2 emission cap. Costs minimized by the CE model equal fixed operation and maintenance (O&M) and capital costs of added generators, plus variable electricity generation and start-up costs of added and existing generators. In order to isolate the effect of adding storage to our system and given significant uncertainty in future demand, we use 2015 hourly demand from ERCOT [32] (Appendix C) and assume no load growth over our study period, deferring analysis on how storage affects emissions under future demand scenarios to future work.

In each time step, the CE model can add any number of coal steam with carbon capture and sequestration (CCS), natural gas combined cycle (NGCC), NGCC with CCS, nuclear, wind, and solar generators (see Appendix C for technology parameters). Given our focus on storage operations, we do not include storage in the CE model, but rather perform a parametric analysis of storage additions to the generator fleet optimized in the CE model. To account for generator retirements, we retire generators based on age before each CE run and based on economic performance before and after each CE run [33] (Appendix C).

To account for variable wind and solar generation and for generator and transmission outages, the CE model includes three reserve types [16] (Table 4.1) (Appendix C). Given grid flexibility challenges of insufficient generation and the ability to curtail excessive (i.e., under-forecasted) renewable generation, we model all three reserve types as positive reserves, i.e. procure capacity for increasing generation [16]. Additionally, given current standard operations, only coal steam, oil and gas steam, and NGCC units can provide reserves [14]. For computational tractability, we run the CE model in hourly intervals for two representative contiguous days per season, the day with peak annual net demand, and the day with the peak annual change in hourly net demand, where net demand equals demand minus solar and wind generation (Appendix C).

Table 4.1: Reserve types, response timeframes, and hourly requirements in the CE and UCED models. Reserve types and requirements equal those used in Lew et al.[16], who model similar renewable penetrations as we do. *SR* and *WR* indicate reserve requirement components based on wind and solar generation, respectively, and *r* and *f* index regulation and flexibility reserves. Reserve requirements vary hourly with load and wind and solar generation.

Type	Response Timeframe (min.)	Hourly Requirement
Regulation	5	$\sqrt{(1\%\ hourly\ load)^2 + SR_r^2 + WR_r^2}$
Flexibility	10	$\sqrt{SR_f^2 + WR_f^2}$
Contingency	30	$3\%\ hourly\ load$

4.3.2 UCED Model

The UCED model optimizes electricity generation and reserve provision in order to minimize operational costs while meeting electricity demand, reserve requirement, and generator-level unit commitment constraints (Appendix C). The UCED model includes the same reserve types, timeframes, and requirements as the CE model (Table 4.1). Minimized operational costs equal variable electricity generation, regulation reserve provision, and start-up costs.

Regulation provision costs, which account for increased variable operation and maintenance costs and heat rate degradation, equal \$10, \$6, and \$4 ($\$_{2012}$) per megawatt-hour (MWh) for coal, NGCC, and oil and gas steam units, respectively [14], [17], [34]. These regulation provision costs generally agree with the median day-ahead regulation up clearing price in ERCOT from 2013 through 2015 of \$5.9 per MWh (75% CI of [2.6,16.9] \$/MWh) [35]. Since the UCED model determines the commitment but not dispatch of reserves, we provide a first-order estimate of the effect of emissions due to dispatching reserves provided by storage on our results (Appendix C).

In order to account for inter-day generator operations, the UCED model runs hourly for a 24-hour optimization window plus a 24-hour look-ahead period. The solution of the first 24-hour period determines the initial conditions for the following UCED run. Since we run the UCED model in overlapping 48-hour periods for an entire year, we cannot include a constraint on annual CO_2 emissions. Consequently, from 2020 through 2045 when we enforce a CO_2 emission limit, we convert the relevant annual CO_2 emission limit to a shadow CO_2 price using a simple economic dispatch model (Appendix C), then include that shadow CO_2 price in generators' operational costs in the UCED model. Note that these shadow CO_2 prices do not represent real costs, but rather function as a compliance mechanism with the annual CO_2 emission limit in the UCED model [28].

4.3.3 Storage Model

We quantify system CO_2 emissions with the UCED model without storage and with storage participating in only energy, only reserve, and energy and reserve markets. To reflect variable O&M costs [36], we assume electricity generation and regulation reserve provision

costs of storage equal $2/MWh [37]. To model initial large-scale storage deployment in ERCOT, we add 500 MW of storage to the fleet optimized in the CE model regardless of the market in which storage participates. This storage capacity equals less than 1% of our 2015 generator fleet and 40% of the 2020 California storage mandate [38], although we also parametrically model 1.5 GW of storage as detailed below. Based on real-world storage applications, we parametrize storage as a pumped hydropower facility when participating only in the energy market [8] and as a lithium ion facility when participating in only reserve or energy and reserve markets [39] (Table 4.2).

Table 4.2: Storage parameters given the market in which it participates, and which storage technology each set of parameters is based on given real-world applications of each technology [8], [39], [40]. Across markets in which storage participates, we set storage capacity to 500 MW and storage efficiency to 81%.

Market(s) Storage Participates In	Energy Capacity (MWh)	Max Ramp Rate (MW/ minute)	Represented Storage Technology
Only Energy	4,000	8.3	Pumped hydropower
Only Reserves	2,000	500	Lithium ion battery
Energy and Reserves	2,000	500	Lithium ion battery

4.3.4 Scenarios

We assess moderate and strong power system decarbonization targets of 50% and 70% below 2015 levels by 2050, respectively. To ensure annual CO_2 emission caps bind emissions each year, we estimate 2015 CO_2 emissions from electricity generation in ERCOT as 175 million tons by running our UCED model with our 2015 fleet and no shadow CO_2 price. The moderate (50%) decarbonization target roughly aligns with targets set by the U.S. Clean Power Plan (CPP) [41] extrapolated through 2050 and applied to our baseline emissions of 175 million tons,

although the Trump administration moved to repeal the CPP in late 2017 [42]. Notably, even without the CPP, preliminary analysis suggests U.S. power sector emissions may meet CPP targets [43].

To test the sensitivity of our results to the type of decarbonization policy, we also consider two scenarios in which we enforce each decarbonization target in the CE but not UCED model. These scenarios approximate decarbonizing only through changes to fleet composition, e.g. with a Clean Energy Standard. To test the sensitivity of our results to key storage and fleet parameters under each decarbonization target, we also consider scenarios with early coal-fired generator retirements (at 45 rather than 65 years old), low natural gas prices (3.1-3.8 $\$_{2012}$/MMBtu rather than 3.2-5.2 $\$_{2012}$/MMBtu from 2020-2045), and high storage capacity (1.5 GW) and storage efficiency (90%) (Appendix C).

4.4 RESULTS

4.4.1 Annual Generation and Reserve Provision by Fuel Type without Storage

Figure 4.1 provides annual generation by fuel type output by our UCED model without storage across years and decarbonization targets. Our 2015 generation mix largely agrees with the observed 2015 generation mix in ERCOT of 48% NGCC, 28% coal, 11% nuclear, and 11% wind [44]. Coal-fired generation increases in 2025 under the moderate decarbonization target due to rising natural gas prices and a weak CO_2 emission limit. Otherwise, as CO_2 emission limits tighten, wind, solar, and NGCC generation gradually displace coal-fired generation. Without storage in the fleet, NGCC generators provide more than 80% of each reserve type across years and decarbonization targets, while coal-fired generators provide most of the

remainder (Appendix C). Through 2045, reserve provision by NGCC generators partially or fully displaces that by coal-fired generators, depending on the reserve type and decarbonization target.

In the scenarios without storage, tightening annual CO_2 emission limits drive changes in electricity generation and reserve provision through changes in fleet composition and operations. Fleet capacity increases from 93 GW in 2015 to 100 and 104 GW in 2045 under the moderate and strong decarbonization targets, respectively, as combined wind and solar capacity grows from 14 GW to 32 and 37 GW, respectively, and coal-fired capacity shrinks from 19 GW to 8 and 3 GW, respectively (Appendix C). Shadow CO_2 prices, which capture operational changes in the UCED model, range from \$0-13/ton and \$0-43/ton under the moderate and strong decarbonization targets, respectively, from 2015 to 2045 (Appendix C).

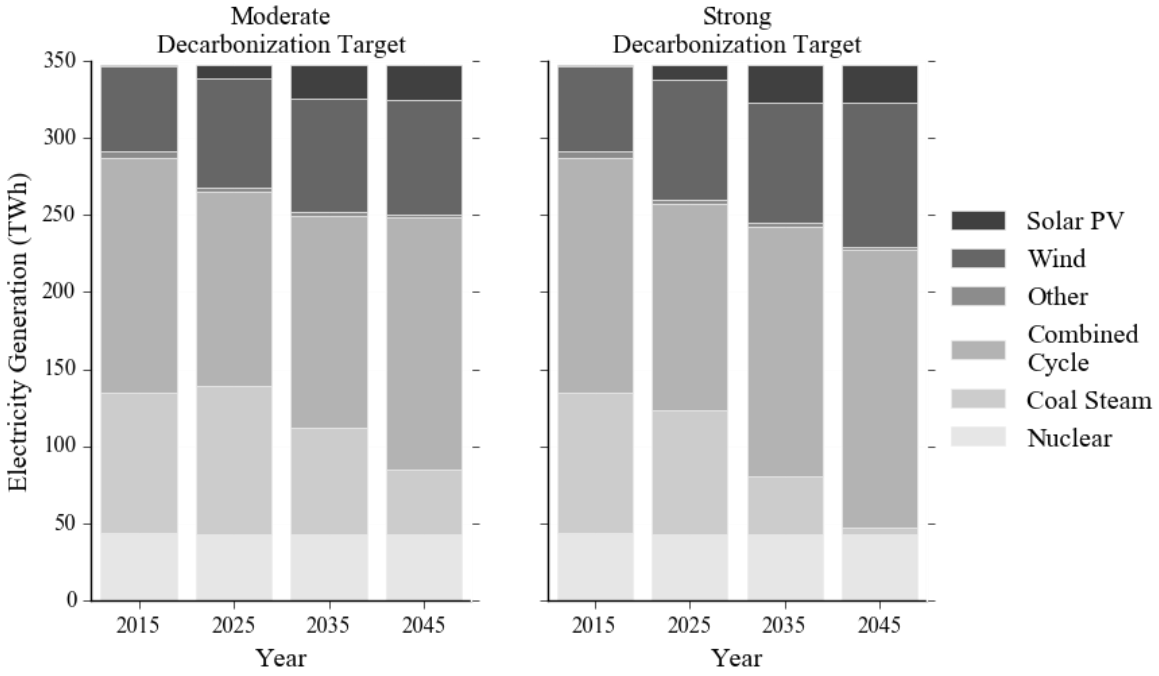

Figure 4.1: Electricity generation by fuel type in each analyzed year under the moderate (left) and strong (right) decarbonization target.

4.4.2 Storage Operations

Across years and decarbonization targets, utilization of storage is significantly less when it participates only in the energy market than when it participates only in reserve markets or in both energy and reserve markets (Figure 4.2). Furthermore, when participating in energy and reserve markets, storage provides 10-40 times more reserves than energy. When providing reserves, storage primarily provides regulation reserves due to its operational flexibility and low offer cost. In fact, storage provides 50-80% of regulation reserve requirements when participating in only reserve or both energy and reserve markets across years and decarbonization targets.

Over time, two shifts in storage operations occur that indicate increasing value of storage for load balancing. First, when participating in energy and reserve markets, storage provides progressively more energy and less reserves through 2045, such that provided energy increases from 2015 to 2045 by 4 and 5 times under the moderate and strong decarbonization targets, respectively (Figure 4.2). Second, when only participating in energy markets, daily peak discharge by storage shifts with daily peak net demand as increasing wind and solar generation shift the latter from late afternoon in 2015 to early evening in 2045 (Figure 4.3). When participating in both energy and reserve markets, peak daily discharge by storage occurs later in the evening than when only participating in energy markets in order to maintain a sufficient charge for reserve provision throughout the day (Figure 4.3). Notably, charging operations also change across years, as storage begins to charge mid-day in 2035 when participating in only energy and in both energy and reserve markets, paralleling growth in solar generation.

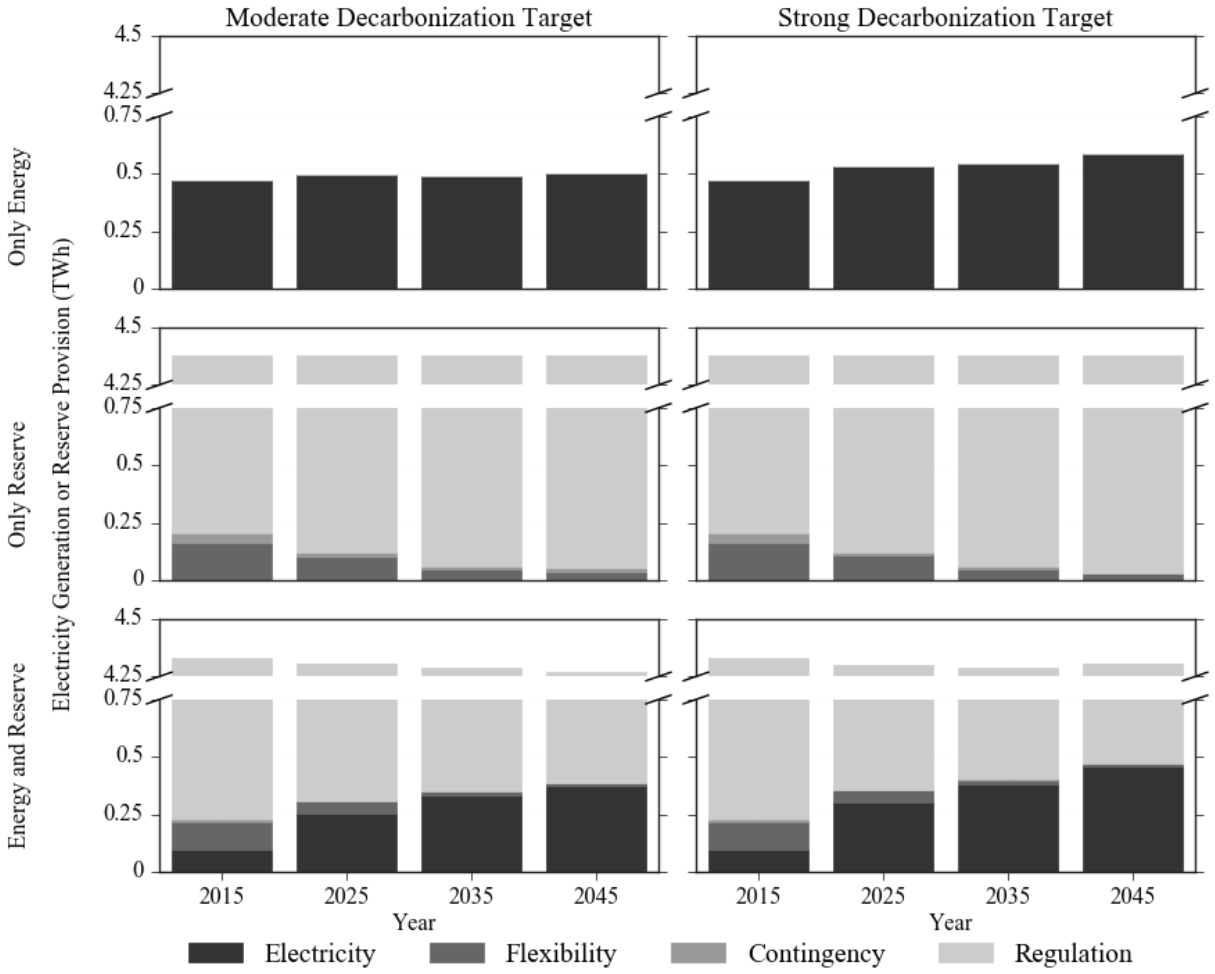

Figure 4.2: Storage electricity generation or flexibility, contingency, or regulation reserve provision under the moderate (left) and strong (right) decarbonization targets when storage participates in only energy (top row), only reserve (middle row), or energy and reserve (bottom row) markets.

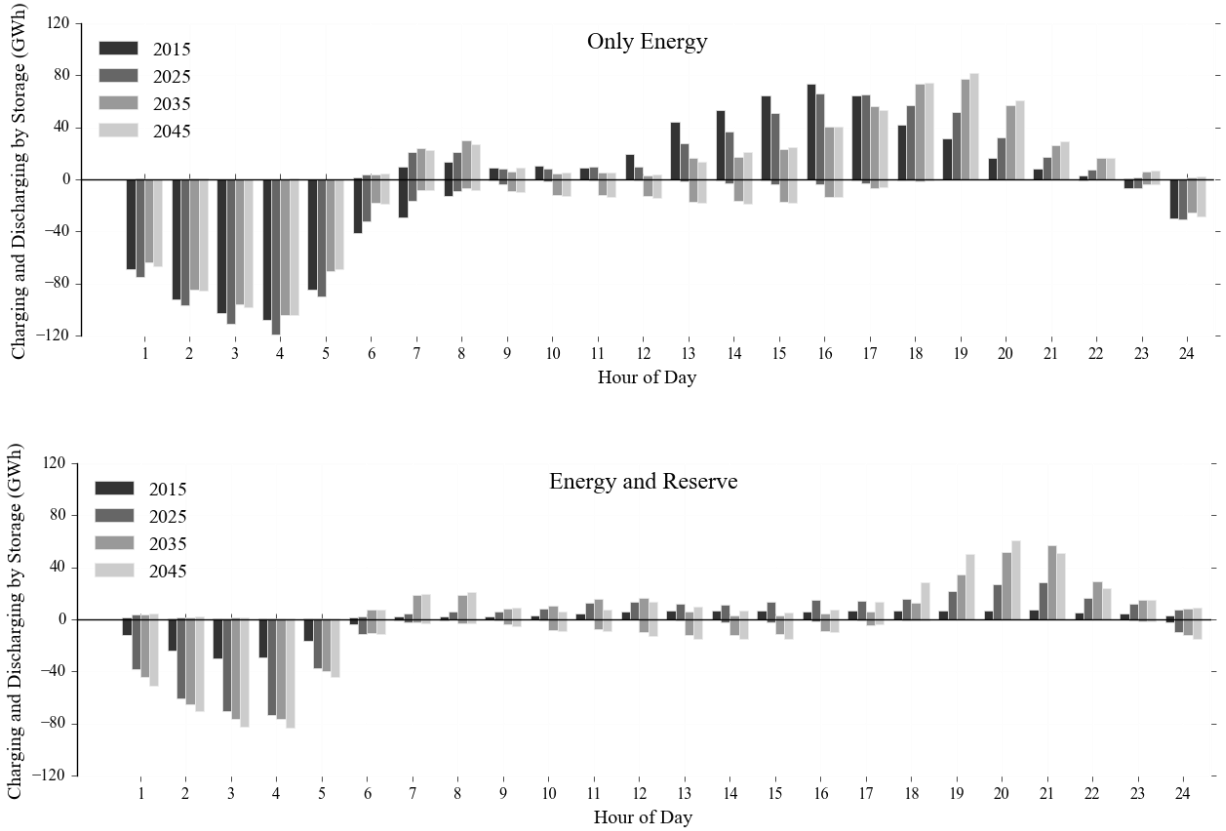

Figure 4.3: Discharging (positive values) and charging (negative values) by storage for each hour of the day summed across all days in each year from 2015 through 2045 under the moderate decarbonization target when only participating in the energy market (top) and when participating in both energy and reserve markets (bottom). Similar results occur under the strong decarbonization target. Note that hours with charging and discharging do not indicate concurrent charging and discharging, but rather that over all days in the year, storage charges in that hour on some days and discharges in that hour on other days.

4.4.3 Effect of Storage on Generation by Fuel Type

Generator-level electricity generation output by our UCED model indicates that storage affects system CO_2 emissions by changing other generators' operations in several ways. When providing energy, charging and discharge storage enables a shift in power output between generators across time. Additionally, when providing reserves, storage offsets reserves from other generators. Consequently, economic generators may increase their generation, whereas uneconomic generators primarily online to provide reserves may turn off.

When participating in only the energy market, storage enables a shift from gas-fired to coal-fired generation in 2015 and 2025 under both decarbonization targets (Figure 4.4), when CO_2 emission limits are weak. In 2035, storage switches to enabling a shift from coal-fired to gas-fired generation under the moderate target and from coal-fired to gas-fired, wind, and solar generation under the strong target. In 2045 under the moderate target, storage enables a shift from coal-fired to gas-fired generation to a greater extent than in 2035. In 2045 under the strong target, though, a tight CO_2 emission limit and the near elimination of coal-fired generation leads storage to enable a switch from inefficient gas-fired to lower-CO_2-emitting gas-fired, wind, and solar generation (Appendix C). Across years, storage reduces wind curtailment under both decarbonization targets and reduces solar curtailment under the strong target. Across years and decarbonization targets, storage reduces wind curtailment by 10-30% and solar curtailment by 0-20% so that wind and solar curtailments are each less than 2% of total wind and solar generation. Reduced curtailments as a result of storage are higher for wind than solar due to wind's higher generation share (Figure 4.1) and the lower correlation of demand with wind (-0.1) than solar (0.4) generation. As wind and solar penetration increase through 2045, storage tends to reduce wind and solar curtailment more.

When participating only in reserve markets, storage enables a shift from gas-fired to coal-fired generation in 2015 under both decarbonization targets (Figure 4.4). Specifically, reserves provided by storage allow economic coal-fired generators to shift from reserve provision to electricity generation. Furthermore, due to higher storage utilization in reserve than energy markets, storage increases coal-fired generation by an order of magnitude more in 2015 when providing reserves instead of energy. In 2025, storage switches to enabling a shift from coal-fired to gas-fired generation under both targets. Due to higher storage utilization in reserve than energy markets, storage increases gas-fired generation significantly more in 2025 and 2035 when providing reserves instead of energy. However, under the moderate target, storage shifting coal-fired to gas-fired generation decreases each year through 2045, such that by 2045, storage has a smaller effect on generation by fuel type when participating in only reserve markets than in only the energy market. This downward trend reflects decreasing reserve provision by coal-fired generators (Appendix C). In 2045 under the strong decarbonization target, storage switches to causing a shift from inefficient gas-fired to lower-CO_2-emitting gas-fired, wind, and solar generation (Appendix C).

When participating in reserve and energy markets, storage has similar but larger effects on generation by fuel type compared to when it participates in only energy or in only reserve markets across most years and decarbonization targets (Figure 4.4). In 2015, storage enables a shift from gas-fired to coal-fired generation, then switches in 2025 to enabling a shift from coal-fired to gas-fired generation. In 2045 under the strong decarbonization target, storage further switches to enabling a shift from inefficient gas-fired to efficient gas-fired, wind, and solar generation (Appendix C). Notably, across years and decarbonization targets, storage also reduces

wind curtailments by 25-50% more and solar curtailments by 0-100% more when participating in energy and reserve markets than in only energy or in only reserve markets.

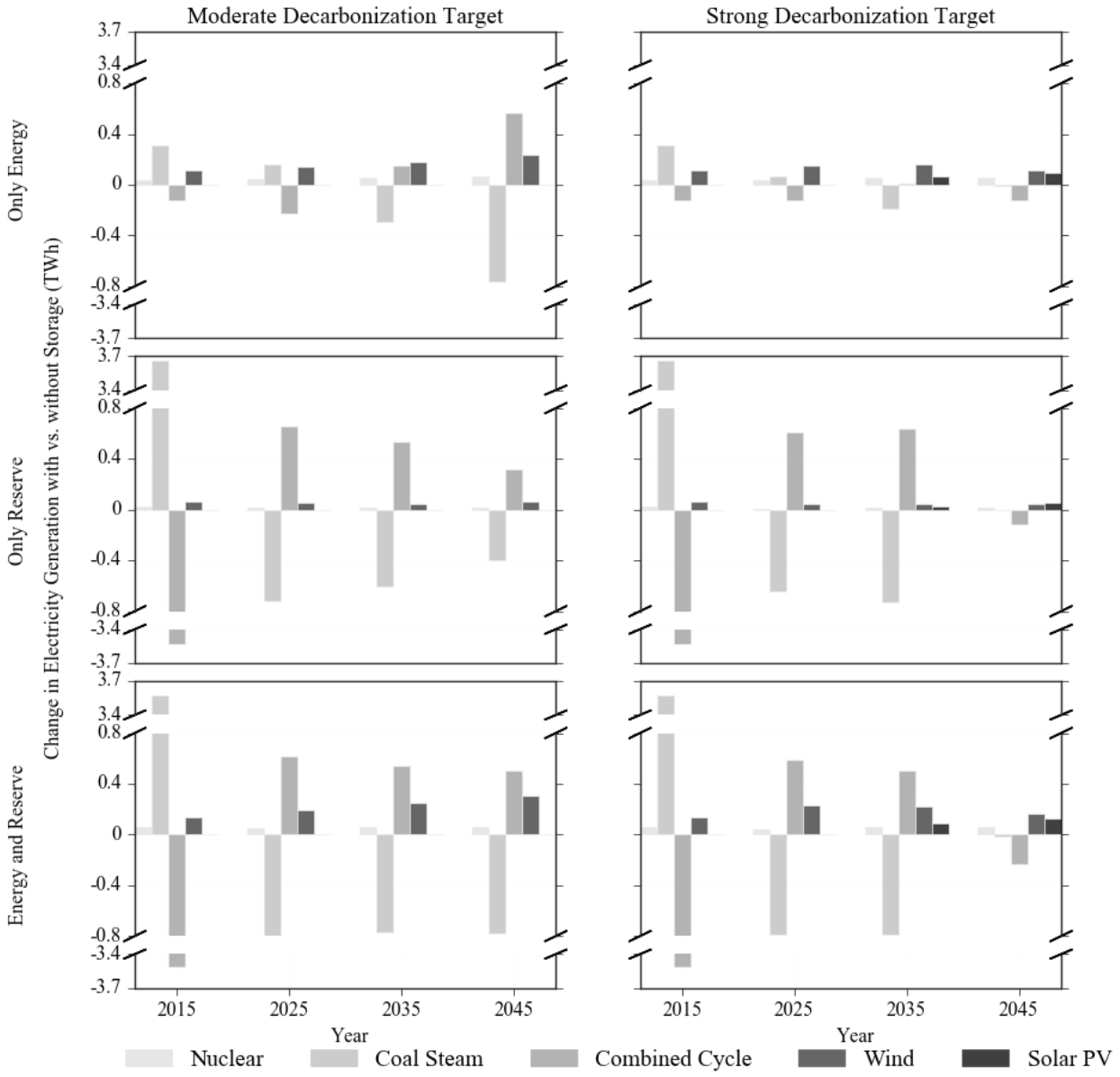

Figure 4.4: Change in generation by fuel type with storage versus without storage under the moderate (left) and strong (right) decarbonization targets when storage participates in only energy (top row), only reserve (middle row), or energy and reserve (bottom row) markets. Positive values indicate storage increases generation.

4.4.4 Change in System CO_2 Emissions

Storage's effect on generation by fuel type as determined by our UCED model largely drives its effect on operational system CO_2 emissions (see Appendix C for equation used to calculate change in CO_2 emissions) (Figure 4.5). Across our analysis, storage only increases CO_2 emissions in 2015, when storage enables a shift from gas-fired to coal-fired generation (Figure 4.4). Furthermore, in 2015, storage increases CO_2 emissions by over an order of magnitude more when participating in only reserve or in both energy and reserve markets than in only the energy market. This result reflects large differences in how much storage increases coal-fired generation in 2015 when participating in different markets (Figure 4.4).

Under the moderate decarbonization target, storage decreases system CO_2 emissions from 2025 through 2045, regardless of the market in which it participates (Figure 4.5). When only participating in the energy market, storage enables progressively greater CO_2 emission reductions through 2045. Conversely, when only participating in reserve markets, storage enables diminishing reductions in CO_2 emissions through 2045. These results parallel trends in how storage reduces coal-fired generation (Figure 4.4). However, from 2025 to 2045 storage achieves the greatest system CO_2 emission reductions when participating in both energy and reserve markets.

Under the strong decarbonization target, storage reduces CO_2 emissions from 2025 through 2045 regardless of the market in which it participates, like under the moderate decarbonization target (Figure 4.5). Furthermore, the effect of storage on CO_2 emissions in 2025 and 2035 is similar in relative and absolute magnitude across markets under both decarbonization targets. Unlike under the moderate target, though, CO_2 emission reductions from storage are lower in 2045 than in 2035, by 75-85%. These diminishing reductions associated

with storage in the strong decarbonization target do not correspond to lower storage utilization (Figure 4.2), but rather to storage switching from enabling a shift from coal-fired to gas-fired, wind, and solar generation to enabling a shift from inefficient gas-fired to lower-CO_2-emitting gas-fired, wind, and solar generation (Figure 4.4, Appendix C).

Changes in CO_2 emissions due to storage when participating in only reserve or in both energy and reserve markets shown in Figure 4.5 only account for commitment of reserves, but dispatching of reserves provided by storage could incur additional CO_2 emissions. As detailed in Appendix C, we conduct a first-order analysis of emissions associated with the dispatch of regulation reserves provided by storage. From 2025 to 2045 under both decarbonization targets, these emissions would negate 6-51% of CO_2 emission reductions due to storage when participating in only reserve or in both energy and reserve markets.

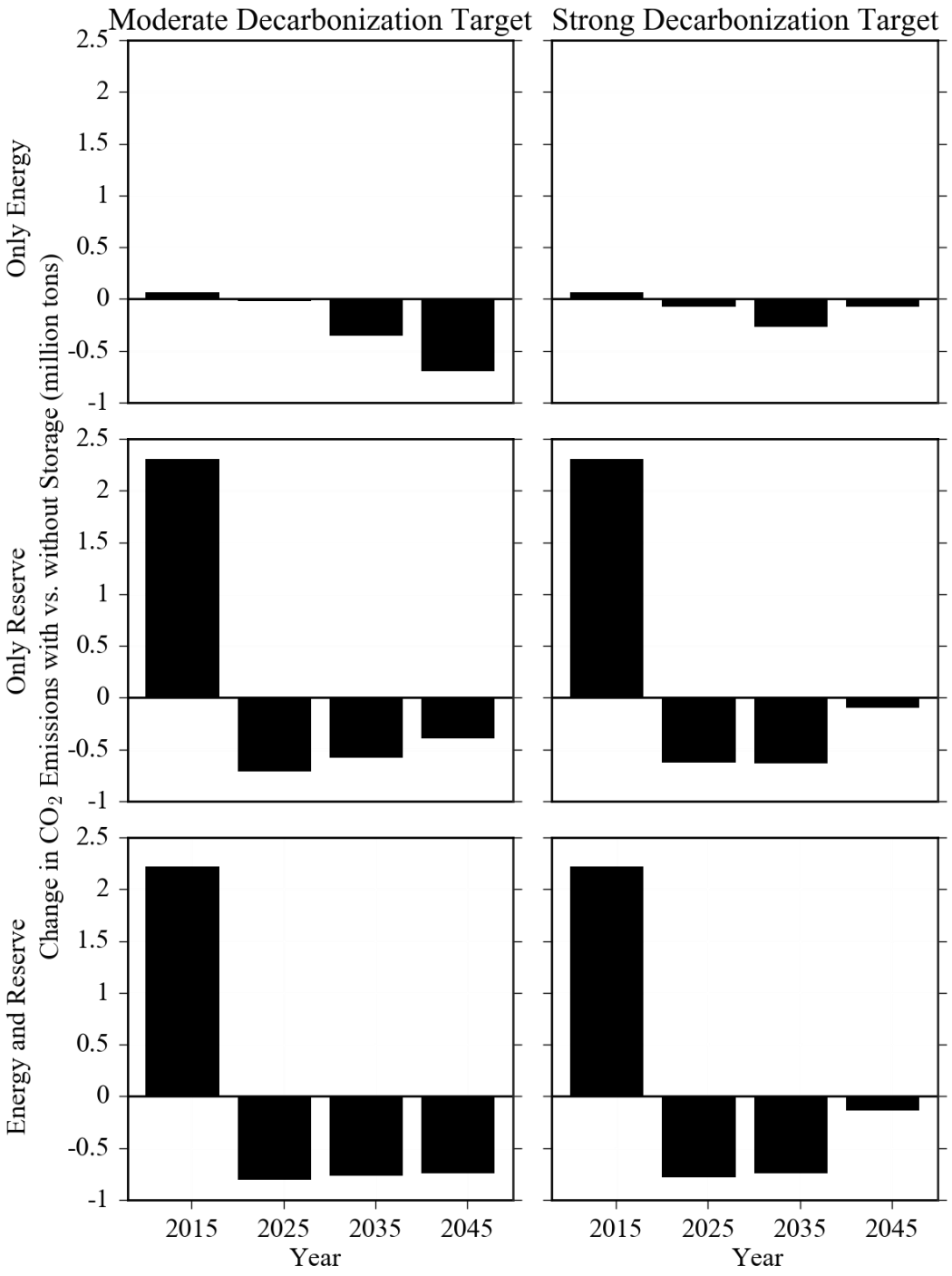

Figure 4.5: Change in system CO_2 emissions with storage versus without storage under the moderate (left) and strong (right) decarbonization targets when storage participates in only energy (top row), only reserve (middle row), or energy and reserve (bottom row) markets. Positive values indicate storage increases CO_2 emissions.

4.4.5 Sensitivity Analysis

To test the robustness of our results, we conduct several sensitivity analyses under the moderate and strong decarbonization targets (Appendix C). When we include CO_2 emission limits in our CE model but do not include shadow CO_2 prices in our UCED model, storage increases CO_2 emissions through 2035 under both decarbonization targets and in 2045 under the moderate decarbonization target regardless of the market in which it participates. In these instances, although NGCC and renewable capacity supplant some coal-fired capacity over time, storage primarily enables a shift from gas-fired to cheaper coal-fired generation. While storage also reduces wind and solar curtailment, consequent emission reductions are less than emissions from greater coal-fired generation. Conversely, in 2045 under the strong decarbonization target, storage reduces CO_2 emissions with no shadow CO_2 price across markets in which it participates, as storage primarily enables a shift from gas-fired to wind and solar generation. Notably, in that year coal-fired generation is nearly eliminated and wind and solar generation account for a third of total electricity (Figure 4.1), roughly indicating the fleet mix at which storage would begin to reduce emissions when decarbonizing only via fleet composition changes.

Under both decarbonization targets, tripling storage capacity from 0.5 to 1.5 GW amplifies the effect of storage on CO_2 emissions. For example, under the moderate decarbonization target, 1.5 GW of storage increases CO_2 emissions 1-4 times more in 2015 and decreases CO_2 emissions 2-4 times more in 2025 through 2045 than 0.5 GW of storage. While these emission reductions account for less than 2% of total system emissions, increasing reductions with increasing storage capacity demonstrated here indicate further potential for emission reductions with even greater storage capacities, a potential topic for future research. At a higher capacity, storage provides more energy and reserves, which enables larger changes in

generation by fuel type in each year. Increasing storage efficiency from 81% to 90% does not significantly change how storage affects system CO_2 emissions.

Under both decarbonization targets, low natural gas prices also do not significantly change our results, as adding storage to the generator fleet reduces CO_2 emissions from 2025 through 2045. Across years, decarbonization targets, and which market storage participates in, these emission reductions are greater than, equal to, or less than those achieved by storage under the base scenarios. Under both decarbonization targets and low natural gas prices, gas-fired capacity, including with CCS under the strong decarbonization target, increases through 2045 and fully displaces coal-fired capacity in 2045. Consequently, through 2035 storage reduces CO_2 emissions primarily by enabling a shift from coal-fired to gas-fired and wind generation, and in 2045 reduces emissions primarily by enabling a shift from higher-CO_2-emitting gas-fired to CCS-equipped gas-fired and wind generation. Although we do not test high (greater than $5.2/MMBtu) natural gas prices, reversing the differences observed at low versus moderate natural gas prices provides some indication of expected outcomes at high gas prices. Specifically, less gas-fired generation would occur at high gas prices than in the base scenarios, likely resulting in greater coal-fired (and renewable) generation in later years. Consequently, storage may achieve greater emission reductions at high gas prices than in the base scenarios.

In the early coal-fired generator retirements scenarios, storage leads to smaller CO_2 emission reductions than in the base scenarios under both decarbonization targets. Early coal-fired retirements rapidly decrease coal-fired capacity and generation. Under the moderate decarbonization target, adding storage to the generator fleet increases coal-fired generation from remaining coal plants without exceeding the CO_2 emission limit through 2045. Consequently, under the moderate target, storage either increases CO_2 emissions or reduces them significantly

less than in the base scenario through 2045. Conversely, under the strong decarbonization target, storage reduces coal-fired generation from remaining coal plants due to the strong CO_2 emission limits through 2045, like in the base scenario. Consequently, under the strong target, storage reduces CO_2 emissions, albeit often by less than in the base scenario, through 2045.

4.5 DISCUSSION

To better understand how storage affects operational system CO_2 emissions as a power system decarbonizes, we quantified how storage affects CO_2 emissions from 2015 through 2045 under CO_2 emission reduction targets of 50% and 70% below 2015 levels by 2050. Like prior studies [8], [9], we found that storage would increase CO_2 emissions in the 2015 ERCOT system. However, under both decarbonization targets, we found that storage would reduce CO_2 emissions within 10-20 years, well before deep decarbonization. Storage achieves these emission reductions by enabling a shift from coal-fired to gas-fired generation and, to a lesser extent, by reducing wind curtailment. Furthermore, we found that storage achieved greater emission reductions in systems with significant coal-fired capacity than in systems where gas-fired, wind, and solar capacity had nearly eliminated coal-fired capacity. Thus, storage can further decarbonization efforts not only in deeply decarbonized systems with high renewable penetrations, but also in moderately decarbonized power systems with high coal-fired capacity and relatively low renewable penetrations.

Given that storage units will participate in reserve markets rather than or in addition to the energy market, we also compared how storage affects CO_2 emissions while participating in only energy, only reserve, or energy and reserve markets. We found that the market in which storage participates can significantly change the magnitude, but not the direction, of the effect of

storage on system CO_2 emissions. Across years and decarbonization targets, storage reduces CO_2 emissions the most when participating in both energy and reserve markets.

Via sensitivity analysis, we found that decarbonizing only through fleet composition (and not operational) changes flipped storage from a net-negative to net-positive CO_2 emission technology except when coal-fired generation was nearly eliminated and wind and solar generated a third of total electricity. Thus, storage may have significantly different effects on CO_2 emissions in systems with decarbonization policies that affect system composition and operation, e.g. a carbon tax, versus only system composition, e.g. a Clean Energy Standard. We also found that early coal-fired generator retirements, by reducing CO_2 emissions and consequently the implicit cost of CO_2 emissions under an emission limit, could reduce or negate the emission benefits of storage, although storage applications in other contexts, e.g. co-located with wind farms, may still yield emission benefits. Conversely, our results were robust to higher storage capacity and efficiency and lower natural gas prices.

Our analysis has several limitations that could be addressed in future work. First, we do not optimize for storage deployment in our CE model, which would likely increase wind and solar deployment [3], [7]. Higher renewable penetrations would likely cause storage to reduce renewable curtailment and emissions more. However, it would also reduce the implicit CO_2 emission cost under the cap and, consequently, potentially reduce the shift from coal- to gas-fired generation enabled by storage. Thus, the net effect of optimizing storage deployment in our CE model on how storage affects operational system CO_2 emissions is uncertain. Future research could address this question by translating by translating constraints on storage operations from our UCED model to CE model, although subsequent CE model simplifications may be necessary for computational tractability.

Second, we estimate storage energy losses and emissions associated with dispatching of reserves after rather than within the UCED model, which could lead to overestimation of reserves provided by storage. Third, by dispatching generators at an hourly resolution, we may underestimate renewable energy curtailment and renewable integration benefits of storage. Fourth, transmission constraints, which we ignore here, could drive spatial heterogeneity in the effects of storage on system CO_2 emissions. Fifth, we do not consider load growth through 2045 here, deferring that to future analysis. Meeting growing demand while imposing the same decarbonization targets would require greater deployment of renewables, CCS, and/or nuclear, which could alter how storage affects generation by fuel type and, in turn, emissions. In particular, storage would likely provide greater curtailment benefits at higher renewable penetrations, and could even reduce curtailment of relatively-inflexible CCS and nuclear generators if deployed at high capacities.

Finally, considering system operational costs in addition to emissions associated with storage could highlight win-wins or trade-offs between the two and further inform policymaking. For instance, in the near-term, our analysis indicates that using storage to provide energy leads to a smaller increase in emissions compared to using storage only for reserves or for energy and reserves. If storage used only for energy also leads to lower costs, then given a storage deployment mandate, policies encouraging storage to participate in energy rather than reserve markets could yield best possible cost and emission outcomes.

4.6 CONCLUSION

Our results indicate that policies promoting storage can yield operational CO_2 emission reductions in the mid-term if comprehensive decarbonization policies, like a carbon tax, exist.

Furthermore, policies can significantly change how storage affects CO_2 emissions by encouraging participation in energy and/or reserve markets. Thus, storage can play a significant role in decarbonization efforts in the mid- and long-term, but storage-specific and decarbonization policies play a key role in determining whether and to what extent this occurs.

4.7 REFERENCES

[1] R. W. Fri, M. A. Brown, D. Arent, A. Carlson, M. Carter, L. Clarke, F. de la Chesnaye, G. C. Eads, G. Giuliano, A. Hoffman, R. O. Keohane, L. Lutzenhiser, B. McCarl, M. McFarland, M. D. Nichols, E. S. Rubin, T. H. Tietenberg, J. A. Trainham, L. Geller, A. Crane, T. Menzies, K. Weller, and S. Freeland, "Limiting the Magnitude of Future Climate Change," 2010.

[2] A. Mileva, J. Johnston, J. H. Nelson, and D. M. Kammen, "Power system balancing for deep decarbonization of the electricity sector," *Appl. Energy*, vol. 162, pp. 1001–1009, 2016.

[3] F. J. De Sisternes, J. D. Jenkins, and A. Botterud, "The value of energy storage in decarbonizing the electricity sector," *Appl. Energy*, vol. 175, pp. 368–379, 2016.

[4] P. Denholm and M. Hand, "Grid flexibility and storage required to achieve very high penetration of variable renewable electricity," *Energy Policy*, vol. 39, no. 3, pp. 1817–1830, 2011.

[5] Deep Decarbonization Pathways Project, "Pathways to Deep Decarbonization," 2015.

[6] T. Das, V. Krishnan, and J. D. Mccalley, "Assessing the benefits and economics of bulk energy storage technologies in the power grid," *Appl. Energy*, vol. 139, pp. 104–118, 2015.

[7] J. Linn and J. Shih, "Does electricity storage innovation reduce greenhouse gas emissions?," *Resources for the Future*, 2016. [Online]. Available: http://www.rff.org/research/publications/does-electricity-storage-innovation-reduce-greenhouse-gas-emissions.

[8] E. S. Hittinger and I. M. L. Azevedo, "Bulk energy storage increases United States electricity system emissions," *Environ. Sci. Technol.*, vol. 49, pp. 3203–3210, 2015.

[9] R. T. Carson and K. Novan, "The private and social economics of bulk electricity storage," *J. Environ. Econ. Manage.*, vol. 66, no. 3, pp. 404–423, 2013.

[10] M. J. Fisher and J. Apt, "Emissions and economics of behind-the-meter electricity storage," *Environ. Sci. Technol.*, vol. 51, no. 3, pp. 1094–1101, 2017.

[11] K. Siler-Evans, I. L. Azevedo, and M. G. Morgan, "Marginal emissions factors for the U.S. electricity system," *Environ. Sci. Technol.*, vol. 46, no. 9, pp. 4742–4748, 2012.

[12] A. Tuohy and M. O'Malley, "Impact of pumped storage on power systems with increasing wind penetration," in *Power & Energy Society General Meeting*, 2009.

[13] M. Arbabzadeh, J. X. Johnson, G. A. Keoleian, P. G. Rasmussen, and L. T. Thompson, "Twelve principles for green energy storage in grid applications," *Environ. Sci. Technol.*, vol. 50, pp. 1046–1055, 2016.

[14] P. Denholm, J. Jorgenson, T. Jenkin, D. Palchak, B. Kirby, M. O. Malley, P. Denholm, J. Jorgenson, T. Jenkin, D. Palchak, B. Kirby, O. Ma, and M. O'Malley, "The value of energy storage for grid applications," *U.S. National Renewable Energy Laboratory*, 2013. .

[15] GTMResearch, "U.S. Energy Storage Monitor: Q4 2016 Executive Summary," 2016.

[16] D. Lew, G. Brinkman, E. Ibanez, A. Florita, M. Heaney, B. Hodge, M. Hummon, and J. King, "The Western Wind and Solar Integration Study Phase 2," *U.S. National Renewable Energy Laboratory*, 2013. .

[17] Y. Lin, J. X. Johnson, and J. L. Mathieu, "Emissions impacts of using energy storage for power system reserves," *Appl. Energy*, vol. 168, no. 784, pp. 444–456, 2016.

[18] R. Sioshansi and P. Denholm, "Emissions impacts and benefits of plug-in hybrid electric vehicles and vehicle-to-grid services," *Environ. Sci. Technol.*, vol. 43, no. 4, pp. 1199–204, Feb. 2009.

[19] GAMS Development Corporation, "The GAMS Development Corporation Website," 2013. [Online]. Available: http://www.gams.com/.

[20] IBM, "IBM ILOG CPLEX Optimization Studio: CPLEX User's Manual. Version 12 Release 6.," 2014.

[21] U.S. National Renewable Energy Laboratory, "Renewable resource data center," *NREL.gov*, 2016. [Online]. Available: http://www.nrel.gov/rredc/. [Accessed: 14-Feb-2017].

[22] ERCOT, "Report on the capacity, demand, and reserves (CDR) in the ERCOT region, 2017-2026," 2016. [Online]. Available: http://www.ercot.com/content/wcm/lists/96607/CapacityDemandandReserveReport_May2016.pdf.

[23] U.S. Environmental Protection Agency, "National Electric Energy Data System (Version 5.15)." 2015.

[24] U.S. Energy Information Administration, "Annual Energy Outlook 2016," 2016.

[25] U.S. Energy Information Administration, "Annual Energy Outlook 2015," 2015.

[26] U.S. Environmental Protection Agency, "Documentation for EPA Base Case v.5.13 Using the Integrated Planning Model," 2013.

[27] ERCOT, "Report on existing and potential electric system constraints and needs," 2015. [Online]. Available: http://www.ercot.com/content/news/presentations/2016/2015ERCOTConstraintsAndNeed

sReport.pdf.

[28] M. Craig, P. Jaramillo, H. Zhai, and K. Klima, “The economic merits of flexible carbon capture and sequestration as a compliance strategy with the Clean Power Plan,” *Environ. Sci. Technol.*, vol. 51, pp. 1102–1109, 2017.

[29] U.S. National Renewable Energy Laboratory, “Transmission Grid Integration: Eastern Wind Dataset,” 2012.

[30] U.S. National Renewable Energy Laboratory, “Transmission Grid Integration: Solar Power Data for Integration Studies Dataset,” 2010.

[31] P. Peterson, M. Whited, and S. Fields, “Demonstrating resource adequacy in ERCOT,” *Synapse Energy Economics, Inc.*, 2014. [Online]. Available: http://www.synapse-energy.com/sites/default/files/SynapseReport.2014-02.SC_.ERCOT-Resource-Adequacy.13-122.pdf.

[32] ERCOT, “2015 ERCOT hourly load data,” 2016. [Online]. Available: http://www.ercot.com/gridinfo/load/load_hist/.

[33] W. Short, P. Sullivan, T. Mai, M. Mowers, C. Uriarte, N. Blair, D. Heimiller, and A. Martinez, “Regional energy deployment system (ReEDS),” *U.S. National Renewable Energy Laboratory*, 2011. .

[34] PJM, “PJM Manual 15: Cost Development Guidelines,” 2016.

[35] ERCOT, “Historical DAM clearing prices for capacity,” 2015. [Online]. Available: http://www.ercot.com/mktinfo/prices. [Accessed: 07-Apr-2017].

[36] G. He, Q. Chen, C. Kang, P. Pinson, and Q. Xia, “Optimal bidding strategy of battery storage in power markets considering performance-based regulation and battery cycle life,” *IEEE Trans. Smart Grid*, vol. 7, no. 5, pp. 2359–2367, 2016.

[37] Lazard, “Lazard’s Levelized Cost of Storage - Version 2.0,” 2016.

[38] California Public Utilities Commission, “Decision approving San Diego Gas & Electric Company, Pacific Gas and Electric Company, and Southern California Edison Company’s storage procurement framework and program applications for the 2014 biennial procurement period (Decision 14-10-045),” 2014.

[39] T. Randall, “Tesla’s battery revolution just reached critical mass,” *Bloomberg Technology*, 30-Jan-2017.

[40] J. I. San Martin, I. Zamora, J. J. San Martín, V. Aperribay, and P. Eguía, “Energy storage technologies for electric applications,” *Int. Conf. Renew. Energies Power Qual.*, vol. 1, no. 2, pp. 1–6, 2013.

[41] U.S. Environmental Protection Agency, “Carbon pollution emission guidelines for existing stationary sources: Electric utility generating units. Federal Register Vol. 80: 64661-65120,” 2015.

[42] U.S. Environmental Protection Agency, “Repeal of carbon pollution emission guidelines for existing stationary sources: Electric utility generating Units. Federal Register Vol. 82:

48035-48049," 2017.

[43] J. Larsen and W. Herndon, "What the CPP would have done," *Rhodium Group*, 2017. [Online]. Available: http://rhg.com/notes/what-the-cpp-would-have-done. [Accessed: 05-Dec-2017].

[44] ERCOT, "Energy by Fuel Type 2002-2015," 2016. [Online]. Available: http://www.ercot.com/news/presentations.

CHAPTER 5: A RETROSPECTIVE ANALYSIS OF THE MARKET PRICE RESPONSE TO DISTRIBUTED PHOTOVOLTAIC GENERATION IN CALIFORNIA

5.1 ABSTRACT

In response to rapid growth of distributed solar photovoltaic (PV) capacity in the U.S., numerous "value of solar" studies have attempted to quantify avoided costs associated with distributed PV. One such avoided cost that has received little attention is the market price response, or how distributed PV generation reduces utilities' procurement costs and, consequently, consumers' costs through reduced wholesale electricity prices in the short-term. Here, we quantify the reduction in day-ahead wholesale electricity prices to distributed PV generation in California (CA) from 2013 through 2015. Using a database of all distributed PV systems in the three CA investor owned utilities, we estimate historic hourly distributed PV generation using three methods that we validate with metered generation from 205 PV systems. Via multiple linear regression, we then estimate electricity price reductions due to distributed PV generation. Across the three methods used to estimate PV generation, we find that distributed PV generation reduced hourly median (mean) wholesale electricity prices by up to \$2.7-3.1/MWh (\$2.9-3.2/MWh) ($\$_{2015}$), or by 7-8% (8-9%). Lower wholesale prices, in turn, reduced utilities' energy procurement costs in the day-ahead market by up to \$650-730 million ($\$_{2015}$) from 2013 through 2015. These avoided costs are similar to other avoided costs commonly included in value of solar studies.

This paper is being prepared for submission with co-authors Paulina Jaramillo, Bri-Mathias Hodge, Nathan Williams, and Edson Severnini.

5.2 INTRODUCTION

Installed solar photovoltaic (PV) capacity has grown rapidly in recent years, increasing from 2.5 to 21.7 GW in the U.S. from 2010 to 2015 [1], [2] and from 10 to 230 GW globally over the same period [3]. In the U.S., numerous factors have driven this growth, including falling PV panel and balance-of-system costs [4] and policy support such as deployment mandates and financial incentives [5], [6]. Forecasts project continued rapid growth in installed PV capacity in the U.S. [7] and globally [8].

PV projects can be broadly categorized as utility-scale or distributed PV. Utility-scale PV typically connects to the transmission grid, while distributed PV, also known as behind-the-meter or rooftop solar, generates electricity to be consumed on-site by industrial, commercial, or residential facilities. In the U.S., utility-scale PV capacities typically range from 1-20 MW [9], whereas residential distributed PV capacities typically range from 2-10 kW [10]. As of 2015, distributed PV accounted for 45% of installed PV capacity in the U.S. [1].

Rapid growth of distributed PV has led to questions regarding its costs and benefits. In response, numerous "value of solar" studies have attempted to quantify incurred and avoided system costs associated with distributed PV generation in order to determine how to compensate distributed PV generation [11]–[13]. While avoided and incurred costs included in these studies vary widely [11], [12], avoided costs can include avoided power system costs, such as through deferred or reduced grid infrastructure investment, reduced system losses, and avoided generation [11], [12], [14]; avoided environmental and health costs due to reduced global and local air emissions [11], [15], [16]; and social and reliability benefits [11], [12]. Incurred costs can include grid integration costs, such as grid infrastructure upgrades and higher ancillary

service requirements, and subsidies [11], [12]. Avoided and incurred costs of distributed PV vary significantly by location, PV penetration, and other variables [15], [17], [18].

This paper focuses on one avoided cost associated with distributed PV that has received less attention than other benefits [11], [12], namely the market price response to distributed PV generation, or how distributed PV generation suppresses wholesale electricity prices in the short-term. Since electricity generated by distributed PV partially or fully meets on-site electricity demand, distributed PV reduces net electricity demand. In the near-term, given a static supply curve, reduced demand eliminates the need for marginal, high cost generation, thus suppressing wholesale electricity prices [19]. Lower wholesale prices, in turn, reduce utility expenditures in wholesale markets, which should ultimately reduce consumers' costs through lower retail rates.

Notably, short-term reductions in electricity prices due to distributed PV generation may alter generator retirements and investments, which can affect electricity prices in the long-term. Additionally, revenues originally obtained by producers in wholesale energy markets may instead move to capacity markets or similar mechanisms [20]. Such long-term effects may reduce (or eliminate) short-term avoided costs due to reduced wholesale electricity prices. To understand the extent of short-term price effects and potential long-term market shifts due to distributed PV, here we quantify short-term price reductions and avoided costs, deferring long-term analyses to future work.

Numerous studies have examined how renewables affect wholesale electricity prices [19], [21]–[27], but most have focused on utility-scale renewables or have not differentiated between utility-scale and distributed facilities. Studies on wholesale price, or "merit-order", effects of utility-scale renewables fall into two groups. One group conducts retrospective or *ex-post* analyses using empirical data [22]–[25]. Due to the rapid deployment of renewables in

response to feed-in tariffs and other policies, most studies in this group have focused on European nations [23]–[25]. Conversely, Woo et al. [22] focused on California. Using multiple linear regression, they found that each hourly GWh increase in utility-scale solar and wind generation decreased day-ahead locational marginal prices by $2-5/MWh and $1-3/MWh, respectively, from 2013 through 2015. The second group of studies assesses merit-order effects of utility-scale renewables with dispatch models or simulation [19], [26], [27]. Bode and Groscurth [26], for instance, used a simplified dispatch model to estimate how parametrically increasing capacities of PV would depress future electricity prices relative to no additional PV. Similar analyses have also been conducted on energy efficiency, where wholesale price effects are called "demand reduction induced price effects" [28], [29].

Unlike the above studies, McConnell et al. [30] conducted a retrospective analysis focused on the market price response to distributed PV in Australia. The authors estimated electricity generation by a representative PV system in four state capitals with historic meteorological and solar irradiance data, then scaled generation from those four PV systems to estimate generation by an assumed 1 to 5 GW of installed PV. By coupling these generation estimates with a dispatch model, they found that distributed PV would reduce wholesale electricity prices throughout the year but particularly in the summer, yielding total cost savings of $310-970 million and $150-550 million ($_{2015}$) in 2009 and 2010, respectively, with 1-5 GW of distributed PV. Notably, by estimating generation by a single representative system in only four locations, McConnell et al. ignored heterogeneity among distributed PV systems' orientations and locations. Additionally, rather than using historic PV capacity and market data, McConnell et al. simulated the effects of parametrically increasing distributed PV capacities.

In this paper, we quantify the market price response to distributed PV generation in California from 2013 through 2015. As of 2015, California installed 7.3 GW of utility-scale thermal and PV capacity [31] and 3.4 GW of distributed PV capacity (Table 5.1). Using a database of all distributed PV systems (439,010) in the three California investor owned utilities (IOUs), namely Pacific Gas and Electric (PGE), Southern California Edison (SCE), and San Diego Gas and Electric (SDGE), we estimate historic hourly generation by each distributed PV system while accounting for heterogeneity in PV system orientation and location. Using historic price data and multiple linear regression, we then estimate how distributed PV generation reduced wholesale electricity prices in the day-ahead market. We also test the sensitivity of our results to PV efficiency degradation and high inverter loading ratios.

5.3 METHODS

5.3.1 Estimating Distributed PV Generation

From the Net Energy Metering ("NEM") dataset, we obtain system information, including zip code, capacity, orientation, and interconnection date, for all commercial, residential, and industrial distributed PV systems in PGE, SCE, and SDGE approved for interconnection as of 2016 [10] (see Table 5.1 for summary statistics and Appendix D.1 for histograms of PV system orientations). Since we lack metered generation, we estimate hourly electricity generation by each PV system in the NEM dataset from 2013 through 2015. To do so, we validate four methods (summarized in Table 5.2) with metered generation from 205 distributed PV systems, then apply the three most accurate methods to estimate generation by all distributed PV systems. In so doing, we hedge against biases of any single method. Across methods, we assume PV systems begin generating electricity on their interconnection approval

date. Given that 99.5% of PV systems with tracking data in the NEM dataset are fixed array systems, we also assume all PV systems are fixed array systems.

Table 5.1: Summary statistics for distributed PV systems in the NEM and CSI datasets interconnected through 2015, the end of our period of analysis.

Summary Statistic	**Value in NEM Dataset**	**Value in CSI Dataset**
Total number of PV systems	439,010	492
Total capacity of PV systems [MW]	3,434	3
Average PV system capacity [kW]	8	5.9
Median interconnection date	Apr. 9, 2014	Sep. 3, 2008
Average nominal efficiency of 10 most common panels [%]	16.6	15.8
Percent of PV systems with tracking data that are fixed array [%]	99.7	94
Minimum / average / maximum azimuth [degrees]	0 / 174 / 360	0 / 191 / 355
Minimum / average / maximum tilt [degrees]	0 / 18 / 90	0 / 21 / 75
Number of PV systems in PGE / SCE / SDGE	211,026 / 156,423 / 71,561	201 / 188 / 103
Total capacity of PV systems in PGE / SCE / SDGE [MW]	1,772 / 1,210 / 451	1.4 / 0.9 / 0.6

Table 5.2: Summary of methods we use to estimate distributed PV generation. Based on our validation of each method, we use all but the specific configuration method to estimate generation by all distributed PV systems.

Method Name	**Method Description**
Scale up	Scale up metered generation from subset of PV systems
Specific configuration	Input location-specific historic solar irradiance and meteorology into a PV system performance model, using each PV system's specific panel and inverter configuration
Generic configuration	Input location-specific historic solar irradiance and meteorology into a PV system performance model, using a generic configuration for all PV systems
Adjusted generic configuration	Modify generation estimates from the generic configuration method using hour-of-day correction factors

5.3.1.1 Method Type 1: Scale-up Metered Generation

In our first method (the scale up method), we estimate hourly generation by distributed PV systems by scaling up 15-minute metered generation from 492 distributed PV systems in PGE, SCE, and SDGE collected through the California Solar Initiative ("CSI") [32] (see Table 5.1 for summary statistics and Appendix D.2 for histograms of system orientations). To maximize metered generation availability, we conduct our analysis through 2015. Given our focus on day-ahead hourly electricity prices, we sum 15-minute to hourly generation. Due to data gaps, each PV system on average lacks 25% of hourly metered generation over our study period (Appendix D.2).

To scale up metered generation from 492 distributed PV systems in the CSI dataset to the 439,010 distributed PV systems in the NEM dataset, we assume nearby distributed PV systems share meteorology and solar irradiance and, consequently, generation profiles. The finest spatial resolution in the NEM and CSI datasets is zip code. As such, using metered generation we calculate average historic hourly capacity factors (CFs) by zip code, then use the nearest zip-code-level CFs to each PV system in the NEM dataset to estimate its historic hourly generation (see Appendix D.3 for flowchart). For roughly 86% of PV systems in the NEM dataset, the nearest zip code with CFs is within 20 km, distances at which hourly solar generation between PV plants is highly correlated [33], [34]. While we do not account for PV system orientation in this method, PV systems in the CSI and NEM datasets have similar distributions of azimuths and tilts (Appendices A.1 and A.2), so this omission should not significantly bias our results. We fill gaps in zip-code-level hourly CFs, which on average account for 8% of hours from 2013 through 2015, with IOU-level average hourly CFs (Appendix D.3).

5.3.1.2 Methods that Input Solar Irradiance and Meteorology into a PV System Performance Model

In our other three methods (the specific configuration, generic configuration, and adjusted generic configuration methods), we estimate hourly generation by each distributed PV system using location-specific historic meteorology and solar irradiance and PVLib [35], a PV system performance model. We obtain hourly meteorology (wind speed and temperature) and solar irradiance (diffuse horizontal, direct normal, and global horizontal irradiance) by zip code from 2013 through 2015 from the National Solar Radiation Database (NSRDB) [36] (see Appendix D.4 for summary statistics). NSRDB meteorology and solar irradiance are based on remote sensing and satellite imagery, respectively, and are provided at hourly and 4x4 km resolution [37]. Given user-input meteorology and solar irradiance, PVLib [35] uses the Sandia PV Array Performance Model to simulate electricity generation by a user-defined PV system model. Each PV system model requires location, orientation, panel, and inverter information.

To set panel and inverter information, we use a different approach in the specific configuration method than in the generic and adjusted generic configuration methods. In the specific configuration method, we use each PV system's given panel and inverter names and numbers. Conversely, in the generic and adjusted generic configuration methods, we use a generic panel and inverter configuration (Table 5.3) and scale this configuration's generation by each system's actual DC capacity divided by the configuration's DC capacity. By scaling generation, we incorporate each PV system's capacity in the NEM dataset. The generic configuration uses a panel with a similar efficiency (16.9%) as common panels in the NEM dataset (Table 5.1) and a standard inverter loading, i.e. DC to AC, ratio of 1.2.

During validation (Section 5.4.1), estimated generation with the generic configuration method exhibits biases relative to metered generation. To correct for those biases, which vary by hour of day and IOU, the adjusted generic configuration method uses hour-of-day- and IOU-specific correction factors (*F*) that equal the median normalized error between IOU-level hourly metered generation and estimated generation during validation, or:

$$F_{hd,IOU} = median\left(\frac{p_{t,IOU}^{Metered} - p_{t,IOU}^{Estimated}}{p_{t,IOU}^{Estimated}}\right) \qquad \forall\ t \in hd \qquad (Equation\ 1)$$

where *t*, *IOU*, and *hd* index hour, IOU, and hour of day, respectively; $p^{Metered}$ = hourly metered generation [kWh]; and $p^{Estimated}$ = hourly estimated generation using the generic configuration method [kWh]. These correction factors indirectly account for variables not captured in our data, such as shading, that could bias the generic configuration method. With these correction factors, we estimate "adjusted" generation ($p^{Adjusted}$) as:

$$p_{t,IOU}^{Adjusted} = p_{t,IOU}^{Estimated} * \left(1 + F_{hd,IOU}\right) \qquad \forall\ t \in hd \qquad (Equation\ 2)$$

Using cross-validation, we demonstrate these correction factors do not result in overfitting (Appendix D.5).

In the specific, generic, and adjusted generic configuration methods, we assume DC generation losses of 4.4% per the Solar Advisor Model [38]. Additionally, we use each PV system's azimuth and tilt when given in the NEM dataset or a randomly sampled azimuth and tilt from the NEM dataset in each PV system's IOU (Appendix D.1) to capture variability in actual PV systems' orientations. Finally, we set PV systems' locations by zip codes in the NEM dataset.

Table 5.3: PV system configuration used in the generic and adjusted generic configuration methods.

System Parameter	Value
Panel name	SunPower SPR-210-WHT
Panel type	Crystalline silicon
Inverter name	iPower SHO 5-2
Number of panels	28
Number of inverters	1
Number of strings per inverter	4
Inverter loading ratio	1.16

5.3.1.3 Sensitivity Analyses on Distributed PV Generation

By modifying the generic configuration method, we test the sensitivity of our distributed PV generation estimates to two PV system parameters. First, to test the effect of efficiency degradation, we assume each system's efficiency decreases by 0.5% annually [39]. Second, to test the effect of a higher inverter loading ratio, we use an iPower SHO 4-6 inverter in the generic configuration, yielding an inverter loading ratio of 1.30.

5.3.2 Estimating the Response of Day-Ahead Wholesale Electricity Prices to Distributed PV Generation

The California Independent System Operator (CAISO) operates the electric grid that provides roughly 80% of California electricity [40]. In order to balance supply and demand, CAISO operates a day-ahead market (DAM) and a real-time market. Over 95% of total energy procured by PGE, SCE, and SDGE, including through long-term bilateral contracts, passes through the DAM [41]. DAM wholesale electricity prices take the form of hourly locational marginal prices (LMPs), which account for energy, congestion, and transmission losses. Changes in LMPs as a result of distributed PV generation would affect the costs PGE, SCE, and SDGE incur to meet their customer's demand for electricity. To capture this change in costs, between

2013 and 2015 we calculate the difference between historic LMPs and counterfactual LMPs that would have occurred if distributed PV generation had not met some electricity demand. To estimate counterfactual LMPs, we first fit two regressions on historic net demand and supply-related variables [22] since supply and demand drive LMP formation. We then use those regressions to predict LMPs after replacing net demand with total demand, which we estimate as net demand plus distributed PV generation. We provide all monetary results in 2015 dollars using the Producer Price Index for electric utilities [42].

Our two regressions are:

$$LMP_t^{NP15} = \alpha_1 * D_t^{NP15} + \alpha_2 * D_t^{SP15} + \alpha_3 * W_t^{NP15} + \alpha_4 * S_t^{NP15} + \alpha_5 * W_t^{SP15} + \alpha_6 * S_t^{SP15} + \alpha_7 * V_t + \alpha_8 * C_t + \alpha_9 * NG_t + \alpha_{10} * KR_t + \alpha_{11} * SR_t + \alpha_{12} * HI_t + (\beta_1 * HD_2 + \cdots + \beta_{23} * HD_{24} + \beta_{24} * DW_2 + \cdots + \beta_{29} * DW_7 + \beta_{30} * M_2 + \cdots + \beta_{40} * M_{12} + \beta_{41} * Y_{2014} + \beta_{42} * Y_{2015}) + \varepsilon_t \quad (Regression\ 1)$$

$$LMP_t^{SP15} = \gamma_1 * D_t^{NP15} + \gamma_2 * D_t^{SP15} + \gamma_3 * W_t^{NP15} + \gamma_4 * S_t^{NP15} + \gamma_5 * W_t^{SP15} + \gamma_6 * S_t^{SP15} + \gamma_7 * V_t + \gamma_8 * C_t + \gamma_9 * NG_t + \gamma_{10} * KR_t + \gamma_{11} * SR_t + \gamma_{12} * HI_t + (\theta_1 * HD_2 + \cdots + \theta_{23} * HD_{24} + \theta_{24} * DW_2 + \cdots + \theta_{29} * DW_7 + \theta_{30} * M_2 + \cdots + \theta_{40} * M_{12} + \theta_{41} * Y_{2014} + \theta_{42} * Y_{2015}) + \tau_t \quad (Regression\ 2)$$

where *t* indexes hour and *NP15* and *SP15* index CAISO zones; *LMP* = forecasted average, or trading hub, LMP [$$_{2015}$/MWh] [43]; *D* = forecasted net demand [MWh] [44]; *W* = forecasted utility-scale wind generation [MWh] [45]; *S* = forecasted utility-scale solar generation [MWh] [45]; *V* = Palo Verde nuclear plant generation [MWh] [46]; *C* = Diablo Canyon nuclear plant generation [MWh] [46]; *NG* = Henry Hub natural gas price [$$_{2015}$/MMBtu] [47]; *KR* = Klamath

River flow [ft^3/s] [48]; *SR* = Sacramento River flow [ft^3/s] [49]; *HI* = average California stream flow index [1-7] [50]; *HD*, *DW*, *M*, and *Y* = dummy variables for hour of day, day of week, month, and year, respectively; ε and τ = random errors; and α, β, γ, and θ = coefficients.

Non-dummy variables capture the effect of generation by major fuel types [51] and of net demand on LMPs. Based on the availability of utility-scale wind and solar generation, we begin our analysis in 2013. Since PGE, SCE, and SDGE serve most demand in their respective zones [22], we approximate forecasted net demand in NP15 and SP15 as that in PGE and SCE plus SDGE, respectively. Augmented Dickey-Fuller tests [52] indicate all dependent and independent variables are stationary over our study period (p-values < 0.02). Furthermore, all non-dummy variables except *HI* (average California stream flow index) and *V* (Palo Verde nuclear plant generation) pass the Granger causality test (p-values < 0.01), although we retain both for price estimation. Dummy variables account for temporal trends in power system operations (see SI for specification without year dummy variables). Appendix D.6 further discusses and provides descriptive statistics for each variable.

Table 5.4 reports the results of Regressions 1 ($R^2 = 0.77$) and 2 ($R^2 = 0.79$). To account for autocorrelation in the residuals of Regressions 1 and 2 (Appendix D.6), we provide Newey-West standard errors [53] (Table 5.4) and block bootstrapped standard errors (Appendix D.6). Regressions 1 and 2 accurately predict most prices, but underestimate peak prices over our study period (Appendix D.6). While we use our regressions for prediction rather than causal inference, we note that all variables have statistically significant coefficients (p-value < 0.01) except *HI* and, in Regression 1, S^{NP15}. Furthermore, consistent with Woo et al. [22], coefficients indicate greater load and natural gas prices increase LMPs, while greater utility-scale wind and solar, nuclear, and hydropower generation decrease LMPs.

Table 5.4: Coefficients and standard errors for Regressions 1 and 2 using Newey-West standard errors with a maximum time lag of $4(T/100)^{2/9}$, where T = the number of observations in our dataset (26,280) [54]. For clarity, we provide regression results for data standardized as $(X/(X^{MAX} - X^{MIN}))$, where X^{MAX} and X^{MIN} equal the maximum and minimum variable value, respectively, and for dependent variables (LMPs) scaled to $\$_{2015}$/GWh. **Bold** values indicate statistical significance (p-value < 0.01). Appendix D.6 provides coefficients on dummy variables and bootstrapped standard errors.

	Regression 1		**Regression 2**	
Variable: definition	**Coeff.**	**Std. Error**	**Coeff.**	**Std. Error**
W_t^{NP15}: Hourly forecasted wind generation in NP15	**-20.92**	3.08	**-12.7**	3.45
S_t^{NP15}: Hourly forecasted solar generation in NP15	-5.22	3.88	**-12.9**	4.23
W_t^{SP15}: Hourly forecasted wind generation in SP15	**-13.21**	2.47	**-37.2**	3.15
S_t^{SP15}: Hourly forecasted solar generation in SP15	**-34.59**	2.42	**-81.0**	3.37
D_t^{NP15}: Hourly forecasted net demand in PGE	**317.23**	32.14	**227.9**	24.70
D_t^{SP15}: Hourly forecasted net demand in SCE + SDGE	**56.58**	16.08	**189.9**	16.15
C_t: Daily generation by Diablo Canyon	**-26.12**	3.50	**-33.5**	3.29
V_t: Daily generation by Palo Verde	**-26.06**	3.35	**-15.5**	3.35
NG_t: Daily natural gas Henry Hub price	**244.96**	18.56	**235.3**	17.58
HI_t: Daily California hydro index	-5.28	7.89	9.6	7.65
KR_t: Hourly Klamath river flow	**-29.37**	10.47	**-23.9**	9.29
SR_t: Hourly Sacramento river flow	**-18.85**	3.47	**-22.7**	3.81

5.4 RESULTS

5.4.1 Validation of Methods for Estimating Historic Distributed PV Generation

Using hourly metered generation from 2010 through 2016 for 205 distributed PV systems with a total capacity of 1.1 MW spread across 173 zip codes in SCE, SDGE, and PGE, we validate our four methods for estimating hourly distributed PV generation (Table 5.2). We select these 205 systems because we can model each system with the specific configuration method, meaning these systems are fixed array systems with a numeric azimuth and tilt, a single type of panel and inverter, and a panel and inverter that we can match to entries in the California Energy Commission Inverter and Sandia Module databases. To validate the scale up method, we

estimate generation by each of the 205 PV systems using the generation profile from the zip code nearest each PV system. Notably, when historic generation is available in a PV system's own zip code, the scale up method uses that generation. During validation, however, to understand error introduced from using generation profiles in nearby zip codes, we do not use generation profiles from a PV systems' own zip codes in the scale up method.

On average across individual PV systems, the generic and adjusted generic configuration methods estimate historic generation with less error relative to metered generation than the scale up or specific configuration methods (Table 5.5). Summing distributed PV generation by IOU improves the performance of each method (Table 5.6). Specifically, normalized root mean square errors (NMRSEs) decrease by 31-66% across the four methods when aggregating generation at the IOU level. Reduced error could be due to averaging out uncontrolled variables, e.g. shading, and/or to spatiotemporal smoothing, as generation errors between PV systems are not perfectly correlated. The generic and adjusted generic configuration methods estimate generation at the IOU level with less error relative to metered generation than the other two methods (Table 5.6). Lower accuracy with the specific than generic configuration method could be due to imperfect mapping from the NEM dataset to inverter and module databases used with PVLib and missing configuration details (e.g., strings per inverter).

Table 5.5: Means and standard deviations for root mean square errors (RMSEs) and normalized RMSEs (NRMSEs) during daytime hours between hourly metered and estimated generation across individual PV systems by method used to estimate generation.

Method	**Mean (standard deviation) of RMSEs [kWh]**	**Mean (standard deviation) of NRMSEs**
Specific configuration	0.89 (1.3)	0.16 (0.06)
Generic configuration	0.78 (1.1)	0.15 (0.05)
Adjusted generic configuration	0.74 (1.0)	0.14 (0.05)
Scale up	0.87 (1.0)	0.16 (0.06)

Table 5.6: Normalized root mean square errors (NRMSE) and mean bias errors (MBE) during daytime hours between hourly metered and estimated generation at the IOU level by method used to estimate generation.

	Specific Config. Method		**Generic Config. Method**		**Adjusted Generic Config. Method**		**Scale Up Method**	
IOU	NRMSE	MBE [kWh]	NRMSE	MBE [kWh]	NRMSE	MBE [kWh]	NRMSE	MBE [kWh]
PGE	0.09	31.1	0.05	8.7	0.04	0.7	0.11	-39.2
SCE	0.07	18.6	0.05	-1.4	0.03	0.6	0.07	-17.6
SDGE	0.09	9.9	0.06	0.18	0.05	-0.4	0.06	-6.2

Mean bias errors (MBEs) for estimated versus metered generation at the IOU level (Table 5.6) indicate that the specific, generic, and adjusted generic configuration methods tend to overestimate generation, while the scale up method tends to underestimate generation. The generic and adjusted generic configuration methods have lower MBEs than the specific configuration and scale up methods, further indicating the former two estimate metered generation with less error than the latter two. We observe similar biases for each method when estimating total generation by individual PV systems (Appendix D.7). Biases in generation at the IOU level vary throughout the day (Figure 5.1). For instance, the specific and generic configuration methods overestimate generation most in the late afternoon, which could be driven by shading not captured in our data. Due to hour-of-day correction factors, the adjusted generic configuration method has zero median error across hours and IOUs.

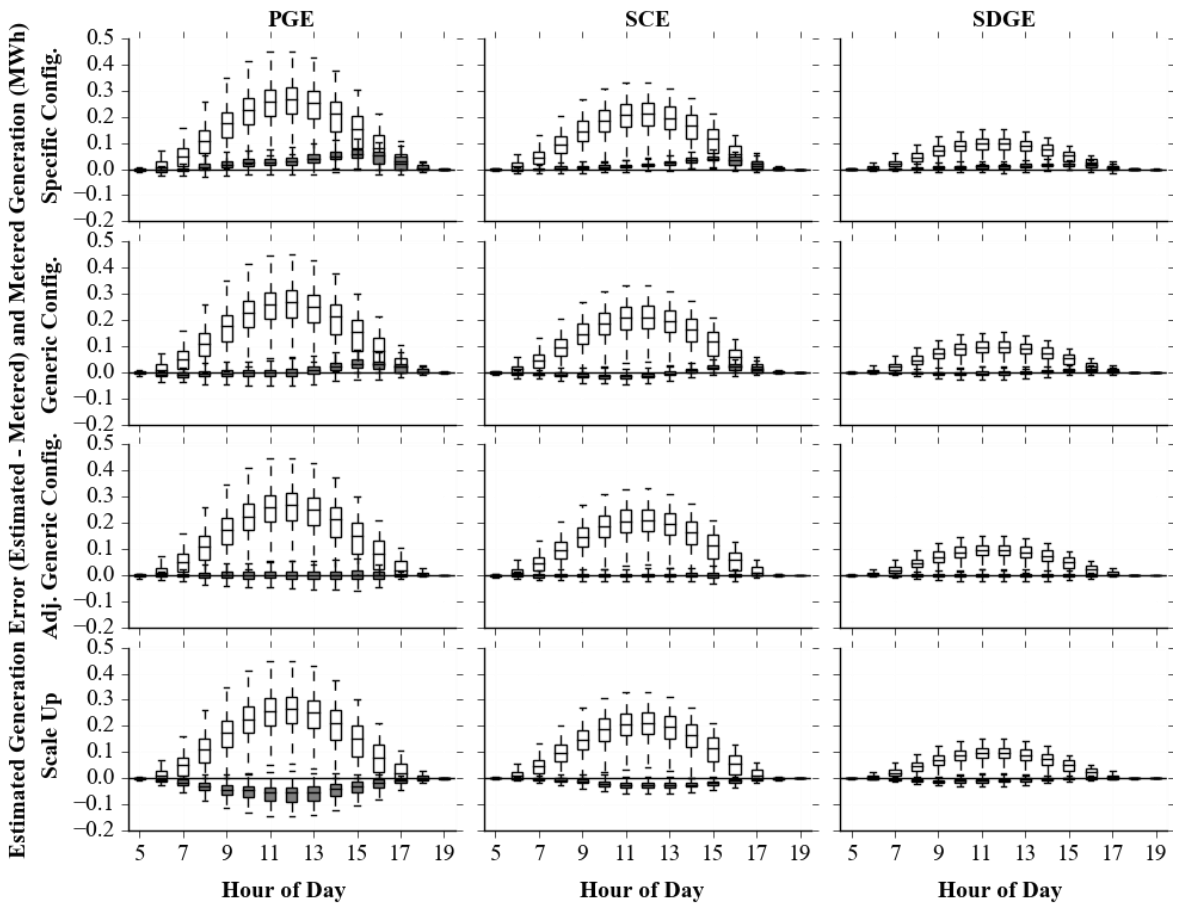

Figure 5.1: Box plots of metered generation (unshaded boxes) and the error in estimated generation (defined as estimated minus metered generation) (shaded boxes) by hour of day and IOU for the specific configuration (first row), generic configuration (second row), adjusted generic configuration (third row), and scale up method (fourth row). Boxes indicate the first, second, and third quartiles, while whiskers extend to 1.5 times the first and third quartiles.

Given that the specific, generic, and adjusted generic configuration methods use a similar approach to estimate distributed PV generation and that the latter two estimate generation with less error than the former, we do not use the specific configuration method to estimate generation by all distributed PV in California. While the scale up method also estimated generation with more error than the generic and adjusted generic configuration methods, it uses a significantly different approach than the generic configuration methods. Additionally, whereas the generic configuration method tends to overestimate generation, the scale up method tends to

underestimate generation. Thus, by using the generic configuration, adjusted generic configuration, and scale up methods to estimate generation by all distributed PV systems, we may bound historic distributed PV generation.

5.4.2 Generation by All Distributed PV Systems in Each IOU

Having validated our methods for estimating distributed PV generation against metered generation for a subset of PV systems, we now use the generic configuration, adjusted generic configuration, and scale up methods to estimate hourly generation by all distributed PV systems in PGE, SCE, and SDGE (Table 5.1). Across those three methods, total distributed PV generation from 2013 through 2015 in PGE, SCE, and SDGE ranges from 5.3-6.2, 3.8-3.9, and 1.3-1.4 TWh, respectively (Table 5.7). These generation levels correspond to capacity factors of 18-21% across IOUs, similar to the 21% average capacity factor of distributed PV in California in 2016 [55]. Decreasing generation from PGE to SCE to SDGE is consistent with decreasing distributed PV capacities (Table 5.1). As during validation, the scale up method estimates the least distributed PV generation across IOUs, while the generic configuration method estimates the greatest generation in PGE and SDGE while the adjusted generic configuration method estimates the greatest generation in SCE. Thus, as during validation, generation estimates with these methods may bound historic distributed PV generation.

Table 5.7: Total distributed PV generation from 2013 through 2015 in PGE, SCE, and SDGE by method used to estimate generation.

Method Used to Estimate Distributed PV Generation	**Total Distributed PV Generation (TWh)**		
	PGE	**SCE**	**SDGE**
Generic Configuration	6.21	3.92	1.40
Adjusted Generic Configuration	5.92	4.00	1.38
Scale Up	5.33	3.83	1.35

All three methods estimate a similar daily median generation profile that begins at 6 a.m., peaks around noon, and ends at 6 p.m. PST (Figure 5.2). For a given hour of the day, hourly distributed PV generation varies significantly between days (Figure 5.2, Appendix D.8) due to variable irradiance and meteorology. Across estimation methods, max hourly distributed PV generation over our study period equals 1.20-1.30, 0.87-0.90, and 0.32-0.34 GW in PGE, SCE, and SDGE, respectively, on the order of utility-scale generators. For context, net demand in PGE, SCE, and SDGE ranges from 8.3-23.2, 7.9-24.0, and 1.6-4.9 GW, respectively, over our study period. In addition to significant daily variability, distributed PV generation also varies seasonally in magnitude and duration (Appendix D.8).

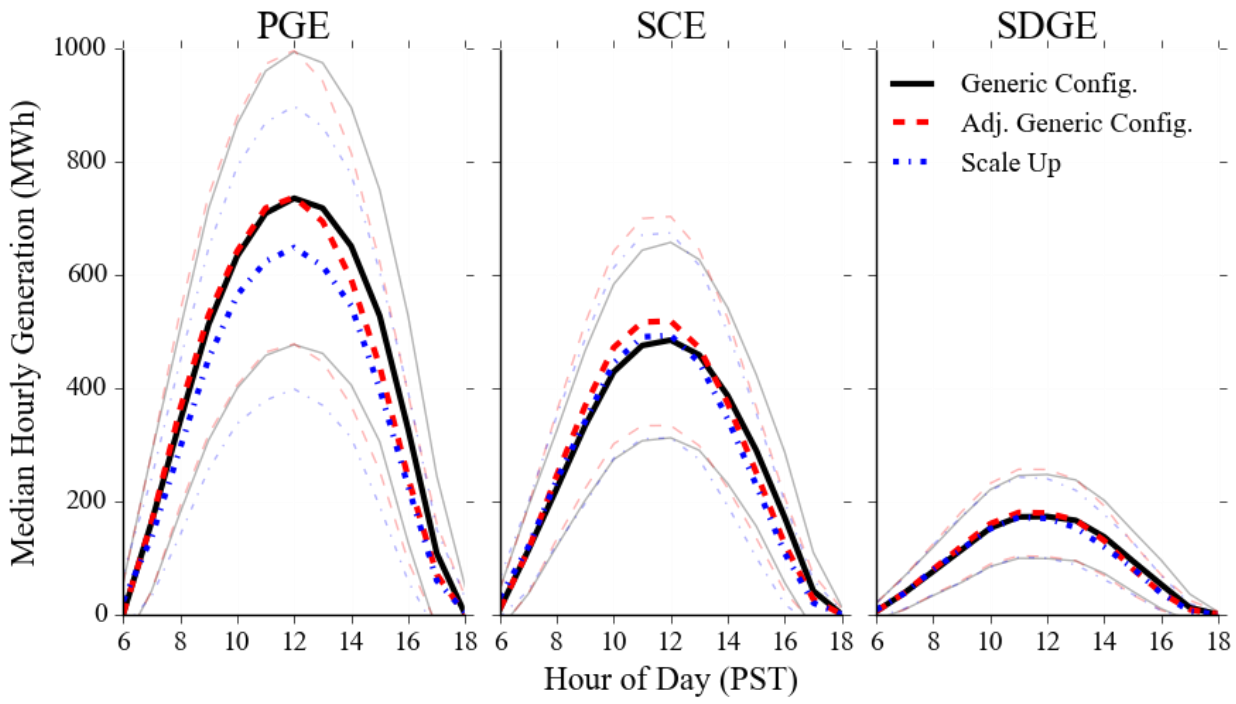

Figure 5.2: Median electricity generation (dark lines) +/- 1 standard deviation (faded lines) for all distributed PV systems in PGE, SCE, and SDGE by hour of day and method used to estimate generation from 2013 through 2015.

5.4.3 Wholesale Electricity Price Response to Distributed PV Generation

To estimate the wholesale electricity price response to distributed PV generation, we calculate the difference between LMPs based on historic net demand and total demand. We estimate total demand as net demand plus estimated distributed PV generation, where distributed PV generation in NP15 and SP15 equal that in PGE and in SCE plus SDGE, respectively. Median LMP reductions due to distributed PV generation are similar in magnitude and daily profile between zones (Figure 5.3). The greatest reductions in median (mean) LMPs, which range from \$2.7-3.1/MWh (\$2.9-3.2/MWh) ($\$_{2015}$) across methods used to estimate generation (Figure 5.3), coincide with peak distributed PV generation from 12-1 p.m. PST (Figure 5.2). LMP reductions are greater in the summer than winter due to greater distributed PV generation (Appendix D.9). Consistent with total distributed PV generation estimates across IOUs (Table 5.7), LMP reductions are greatest with the generic configuration method, followed in decreasing order by the adjusted generic configuration and scale up methods (Figure 5.3). For context, from 2013 through 2015 median (mean) LMPs in each hour of the day ranged from \$29-48/MWh (\$29-49/MWh) ($\$_{2015}$) in NP15 and \$29-52/MWh (\$29-50/MWh) ($\$_{2015}$) in SP15 (Appendix D.9). Over our study period, distributed PV generation reduced median (mean) LMPs from 12-1 p.m. PST by 7-8% (8-9%) across zones and methods used to estimate generation.

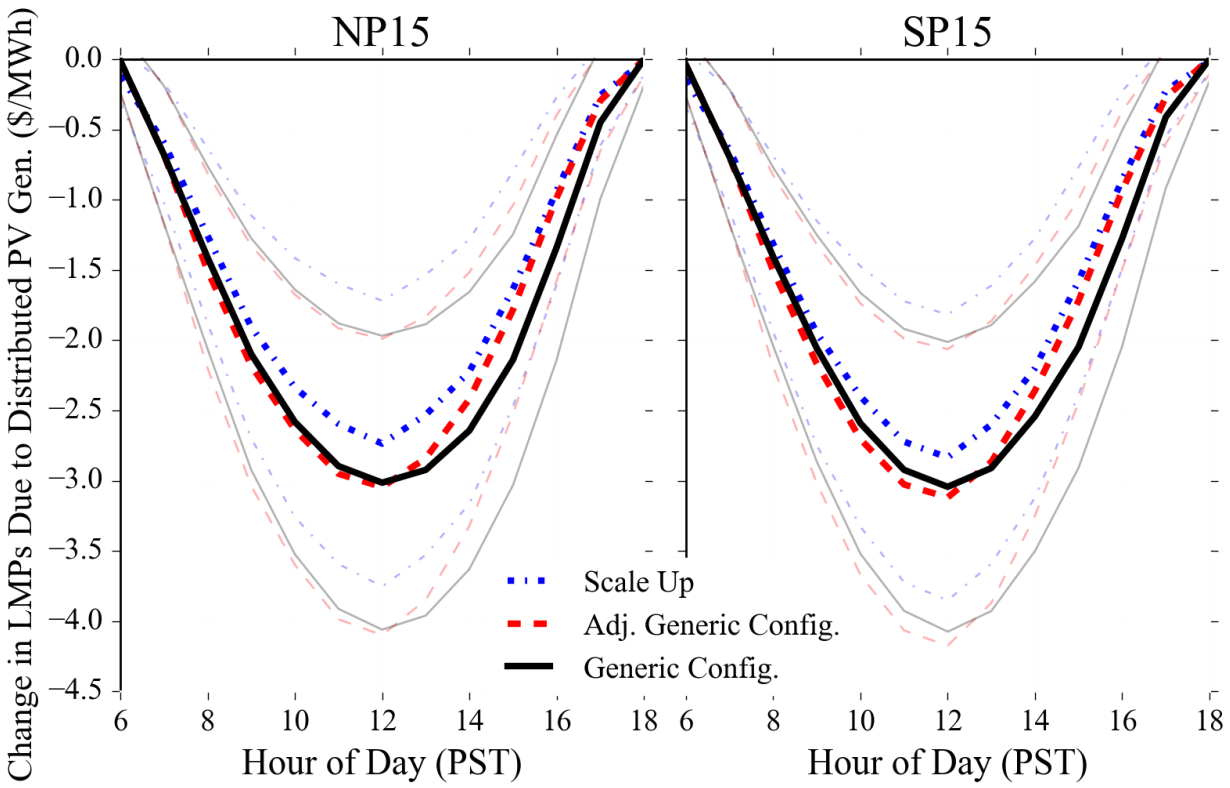

Figure 5.3: Median change in NP15 and SP15 LMPs (dark lines) +/- 1 standard deviation (faded lines) due to distributed PV generation by hour of day and method used to estimate generation from 2013 through 2015.

By reducing LMPs, distributed PV generation reduces the short-term cost to utilities of purchasing energy in the DAM, which translates to avoided consumer costs. To estimate these avoided costs, we multiply hourly LMP reductions due to distributed PV generation by historic hourly net demand, implicitly assuming California IOUs procure all of their energy in the DAM. In reality, California IOUs also procure energy via long-term bilateral contracts [41], so we likely overestimate actual avoided costs here. Under this "best case" assumption, avoided costs by IOUs in the DAM from 2013 through 2015 due to the market price response to distributed PV range from \$650-730 million ($\$_{2015}$) across methods used to estimate distributed PV generation (Table 5.8). For comparison, assuming IOUs purchased all energy required to meet net demand in the DAM, total energy procurement costs from 2013 through 2015 equaled \$12.3 and \$15.1

billion ($2015) in NP15 and SP15, respectively. On a per-generation and per-capacity basis (accounting for varying interconnection times), avoided costs equal 6 cents/kWh of distributed PV generation and 100-120 $/kW of distributed PV capacity across methods used to estimate generation over our study period (see Appendix D.10 for calculation details). Avoided costs are larger in SP15 than NP15 (Table 5.8) due to higher LMP reductions (Figure 5.3) and net demand (Appendix D.6).

Table 5.8: Avoided costs from 2013 through 2015 by zone due to LMP reductions from, i.e. the market price response to, distributed PV generation. Avoided costs equal the sum of hourly LMP reductions due to distributed PV generation multiplied by historic hourly net demand.

Method Used to Estimate Distributed PV Generation	Avoided Cost due to Market Price Response in NP15 (million $2015)	Avoided Cost due to Market Price Response in SP15 (million $2015)
Generic Configuration	330	400
Adjusted Generic Configuration	310	390
Scale Up	290	360

5.4.4 Sensitivity Analysis

Via sensitivity analysis, we find our results with the generic configuration method are robust to accounting for annual module efficiency degradation of 0.5% (versus 0%) and a higher inverter loading ratio of 1.3 (versus 1.16) (Appendix D.11). Since PV systems in our analysis have a median interconnection date of April 2014 (Table 5.1), accounting for PV system efficiency degradation of 0.5% per year reduces total distributed PV generation across IOUs by 2%. Using an inverter loading, i.e. DC to AC, ratio of 1.30 similarly reduces total distributed PV generation across IOUs by 2%, as a lower inverter capacity (and fixed module capacity) results in greater clipping. In both sensitivities, reduced distributed PV generation results in reduced total avoided costs of 1-2%.

5.5 DISCUSSION

To better understand a little-studied avoided cost of distributed PV, we quantified the market price response, or decrease in wholesale electricity prices, due to distributed PV generation in California from 2013 through 2015. To do so, we estimated hourly distributed PV generation in PGE, SCE, and SDGE using three methods that accounted for heterogeneity among PV systems' locations and orientations. Across those three methods, distributed PV generation totaled 5.33-6.21, 3.83-4.00, and 1.35-1.40 TWh in PGE, SCE, and SDGE, respectively, from 2013 through 2015. To determine how this distributed PV generation reduced wholesale electricity prices, we linked hourly LMPs in the DAM to electricity demand and other variables via multiple linear regression. By comparing LMPs predicted on net demand versus total demand, or net demand plus distributed PV generation, we found distributed PV generation reduced historic hourly median (mean) LMPs by \$2.7-3.1/MWh (\$2.9-3.2/MWh) ($\$_{2015}$), or by 7-8% (8-9%), during peak distributed PV generation hours (12-1 p.m. PST). LMP reductions throughout the day reduced IOUs' expenditures in the DAM by \$650-730 million ($\$_{2015}$) from 2013 through 2015, assuming IOUs procured all their energy through the DAM.

Our avoided cost estimate is lower than that of McConnell et al. [30], who projected annual avoided costs due to the market price response to 5 GW of distributed PV would equal \$110-200/kW ($\$_{2015}$). One large driver of this difference could be greater installed solar capacity in California over our study period (up to 10.4 GW) than in Australia over McConnell et al.'s study period (up to 500 MW [56]), as increasing solar capacity yields diminishing returns to electricity price reductions [30]. Differences in avoided costs could also reflect differing methods, as they used a dispatch model with hypothetical distributed PV capacities, and differing

market conditions, as the Australian energy market is an energy-only [57], fossil-heavy market [58].

Our estimates of avoided costs due to the market price response to distributed PV generation are similar to other avoided costs commonly included in value of solar studies. In 16 value of solar studies (including 5 in California) compiled by Hansen et al. [11], avoided costs of reduced generation, deferred generation capacity, and deferred transmission and distribution upgrades averaged about 10, 5, and 5 cents/kWh ($\$_{2015}$), respectively, comparable to our avoided costs of 6 cents/kWh. Vaishnav et al. [15] estimated annual avoided costs due to reduced local and global air pollution as roughly \$50/kW ($\$_{2015}$) in California, half our estimated annual avoided costs of \$100-120/kW. Relative to median installed prices of residential distributed PV of \$5,000/kW and \$4,000/kW ($\$_{2015}$) in 2013 and 2015, respectively [4], our avoided costs are small.

Although we focused here on how distributed PV affected electricity prices in the short-term, distributed PV can also affect prices in the long-term by changing the economics of generator entry and exit. If frequently dispatched units retire, as is the case with many retiring nuclear and coal plants [59], then electricity prices would likely increase, partly counteracting short-term price reductions quantified here. Concurrently, rising wholesale prices would increase wholesale price reductions due to distributed PV generation, tempering such long-term reductions in avoided costs. Also in the long-term, in order for generators to meet revenue requirements, decreasing wholesale prices may shift costs from energy to capacity markets [20]. Our analysis indicates such a shift could entail hundreds of millions of dollars.

Our study has several limitations. First, due to data gaps and limitations, we could not model key parameters like soiling and shading, which could significantly reduce distributed PV

generation in the early morning and/or late afternoon, or each system's specific panel and inverter configuration. Doing so would yield a more accurate estimate of distributed PV generation. The findings of our study also depend on meteorology, solar irradiance, and electricity system and market data specific to California, so our findings may not be applicable to other power systems. By running our analysis on zonal rather than nodal LMPs, we may underestimate avoided costs of some distributed PV systems, as in areas with elevated LMPs due to transmission congestion.

Finally, past studies suggest increasing solar penetration has diminishing returns to decreasing electricity prices [19], [30]. To that end, distributed PV capacity increased in California from 3.4 to 5.4 GW from 2015 through September 2017 [60] and total installed solar capacity reached 10.2 GW in August 2017 [61]. High solar capacities have contributed to negative LMPs in 106 and 132 hours in NP15 and SP15, respectively, in 2017 as of October, versus 0 and 26 hours in NP15 and SP15, respectively, over our study period [43], [62]. Thus, on a per-capacity or per-generation basis, distributed PV likely has a smaller effect on wholesale electricity prices now than in our analysis.

5.6 CONCLUSION

In the short-term, the market price response, or reduction in wholesale electricity prices, due to distributed PV generation can reduce consumer costs. We quantified these avoided costs in California from 2013 through 2015 as $650-730 million ($_{2015}$) or $100-120/kW, similar to other avoided costs commonly included in value of solar studies. In the long-term, price increases or greater capacity market payments may offset these avoided costs. Thus, when valuing or considering policies related to distributed PV, policymakers and regulators should

consider short-term avoided costs quantified here and how those costs may affect long-term market conditions.

5.7 REFERENCES

[1] U.S. Energy Information Administration, "Electric power annual 2015," 2016. [Online]. Available: https://www.eia.gov/electricity/annual/pdf/epa.pdf.

[2] K. Ardani and R. Margolis, "2010 Solar Technologies Market Report," *U.S. Department of Energy*, no. November. pp. 1–136, 2011.

[3] International Energy Agency Photovoltaic Power Systems Programme, "Snapshot of global photovoltaic markets 2016." pp. 1–16, 2017.

[4] G. Barbose, N. Darghouth, D. Millstein, S. Cates, N. DiSanti, and R. Widiss, "Tracking the sun IX: The installed price of residential and non-residential photovoltaic systems in the United States," *Lawrence Berkeley National Laboratory*. 2016.

[5] U.S. Department of Energy, NC Clean Energy Technology Center, and North Carolina State University, "Database of state incentives for renewables and efficiency," 2017. [Online]. Available: http://www.dsireusa.org/. [Accessed: 06-Dec-2015].

[6] K. H. Solangi, M. R. Islam, R. Saidur, N. A. Rahim, and H. Fayaz, "A review on global solar energy policy," *Renew. Sustain. Energy Rev.*, vol. 15, no. 4, pp. 2149–2163, 2011.

[7] W. Cole, B. Frew, P. Gagnon, J. Richards, Y. Sun, J. Zuboy, M. Woodhouse, and R. Margolis, "SunShot 2030 for photovoltaics (PV): Envisioning a low-cost PV future," *U.S. National Renewable Energy Laboratory*. 2017.

[8] F. Creutzig, P. Agoston, J. C. Goldschmidt, G. Luderer, G. Nemet, and R. C. Pietzcker, "The underestimated potential of solar energy to mitigate climate change," *Nat. Energy*, vol. 2, no. 9, p. 17140, 2017.

[9] U.S. Energy Information Administration, "Form EIA-860," *EIA.gov*, 2015. [Online]. Available: https://www.eia.gov/electricity/data/eia860/.

[10] California Distributed Generation Statistics, "California investor owned utility (IOU) interconnection net energy metering (NEM) solar PV data," *CaliforniaDGStats.ca.gov*, 2017. [Online]. Available: http://www.californiadgstats.ca.gov/downloads/. [Accessed: 13-Oct-2017].

[11] L. Hansen, V. Lacy, and D. Glick, "A review of solar PV benefit and cost studies," *Rocky Mountain Institute Electricity Innovation Lab*. p. 59, 2013.

[12] K. Patel, Z. Ming, L. Lavin, G. De Moor, B. Horii, and S. Price, "The benefits and costs of net energy metering in New York," *Energy and Environmental Economics*. 2015.

[13] M. Taylor, J. McLaren, K. Cory, T. Davidovich, J. Sterling, and M. Makhyoun, "Value of solar: program design and implementation considerations," *U.S. National Renewable Energy Laboratory*, no. March. 2015.

[14] M. A. Cohen, P. A. Kauzmann, and D. S. Callaway, “Effects of distributed PV generation on California’s distribution system, part 2: Economic analysis,” *Sol. Energy*, vol. 128, pp. 139–152, 2016.

[15] P. Vaishnav, N. Horner, and I. L. Azevedo, “Was it worthwhile? Where have the benefits of rooftop solar photovoltaic generation exceeded the cost?,” *Environ. Res. Lett.*, vol. 12, pp. 1–13, 2017.

[16] R. Wiser, D. Millstein, T. Mai, J. Macknick, A. Carpenter, S. Cohen, W. Cole, B. Frew, and G. Heath, “The environmental and public health benefits of achieving high penetrations of solar energy in the United States,” *Energy*, vol. 113, pp. 472–486, 2016.

[17] M. A. Cohen and D. S. Callaway, “Effects of distributed PV generation on California’s distribution system, part 1: Engineering simulations,” *Sol. Energy*, vol. 128, pp. 126–138, 2016.

[18] MIT Energy Initiative, *Utility of the future*. 2016.

[19] L. Hirth, “The market value of variable renewables: The effect of solar and wind power variability on their relative price,” *European Energy Institute*. 2013.

[20] S. Borenstein, “The market value and cost of solar photovoltaic electricity production,” *Center for the Study of Energy Materials Working Paper Series*, no. January. p. 38, 2008.

[21] P. E. Morthorst, S. Ray, J. Munksgaard, and A.-F. Sinner, “Wind energy and electricity prices: Exploring the ‘merit order effect,’” *Wind Energy Association*. p. 24, 2010.

[22] C. K. Woo, J. Moore, B. Schneiderman, T. Ho, A. Olson, L. Alagappan, K. Chawla, N. Toyama, and J. Zarnikau, “Merit-order effects of renewable energy and price divergence in California’s day-ahead and real-time electricity markets,” *Energy Policy*, vol. 92, pp. 299–312, 2016.

[23] L. Gelabert, X. Labandeira, and P. Linares, “An ex-post analysis of the effect of renewables and cogeneration on Spanish electricity prices,” *Energy Econ.*, vol. 33, no. SUPPL. 1, pp. S59–S65, 2011.

[24] Å. G. Tveten, T. F. Bolkesjø, T. Martinsen, and H. Hvarnes, “Solar feed-in tariffs and the merit order effect: A study of the German electricity market,” *Energy Policy*, vol. 61, no. June 2011, pp. 761–770, 2013.

[25] S. Clò, A. Cataldi, and P. Zoppoli, “The merit-order effect in the Italian power market: The impact of solar and wind generation on national wholesale electricity prices,” *Energy Policy*, vol. 77, pp. 79–88, 2015.

[26] S. Bode and H.-M. Groscurth, “The impact of PV on the German power market - or why the debate on PV feed-in tariffs needs to be reopened Or Why the Debate on PV Feed-In Tariffs Needs to be Reopened,” *Arrhenius Institute for Energy and Climate Policy*. 2010.

[27] C. Brancucci Martinez-Anido, G. Brinkman, and B.-M. Hodge, “The impact of wind power on electricity prices,” *Renew. Energy*, vol. 94, pp. 474–487, 2016.

[28] N. Mims, T. Eckman, and C. Goldman, “Time-varying value of electric energy efficiency,” *Lawrence Berkeley National Laboratory*. 2017.

[29] Industrial Energy Efficiency and Combined Heat and Power Working Group, “State

approaches to demand reduction induced price effects: examining how energy efficiency can lower prices for all." 2015.

[30] D. McConnell, P. Hearps, D. Eales, M. Sandiford, R. Dunn, M. Wright, and L. Bateman, "Retrospective modeling of the merit-order effect on wholesale electricity prices from distributed photovoltaic generation in the Australian National Electricity Market," *Energy Policy*, vol. 58, pp. 17–27, 2013.

[31] California Energy Commission, "California's installed electric power capacity and generation," *Tracking Progress*, 2017. [Online]. Available: http://www.energy.ca.gov/renewables/tracking_progress/documents/installed_capacity.pdf. [Accessed: 17-Nov-2017].

[32] California Solar Initiative, "California Solar Initiative 15-minute interval data," *CaliforniaDGStats.ca.gov*, 2016. [Online]. Available: http://www.californiadgstats.ca.gov/downloads/. [Accessed: 13-Oct-2017].

[33] C. N. Long and T. P. Ackerman, "Surface measurements of solar irradiance: A study of the spatial correlation between simultaneous measurements at separated sites," *Journal of Applied Meteorology*, vol. 34, no. 5. pp. 1039–1046, 1995.

[34] K. Klima and J. Apt, "Geographic smoothing of solar PV: Results from Gujarat," *Environ. Res. Lett.*, vol. 10, no. 10, 2015.

[35] Sandia National Laboratories, "PV_LIB toolbox," *PVPerformance Modeling Collaborative*, 2014. [Online]. Available: https://pvpmc.sandia.gov/applications/pv_lib-toolbox/. [Accessed: 29-Sep-2017].

[36] U.S. National Renewable Energy Laboratory, "National Solar Radiation Database (NSRDB)," *NREL.gov*, 2017. [Online]. Available: https://nsrdb.nrel.gov/. [Accessed: 08-Oct-2017].

[37] A. Habte, M. Sengupta, and A. Lopez, "Evaluation of the National Solar Radiation Database (NSRDB): 1998-2015," *NREL (National Renewable Energy Laboratory (NREL)*, 2017. [Online]. Available: http://www.nrel.gov/docs/fy17osti/67722.pdf.

[38] U.S. National Renewable Energy Laboratory, "System Advisor Model," *SAM.NREL.gov*, 2017. [Online]. Available: https://sam.nrel.gov/. [Accessed: 13-Oct-2017].

[39] D. C. Jordan, S. R. Kurtz, K. VanSant, and J. Newmiller, "Compendium of photovoltaic degradation rates," *Prog. Photovoltaics Res. Appl.*, vol. 24, pp. 978–989, 2016.

[40] California ISO, "Understanding the ISO," *caiso.com*, 2017. [Online]. Available: https://www.caiso.com/about/Pages/OurBusiness/Default.aspx. [Accessed: 19-Oct-2017].

[41] H. K. Trabish, "How electricity gets bought and sold in California," *Greentech Media*, 2012. [Online]. Available: https://www.greentechmedia.com/articles/read/how-electricity-gets-bought-and-sold-in-california. [Accessed: 19-Oct-2017].

[42] Federal Reserve Bank of St. Louis, "Producer Price Index by industry: Electric power generation: Utilities," *FRED Economic Data*, 2017. [Online]. Available: https://fred.stlouisfed.org/series/PCU2211102211104. [Accessed: 14-Nov-2017].

[43] California ISO, "Locational Marginal Prices (LMP), DAM, for TH_SP15_GEN-APND

and TH_NP15_GEN-APND," *OASIS*, 2017. [Online]. Available: http://oasis.caiso.com/mrioasis/logon.do?reason=application.baseAction.noSession. [Accessed: 29-Sep-2017].

[44] California ISO, "CAISO demand forecast, DAM, for PGE-TAC, SCE-TAC, and SDGE-TAC," *OASIS*, 2017. [Online]. Available: http://oasis.caiso.com/mrioasis/logon.do?reason=application.baseAction.noSession. [Accessed: 29-Sep-2017].

[45] California ISO, "Wind and solar forecast, DAM, for NP15 and SP15," *OASIS*, 2017. [Online]. Available: http://oasis.caiso.com/mrioasis/logon.do?reason=application.baseAction.noSession. [Accessed: 29-Sep-2017].

[46] U.S. Nuclear Regulatory Commission, "Power reactor status reports," *NRC Library*, 2017. [Online]. Available: https://www.nrc.gov/reading-rm/doc-collections/event-status/reactor-status/. [Accessed: 29-Sep-2017].

[47] U.S. Energy Information Administration, "Henry Hub natural gas spot price," *Natural Gas*, 2017. [Online]. Available: https://www.eia.gov/dnav/ng/hist/rngwhhdD.htm. [Accessed: 29-Sep-2017].

[48] U.S. Geological Survey, "USGS site number 11530500," *USGS Current Conditions for California: Build Time Series*, 2017. [Online]. Available: https://waterdata.usgs.gov/ca/nwis/uv?search_criteria=search_site_no&submitted_form=introduction. [Accessed: 29-Sep-2017].

[49] U.S. Geological Survey, "USGS site number 11447650," *USGS Current Conditions for California: Build Time Series*, 2017. [Online]. Available: https://waterdata.usgs.gov/ca/nwis/uv?search_criteria=search_site_no&submitted_form=introduction. [Accessed: 29-Sep-2017].

[50] U.S. Geological Survey, "Table of daily streamflow compared to historical streamflow for all days of the year (California)," *WaterWatch*, 2017. [Online]. Available: https://waterwatch.usgs.gov/index.php?region_cd=ca&map_type=pa01d&web_type=table2. [Accessed: 29-Sep-2017].

[51] California Energy Commission, "Total system electric generation, 2013-2015," *Electricity Data*, 2016. [Online]. Available: http://www.energy.ca.gov/almanac/electricity_data/system_power/2015_total_system_power.html. [Accessed: 29-Sep-2017].

[52] D. A. Dickey and W. A. Fuller, "Distribution of the estimators for autoregressive time series with a unit root," *J. Am. Stat. Assoc.*, vol. 74, no. 366, pp. 427–431, 1979.

[53] W. K. Newey and K. D. West, "A simple, positive semi-definite, heteroskedasticity and autocorrelation consistent covariance matrix," *Econometrica*, vol. 55, pp. 703–708, 1987.

[54] W. K. Newey and K. D. West, "Automatic lag selection in covariance matrix estimation," *Rev. Econ. Stud.*, vol. 61, pp. 631–653, 1994.

[55] D. Feldman, D. Boff, and D. R. Margolis, "Q3/Q4 2016 solar industry update," *U.S. Department of Energy*, 2016. [Online]. Available:

https://www.nrel.gov/docs/fy17osti/67639.pdf.

[56] Australian PV Institute, “Australian PV market since April 2001,” *APVI.org*, 2017. [Online]. Available: http://pv-map.apvi.org.au/analyses. [Accessed: 17-Nov-2017].

[57] Australian Energy Market Commission, “National electricity market,” *AEMC.gov.au*, 2017. [Online]. Available: http://www.aemc.gov.au/Australias-Energy-Market/Markets-Overview/National-electricity-market. [Accessed: 31-Oct-2017].

[58] Australian Energy Regulator, “Generation capacity and output by fuel source,” *AER.gov.au*, 2017. [Online]. Available: https://www.aer.gov.au/wholesale-markets/wholesale-statistics/generation-capacity-and-output-by-fuel-source. [Accessed: 31-Oct-2017].

[59] M. B. Roth and P. Jaramillo, “Going nuclear for climate mitigation: An analysis of the cost effectiveness of preserving existing U.S. nuclear power plants as a carbon avoidance strategy,” *Energy*, vol. 131, pp. 67–77, 2017.

[60] California Distributed Generation Statistics, “Statistics and charts,” *CaliforniaDGStats.ca.gov*, 2017. [Online]. Available: http://www.californiadgstats.ca.gov/charts/. [Accessed: 17-Nov-2017].

[61] U.S. Energy Information Administration, “Table 6.2B,” *Electric Power Monthly*, 2017. [Online]. Available: https://www.eia.gov/electricity/monthly/epm_table_grapher.php?t=epmt_6_02_b. [Accessed: 17-Nov-2017].

[62] California ISO, “Locational Marginal Prices (LMP), node TH_NP15_GEN-APND,” *OASIS*, 2017. [Online]. Available: http://oasis.caiso.com/mrioasis/logon.do?reason=application.baseAction.noSession. [Accessed: 29-Sep-2017].

CHAPTER 6: CONCLUSION

Effectively mitigating climate change will require reducing CO_2 emissions from the electric power sector by 80% or more. Achieving these reductions will require large-scale deployment of numerous low-carbon technologies, which could in turn require significant policy support. In this thesis, I considered three low-carbon technologies that could play an instrumental role in decarbonizing power systems: carbon capture and sequestration (CCS), grid-scale electricity storage, and distributed solar photovoltaic.

One stumbling block to widespread CCS deployment has been high capital and operational costs. To overcome cost issues, prior papers have proposed adding flexibility to amine-based CCS systems by adding on-site solvent storage. These prior papers found "flexible" CCS offers several advantages over "normal" CCS, particularly through increased reserve provision, but did not fully monetize these benefits. Furthermore, in 2015 the U.S. promulgated the Clean Power Plan (CPP), the first national regulation on CO_2 emissions from existing power plants. At that time, it was unclear whether flexible CCS could be an economic compliance strategy with the CPP.

In Chapters 2 and 3, I addressed these questions. In both chapters, I quantified system emissions and costs, including reserve costs, with flexible CCS retrofits versus other low-carbon technologies. In Chapter 2, I specifically compared the cost-effectiveness of reducing carbon emissions to comply with the CPP with flexible CCS retrofits versus normal CCS retrofits, re-dispatching from coal- to gas-fired generators, and additional wind. Using a unit commitment and economic dispatch (UCED) model, a power system optimization model that meets system electricity demand at least cost, I found in Chapter 2 that flexible CCS does not achieve as cost-

effective emissions reductions under the CPP as additional wind and, depending on the CO_2 reduction target, re-dispatching. In Chapter 3, I found that flexible CCS offers a trade-off between system cost and emission reductions under a moderate decarbonization target relative to normal CCS. However, under a stronger decarbonization target, I found that flexible CCS reduces costs and emissions more than normal CCS.

Grid-scale electricity storage is widely seen as a key decarbonization technology, as it can shift supply from variable and uncertain renewables to meet demand. However, several recent studies have indicated that storage would increase carbon emissions from current power systems. In Chapter 4, I quantified how storage would affect carbon emissions as a power system decarbonizes over time, bridging the gap between research on storage in current and decarbonized power systems. I found that under even a moderate decarbonization policy, storage would reduce carbon emissions in the mid-term, e.g. by around 2025. Furthermore, I found that whether storage provides only energy, only reserves, or both can significantly change the magnitude of the effect of storage on system emissions.

Distributed PV has grown rapidly in the U.S. in recent years. To determine fair compensation for distributed PV, regulators and policymakers have commissioned numerous value of solar studies. In Chapter 5, I quantified a little-studied avoided cost of distributed PV, namely the market price response, or how distributed PV reduces wholesale electricity prices and, in turn, utilities' energy procurement costs in the short-term. Using 2013 through 2015 data from California, I found that the market price response reduced utility expenditures in the day-ahead market by up to $650-730 million from 2013 through 2015. These avoided costs are similar to other avoided costs commonly included in value of solar studies.

Several policy recommendations result from the research presented in this thesis. Chapters 2 and 3 suggest that for CCS to play a significant role in deep decarbonization of the electric power sector, carbon emission limits set by the CPP will not sufficiently incentivize CCS deployment. Thus, additional policy support, either through deployment mandates or financial incentives, will be necessary, some of which already exist. Chapter 3 also suggests that policymakers should carefully weigh near- versus long-term goals when incentivizing flexible versus normal CCS, as the former may reduce carbon emissions less but reduce costs more than the latter in the near-term.

Chapter 4 indicates that grid-scale electricity storage can contribute to decarbonization efforts prior to deep decarbonization under comprehensive carbon policies that affect system operation and composition. However, in the absence of comprehensive carbon policies, storage may increase carbon emissions. Thus, policymakers should carefully consider storage incentives and mandates in the context of other existing carbon policies. If policymakers want to promote storage deployment in the near-term while ensuring it reduces carbon emissions, then comprehensive carbon policies should also be put in place or regulations restricting storage operations to, for instance, reducing renewable curtailment. Chapter 4 also indicates that which market storage participates in can change the extent to which storage affects carbon emissions. This provides policymakers a key lever, as they can incentivize storage to participate in energy versus reserve markets.

Finally, Chapter 5 contributes to ongoing debates around the value of distributed PV generation by indicating that avoided costs due to the market price response to distributed PV are similar to other avoided costs commonly included in value of solar studies. Thus, in order to

fully value distributed PV and set compensation for optimal investment levels, policymakers and regulators should include the market price response in future value of solar studies.

Overall, these policy implications indicate roles for policymakers at all levels of government. Given the current political environment at the federal level, significant advances in federal climate policy seem unlikely in the near-term. Conversely, many states and cities are leading the way on climate action in the U.S. by enacting aggressive climate policies and goals, including 100% renewable energy goals, state and regional cap-and-trade programs, renewable energy and storage mandates, and policies aimed at reducing costs and uncertainty associated with CCS. To further these efforts, this thesis illuminates additional actions state and regional policymakers can take to mitigate climate change, such as by supporting flexible CCS, designing storage policies for near- and mid-term emission reductions, and improving value of solar studies. While state- and city-level policies may seem insignificant relative to the grand challenge of mitigating climate change, the accretion of such policies can provide a strong foundation on which further climate mitigation actions can be based.

APPENDIX A:
SUPPLEMENTAL INFORMATION FOR CHAPTER 2

A.1: UNIT COMMITMENT AND ECONOMIC DISPATCH FORMULATION

This appendix provides the complete formulation of the unit commitment and economic dispatch (UCED) model that we use to determine operational costs and emissions of each of our power plant fleets. The UCED model is built and run in PLEXOS [1], a commercial software package. The constraints of our flexible carbon capture and sequestration (CCS) model [2] are added to the UCED formulation provided in this section.

A.1.1: Definition of Variables, Sets and Parameters

Table A.1: Variables, parameters and sets used in the UCED formulation.

Variable	Definition
$c^{UP}_{i,t}$	Increase in electricity generation at generator i in time t (MWh)
$c^{DOWN}_{i,t}$	Decrease in electricity generation at generator i in time t (MWh)
nse_t	Non-served energy at time t (MWh)
$p_{i,t}$	Electricity generation by generator i at time t (MWh)
$r_{i,t}$	Provided spinning reserves by generator i at time t (MW)
$sr_{i,t}$	Spare spinning reserves of generator i at time t (MW)
$u_{i,t}$	Binary variable indicating on/off state of generator i at time t, where 1 indicates on {0,1}
$v_{i,t}$	Binary variable indicating generator i turns on at time t {0,1}
$w_{i,t}$	Binary variable indicating generator i turns off at time t {0,1}

Parameter	Definition
CNSE	Cost of non-served energy ($/MWh)
ER_i^{CO2}	Emissions rate for generator i of CO_2 (ton/MWh)
EC^{CO2}	Emissions cost for CO_2 ($/ton)
FC_i	Fuel cost for generator i ($/MMBtu)
HR_i	Heat rate for generator i (MMBtu/MWh)
MDT_i	Minimum down time for generator i, which indicates the number of hours that must elapse before a generator can turn on once it shuts off (hours)
OC_i	Operating cost of generator i ($/MWh)
OQ_i^{TYPE}	Offered quantity of reserves of a given type by generator i in time t (MW)
P_i	Electricity generation by generator i in the last period of the prior optimization horizon (MWh)

P^{D}_{t}	Electricity demand at time t (MWh)
P^{MAX}_{i}	Maximum electricity generation capacity of generator i (MWh)
P^{MIN}_{i}	Minimum stable load of generator i (MW)
R_t	Required spinning reserves at time t (MW)
RL_i	Ramping limit of generator i (MW)
ROS	Reserve offer scalar for spinning reserves
SU_i	Start-up cost for generator i ($)
U_i	On/off state of generator i in the last period of the prior optimization horizon {0,1}
VOM_i	Variable operations and maintenance cost of generator i ($/MWh)

Set	**Definition**
F	Offline generators eligible to provide replacement reserves
I	Generators in the fleet
K_i	Number of hours before which a generator can turn on in the current optimization horizon. $K = MDT_i - (24\text{-}H\text{-}1)$, where H equals the last hour in which the generator turned off in the prior optimization period. K is used to enforce the MDT for a generator for shut-off decisions in the last optimization period (hours)
N	Online generators eligible to provide regulation and spinning reserves
T	Time periods in the optimization horizon

A.1.2: Objective Function

The UCED model minimizes total operational costs, which include costs of electricity generation, reserves, start-ups, and non-served energy. The UCED runs over a 24-hour optimization horizon in hourly increments and includes an additional 24-hour period in 6-hour increments. The second 24-hour period is a "look-ahead period", in that solutions to variables in that period of time are not fixed in the final UCED solution, but rather are re-solved for in the subsequent UCED run. In this way, the additional 24-hour period functions only to bring additional information into the current 24-hour optimization horizon.

For intervals in the 24-hour look-ahead period, objective function coefficients are multiplied by 6, the number of hours in each interval. Demand for each interval equals the average demand over the 6-hour period.

Total operational costs (*TC*) are calculated as:

$$TC = \sum_{i,t}\left[p_{i,t} * OC_i + r_{i,t} * OC_i * ROS + v_{i,t} * SU_i\right] + \sum_t nse_t * CNSE \qquad \forall t \in T, i \in I \quad (1)$$

where *i* and *t* index generators and hours, respectively; *p* = electricity generation [MWh]; *OC* = operating cost [$/MWh], as defined in Equation 2; *r* = provided spinning reserves [MWh]; *ROS* = reserve offer scalar [$/MWh], or the ratio of operating cost to reserve offer cost (0.26); *v* = binary indicator of whether the unit turned on; *SU* = start-up costs [$]; *nse* = non-served energy [MWh]; and *CNSE* = the cost of non-served energy [$/MWh]. Operating costs (*OC*) equal:

$$OC_i = HR_i * FC_i + ER_i^{CO_2} * EC^{CO_2} + VOM_i \quad (2)$$

where *HR* = heat rate [MMBtu/MWh]; *FC* = fuel cost [$/MMBtu]; ER^{CO2} = CO_2 emissions rate [kg/MWh]; EC^{CO2} = CO_2 emissions price [$/kg]; and *VOM* = variable operations and maintenance [$/MWh].

A.1.3: System-wide Electricity Demand and Reserve Requirement Constraints

Combined electricity generation plus non-served energy must equal system-wide demand (P^D [MWh]) in each time period:

$$\sum_i p_{i,t} + nse_t = P_t^D \qquad \forall t \in T, i \in I \quad (3)$$

Provided reserves must equal system reserve requirements (*R* [MWh]) in each time period for each type of reserve:

$$\sum_i r_{i,t} = R_t \qquad \forall t \in T, i \in I \quad (4)$$

Given the large penetration of wind power in our scenarios, we set hourly spinning reserve requirements equal to 3% of maximum daily load plus 5% of hourly wind generation [3], [4]. Spinning reserves in our model have a 10-minute response time.

A.1.4: Reserve Provision Constraints

Provided spinning reserves from online generators cannot exceed spare reserves (*sr* [MWh]) of each generator:

$$r_{i,t} \leq sr_{i,t} \qquad \forall t \in T, i \in I \quad (5)$$

Provided spinning reserves of each generator also cannot exceed the maximum reserve offer quantity (*OQ* [MWh]) of each generator, which is set based on the ramp rate of the generator and the reserve timeframe:

$$r_{i,t} \leq OQ_i * u_{i,t} \qquad \forall t \in T, i \in I \quad (6)$$

where *u* = binary indicator of whether the generator is on or off. Spare reserves are non-zero for online generators, and cannot exceed the spare capacity at the generator, defined as the difference between the maximum capacity (P^{MAX} [MWh]) and the electricity generation at the generator at time t:

$$sr_{i,t} \leq P_i^{MAX} * u_{i,t} - p_{i,t} \qquad \forall t \in T, i \in I \quad (7)$$

A.1.5: Generator-Specific Operational Constraints

A.1.5.1: Maximum and Minimum Electricity Generation Constraints

Several operational constraints are applied at the generator level. Electricity generation cannot exceed maximum capacity:

$$p_{i,t} \leq P_i^{MAX} * u_{i,t} \qquad \forall t \in T, i \in I \quad (8)$$

Electricity generation must be greater than the minimum stable load (P^{MIN} [MWh]):

$$p_{i,t} \geq P_i^{MIN} * u_{i,t} \qquad \forall t \in T, i \in I \quad (9)$$

A.1.5.2: Ramping Constraints

Up (c^{UP} [MWh]) and down (c^{DOWN} [MWh]) ramps are defined by the change in electricity generation from one hour to the next:

$$c_{i,t}^{UP} - c_{i,t}^{DOWN} = p_{i,t} - p_{i,t-1} \qquad \forall t > 1, i \in I \quad (10)$$

$$c_{i,t}^{UP} - c_{i,t}^{DOWN} = p_{i,t} - P_i \qquad \forall t = 1, i \in I \quad (11)$$

At t=1, the electricity generation of the unit in the last period of the prior optimization is input. In the case of the very first hour of the entire optimization period (e.g., the first hour in 2030 when running the UCED for all of 2030), the right-hand side of the constraint is set equal to zero.

Increases in electricity generation from one time period to the next (i.e., ramp ups) must be less than the ramping limit plus the minimum stable load of the generator if the generator turned on at time t:

$$c_{i,t}^{UP} - c_{i,t}^{DOWN} \leq RL_i * u_{i,t} + P_i^{MIN} * v_{i,t} \qquad \forall t \in T, i \in I \quad (12)$$

Ramp downs must be less than the ramping limit (*RL* [MWh]) plus the minimum stable load of the generator if the generator turned off at time *t* (*w*):

$$c_{i,t}^{DOWN} - c_{i,t}^{UP} \leq RL_i * u_{i,t-1} + P_i^{MIN} * w_{i,t} \qquad \forall t > 1, i \in I \quad (13)$$

At *t*=1, whether the unit was on or off in the last period (*U*) of the prior optimization horizon is input instead.

$$c_{i,t}^{DOWN} - c_{i,t}^{UP} \leq RL_i * U_i + P_i^{MIN} * w_{i,t} \qquad \forall t = 1, i \in I \quad (14)$$

In the very first hour of the entire optimization period, *U* is set equal to 1:

A.1.5.3: On/Off Constraints

The unit must be marked as on if the unit turns on in that hour:

$$u_{i,t} \geq v_{i,t} \qquad \forall t \in T, i \in I \quad (15)$$

The unit also cannot turn off if it is not on in the prior hour:

$$u_{i,t-1} + v_{i,t} \leq 1 \qquad \forall t > 1, i \in I \quad (16)$$

At *t*=1, the on/off state in the last period of the prior optimization horizon is input:

$$U_i + v_{i,t} \leq 1 \qquad \forall t = 1, i \in I \quad (17)$$

The following constraint defines when the unit turns off; it cannot turn off in the same hour it turns on, and cannot turn off if the unit was not on in the prior hour:

$$w_{i,t} = u_{i,t-1} - u_{i,t} + v_{i,t} \qquad \forall t > 1, i \in I \quad (18)$$

At *t*=1, the on/off state in the last period of the prior optimization horizon is input:

$$w_{i,t} = U_i - u_{i,t} + v_{i,t} \qquad \forall t = 1, i \in I \quad (19)$$

A minimum down time (*MDT* [hr]) is enforced on each generator, such that it cannot turn off twice within its minimum down time period. Several constraints are used to enforce the MDT. When t is greater than or equal to *MDT*, then the generator can only turn off once in a period determined by the *MDT*, and cannot be on in any hour within that period:

$$u_{i,t} + w_{i,t-(MDT_i-1)} + w_{i,t-(MDT_i-2)} + \cdots + w_{i,t} \leq 1 \qquad \forall t \geq MDT_i, i \in I \quad (20)$$

At *t*<*MDT*, the number of intervals included in the optimization is reduced, and an extra constraint is included that forces the unit off for a given number of hours, *K*, where *K* is determined by the most recent hour in the prior optimization window in which the generator turned off:

$$u_{i,t} + w_{i,1} + \cdots + w_{i,t} \leq 1 \qquad \forall t < MDT_i, i \in I \quad (21)$$

$$u_{i,t} \leq 0 \qquad \forall t = K_i, i \in I \quad (22)$$

A.2: MODIFICATIONS TO IPM FLEET

We make several modifications to the Integrated Planning Model (IPM) fleet in order to derive our 2030 base fleet. First, the IPM forecasts heat rate improvements and control technology retrofits, but does not adjust heat rates to reflect these modifications in the parsed file. We adjust generator heat rates downwards to account for heat rate improvements by 4.3%, the value assumed in the CPP [5], and upwards to account for control technology retrofits, such as Selective Catalytic Reduction, using heat rate penalties as a function of generator heat rate from the IPM [6].

New generators forecast by the IPM can be very small (<10 MW) and very large (>1 GW) units. To obtain more realistic generator sizes, we divide new generators greater than 800 MW into 250 MW units, with any remaining capacity split evenly among the newly-created 250 MW units, and remove new fossil units smaller than 10 MW. Most of these deleted units are much smaller than 10 MW, such that the combined capacity of deleted units is 12 MW.

The IPM model forecasts roughly 2 GW of added hydropower capacity in our study region. However, less than 30 MW of hydropower was built in our study region from 2005 through 2015 [7]. Thus, we remove these added hydropower plants from our fleet. We also remove 2.5 GW of pumped hydropower units from our fleet given the small size of these units relative to our fleet and the lack of necessary public data, e.g. round-trip efficiency, essential to model these units. Table A.2 provides capacity by fuel type of the base fleet.

Table A.2: Capacity by fuel type of the base fleet.

Fuel Type	Coal	Natural Gas	Oil	Nuclear	Wind	Solar	Other	Total
Capacity (GW)	50.7	53.8	5.8	18	33.1	1.2	1.5	164.1

A.3: PARAMETERS ADDED TO IPM FLEET

Several parameters must be added to the base fleet so it can be run in the UCED model. We add variable operations and maintenance costs and heat rates for new generators using data from the IPM documentation [6].

Three unit commitment parameters – minimum stable load (MSL), minimum down time, and start-up costs – are added based on values in PHORUM [8], a price-validated reduced form UCED model of PJM [9]. Unit commitment parameters are assigned based on fuel type and, in some instances, plant type and plant size in order to capture nonlinearities in unit commitment parameter values for some plant types, e.g. coal-fired generators. With respect to ramp rates, we rely on several sources for hourly values specific to fuel and plant type [10]–[13]. However, our UCED model requires per-minute ramp rates to model sub-hourly reserves. To obtain per-minute ramp rates, we scale up PHORUM ramp rates such that they are in agreement with the hourly ramp rates obtained from other sources. Table A.3 provides the unit commitment parameter values used in our model.

Table A.3: Unit commitment parameter values by plant and fuel type and plant size, if applicable, used in our model.

Unit Commitment Parameter	**Plant and Fuel Type**	**Plant Size**	**Value**
Minimum Stable Load (% of total capacity)	Oil-fired combustion turbine	All	25%
	Oil-fired O/G steam turbine	All	25%
	Hydropower	All	0%
	Nuclear	All	90%
	All other generators	All	40%
Ramp Rate (Up and Down) (% of total capacity)	Coal	>150 MW	1.5%/min.
	Coal	<150 MW	2.9%/min.
	Natural gas combined cycle	>100 MW	2.7%/min.
	Natural gas combined cycle	<100 MW	5.3%/min.
	Combustion turbine (natural gas and oil)	All	2.9%/min.
	O/G steam turbine (natural gas and oil)	All	1.9%/min.

	Landfill gas, municipal solid waste, biomass, hydropower, fossil waste	All	8.3%/min.
	Nuclear	All	0.7%/min.
Startup Costs ($, as multiple of nameplate capacity)	Coal	All	100x
	Natural gas combined cycle	All	100x
	Combustion turbine (natural gas and oil)	All	25x
	Hydropower	All	0
	Fossil waste	All	100x
	Municipal solid waste	All	100x
	Landfill gas	All	50x
	Nuclear	All	500x
	O/G Steam (natural gas and oil)	All	100x
Minimum Down Time (hours)	Coal	>150 MW	12
	Coal	<150 MW	6
	Nuclear	All	20
	Natural gas combined cycle	All	4
	Combustion turbine (natural gas and oil)	<60 MW	1
	Combustion turbine (natural gas and oil)	60-140 MW	2
	Combustion turbine (natural gas and oil)	>140 MW	3
	Landfill gas	All	4
	Municipal solid waste	All	4
	Fossil waste	All	8
	O/G Steam (natural gas and oil)	All	7

We also add fuel prices and CO_2, NO_x and SO_2 emissions rates using data from the IPM [14]. We calculate generator-specific values where possible, including for all coal-fired generators (accounting for coal type), using total annual electricity generation, fuel input, and emissions values. Those data are not available for generators that do not generate electricity (i.e., are not dispatched) in the IPM, which tend to be generators with high operational costs. For these generators, we use a capacity-weighted average value for generators of the same fuel and plant type, e.g. natural gas combustion turbines. Oil-fired generators do not generate any electricity in the IPM, so external fuel and emissions rates values are obtained from Oates [15] and the U.S. Environmental Protection Agency's (EPA's) AP-42 [16] (specifically for distillate-oil fired

stationary gas turbines). Table A.4 provides the capacity-weighted fuel price by fuel type of the base fleet.

Table A.4: Capacity-weighted fuel prices for the base fleet.

Fuel	Fuel Price ($/GJ)
Coal	2.4
Natural Gas	5.7
Nuclear	0.9
Oil	24.4
Biomass	4
Landfill gas, municipal solid waste, fossil waste	0
Petroleum coke	2.9

Forecasted NOx and SO_2 emission prices under the Cross-State Air Pollution Rule (CSAPR) are added to generators covered by CSAPR. The CSAPR applies to oil-, coal-, and natural gas-fired generators over 25 MW in capacity for all states in our region except North and South Dakota [17]. We apply a NOx permit price of $600/ton to those generators, and SO_2 prices of $700/ton and $1,100/ton to generators in Minnesota and all other states, respectively, to reflect different SO_2 pricing groups under CSAPR [17].

A.4: GENERATION PROFILES FOR HYDROPOWER, WIND, AND SOLAR PLANTS

Rather than use seasonal capacity factors as in the IPM to determine electricity generation at hydropower plants remaining in our fleet (as reported in Oates et al. [18]), we set hourly electricity generation by hydropower plants using plant-specific average monthly capacity factors from 2008 to 2013 [19]. We reduce demand in the UCED model by generation from these hydropower plants (estimate net load) and can thus remove them from our fleet to reduce the fleet size for the optimization problem.

In order to capture spatial and temporal variability in output among wind and solar farms, we match wind and solar power plants in the parsed file to simulated wind and solar generation profiles from the National Renewable Energy Laboratory (NREL) [20], [21]. These wind and solar generation databases provide simulated generation profiles for hypothetical plants at 10- and 5-minute increments, respectively. We downscale generation data to hourly increments by calculating the average generation values for all time steps in each hour [3]. For each state in our system, we then calculate the installed capacity of wind in our base fleet, and add wind farms in the NREL dataset in that state to our fleet in order of decreasing capacity factor. We perform the same process for solar. The resulting wind and solar plants in our fleet have capacity factors between 30-45% and 13-16%, respectively. Given that each wind and solar generator varies only by capacity and generation profile once included in our UCED model (as we do not include the transmission system), we then collapse all wind and solar generators into a single generator of each type by combining their capacities and hourly generation profiles.

A.5: BASE FLEET SIMPLIFICATIONS FOR COMPUTATIONAL EFFICIENCY

After the above modifications, running the UCED model with the base fleet takes a prohibitively long time given the hundreds of runs necessary for our analysis. As such, we simplify our base fleet by aggregating plants for some generator types.

Oil-fired combustion turbine generators are rarely dispatched due to high fuel costs and emissions, whereas municipal solid waste and landfill gas generators are almost always operated because they have no fuel cost in our model. Thus, we can group oil-fired combustion turbine generators as a single power plant, and also aggregate landfill gas and municipal solid waste generators while minimally affecting our UCED model. We also aggregate inefficient natural

gas-fired combustion turbine generators with heat rates above 18 MMBtu/MWh, as these generators would be infrequently dispatched due to low efficiencies. We only aggregate units less than 50 MW in capacity and differentiate by heat rate to preserve some differentiation by efficiency. For instance, we aggregate natural gas-fired combustion turbine generators with heat rates between 18 and 20 MMBtu/MWh, 20 and 22 MMBtu/MWh, and so on. These heat rate intervals strike a compromise between reduction in fleet size and maintaining some differentiation in efficiency among units. Table A.5 provides the heat rate intervals used for all unit types. Note that natural gas-fired combustion turbines with heat rates below 18,000 Btu/kWh are not aggregated together, as these plants may be dispatched regularly given their greater efficiency.

Table A.5: Heat rate intervals (Btu/kWh) for each type of unit aggregated in the base fleet.

	Heat Rate Intervals (Btu/kWh)				
Unit Type	**Bin 1**	**Bin 2**	**Bin 3**	**Bin 4**	**Bin 5**
Oil-fired combustion turbine	1-10,000	10,000-12,000	12,000-16,000	16,000-20,000	>20,000
Landfill gas	1-14,000	14,000-18,000	18,000-20,000	>20,000	N/A
Municipal solid waste	1-10,000	10,000-20,000	>20,000	N/A	N/A
Natural gas-fired combustion turbine	18,000-20,000	20,000-22,000	22,000-24,000	>24,000	N/A

A.6: HOURLY DEMAND PROFILE IN 2030

Demand in our study system increased from 2004 through 2008, then held largely constant from 2009 to 2013 (Table A.6) [22]. To forecast future demand in our region, rather than rely on aggressive sustained energy efficiency assumptions by the EPA, we instead assume

a continuation of historic demand growth for our region of analysis. Specifically, we assume 0.5% per year incremental energy efficiency savings across the region from 2022-2030 (the phase-in period of the CPP) relative to business as usual load growth as forecast by the EPA [23]. Under this assumption, total and peak demand in 2030 equals 673 TWh and 117.4 GW, respectively. The combined hourly profiles of each state in our study system [6] are scaled up such that annual demand equals forecasted 2030 demand, thereby maintaining the shape of the regional demand curve.

Table A.6: Combined annual demand from 2004 to 2013 of the states included in our study system, based on data from the Energy Information Administration Form 861 [22].

Year	Total Annual Demand (TWh)	Year-to-Year Growth (%)
2013	646	0.2%
2012	645	-0.2%
2011	646	-0.1%
2010	647	5.8%
2009	612	-5.8%
2008	650	-1.2%
2007	658	2.9%
2006	639	-0.5%
2005	643	4.5%
2004	615	0.7%

A.7: DETERMINING AFFECTED EGUS FOR APPLICATION OF SHADOW CO_2 PRICE

We apply the shadow CO_2 price that enforces re-dispatching in our fleet only to affected EGUs under the CPP. Specifically, we include the shadow CO_2 price in the operating cost and reserve offer prices of affected EGUs. This section details the selection of affected EGUs in our

fleets by first describing how the EPA defines affected EGUs in the CPP final rule, then specifying how we operationalize that definition.

In the final CPP, the Environmental Protection Agency (EPA) defines affected electricity generating units (EGUs) as steam generating units, integrated gasification combined cycle units (IGCCs), or stationary combustion turbines that are larger than 25 MW in size, have a fuel burn capability greater than 250 MMBtu per hour of fossil fuel, and began construction before January 8, 2014 [5]. Stationary combustion turbines are only included under the rule if they are either combined cycle units that burn natural gas or combined heat and power combustion turbines.

To account for unit size and fuel burn capability, unit type, and fuel type requirements, we identify units in our base fleet of the above generator types (fossil steam, IGCC, or natural gas combined cycle) that have a capacity greater than 25 MW and fuel burn capability greater than 250 MMBtu per hour. Fossil waste units are listed as steam units in Form 860 from the Energy Information Administration (EIA) [7], so we classify fossil waste units as affected units. Petroleum coke and waste coal units are labeled as steam units in the IPM's parsed file output [14] that we use as the basis for our base fleet, so units of either fuel type are also considered affected units. Landfill gas is not classified as an affected EGU in our model, as it is not defined as natural gas in the CPP [5]. Since all coal-fired generators retrofit with CCS in our compliance scenarios are over 300 MW in size, all flexible CCS generators – including the associated generators – are also considered affected units in our fleets.

None of the parsed IPM file [14], the National Electric Energy Data System [24], and EIA Form 923 [19] contain the date at which generators began construction. As such, we cannot directly determine which generators began construction before January 8, 2014 in order to

account for the start of construction deadline in the CPP. However, according to the National Energy Technology Laboratory [25] and the National Renewable Energy Laboratory [26], natural gas combined cycle (NGCCs) units take roughly 3 years to build, and furthermore have shorter construction times than fossil steam or IGCC units. This information, in conjunction with the year each generator came online in the NEEDS dataset [24], yields a year in which construction began for each generator. If this year is 2013 or earlier, we considered it an affected EGU.

A.8: ECONOMIC DISPATCH MODEL TO DETERMINE SHADOW CO_2 PRICE

We use a simple economic dispatch (ED) model to determine a shadow CO_2 price for each compliance fleet such that total CO_2 emissions from affected EGUs meet the regional mass limit. The ED model minimizes total energy costs subject to the constraints that supply equals demand and each generator's electricity generation varies between zero and its maximum capacity [18]. Total energy costs are defined as:

$$TC = \sum_{i,t} p_{i,t} * OC_i$$

where *i* and *t* index generators and time; *p* = electricity generation; and *OC* = the operating cost of each generator in each period, which accounts for fuel, variable operations and maintenance, and emissions costs. We remove wind and solar generation from demand prior to running the ED model.

A.9: CAPITAL RECOVERY FACTOR AND TOTAL OPERATIONAL COST IN COST-EFFECTIVENESS CALCULATION

To compare capital costs to operational costs and emissions reductions in a single modeling year, we annualize capital costs using a capital recovery factor (CRF) assuming a discount rate of 7% [27], a lifetime for wind of 20 years [28], and a lifetime for CCS retrofits of 30 years [29]. We calculate the CRF as:

$$CRF = \frac{i * (1+i)^n}{(1+i)^n - 1}$$

Total operational costs (TOC) are defined as:

$$TOC = \sum_{i,j,t} \left(p_{i,t} * OC_i + r_{i,t}^j * ROP_i^j + v_{i,t} * SC_i \right) + \sum_t nse_t * CNSE$$

where *i, j* and *t* index generators, reserve types, and time; *p* = electricity generation [MWh]; *OC* = operating cost [$/MWh]; *r* = provided reserves [MWh]; *ROP* = reserve offer price [$/MWh]; *v* = start-ups; *SC* = start-up costs [$]; *nse* = non-served energy [MWh]; and *CNSE* = cost of non-served energy [$/MWh].

A.10: CAPITAL COSTS USED IN COST-EFFECTIVENESS AND BREAK-EVEN CALCULATIONS

In order to account for uncertainty in capital costs, we calculate cost-effectiveness across a range of capital costs. Table A.7 provides the minimum, best guess, and maximum capital costs for wind and normal and flexible CCS used in our analysis. These values are also used when calculating the flexible CCS break-even capital cost.

Table A.7: Range of capital costs included in cost-effectiveness calculations. Flexible CCS capital costs equal the sum of normal CCS and solvent storage capital costs. Normal CCS capital costs from the IECM [30] and National Energy Technology Laboratory [31] include a retrofit factor of 1.25 [29].

Technology	Capital Cost (Minimum / Best Guess / Maximum) ($2011/net kW)	Annualized Capital Cost (Minimum / Best Guess / Maximum) ($2011/net kW)	Sources
Wind	1,300 / 1,800 / 2,270	126 / 170 / 214	[6], [32], [33]
Normal CCS Retrofit	1,160 / 1,270 / 1,380	93 / 102 / 111	[30], [31], [34]
Solvent Storage	7 / 32 / 110	1 / 3 / 9	[35]–[38]
Flexible CCS Retrofit	1,167 / 1,302 / 1,490	94 / 105 / 120	[30], [34]–[38]

A.11: SHADOW CO_2 PRICES NECESSARY TO ACHIEVE COMPLIANCE WITH THE CLEAN POWER PLAN OR STRONGER CLEAN POWER PLAN

Table A.8 provides the shadow CO_2 price necessary for each compliance scenario to comply with the CPP or stronger CPP.

Table A.8: CO_2 price necessary for each compliance scenario to comply with the CPP or stronger CPP. Provided CCS retrofit capacities are de-rated capacities that account for the energy penalty of the CCS system. Scenarios with a CO_2 price include re-dispatching based on that CO_2 price. N/As indicate the compliance scenarios that are not analyzed under either the CPP or stronger CPP.

Compliance Scenarios	CO_2 Price to Comply with the CPP ($/ton)	CO_2 Price to Comply with the Stronger CPP ($/ton)
Re-dispatch	9	39
Normal CCS retrofits, 1.6 GW	7	36
Flexible CCS retrofits, 1.6 GW	7	36
Wind, 2.5 GW	7	N/A
Wind, 3 GW	N/A	36
Normal CCS retrofits, 3.9 GW	3	31
Flexible CCS retrofits, 3.9 GW	3	31
Wind, 5.5 GW	3	N/A

Wind, 9 GW	N/A	31
Normal CCS retrofits, 6.2 GW	0	27
Flexible CCS retrofits, 6.2 GW	0	27
Wind, 6.5 GW	0	N/A
Wind, 14 GW	N/A	27

A.12: GENERATION MIX OF CLEAN POWER PLAN AND STRONGER CLEAN POWER PLAN SCENARIOS

Figure A.1 provides the 2030 generation mix for the base and compliance scenarios with the Clean Power Plan and hypothetical stronger Clean Power Plan.

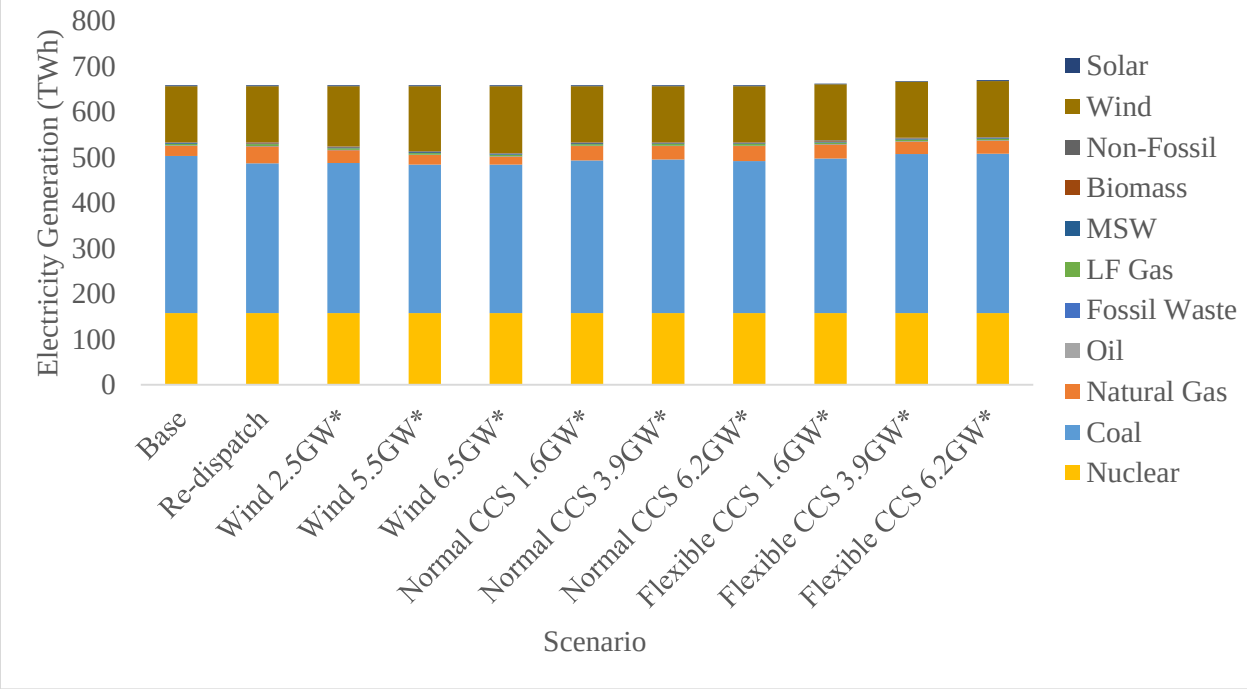

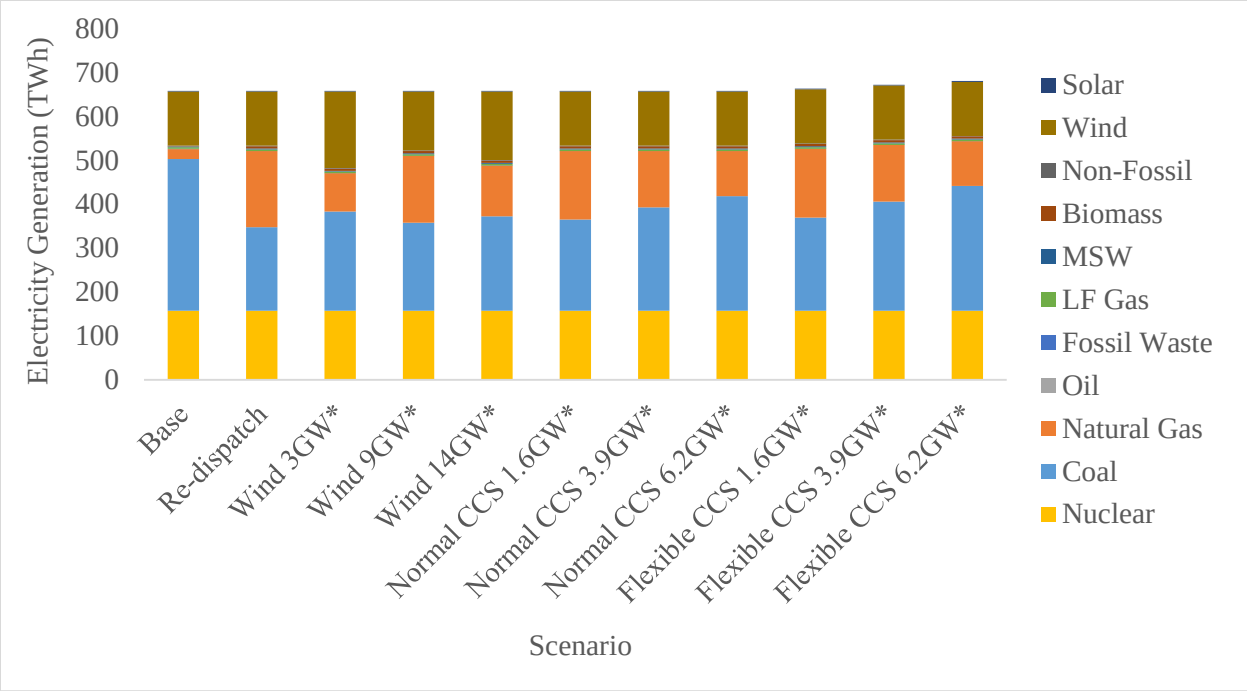

Figure A.1: Generation mix for base and compliance scenarios with the Clean Power Plan (top) and stronger Clean Power Plan (bottom) for 2030. * denotes wind or CCS compliance scenarios that include some re-dispatching.

A.13: FLEXIBLE CCS EQUIVALENT CAPITAL COSTS

Table A.9 and Table A.10 provide equivalent capital costs (ECCs) for flexible CCS under the CPP and stronger CPP, respectively, relative to additional wind capacity and normal CCS retrofits. Each ECC indicates the flexible CCS capital cost at which flexible CCS would achieve as cost-effective CO_2 emissions reductions as, and thereby be competitive with, an alternative compliance strategy. Higher ECCs are better, while negative ECCs suggest that even if the capital costs of flexible CCS were zero, flexible CCS would still be less desirable than the alternative compliance strategy.

Table A.9: ECCs for flexible CCS to achieve as cost-effective emissions reductions as additional wind or normal CCS retrofits under the CPP. ECCs are provided for low, best guess and high capital costs for wind or normal CCS.

Alternative Compliance Scenario	ECC at Low Capital Cost ($/kW)	ECC at Best Guess Capital Cost ($/kW)	ECC at High Capital Cost ($/kW)
Wind, 2.5 GW	-1,120	-240	650
Wind, 5.5 GW	-1,230	-460	310
Wind, 6.5 GW	-1,130	-550	30
Normal CCS, 1.6 GW	1,350	1,460	1,570
Normal CCS, 3.9 GW	1,360	1,470	1,580
Normal CCS, 6.2 GW	1,370	1,480	1,590

Table A.10: ECCs for flexible CCS to achieve as cost-effective emissions reductions as additional wind or normal CCS retrofits under the stronger CPP. ECCs are provided for low, best guess and high capital costs for wind or normal CCS.

Alternative Compliance Scenario	ECC at Low Capital Cost ($/kW)	ECC at Best Guess Capital Cost ($/kW)	ECC at High Capital Cost ($/kW)
Wind, 3 GW	-1,710	-650	410
Wind, 9 GW	-1,770	-510	750
Wind, 14 GW	-1,610	-370	880
Normal CCS, 1.6 GW	1,310	1,420	1,530
Normal CCS, 3.9 GW	1,300	1,410	1,530
Normal CCS, 6.2 GW	1,360	1,470	1,580

A.14: REFERENCES

[1] Energy Exemplar, "PLEXOS Integrated Energy Model. Version 7.2," 2015.

[2] M. Craig, P. Jaramillo, H. Zhai, and K. Klima, "The economic merits of flexible carbon capture and sequestration as a compliance strategy with the Clean Power Plan," *Environ. Sci. Technol.*, vol. 51, pp. 1102–1109, 2017.

[3] D. L. Oates and P. Jaramillo, "Production cost and air emissions impacts of coal cycling in power systems with large-scale wind penetration," *Environ. Res. Lett.*, vol. 8, no. 2, p. 24022, Jun. 2013.

[4] D. Lew, "Western Wind and Solar Integration Study," 2010.

[5] U.S. Environmental Protection Agency, "Carbon pollution emission guidelines for existing stationary sources: Electric utility generating units. Federal Register Vol. 80: 64661-65120," 2015.

[6] U.S. Environmental Protection Agency, "Documentation for EPA Base Case v.5.13 Using

the Integrated Planning Model," 2013.

[7] U.S. Energy Information Administration, "Form EIA-860," *EIA.gov*, 2015. [Online]. Available: https://www.eia.gov/electricity/data/eia860/.

[8] R. Lueken, "PJM Hourly Open-source Reduced-form Unit Commitment Model (PHORUM)," 2013. [Online]. Available: https://github.com/rlueken/PHORUM. [Accessed: 12-Mar-2015].

[9] R. Lueken, "Reducing Carbon Intensity in Restructured Markets: Challenges and Potential Solutions," Carnegie Mellon University, 2014.

[10] U.S. National Energy Technology Laboratory, "Impact of Load Following on Power Plant Cost and Performance: Literature Review and Industry Interviews," 2012.

[11] IEAGHG, "Operating Flexibility of Power Plants with CCS," 2012.

[12] MIT Energy Initiative, "Symposium on Managing Large-scale Penetration of Intermittent Renewables: Findings in brief," 2011.

[13] E. McDonald-Buller, Y. Kimura, M. Craig, G. McGaughey, D. Allen, and M. Webster, "Dynamic Management of NOx and SO2 Emissions in the Texas and Mid-Atlantic Electric Power Systems and Implications for Air Quality," *Environ. Sci. Technol.*, vol. 50, no. x, pp. 1611–1619, 2016.

[14] U.S. Environmental Protection Agency, "Parsed File: Mass-Based, 2030. Docket No. EPA-HQ-OAR-2013-0602," 2015.

[15] D. L. Oates, "Low Carbon Policy and Technology in the Power Sector: Evaluating Economic and Environmental Effects," Carnegie Mellon University, 2015.

[16] U.S. Environmental Protection Agency, "Stationary Gas Turbines," in *Compilation of Air Pollutant Emissions Factors, Volume 1: Stationary Point and Area Sources, AP-42*, 5th ed., 2000.

[17] U.S. Environmental Protection Agency, "Federal Implementation Plans: Interstate Transport of Fine Particulate Matter and Ozone and Correction of SIP Approvals, 76 Federal Register 152 (8 Aug 2011), pp. 48207-48712.," 2011.

[18] D. L. Oates and P. Jaramillo, "State cooperation under the EPA's proposed clean power plan," *Electr. J.*, vol. 28, no. 3, pp. 26–40, 2015.

[19] U.S. Energy Information Administration, "Form EIA-923," 2015.

[20] U.S. National Renewable Energy Laboratory, "Transmission Grid Integration: Eastern Wind Dataset," 2012.

[21] U.S. National Renewable Energy Laboratory, "Transmission Grid Integration: Solar Power Data for Integration Studies Dataset," 2010.

[22] U.S. Energy Information Administration, "Form EIA-861," 2015.

[23] U.S. Environmental Protection Agency, "Data File: Demand-Side Energy Efficiency Appendix – Illustrative 3% Scenario." 2015.

[24] U.S. Environmental Protection Agency, “National Electric Energy Data System (Version 5.15).” 2015.

[25] U.S. National Energy Technology Laboratory, “NGCC Plant – Combined Cycle,” 2007. [Online]. Available: http://www.netl.doe.gov/KMD/cds/disk50/NGCC Plant Case_FClass_051607.pdf.

[26] U.S. National Renewable Energy Laboratory, “Annual Technology Baseline 2015,” 2015.

[27] The White House Office of Management and Budget, “Guidelines and discount rates for benefit-cost analysis of federal programs. Circular No. A-94 Revised.,” 1992.

[28] J. Lamy, I. L. Azevedo, and P. Jaramillo, “The role of energy storage in accessing remote wind resources in the Midwest,” *Energy Policy*, vol. 68, no. 2006, pp. 123–131, 2014.

[29] H. Zhai, Y. Ou, and E. S. Rubin, “Opportunities for decarbonizing existing U.S. coal-fired power plants via CO2 capture, utilization and storage,” *Environ. Sci. Technol.*, vol. 49, no. 13, pp. 7571–9, 2015.

[30] Carnegie Mellon University, “Integrated Environmental Control Model. Version 8.0.2.” 2015.

[31] U.S. National Energy Technology Laboratory, “Cost and Performance Baseline for Fossil Energy Plants. Volume 1,” 2013.

[32] Lazard, “Lazard’s Levelized Cost of Energy Analysis. Version 8.0,” 2014.

[33] U.S. Energy Information Administration, “Updated Capital Cost Estimates for Utility Scale Electricity Generating Plants,” 2013.

[34] S. Specker, J. Phillips, and D. Dillon, “The Potential Growing Role of Post-combustion CO2 Capture Retrofits in Early Commercial Applications of CCS to Coal-fired Power Plants,” 2009.

[35] P. C. Van der Wijk, A. S. Brouwer, M. Van den Broek, T. Slot, G. Stienstra, W. Van der Veen, and A. P. C. Faaij, “Benefits of coal-fired power generation with flexible CCS in a future northwest European power system with large scale wind power,” *Int. J. Greenh. Gas Control*, vol. 28, pp. 216–233, 2014.

[36] D. L. Oates, P. Versteeg, E. Hittinger, and P. Jaramillo, “Profitability of CCS with flue gas bypass and solvent storage,” *Int. J. Greenh. Gas Control*, vol. 27, pp. 279–288, 2014.

[37] P. Versteeg, D. L. Oates, E. Hittinger, and E. S. Rubin, “Cycling coal and natural gas-fired power plants with CCS,” *Energy Procedia*, vol. 37, pp. 2676–2683, 2013.

[38] D. Patiño-Echeverri and D. C. Hoppock, “Reducing the energy penalty costs of postcombustion CCS systems with amine-storage,” *Environ. Sci. Technol.*, vol. 46, pp. 1243–1252, 2012.

APPENDIX B:
SUPPLEMENTAL INFORMATION FOR CHAPTER 3

B.1: DESCRIPTION OF VENTING COMPONENTS OF FLEXIBLE CCS MODEL

While we do not assess flexible CCS with venting in the main text of this paper, we do assess operations of flexible CCS with solvent storage and venting in Section B.7. Additionally, providing the option to include venting capabilities in our flexible CCS model affects the structure of our model for flexible CCS generators equipped only with solvent storage, as discussed in Section B.4. For both reasons, we explain the venting components of our flexible CCS model in this section. These venting components can be modeled together or separate from the solvent storage components.

Figure B.1 provides a schematic of a flexible CCS generator that includes a flue gas bypass and solvent storage system. With respect to design assumptions, as when discharging stored solvent, we assume that venting can reduce the CCS system's parasitic load by up to 90%, which corresponds to eliminating the parasitic load of the solvent regenerator and CO_2 compressor [1]. Also, as when discharging stored solvent, venting flue gas while not charging stored solvent enables greater net electricity output at greater efficiency than during normal CCS operations. In this operational mode, venting allows for faster ramping than during normal CCS operations, as venting entails increasing the steam turbine load rather than fuel input. We also allow our flexible CCS generator to vent CO_2 emissions while charging stored solvent. Doing so results in a lower CO_2 capture rate, but allows a flexible CCS generator to maintain constant fuel input and net electricity output relative to normal CCS operations.

To represent flexible CCS operations while venting, we use two proxy units, vent and vent while charging. Figure B.2 provides a tree depicting which venting and solvent storage

proxy units are on or off given flexible CCS operations. The vent proxy unit accounts for increased net electricity output and efficiency relative to normal CCS operations when venting. Conversely, the vent while charging unit allows for the same net electricity output as during normal CCS operations when venting while charging stored lean solvent. As for stored solvent proxy units, we parametrize venting proxy units with IECM-derived linear regressions, as described in Section B.3. The full mathematical formulation of our flexible CCS model, provided in Section B.4, accounts for venting operations as well as solvent storage.

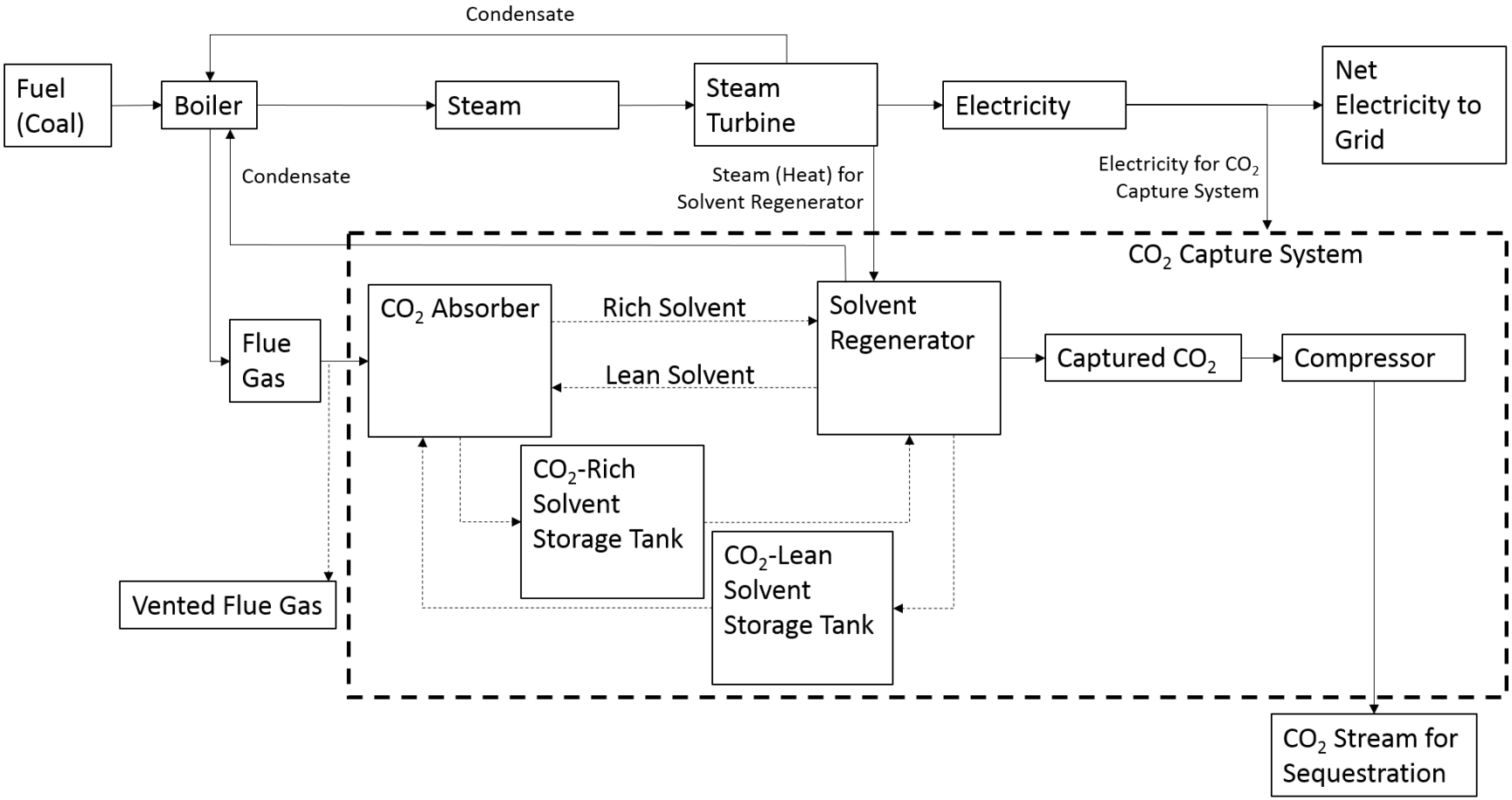

Figure B.1: A full schematic of a flexible CCS generator equipped with a flue gas bypass and solvent storage system. The dashed box indicates the CO_2 capture system. Dashed lines indicate operational choices at the generator: venting flue gas or using stored solvent in place of continuously-regenerated solvent.

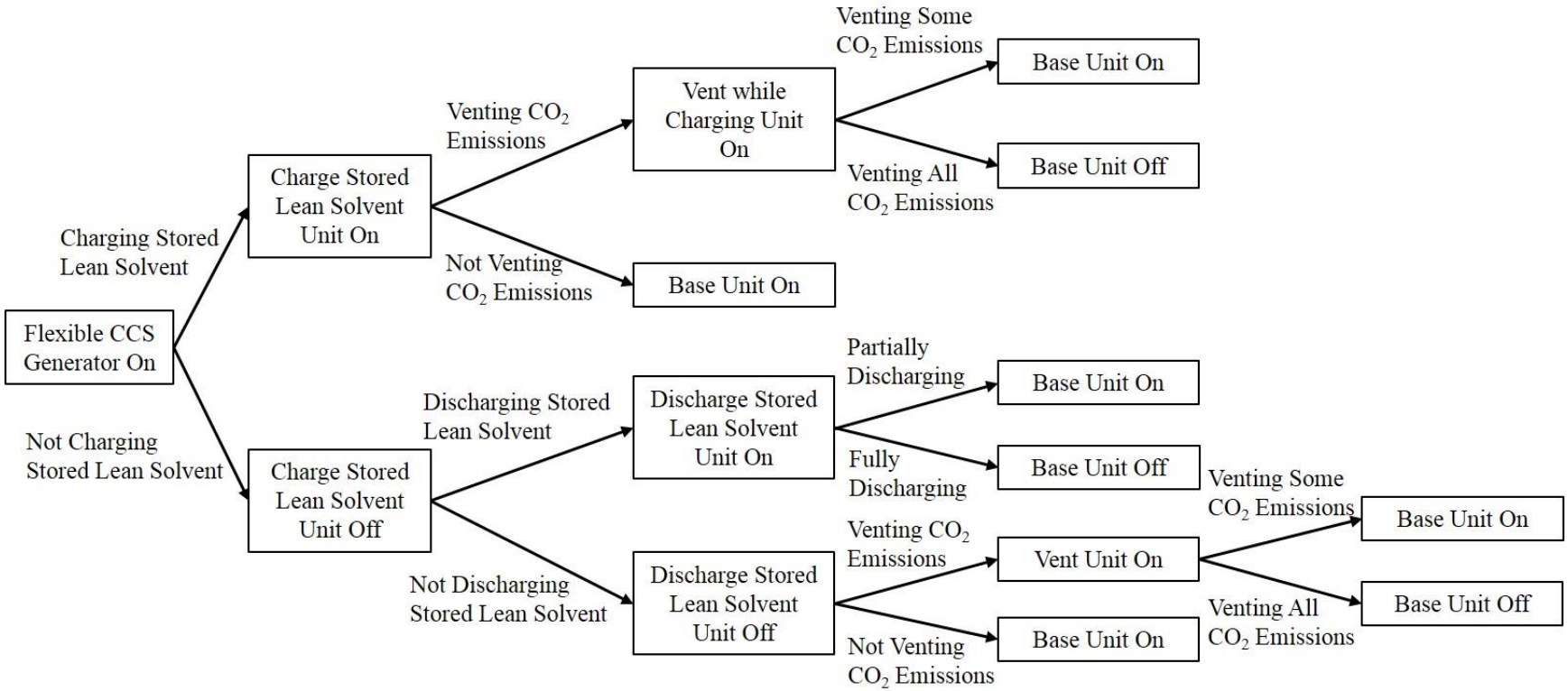

Figure B.2: Tree showing which venting and solvent storage proxy units are on or off given the operations of a flexible CCS generator equipped with a flue gas bypass and solvent storage system at any given time. When the base proxy unit is on, the continuous solvent proxy unit is also on.

B.2: JUSTIFICATION OF FLEXIBLE CCS DESIGN PARAMETERS

This section details the justification of the flexible CCS design parameters. We assume CCS retrofits occur at existing coal-fired power generators.

Maximum power output of steam turbine: We assume the only modification to the steam turbine during a CCS retrofit is the installation of a steam extractor. As such, the maximum power output of the steam turbine at each coal-fired generator retrofit with CCS equals the net capacity of the generator prior to the CCS retrofit.

Solvent storage tank capacity: The solvent storage tanks' capacities determine how many hours of full load the stored lean solvent can enable while maintaining a 90% capture rate. Previous papers on flexible CCS have used stored solvent capacities ranging from 1 to 4 hours [2]–[4]. For this model, we assume solvent storage tank sizes of 1 or 2 hours.

Regenerator size: The solvent throughput capacity of the regenerator train affects operations while charging stored lean solvent by limiting the amount of continuous and stored solvent that can be regenerated at once. At a normal CCS generator, only continuous solvent passes through the regenerator train, so the throughput capacity of the train can be set to the maximum flow rate of continuous solvent. But at a flexible CCS generator, two solvent streams – continuous and stored rich solvent – can pass through the regenerator train. The solvent throughput capacity of the train dictates whether the two solvent streams can be regenerated simultaneously or if one displaces the other. For instance, an "over-sized" solvent regenerator train – that is, a regenerator train at a flexible CCS generator with a *greater* solvent throughput capacity than that of a train at a normal CCS facility of the same net power output capacity during normal operations – could regenerate some stored lean solvent while simultaneously regenerating continuous lean solvent at its maximum flow rate. If, on the other hand, the

throughput solvent capacity of the regenerator train at a flexible CCS generator equals that of a train at a normal CCS generator of equal net power output capacity – which we call an "equally-sized" solvent regenerator train – stored rich solvent sent to the regenerator train displaces continuous rich solvent.

Wijk et al. [4] assume two solvent regenerator train throughput capacities, equally-sized and 25% over-sized, whereas Cohen et al. [5] base their decision to use an over-sized solvent regenerator train on a simple solvent discharge potential heuristic. Alternatively, Versteeg et al. [3] and Oates et al. [2] use profit-maximizing optimization models to determine the optimal solvent regenerator throughput capacity. Under complete information, Versteeg et al. [3] determine the optimal throughput capacity as equally-sized, whereas Oates et al. [2] determine that an under-sized solvent regenerator is optimal. However, these profit-maximizing optimization models may neglect public (i.e., system) benefits of flexible CCS that we aim to quantify and therefore may undervalue larger regenerators. As such, we model an equally-sized solvent regenerator in this research. With an equally-sized solvent regenerator, charging stored lean solvent necessarily reduces regeneration of continuous solvent, which in turn necessitates a reduction in fuel input and net electricity to the grid in order to maintain a constant CO_2 capture rate (i.e., in order to continue capturing 90% of CO_2 emissions).

Maximum achievable reduction in parasitic load while discharging: Patiño-Echeverri and Hoppock [1] summarize the results of three studies that divide the parasitic load, or overall energy penalty in net plant efficiency, of a CCS system among its components. They find that pumps, fans, and other losses account for roughly 8-9% of the total parasitic load of the CCS system, whereas the solvent regenerator and CO_2 compressor largely account for the remainder. Like Patiño-Echeverri and Hoppock [1], we assume that discharging stored lean solvent can

eliminate the parasitic load of the solvent regenerator and CO_2 compressor. Consequently, while discharging stored lean solvent, the portion of the parasitic load from pumps, fans and other losses would remain. We set this remaining parasitic load to 10% of the total parasitic load of the CCS system, or 10% of the overall energy penalty in net plant efficiency of the CCS system.

B.3: REGRESSIONS BASED ON DATA FROM THE INTEGRATED ENVIRONMENTAL CONTROL MODEL

To estimate seven normal and/or flexible CCS parameters (Table B.1), we constructed linear regression models with output from the Integrated Environmental Control Model (IECM), a computational tool for evaluating fossil fuel-fired power plants with and without CCS [6]. More specifically, we regress each parameter separately against heat rate for bituminous and sub-bituminous fuel, which then allows us to estimate the parameter value for retrofitting a given generator as a function of heat rate and fuel type. In this section, we first discuss how we obtain the necessary data from the IECM, then further define each parameter estimated this way, and finally provide the linear regressions.

Table B.1: Flexible and, in some cases, normal CCS operational parameters estimated using regressions based on data from the IECM.

CCS Type	Parameter Based on IECM Data
Normal and flexible	Net capacity penalty from normal or flexible CCS retrofit during normal operations (%)
Normal and flexible	Net heat rate penalty from normal or flexible CCS retrofit during normal operations (%)
Flexible	Net capacity penalty at maximum achievable reduction of CO_2 capture system parasitic load while discharging stored solvent or venting (%)

Flexible	Net heat rate penalty at maximum achievable reduction of CO_2 capture system parasitic load while discharging stored solvent or venting (%)
Flexible	Net electricity delivered to grid per unit of thermal and electric energy (hereafter "equivalent energy") used by CO_2 capture system during normal operations (MWh)
Flexible	Net electricity delivered to grid enabled by discharging stored lean solvent per unit of equivalent energy used to store lean solvent (MWh)
Flexible	Equivalent energy required to regenerate continuous lean solvent in order to capture CO_2 emissions from fuel input to regenerate stored lean solvent per unit of equivalent energy used to store lean solvent (MWh)

B.3.1: Obtaining Data from IECM

To obtain data from IECM for use in our regressions, we construct three generator configurations for a given generator efficiency: 1) a non-CCS coal-fired generator, 2) a CCS-retrofitted coal-fired generator, and 3) a flexible CCS coal-fired generator engaged in full discharge of its stored solvent. We construct these three model generators for each of sub-, super- and ultrasuper-critical coal-fired power plant types, thereby yielding parameter values across different heat rates. We repeat this process using bituminous (Illinois #6 coal) and sub-bituminous (Wyoming Powder River Basin coal) coal types.

We begin with the default IECM coal-fired generator to model the non-CCS coal-fired generator. The non-CCS coal-fired generator is equipped with in-furnace NOx controls, hot-side selective catalytic reduction (SCR), cold-side electrostatic precipitator (ESP), wet flue gas desulfurization (FGD), and carbon injection control technologies, as our CCS retrofit criteria assumes installation of these control technologies, and the generator uses once-through cooling. The base non-CCS coal-fired generator has a gross output of 650 MW.

We then build the CCS-retrofit coal-fired generator. Crucially, we assume constant fuel input capacity at the generator post-CCS retrofit. Thus, to model a CCS-retrofit generator with

the same fuel input as the non-CCS generator, we install an amine CO_2 capture system on the non-CCS generator, and then reduce its gross output until the fuel input equals that of the non-CCS generator.

To construct the flexible CCS generator while fully discharging stored lean solvent, we begin with the CCS-retrofit generator and set its gross electrical output to 650 MW. Since we assume a 90% reduction in the parasitic load of the CO_2 capture system while fully discharging stored solvent based Patiño-Echeverri and Hoppock (2012), we reduce the energy requirements of the CO_2 capture system to mirror eliminating 90% of the parasitic load of the CO_2 capture system while discharging stored lean solvent. Specifically, we set the solvent regenerator heat requirement to 0, and then simultaneously vary the amine scrubber power requirement and CO_2 unit compression energy values until the energy use of the CO_2 capture system equals roughly 10% of the CO_2 capture system energy use of the CCS-retrofit generator. Note that when the total CO_2 capture system energy use equals 10% of that for the CCS-retrofit generator, the amine scrubber power requirement and CO_2 unit compression energy may not necessarily equal 10% of those values for the CCS-retrofit generator. Table B.2 provides the CO_2 unit compression energy and amine scrubber power requirement values used for each generator.

Table B.2: Amine scrubber power requirement and CO_2 unit compression energy values used to model flexible CCS generators during full discharging of stored lean solvent in the IECM.

IECM Field	**Coal Type**	**Coal-Fired Plant Type**	**Normal CCS Value**	**Flexible CCS Value**
Amine Scrubber Power Requirement (% MWg)	Subbit	Subcritical	10.6	2.1
CO_2 Unit Compression Energy (kWh/ton CO_2)	Subbit	Subcritical	84.4	16.9
Amine Scrubber Power Requirement (% MWg)	Subbit	Supercritical	9.7	1.9

CO_2 Unit Compression Energy (kWh/ton CO_2)	Subbit	Supercritical	84.4	16.9
Amine Scrubber Power Requirement (% MWg)	Subbit	Ultra-supercritical	8.7	1.7
CO_2 Unit Compression Energy (kWh/ton CO_2)	Subbit	Ultra-supercritical	84.4	16.9
Amine Scrubber Power Requirement (% MWg)	Bit	Subcritical	9.5	1.9
CO_2 Unit Compression Energy (kWh/ton CO_2)	Bit	Subcritical	84.4	16.9
Amine Scrubber Power Requirement (% MWg)	Bit	Supercritical	8.8	1.8
CO_2 Unit Compression Energy (kWh/ton CO_2)	Bit	Supercritical	84.4	16.9
Amine Scrubber Power Requirement (% MWg)	Bit	Ultra-supercritical	7.9	1.6
CO_2 Unit Compression Energy (kWh/ton CO_2)	Bit	Ultra-supercritical	84.4	16.9

B.3.2: Description of Parameters Estimated with Regressions

From these 18 generators (3 types of plants for each of 3 heat rates and 2 fuel types), we extract several design values that we use to estimate the desired parameters. We calculate the capacity and net heat rate penalties as:

$$HRP^{CCSRetrofit} = \frac{HR^{CCSRetrofit} - HR^{NoCCS}}{HR^{NoCCS}} \quad (1)$$

$$CP^{CCSRetrofit} = \frac{\bar{P}^{CCSRetrofit} - \bar{P}^{NoCCS}}{\bar{P}^{NoCCS}} \quad (2)$$

$$HRP^{FullDischarging} = \frac{HR^{FullDischarging} - HR^{NoCCS}}{HR^{NoCCS}} \quad (3)$$

$$CP^{FullDischarging} = \frac{\bar{P}^{FullDischarging} - \bar{P}^{NoCCS}}{\bar{P}^{NoCCS}} \quad (4)$$

where *CCSRetrofit* refers to the coal-fired generator after CCS retrofit, *FullDischarging* refers to the coal-fired generator retrofit with flexible CCS while fully discharging stored solvent, *NoCCS* refers to the coal-fired generator prior to CCS retrofit, *HR* = net heat rate (MMBtu/MWh), *HRP*

= net heat rate penalty (MMBtu/MWh), *CP* = capacity penalty (as fraction of maximum capacity), and $\bar{P}$ = maximum capacity (MW).

We extract three other parameters from the IECM data and include them in the unit constraints detailed below. We use two of these parameters to calculate net output to the grid during stored solvent charging: (1) electricity delivered to the grid during normal CCS operations per unit of energy used to capture CO_2 and (2) energy used to continuously regenerate solvent to capture CO_2 emissions from the fuel used to store solvent per unit of energy used to store solvent. We calculate the former parameter by dividing the net electricity output of the normal CCS IECM generator by the CCS net capacity penalty. To calculate the latter parameter, we begin by calculating the tons of fuel to provide the energy to regenerate each ton of solvent at the normal CCS generator:

$$\frac{Tons\ Fuel\ for\ Energy}{Regenerate\ 1\ Ton\ Solvent} = \frac{Gross\ HR}{\frac{Solvent\ Flow\ Rate}{E\ to\ CO_2\ Capture}}$$

With that value, we know the tons of fuel that need to be input for each ton of solvent regenerated to be stored. We then need to calculate the amount of solvent that needs to be regenerated to capture the CO_2 emissions from that fuel. To do so, we divide the total solvent flow rate by the total fuel input for the normal CCS generator.

$$\frac{Tons\ Solvent}{Capture\ 1\ Ton\ Fuel's\ CO_2\ Emissions} = \frac{Total\ Solvent\ Flow\ Rate}{Total\ Fuel\ Input}$$

Finally, we can calculate the tons of extra solvent that needs to be continuously regenerated to capture the CO_2 emissions from the fuel used to store each ton of solvent. If we let X = tons fuel to regenerate 1 ton of solvent, Z = tons solvent to capture 1 ton of fuel's CO_2 emissions, B = tons of solvent to be stored, and A = tons of extra solvent to be continuously regenerated, then:

$$Total\ Fuel\ Consumption = X * A + X * B$$

Since only A captures CO_2 emissions:

$$Tons\ Fuel's\ CO_2 Emissions\ to\ be\ Captured = A * \frac{1}{Z}$$

If all CO_2 emissions are captured, then they must be captured by A, as B does not capture CO_2:

$$A * \frac{1}{Z} = X * A + X * B$$

$$A * \frac{1}{Z} = X * A + X * B$$

$$A * (\frac{1}{Z} - X) = X * B$$

$$A = \frac{X * B}{\frac{1}{Z} - X}$$

$$\frac{A}{B} = \frac{X}{\frac{1}{Z} - X}$$

Or:

$$\frac{Ton\ Extra\ Continuous\ Solvent}{Ton\ Stored\ Solvent}$$

$$= \frac{\frac{Tons\ Fuel}{Regenerate\ 1\ Ton\ Solvent}}{\frac{1}{\frac{Tons\ Solvent}{Capture\ 1\ Ton\ Fuel's\ CO_2\ Emissions}} - \frac{Tons\ Fuel}{Regenerate\ 1\ Ton\ Solvent}} \quad (5)$$

Note that the energy required to regenerate a ton of solvent is the same for continuously regenerated and stored solvent. As a result, tons of extra continuous solvent per ton of stored solvent is equivalent to energy required to continuously regenerate solvent per energy required to regenerate stored solvent.

The third of the remaining IECM-derived parameters, energy delivered to the grid while discharging stored solvent per energy used to store lean solvent, determines how much energy

can be output while discharging stored lean solvent for each unit of energy input to store solvent during charging. We calculate this value using data from the normal and solvent discharging CCS IECM generators:

$$\frac{E\ to\ Grid\ While\ Discharging\ Stored\ Solvent}{E\ Used\ to\ Store\ Solvent} = \frac{Tons\ Solvent\ Regenerated}{E\ CO_2\ Capture} * \frac{E\ to\ Grid\ While\ Discharing}{Ton\ Solvent\ Discharged} \quad (6)$$

B.3.3: Regressions

The regressions of the previously described seven parameters estimated from the IECM data are provided in Figure B.3.

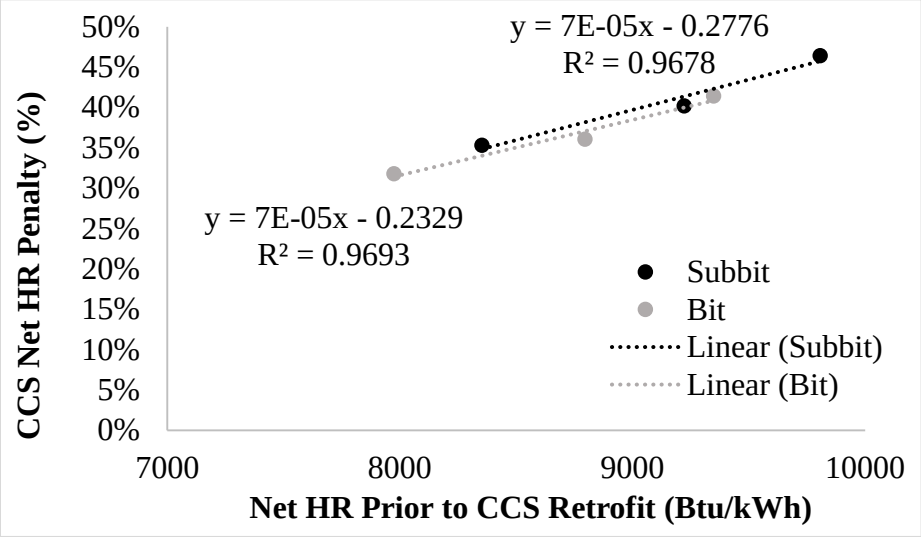

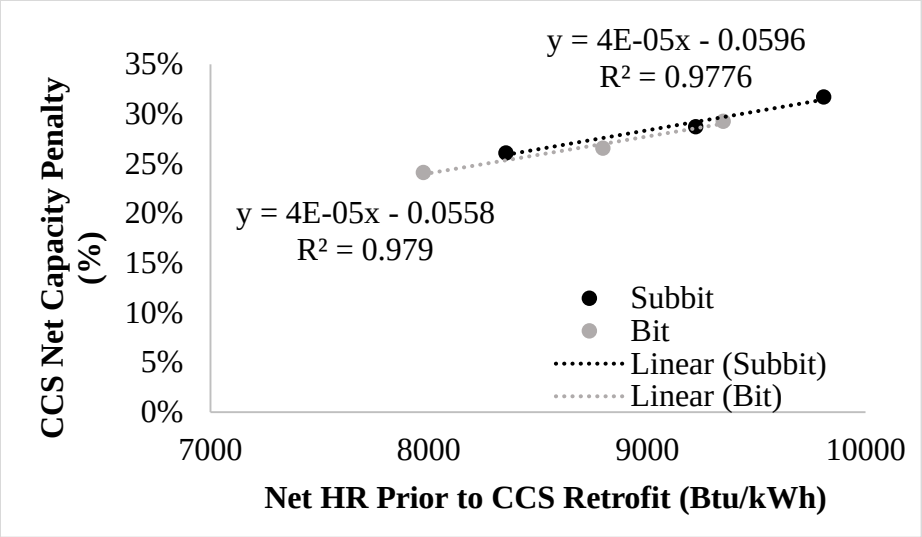
y = 4E-05x - 0.0596
R² = 0.9776
y = 4E-05x - 0.0558
R² = 0.979
CCS Net Capacity Penalty (%)
35%
30%
25%
20%
15%
10%
5%
0%
7000
8000
9000
10000
Net HR Prior to CCS Retrofit (Btu/kWh)
Subbit
Bit
Linear (Subbit)
Linear (Bit)

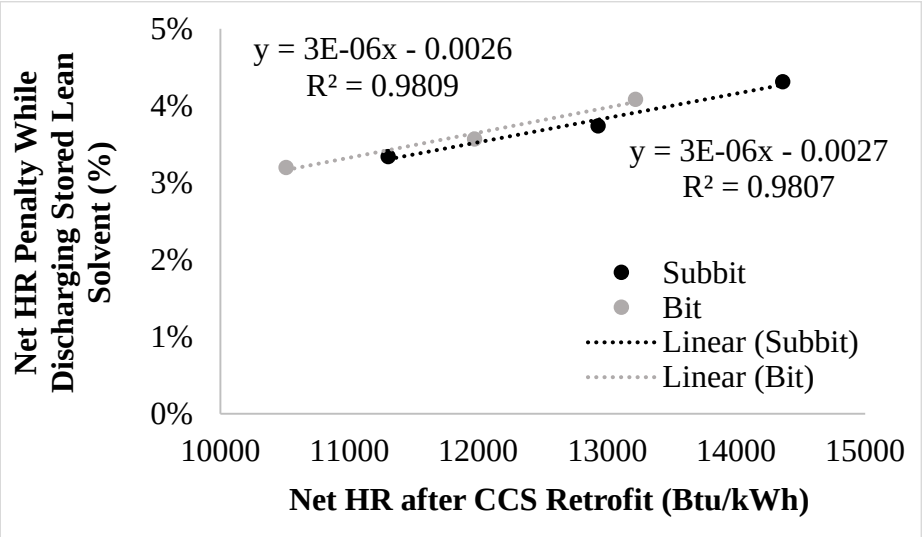
y = 3E-06x - 0.0026
R² = 0.9809
y = 3E-06x - 0.0027
R² = 0.9807
Net HR Penalty While Discharging Stored Lean Solvent (%)
5%
4%
3%
2%
1%
0%
10000
11000
12000
13000
14000
15000
Net HR after CCS Retrofit (Btu/kWh)
Subbit
Bit
Linear (Subbit)
Linear (Bit)

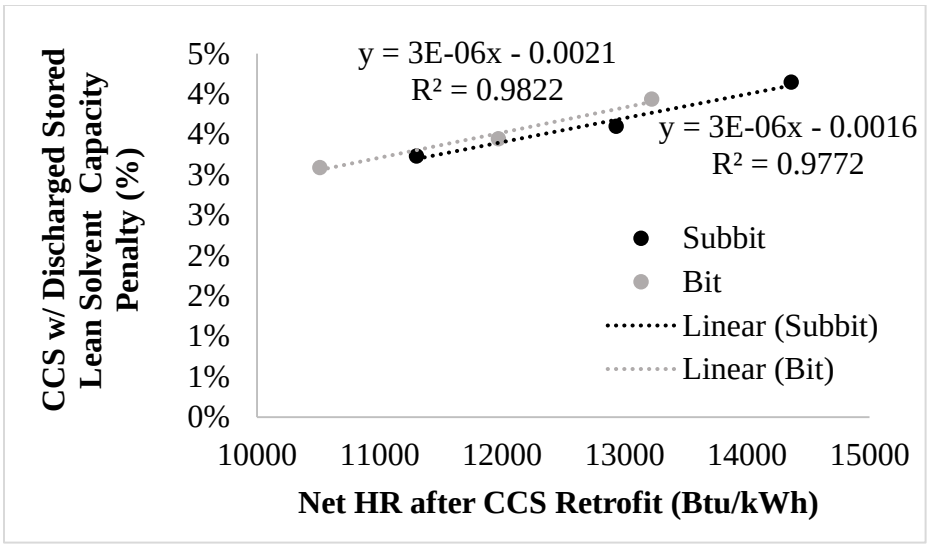
CCS w/ Discharged Stored Lean Solvent Capacity Penalty (%)
5%
4%
4%
3%
3%
2%
2%
1%
1%
0%
y = 3E-06x - 0.0021
R² = 0.9822
y = 3E-06x - 0.0016
R² = 0.9772
Subbit
Bit
Linear (Subbit)
Linear (Bit)
10000
11000
12000
13000
14000
15000
Net HR after CCS Retrofit (Btu/kWh)

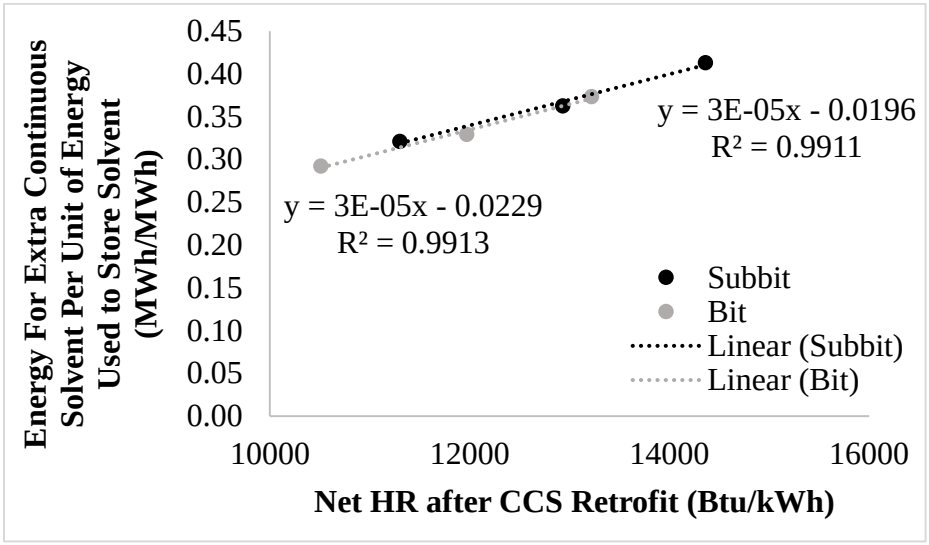
Energy For Extra Continuous Solvent Per Unit of Energy Used to Store Solvent (MWh/MWh)
0.45
0.40
0.35
0.30
0.25
0.20
0.15
0.10
0.05
0.00
y = 3E-05x - 0.0196
R² = 0.9911
y = 3E-05x - 0.0229
R² = 0.9913
Subbit
Bit
Linear (Subbit)
Linear (Bit)
10000
12000
14000
16000
Net HR after CCS Retrofit (Btu/kWh)

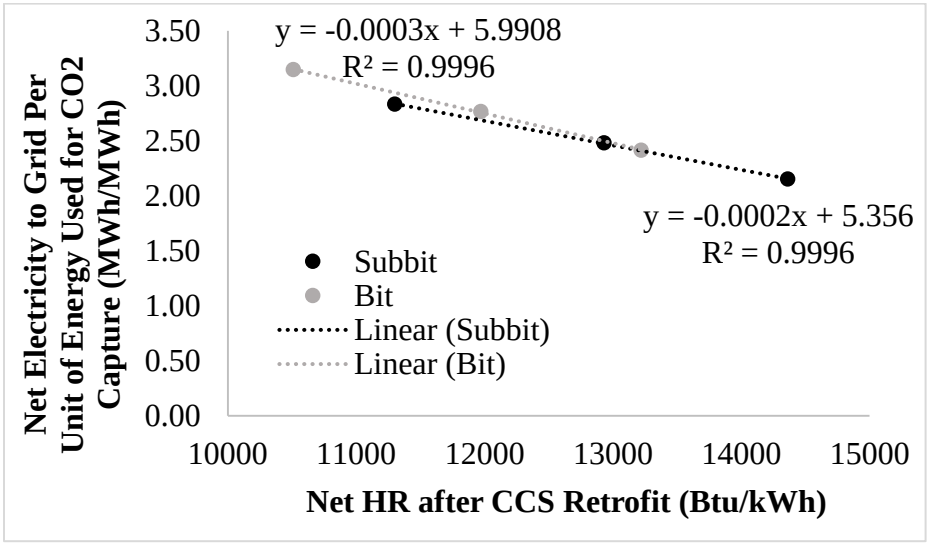
Net Electricity to Grid Per Unit of Energy Used for CO2 Capture (MWh/MWh)
3.50
3.00
2.50
2.00
1.50
1.00
0.50
0.00
y = -0.0003x + 5.9908
R² = 0.9996
y = -0.0002x + 5.356
R² = 0.9996
Subbit
Bit
Linear (Subbit)
Linear (Bit)
10000
11000
12000
13000
14000
15000
Net HR after CCS Retrofit (Btu/kWh)

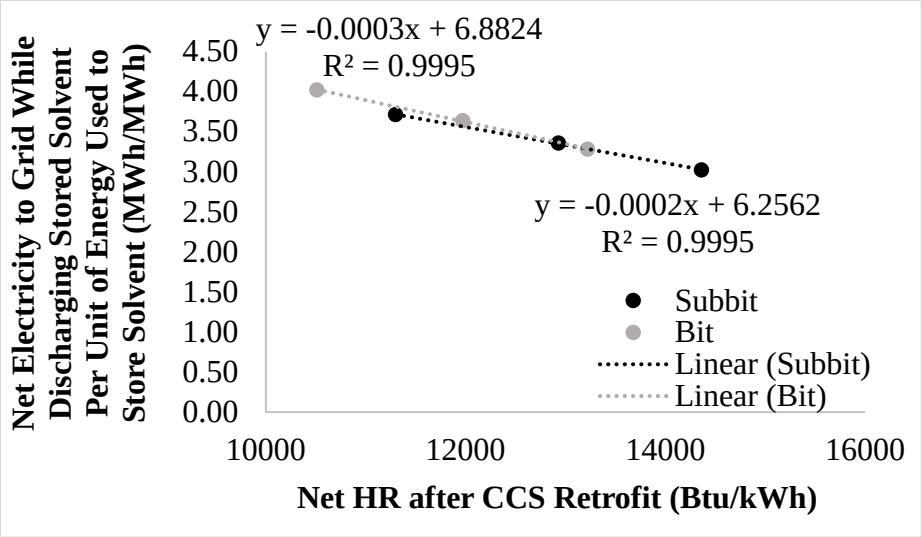

Figure B.3: Regressions of various CCS operational and design parameters estimated using data from the IECM.

Using these regressions, we estimate a unique value for each of the seven parameters for each coal generator retrofit with CCS. We determine the coal type for each generator in our power plant fleet using data from the IPM parsed files and use the regressions for that fuel type. We estimate the CCS capacity and heat rate penalties with the generator's pre-CCS retrofit heat rate, and the other five parameters using the generator's net heat rate post-CCS retrofit. Most of the pre-CCS net heat rates of the generators retrofit with CCS fall within the range of heat rates of the IECM generators used in the above regressions, as shown in Figure B.4.

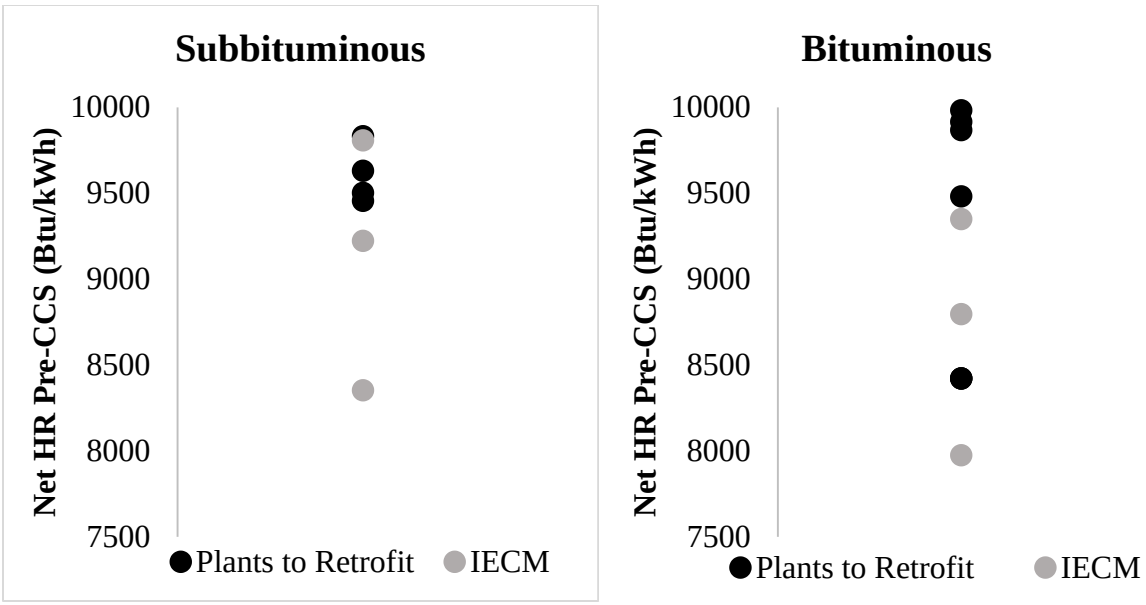

Figure B.4: Net heat rates pre-CCS retrofit of coal-fired generators eligible for CCS retrofits in our fleet (blue dots) and of coal-fired generators modeled in IECM to derive our CCS parameters (orange dots).

B.4: MATHEMATICAL FORMULATION OF FLEXIBLE CCS MODEL

This section provides a detailed mathematical formulation of our model of a flexible CCS generator equipped with solvent storage and venting. To model a flexible CCS generator equipped only with solvent storage, as done for the analysis in this paper, the venting components of our model are removed. Table B.3 provides the definitions of variables and parameters used in the subsequent parametrization of proxy units and proxy unit constraints.

Table B.3: Definitions of variables and parameters used in flexible CCS model formulation. Note that "equivalent energy" equals thermal and electric energy.

Decision Variable	Definition
$c_{i,t}$	Change in power output from generator i at time t (MW)
$e_{i,t}$	Equivalent energy consumed by generator i at time t (MWh)
$ev^{LEAN}{}_{i,t}$	Amount of solvent lean stored in tank i at the end of time t (MWh)

$f_{i,t}$	Stored lean solvent inflow at generator i and time t (MWh)
$m_{i,t}$	Equivalent energy consumed to charge stored lean solvent by generator i at time t (MWh)
$n^{HEAD}{}_{i,t}$	Electricity consumed in pumping water into reservoir head at pumped hydropower facility i in hour t (MWh)
$n^{TAILi}{}_{,t}$	Electricity generated by releasing water into reservoir tail from reservoir head at pumped hydropower facility i in hour t (MWh)
$o_{i,t}$	Stored lean solvent outflow at generator i and time t (MWh)
$p_{i,t}$	Net electricity generation by generator i at time t (MWh)
$r_{i,t}$	Provided reserves of given type by generator i at time t(MW)
$u_{i,t}$	Binary variable indicating on/off state of generator i at time t, where 1 indicates on {0,1}
Parameter	**Definition**
$C^{MAX}{}_i$	Max ramp rate in up and down direction of generator i (MW/min.)
CP^{CCS}	Net capacity penalty from normal or flexible CCS retrofit during normal operations (%) (estimated with IECM)
$CP^{Discharge}$	Net capacity penalty at maximum achievable reduction of CO_2 capture system parasitic load while discharging stored solvent or venting (%) (estimated with IECM)
E^{Grid}	Net electricity delivered to grid per unit of equivalent energy used by CO_2 capture system during normal operations (MWh) (estimated with IECM)
$E^{Discharge}$	Net electricity delivered to grid enabled by discharging stored lean solvent per unit of equivalent energy used to store lean solvent (MWh) (estimated with IECM)
$E^{ContSolvent}$	Equivalent energy required to regenerate continuous lean solvent in order to capture CO_2 emissions from fuel input to regenerate stored lean solvent per unit of energy used to store lean solvent (MWh) (estimated with IECM)
$E^{MAX}{}_i$	Maximum equivalent energy consumption capacity by generator i (MWh)
ER_i	CO_2 emissions rate for generator i (ton/MWh)
ERR_{CCS}	Emissions rate reduction from CCS retrofit (fraction)
$EV^{MAX,Lean}{}_{i,t}$	Max amount of lean solvent that can be stored in tank i (MWh)
$F^{MAX}{}_i$	Maximum stored lean solvent inflow (MWh)
HR_i	Heat rate of generator i used in UCED model (MMBtu/MWh)
$HR^{GROSS}{}_i$	Gross heat rate of generator i (MMBtu/MWh)
HRP^{CCS}	Net heat rate penalty from normal or flexible CCS retrofit during normal operations (%) (estimated with IECM)
$HRP^{Discharge}$	Net heat rate penalty at maximum achievable reduction of CO_2 capture system parasitic load while discharging stored solvent or venting (%) (estimated with IECM)
$M^{MAX}{}_i$	Maximum capacity to charge stored lean solvent by generator i (MWh)
$O^{MAX}{}_i$	Maximum stored lean solvent outflow (MWh)
$P^{MAX}{}_i$	Maximum net electricity generation capacity of generator i (MWh)
$P^{MIN}{}_{i,ST}$	Minimum stable load of the steam turbine at generator i (MWh)
$P^{MIN}{}_{i,Boiler}$	Minimum stable load of the boiler at generator i (MWh)

PC_i	Maximum pump capacity of pumped hydropower facility i (MWh)
R^{MAX}	Maximum reserve offer for a given reserve type by generator i (MW)
RR_i	Ramp rate for generator i (%/min.)

B.4.1: Proxy Unit Structure and Parametrization

B.4.1.1: Division of Solvent Storage Proxy Units

While charging stored solvent at a constant CO_2 capture rate, continuously regenerated solvent must capture CO_2 emissions from fuel combustion to regenerate stored lean solvent ($E^{ContSolvent}$). The thermal energy required by this additional continuously regenerated solvent reduces available energy to be converted to electricity and delivered to the grid. If emissions are vented while charging, though, this additional penalty on net electricity generation is not incurred. As a result, the maximum amount of stored lean solvent that can be charged in a given period of time differs depending on whether venting occurs. In order to accommodate varying CO_2 capture rates while charging, our model includes two sets of tank and charge proxy units, as well as two sets of discharge proxy units that correspond with each tank proxy unit.

B.4.1.2: Parametrization of Proxy Units

We determine proxy unit-specific values for six parameters: maximum capacity, heat rate, CO_2 and SO_2 emission rates, ramp rate, and minimum stable load (MSL). Table B.4 details how we calculate the capacity, heat rate, and CO_2 emissions rate of each flexible CCS proxy unit.

Heat rates and capacities of the vent and discharge proxy units reflect the capacity and net heat rate penalties while venting and discharging stored lean solvent. As such, fuel consumption by the vent and discharge proxy units at maximum capacity equals that by the base plus continuous solvent units at maximum capacity. Because all proxy units besides the vent and

solvent storage discharge units indicate operations in which electricity is generated and solvent is regenerated, the other proxy units' heat rates equal that of the base unit, or the gross heat rate of the generator prior to CCS retrofit. Since the vent while charging unit can only substitute for the base unit during charging, the vent while charging capacity equals that of the base unit.

Gradual stored solvent charging over many hours would manifest as charging only at the first charging proxy unit, which is linked to electricity generation by the first discharging proxy unit. Thus, to allow maximum electricity generation while discharging stored lean solvent under such a charging profile, we set the maximum capacity of the first discharging unit equal to the maximum capacity achievable while discharging. The maximum electricity generation capacity of the second discharge unit is scaled down from the capacity of the first discharge unit to reflect the smaller storage capacity of the second tank relative to the first. Solvent outflow capacities of the tank proxy units allow each discharge proxy unit to reach its maximum capacity.

The charging capacity of the first tank unit equals the amount of charging that can occur without venting emissions before net electricity generation by the flexible CCS generator equals zero. At the combined charging capacities of both charge proxy units, charging lean solvent accounts for the entire throughput capacity of the regenerator.

CO_2 emissions rates of proxy units primarily reflect whether CO_2 is captured in each operational mode. Since we model emissions rates in units of emissions per unit of electricity generation, emissions rates also vary according to unit capacity. However, emissions rates of the charging and discharging units are the same, as the two sets of units jointly represent the same operations. Similarly, we set the emissions rates of the base CCS and continuous solvent proxy units to be equal, as both contribute to emissions under normal operations. We zero out SO_2

emissions for all but the two vent units to capture SO_2 removal requirements while using the CCS system.

Two other key parameters for the proxy units are their MSL and ramp rates. In order to allow the proxy units to substitute for one another when generating electricity, we set the MSL for each proxy unit to zero and instead enforce MSL constraints on groups of proxy units. Regarding ramp rates, we set the ramping capability of the discharge and venting generators to 4% of net capacity per minute [3]–[5], [7], which exceeds the ramp rate (1.5-1.7%) of the less-flexible base proxy unit.

Table B.4: Key parameters for flexible CCS proxy units and coal-fired generator pre-CCS retrofit.

Unit in Model	**Maximum Capacity (MWh)**	**Heat Rate (MMBtu/MWh)**	**CO_2 Emissions Rate (ton/MWh)**
Coal-Fired Generator Pre-CCS Retrofit	P^{MAX}_{PreCCS}	HR^{GROSS}_{PreCCS}	ER_{PreCCS}
Flexible CCS Proxy Units			
Base CCS	$P^{MAX}_{CCS} = P^{MAX}_{PreCCS} * (1 - CP^{CCS})$	$HR_{CCS} = HR^{GROSS}_{PreCCS}$	$ER_{CCS} = ER_{PreCCS} * (1-ERR_{CCS}) * P^{MAX}_{PreCCS} / (P^{MAX}_{CCS} + E^{MAX}_{ContSolvent})$
Continuous Solvent	$E^{MAX}_{ContSolvent} = P^{MAX}_{CCS}/E^{Grid}$	$HR_{ContSolvent} = HR_{CCS}$	$ER_{ContSolvent} = ER_{CCS}$
Discharge Stored Lean Solvent 1	$P^{MAX}_{Discharge1} = P^{MAX}_{PreCCS} * (1 - CP^{Discharge})$	$HR_{Discharge1} = HR_{CCS} * (1 + HRP_{Discharge})$	$ER_{Discharge1} = ER_{PreCCS} * (1-ERR_{CCS}) * P^{MAX}_{PreCCS} / P^{MAX}_{Discharge1}$
Stored Lean Solvent Tank 1	$F^{MAX}_{Tank1} = (P^{MAX}_{CCS}-1) / E^{Grid} / (1 + E^{ContSolvent})^{\dagger}$ $O^{MAX}_{Tank1} = P^{MAX}_{Discharge1} / E^{Discharge}$	$HR_{Lean1} = 1$	0
Charge Stored Lean Solvent 1	$M^{MAX}_{Charge1} = F^{MAX}_{Tank1}$	$HR_{Charge1} = HR_{CCS}$	$ER_{Charge1} = ER_{CCS}$
Stored Lean Solvent Tank 2	$O^{MAX}_{Tank2} = F^{MAX}_{Tank2} = E^{MAX}_{ContSolvent} - F^{MAX}_{Tank1}$	$HR_{Lean2} = 1$	0
Charge Stored Lean Solvent 2	$M^{MAX}_{Charge2} = F^{MAX}_{Tank2}$	$HR_{Charge2} = HR_{CCS}$	$ER_{Charge2} = ER_{Charge1}$
Discharge Stored Lean Solvent 2	$P^{MAX}_{Discharge2} = P^{MAX}_{Discharge1} * F^{MAX}_{Tank2} / (F^{MAX}_{Tank1}+F^{MAX}_{Tank2})$	$HR_{Discharge2} = HR_{Discharge1}$	$ER_{Discharge2} = ER_{Discharge1}$

Vent	$P^{MAX}_{Vent} = P^{MAX}_{PreCCS} * (1 - CP^{Discharge})$ ††	$HR_{Vent} = HR_{Discharge1}$	$ER_{Vent} = ER_{PreCCS} * P^{MAX}_{PreCCS} / P^{MAX}_{Vent}$
Vent while Charging	$P^{MAX}_{VentCharge} = P^{MAX}_{CCS}$	$HR_{VentCharge} = HR_{CCS}$	$ER_{VentCharge} = ER_{PreCCS} * P^{MAX}_{PreCCS} / P^{MAX}_{VentCharge} - ER_{Charge1} * (M^{MAX}_{Charge1} + M^{MAX}_{Charge2}) / P^{MAX}_{VentCharge}$

† We subtract 1 from P_{MAX}^{CCS} to avoid shutting down the base CCS proxy unit, which would force the shutdown of all proxy units at the flexible CCS generator, per the below constraints.

B.4.2: Proxy Unit Operational Constraints

In order to force the ten proxy units to jointly operate like a single flexible CCS generator, we formulate a series of constraints on groups of proxy units. These constraints act in addition to individual unit constraints, such as that electricity generation by each proxy unit cannot exceed its maximum capacity.

B.4.2.1: Electricity Generation and Solvent Regeneration Constraints

Since generation at the base proxy unit represents net electricity generation while capturing CO_2, generation at the base unit decreases with stored lean solvent charging at the first tank unit, which decreases continuous solvent regeneration.

$$p_{CCS,t} \leq P_{CCS}^{MAX} - E^{Grid} * (1 + E^{ContSolvent}) * f_{Tank1,t} \quad (1)$$

In order to account for energy used in to capture CO_2 emissions, continuous solvent regeneration increases with net electricity generation at the base CCS proxy unit and charging of stored lean solvent at the first tank proxy unit. Charging at the second tank proxy unit, though, directly replaces continuous solvent regeneration.

$$o_{ContSolvent,t} = \frac{1}{E^{Grid}} * p_{CCS,t} + E^{ContSolvent} * f_{Tank1,t} - f_{Tank2,t} \quad (2)$$

Net electricity generation at the discharge proxy units reflect stored lean solvent outflows at the tank proxy units.

$$p_{Discharge1,t} = E^{Discharge} * o_{Tank1,t} \quad (3)$$

$$p_{Discharge2,t} = E^{Discharge} * o_{Tank2,t} \quad (4)$$

Energy consumption while charging at the charge proxy units reflect stored lean solvent inflows at the tank proxy units.

$$m_{Charge1,t} = f_{Tank1,t} \quad (5)$$

$$m_{Charge2,t} = f_{Tank2,t} \quad (6)$$

Stored lean solvent inflows and outflows and continuously regenerated solvent must be less than the regenerator throughput capacity, or the continuous solvent unit capacity.

$$f_{Tank1,t} + o_{Tank1,t} + f_{Tank2,t} + o_{Tank2,t} + o_{ContSolvent,t} \leq O^{MAX}_{ContSolvent} \quad (7)$$

B.4.2.2: Reserve Provision Constraints

The final set of constraints limit the reserves provided by the flexible CCS units. First, the tank, charging, and continuous solvent units cannot provide any reserves, as none of these units provide electricity to the grid.

$$r_{Charge1,t} = r_{Charge2,t} = 0 \quad (8)$$

$$r_{Tank1,t} = r_{Tank2,t} = 0 \quad (9)$$

$$r_{ContSolvent,t} = 0 \quad (10)$$

The discharge units cannot offer more reserves than the volume of stored lean solvent; any reserves in excess of that value they would unable to be able to provide if called upon.

$$r_{Discharge1,t} \leq ev_{Lean1,t} \quad (11)$$

$$r_{Discharge2,t} \leq ev_{Lean2.t} \quad (12)$$

Reserves that can be offered by the base proxy unit are constrained by the spare throughput capacity of the solvent regenerator:

$$r_{CCS,t} \leq \left(E^{MAX}_{ContSolvent} - e_{ContSolvent,t} - m_{Charge1,t} - m_{Charge1,t}\right) * E^{Grid} \quad (13)$$

Note that in the next constraint, energy consumed by the charging units – which equals energy stored in the tank units – can be offered as reserves at the discharge units. To avoid double counting this energy consumption in reserves, we do not allow the base CCS unit to provide reserves based on energy consumed at the charging units.

We also create several group reserve provision constraints, such that reserves offered by all units cannot exceed the offer value of the solvent storage discharge components, the most flexible components of a flexible CCS system. Implicit in the inclusion of this constraint is that we assume that during charging, the generator can still offer reserves at the solvent storage discharge generators. These reserves, moreover, would be met by reducing the CO_2 capture system load, i.e. by reducing continuously regenerated solvent and possibly solvent being regenerated for storage. If we assume that energy used to charge solvent cannot be used in reserve offers, then the constraints below would not include a term on the right-hand side for the pump load at pump units 1 and 2.

For the discharging units, offered reserves embody two sources of greater electricity: shifting energy from solvent regeneration to electricity generation and increased generation at the CCS unit, which also leads to greater continuous solvent generation that can be shifted to electricity generation during discharging. For every increase in electricity output at the CCS unit, energy use at the continuous solvent unit increases by:

$$\Delta o_{ContSolvent} = \Delta p_{CCS} * \frac{1}{E^{Grid}} \quad (14)$$

Possible reserves from discharging or venting are therefore:

$$r_{Discharge} = \Delta p_{CCS} + \Delta o_{ContSolvent} + o_{ContSolvent} = \Delta p_{CCS} * \left(1 + \frac{1}{E^{Grid}}\right) + o_{ContSolvent} \quad (15)$$

Substituting the maximum possible increase in CCS generation during the reserve timeframe yields the max reserves that can be supplied by the discharge unit. However, the max possible increase in CCS could either be based on its spare capacity, if spare capacity is less than its ramp rate over the reserve timeframe, or its max ramp rate over the reserve timeframe. We translate this, which is essentially a minimum function, into two constraints:

$$r_{CCS,t} + r_{Discharge1,t} + r_{Discharge2,t} \leq R_{CCS}^{MAX} * \left(1 + \frac{1}{E^{Grid}}\right) + o_{ContSolvent,t} + o_{Charge1,t} + o_{Charge2,t} \quad (16)$$

$$r_{CCS,t} + r_{Discharge1,t} + r_{Discharge2,t} \leq \left(P_{CCS}^{MAX} - p_{CCS,t}\right) * \left(1 + \frac{1}{E^{Grid}}\right) + p_{ContSolvent,t} + o_{Charge1,t} + o_{Charge2,t} \quad (17)$$

Finally, we include a group reserve constraint limiting reserves from all proxy units to the maximum reserves that could be offered by the discharge unit.

$$r_{CCS,t} + r_{Discharge1,t} + r_{Discharge2,t} \leq R_{Discharge1}^{MAX} \quad (18)$$

This ensures that reserves provided by the flexible CCS generator do not exceed the maximum reserves that can be offered by the most flexible component of the flexible CCS generator, namely the solvent storage discharge unit.

B.4.2.3: Electricity Generation and Reserve Provision Constraint

Net electricity generation and reserve provision by all eligible units are limited to the maximum electricity generation of the first discharge unit, i.e. the maximum achievable net output by the flexible CCS generator in any operational mode.

$$p_{CCS,t} + p_{Discharge1,t} + p_{Discharge2,t} + r_{CCS,t} + r_{Discharge1,t} + r_{Discharge2,t} \leq P_{Discharge1}^{MAX} \quad (19)$$

The prior constraint also ensures that generation and reserves provided by the two discharging units does not exceed the capacity of discharge unit 1, which equals the capacity of the venting unit.

B.4.2.4: Total Energy Use Constraint

In order to limit reserve provision by the discharge unit during normal operations, we constrain total net electricity generation, provided reserves, and CO_2 capture energy consumption by the maximum energy input during normal operations plus the extra generation achievable by discharging stored solvent relative to normal operations.

$$p_{CCS,t} + p_{Discharge1,t} + p_{Discharge2,t} + r_{CCS,t} + r_{Discharge1,t} + r_{Discharge2,t} + e_{ContSolvent,t} + m_{Charge1,t} + m_{Charge2,t} \leq P_{Base}^{MAX} + O_{ContSolvent}^{MAX} + \left(P_{Discharge1}^{MAX} - P_{Base}^{MAX}\right) = O_{ContSolvent}^{MAX} + P_{Discharge1}^{MAX} \quad (20)$$

B.4.2.5: Volume of Stored Lean Solvent

As previously discussed, the storage volume of pump unit 1 is set equal to the maximum capacity of stored solvent at the flexible CCS generator, and the storage volume of pump unit 2 is set equal to 2 hours of full pump load at pump unit 2. As such, the total storage volume at both pump units is greater than the desired maximum capacity of stored solvent based on our 2-hour storage assumption. Thus, a constraint is included that limits stored solvent at pump units 1 and 2 to the desired stored volume capacity.

$$ev_{Tank1,t}^{Lean} + ev_{Tank2,t}^{Lean} \leq EV_{Tank1}^{MAX,Lean} \quad (21)$$

B.4.2.6: On/Off Constraints

Several constraints limit when the flexible CCS proxy units can be turned on. For one, all flexible CCS units can only turn on when the base CCS unit is on.

$$u_{ContSolvent,t} - u_{CCS,t} \leq 0 \quad (22)$$

$$u_{Discharge1,t} - u_{CCS,t} \leq 0 \quad (23)$$

$$u_{Discharge2,t} - u_{CCS,t} \leq 0 \quad (24)$$

Each solvent storage tank unit can only be on when the base CCS unit is on, and each tank unit can only either charge or discharge solvent at once.

$$u_{Tank1,t}^{Pump} + u_{Tank1,t}^{Generator} \leq u_{CCS,t} \quad (25)$$

$$u_{Tank2,t}^{Pump} + u_{Tank2,t}^{Generator} \leq u_{CCS.t} \quad (26)$$

Finally, the second charge unit cannot turn on until the first charge unit is at maximum capacity. The denominator of the $o_{Charge1}$ term includes a small adjustment to account for any rounding errors that may occur that would prevent the second charging unit from ever turning on.

$$u_{Charge2,t} - \frac{o_{Charge1,t}}{(O_{Charge1}^{MAX} - 0.05)} \leq 0 \quad (27)$$

B.4.2.7: Minimum Load Constraints

Several constraints enforce minimum stable loads on proxy units. For one, net electricity generation at all proxy units must exceed the generator's steam turbine minimum load (30% of base unit capacity).

$$p_{CCS,t} + p_{Discharge1,t} + p_{Discharge2,t} + p_{Vent,t} + p_{VentCharge,t} \geq P_{CCS,ST}^{MIN} * u_{CCS,t} \quad (28)$$

Additionally, all energy input to the flexible CCS generator must exceed the generator's boiler minimum load (40% of base unit capacity).

$$p_{CCS,t} + p_{Discharge1,t} + p_{Discharge2,t} + p_{Vent,t} + p_{VentCharge,t} + e_{ContSolvent,t} + m_{Charge1,t} + m_{Charge2,t} \geq P_{CCS,Biler}^{MIN} * u_{CCS,t} \quad (29)$$

During discharging, the minimum load of the base unit must be adjusted to a minimal non-zero value since discharging units displace generation at the base unit.

$$p_{CCS,t} \geq P_{CCS,ST}^{MIN} * u_{CCS,t} - (u_{Discharge1,t} + u_{Discharge2,t}) * (P_{CCS,ST}^{MIN} - 1) \quad (30)$$

B.4.2.8: Ramping Constraints

In our flexible CCS model, decreases in electricity generation at the base unit offset by an increase in electricity generation at the discharge unit implies no ramping at the flexible CCS generator as a whole. We therefore constrain ramping of proxy units in the aggregate.

$$c_{CCS,t} + c_{Discharge1,t} + c_{Discharge2,t} + c_{Vent,t} + c_{VentCharge,t} + c_{ContSolvent,t} + c_{Charge1,t} + c_{Charge2,t} \leq C_{CCS}^{MAX} \quad (31)$$

We also modify the constraint on ramping of the base CCS proxy unit depending on whether other flexible components are on.

$$c_{CCS,t} \leq C_{CCS}^{MAX} + \left(u_{Discharge1,t} + u_{Discharge2,t}\right) * P_{CCS}^{MAX} \quad (32)$$

B.4.2.9: Modeling Solvent Storage-Only Flexible CCS Generators

In order to model flexible CCS equipped only with solvent storage, and not venting, we add one constraint to the model that prohibits the venting and venting while charging proxy units from turning on.

$$u_{Vent,t} + u_{VentCharge,t} \leq 0 \quad (33)$$

B.4.2.10: Generic Pumped Hydropower Operational Constraints

This section provides the generic constraints on pumped hydropower operations included in our UCED model. We model solvent storage systems at each flexible CCS generator as a pumped hydropower facility. The head, or reservoir, of the pumped hydropower facility corresponds to the stored lean solvent, whereas the tail corresponds to stored rich solvent. Electricity generated while releasing water from the reservoir at the pumped hydropower facility is analogous to generating electricity while discharging stored lean solvent. Conversely, energy consumed in pumping water into the reservoir is analogous to energy consumed while charging stored lean solvent.

The inflow of water to the reservoir head is determined by the pump load. Note that in our solvent storage model, we set the heat rate (HR) and pump efficiency (PE) of the pumped hydropower unit to 1.

$$n_{i,t}^{HEAD} = HR_i * PE_i * m_{i,t} \quad (34)$$

$$e_{i,t}^{TAIL} = HR_i * PE_i * m_{i,t} \quad (35)$$

The amount of water released from the reservoir determines the amount of electricity generated.

$$e_{i,t}^{HEAD} = HR_i * p_{i,t} \quad (36)$$

$$n_{i,t}^{TAIL} = HR_i * p_{i,t} \quad (37)$$

The amount of energy left in the reservoir depends on inflows and outflows to and from the reservoir in time t and the end volume of the prior period. At t=1, the end volume of the last period of the prior optimization is input instead. For the first hour of the entire period for analysis with the UCED, e.g. hour 1 of 2030, EV_i^{HEAD} equals the initial volume of the reservoir.

$$ev_{i,t-1}^{HEAD} - ev_{i,t}^{HEAD} - e_{i,t}^{HEAD} + n_{i,t}^{HEAD} = 0 \quad \forall\, t > 1 \quad (38)$$

$$EV_i^{HEAD} - ev_{i,t}^{HEAD} - e_{i,t}^{HEAD} + n_{i,t}^{HEAD} = 0 \quad \forall\, t = 1 \tag{39}$$

The pump load is constrained by the pump capacity (*PC*), and pumping cannot occur if the pump unit is not on.

$$m_{i,t} \leq PC_i * u_{i,t}^{Pump} \tag{40}$$

The pump load cannot be less than zero.

$$m_{i,t} \geq 0 \tag{41}$$

The pump and electricity generation units at the pumped hydropower facility cannot both be on at the same time.

$$u_{i,t}^{Generator} + u_{i,t}^{Pump} \leq 1 \tag{42}$$

B.5: GENERATOR FLEET CHARACTERISTICS

Table B.5 details the number and key parameters by generator type in the generator fleet. For a full description of how we construct the generator fleet, see Craig et al. [8].

Table B.5: Number of generators, average capacity, and capacity-weighted heat rate and CO_2 emission rate for each non-renewable generator type in the base fleet after generator aggregation, based on data from the U.S. Environmental Protection Agency [9]–[11].

Generator Type	Fuel Type	Number of Generators	Average Capacity (MW)	Capacity-Weighted Heat Rate (Btu/kWh)	Capacity-Weighted CO_2 Emission Rate (kg/MWh)
Biomass	Biomass	26	25	15,090	1,410
Coal Steam	Coal	178	280	10,110	950
Combined Cycle	Natural Gas	171	135	7,370	420
Combustion Turbine	Oil	32	172	17,060	1,220
Combustion Turbine	Natural Gas	717	38	12,980	690
Fossil Waste	Fossil Waste	2	43	18,700	2,720
IGCC	Coal	6	163	8,920	740

Landfill Gas	Landfill Gas	4	105	14,220	0
Municipal Solid Waste	Municipal Solid Waste	3	75	15,200	790
Non-Fossil Waste	Non-Fossil	23	5	8,270	0
Nuclear	Uranium	19	948	10,510	0
O/G Steam	Oil	5	51	14,870	1,060
O/G Steam	Natural Gas	43	73	13,000	1,030

Table B.6 provides the total installed capacity and average fuel price by fuel type of the 2030 base generator fleet to which we add normal or flexible CCS. Coal and natural gas fuel prices vary by generator.

Table B.6: Total installed average fuel price and capacity by fuel type of the base fleet.

Fuel Type	**Coal**	**Natural Gas**	**Oil**	**Nuclear**	**Wind**	**Solar**	**Other**
Fuel Price ($/GJ)	2.4	5.7	24.4	0.9	0	0	Varies
Capacity (GW)	50.7	53.8	5.8	18	33.1	1.2	1.5

B.6: CO_2 PRICES USED TO ACHIEVE COMPLIANCE WITH THE MODERATE AND STRONG CO_2 EMISSION LIMITS

Table B.7 provides the CO_2 prices necessary to comply with the moderate and strong CO_2 emission limits for each installed capacity of normal or flexible CCS retrofits.

Table B.7: CO_2 price necessary to comply with the moderate or strong CO_2 emission limit via re-dispatching at each de-rated installed capacity of flexible or normal CCS.

De-Rated Normal or Flexible CCS Capacity in Fleet (GW)	**CO_2 Price to Comply with Moderate Emission Limit ($/ton)**	**CO_2 Price to Comply with Strong Emission Limit ($/ton)**
1.5	7	36
3	4	33

B.7: FLEXIBLE CCS OPERATIONS WITH SOLVENT STORAGE AND VENTING

In order to demonstrate the venting capabilities of our flexible CCS model, here we describe the operations of flexible CCS equipped with venting and solvent storage under the moderate and strong CO_2 emission constraints. Under the moderate constraint, re-dispatching from high- to low-CO_2-emitting generators (due to the shadow CO_2 price included in the UCED model) provides a sufficient and low cost means of meeting the CO_2 emissions limit, so venting flue gas in order to operate the flexible CCS generator like a coal-fired generator without CCS minimizes system operational costs. Consequently, over 99% of net electricity output by flexible CCS generators occurs while venting CO_2 emissions. Note that in the main text of this paper, flexible CCS does not have the option to vent CO_2 emissions, so using the flexible CCS generator to provide net electricity and reserves to the grid while capturing CO_2 minimizes system operational costs. Unlike the moderate emission limit, the strong emission limit results in higher re-dispatch costs, so flexible CCS becomes an economic strategy for reducing CO_2 emissions. Under this stronger emission constraint, more than 99% of net electricity output by flexible CCS generators equipped with venting and solvent storage occurs while they are not venting CO_2 emissions.

B.8: CAPACITY FACTORS OF CCS GENERATORS

Figure B.5 provides the capacity factors of each generator retrofit with normal and flexible CCS under the moderate and strong CO_2 emission limits. Because the CO_2 price increases from the moderate to strong limit, the capacity factors of all CCS-equipped generators increase from the moderate to strong limit. Within a given scenario, individual units' capacity factors vary depending on various parameters used by the unit commitment and economic

dispatch model in dispatching generators, e.g. marginal cost and minimum stable load. For instance, CCS generator "4078-4" generates the least electricity of all CCS generators under the moderate emission limit (Figure B.5) because it has the highest marginal cost of all CCS generators.

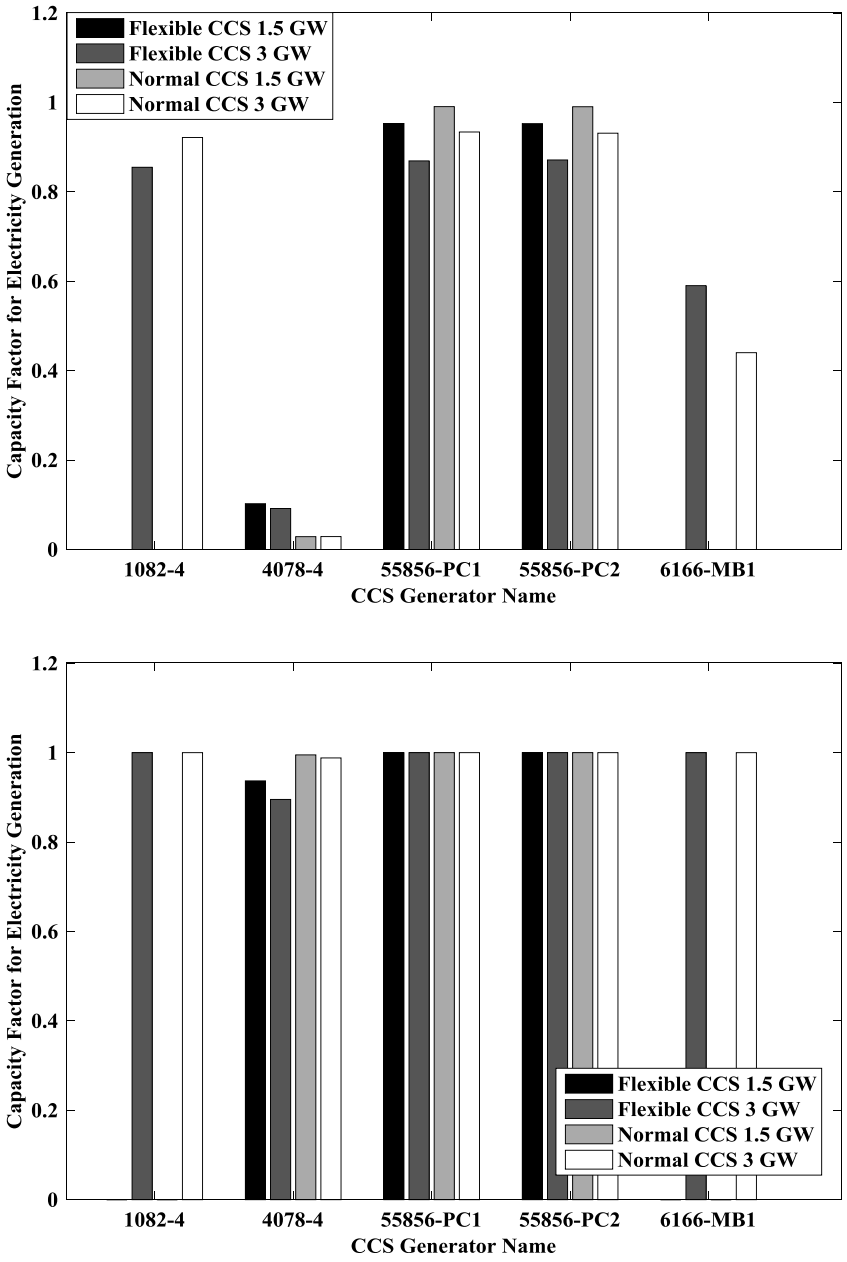

Figure B.5: Capacity factors for each coal-fired generator retrofit with normal and flexible CCS at 1.5 or 3 GW of total installed CCS under the moderate CO_2 emission limit (top) and strong CO_2 emission limit (bottom).

B.9: SENSITIVITY TO HIGH NATURAL GAS PRICES

In order to better understand the trade-off between normal and flexible CCS under the moderate emission limit, we test the sensitivity of our results to high natural gas prices by increasing the generator fleet's capacity-weighted natural gas price from $5.4 per MMBtu to $6.5 per MMBtu. For this sensitivity analysis, we only consider flexible CCS equipped with a 2 hour solvent storage tank size. By making coal-fired generators more economic relative to natural gas-fired generators, higher natural gas prices lead to greater shadow CO_2 prices necessary to comply with the moderate emission limit. Shadow CO_2 prices equal $15 and $7 per ton with 1.5 and 3 GW of CCS installed, respectively. Note that the former shadow CO_2 price exceeds those under the lower natural gas price moderate emission limit scenarios, whereas the latter CO_2 price equals that in the lower natural gas price, 3 GW CCS, moderate emission limit scenario.

Utilization of normal and flexible CCS generators increases with natural gas price (Figure B.6). Notably, with 1.5 GW CCS installed, utilization of generator '4078-4' increases by roughly 20% from normal to flexible CCS, a greater increase than at the lower natural gas price (Figure B.5). As in other scenarios, flexible CCS generators primarily use stored solvent for reserve provision under high natural gas prices (Figure B.7). Consequently, reserve provision by flexible CCS generators exceeds that by normal CCS generators by 9 to 80 times. With respect to electricity generation, at 3 GW CCS, flexible CCS generators use stored solvent for some electricity generation, but most (96-99%) electricity generation occurs during normal operations (i.e., not while discharging stored solvent). Overall electricity generation by CCS generators increases from normal to flexible CCS by roughly 6% with 1.5 GW CCS installed, primarily due

to increased utilization of generator '4078-4.' Conversely, electricity generation by CCS generators decreases from normal to flexible CCS by roughly 2% with 3 GW CCS installed.

At best guess solvent storage capital costs, annual total system costs decrease by $19-58 million from normal to flexible CCS (Figure B.8). Unlike at lower natural gas prices, electricity generation cost reductions ($13-40 million) exceed reserve cost reductions ($9-25 million). High natural gas prices increase electricity generation costs more than reserve provision costs. Consequently, while greater reserve provision from normal to flexible CCS reduces reserve costs, the shift from reserve provision to electricity generation by non-CCS generators yields a greater reduction in electricity generation costs. Total operational cost reductions significantly exceed stored solvent capital costs, resulting in reduced total system costs.

System CO_2 emissions increase by 1 million ton from normal to flexible CCS at 3 GW CCS installed, but remain largely unchanged at 1.5 GW CCS. Utilization of CCS generators, which is driven by natural gas and shadow CO_2 price, explains these divergent outcomes. At 1.5 GW CCS, utilization of CCS generators, particularly '4078-4', significantly increases from normal to flexible CCS. Since CCS generators have lower CO_2 emission rates than non-CCS coal- or gas-fired generation, greater CCS generation reduces system CO_2 emissions. At the same time, greater reserve provision from normal to flexible CCS enables greater electricity generation by coal-fired generators, increasing CO_2 emissions. These two effects offset each other, leading to no change in system CO_2 emissions. At 3 GW CCS, however, utilization of CCS generators does not significantly increase from normal to flexible CCS. Thus, greater electricity generation and consequent CO_2 emissions by coal-fired generators leads to an overall increase in system CO_2 emissions, as seen under the moderate emission limit at lower natural gas prices.

Figure B.9 compares changes in system CO_2 emissions and total costs, including uncertainty in stored solvent capital costs, from normal to flexible CCS. Across solvent storage capital costs, annual total system costs decrease from normal to flexible CCS by $5-65 million, while CO_2 emissions do not change and increase by 1 million ton with 1.5 and 3 GW CCS installed, respectively. Thus, in the 3 GW CCS and high natural gas price scenario, system CO_2 emissions increase more and system costs decrease more from normal to flexible CCS relative to the moderate emission limit scenarios at lower natural gas prices. In the 1.5 GW CCS high natural gas price scenario, though, system CO_2 emissions increase less and system costs decrease less from normal to flexible CCS relative to the moderate emission limit scenarios at lower natural gas prices. However, given that the shadow CO_2 price in the 1.5 GW CCS high natural gas price scenario ($15/ton) exceeds those at the moderate emission limit and lower natural gas price scenarios ($7/ton and $3/ton), the 1.5 GW CCS and high natural gas price scenario is not directly comparable to the moderate emission limit scenarios at lower natural gas prices. Rather, the 1.5 GW CCS and high natural gas price scenario actually lies between the lower natural gas price moderate and strong emission limit scenarios. In fact, changes in system costs and CO_2 emissions from normal to flexible CCS in the 1.5 GW CCS high natural gas price scenario bridge those under the moderate and strong emission limits at lower natural gas prices.

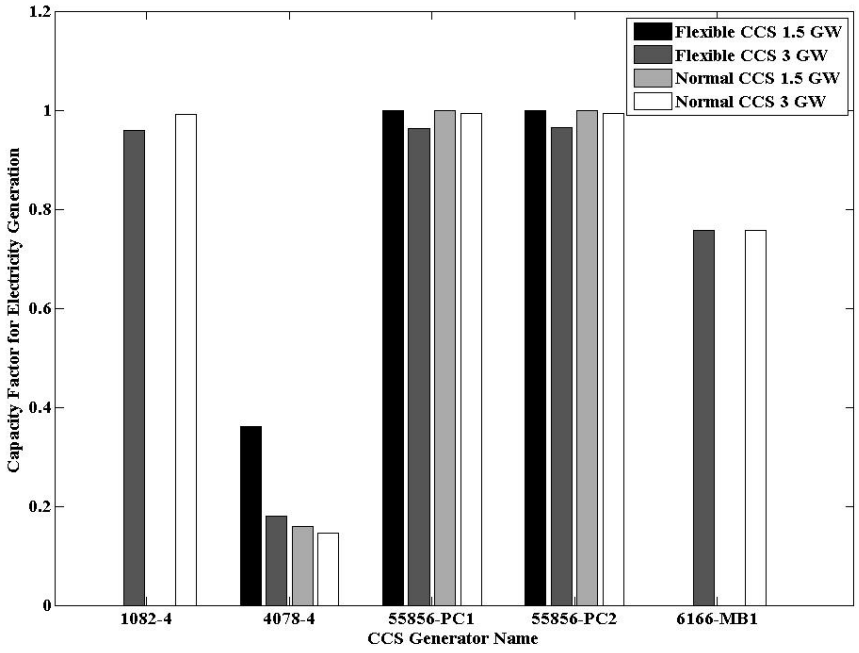

Figure B.6: Capacity factors for each coal-fired generator retrofit with normal and flexible CCS at 1.5 or 3 GW of total installed CCS under moderate emission limit and high natural gas price.

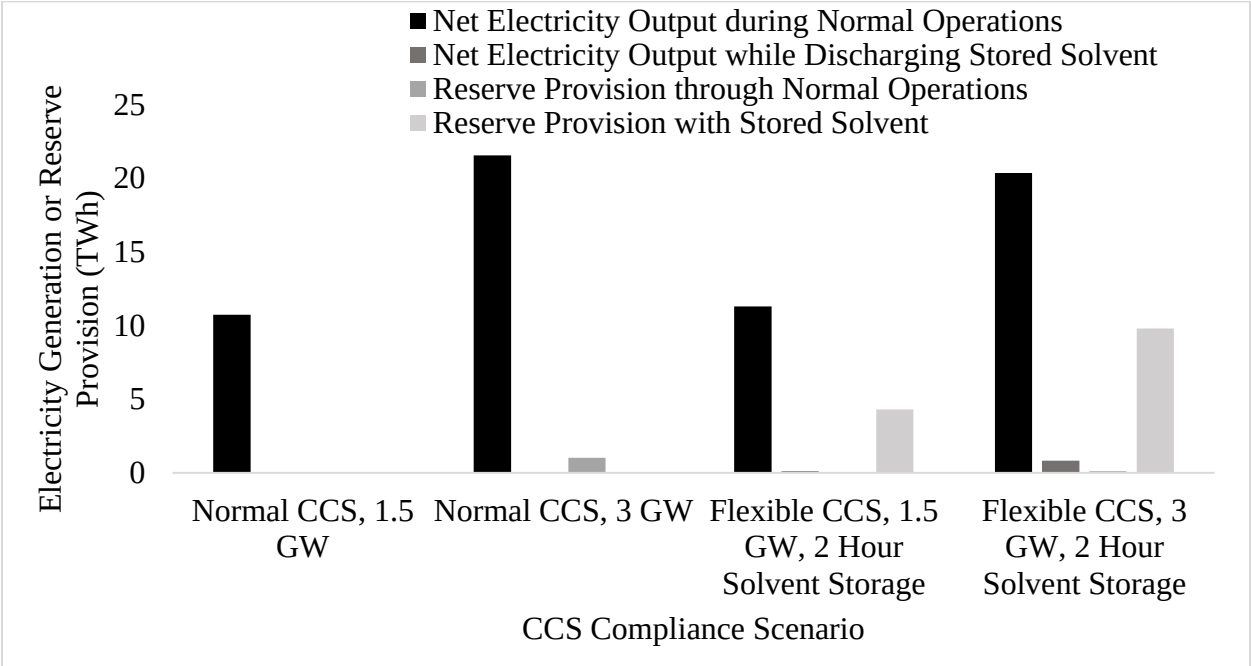

Figure B.7: Annual net electricity output and reserve provision by operational mode for 1.5 and 3 GW of normal and flexible CCS generators under the moderate emission limit and high natural gas price.

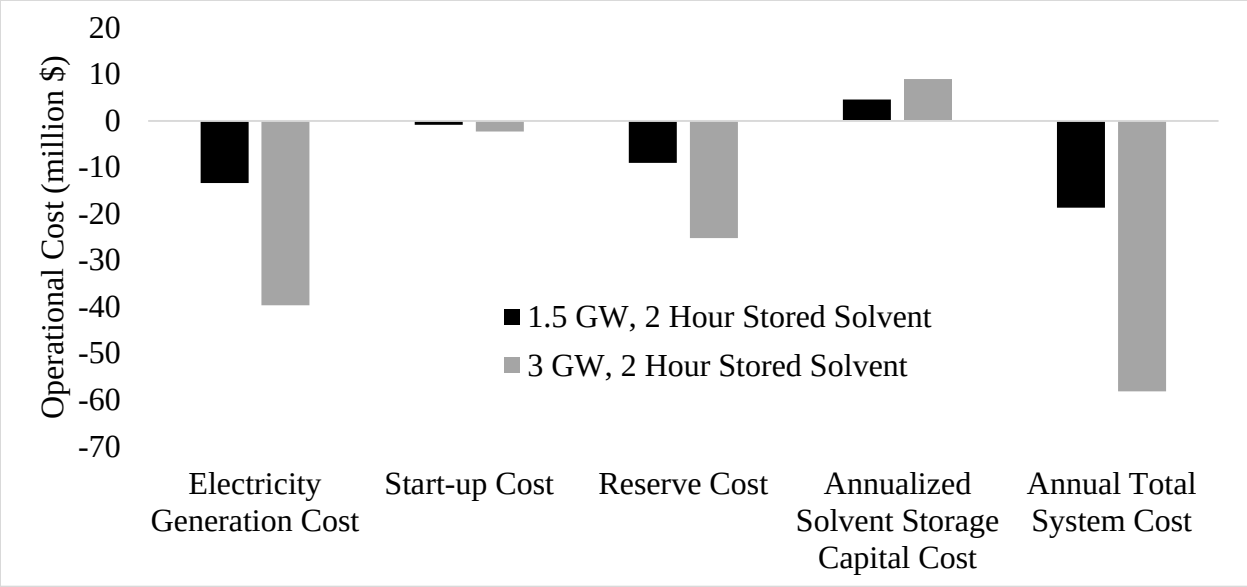

Figure B.8: Change in electricity generation, start-up, and reserve costs, best guess annualized solvent storage capital costs, and the sum of all four (annual total system costs), with 1.5 or 3 GW of flexible CCS instead of normal CCS under the moderate emission limit and high natural gas prices.

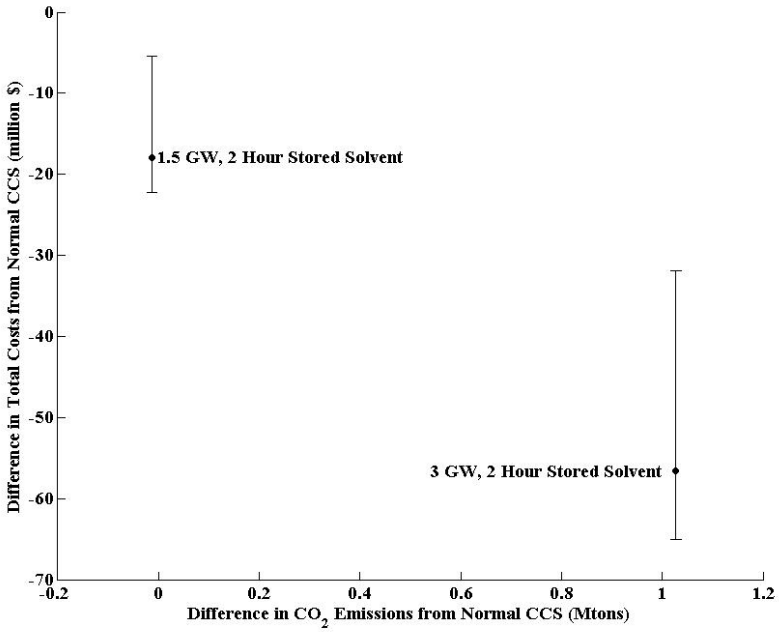

Figure B.9: Annual change in total operational plus capital costs versus annual change in CO_2 emissions with an equal installed capacity of flexible CCS relative to normal CCS for solvent storage tank sizes under the moderate emission limit and high natural gas prices. Negative values indicate reductions with flexible CCS relative to normal CCS. Error bars indicate uncertainty in solvent storage capital costs.

B.10: REFERENCES

[1] D. Patiño-Echeverri and D. C. Hoppock, "Reducing the energy penalty costs of postcombustion CCS systems with amine-storage," *Environ. Sci. Technol.*, vol. 46, pp. 1243–1252, 2012.

[2] D. L. Oates, P. Versteeg, E. Hittinger, and P. Jaramillo, "Profitability of CCS with flue gas bypass and solvent storage," *Int. J. Greenh. Gas Control*, vol. 27, pp. 279–288, 2014.

[3] P. Versteeg, D. L. Oates, E. Hittinger, and E. S. Rubin, "Cycling coal and natural gas-fired power plants with CCS," *Energy Procedia*, vol. 37, pp. 2676–2683, 2013.

[4] P. C. Van der Wijk, A. S. Brouwer, M. Van den Broek, T. Slot, G. Stienstra, W. Van der Veen, and A. P. C. Faaij, "Benefits of coal-fired power generation with flexible CCS in a future northwest European power system with large scale wind power," *Int. J. Greenh. Gas Control*, vol. 28, pp. 216–233, 2014.

[5] S. M. Cohen, G. T. Rochelle, and M. E. Webber, "Optimal CO2 capture operation in an advanced electric grid," *Energy Procedia*, vol. 37, pp. 2585–2594, 2013.

[6] Carnegie Mellon University, "Integrated Environmental Control Model. Version 8.0.2." 2015.

[7] IEAGHG, "Operating Flexibility of Power Plants with CCS," 2012.

[8] M. Craig, P. Jaramillo, H. Zhai, and K. Klima, "The economic merits of flexible carbon capture and sequestration as a compliance strategy with the Clean Power Plan," *Environ. Sci. Technol.*, vol. 51, pp. 1102–1109, 2017.

[9] U.S. Environmental Protection Agency, "Parsed File: Mass-Based, 2030. Docket No. EPA-HQ-OAR-2013-0602," 2015.

[10] U.S. Environmental Protection Agency, "Documentation for EPA Base Case v.5.13 Using the Integrated Planning Model," 2013.

[11] U.S. Environmental Protection Agency, "Stationary Gas Turbines," in *Compilation of Air Pollutant Emissions Factors, Volume 1: Stationary Point and Area Sources, AP-42*, 5th ed., 2000.

APPENDIX C:
SUPPLEMENTAL INFORMATION FOR CHAPTER 4

C.1: INITIAL GENERATOR FLEET

C.1.1: Parameters Added to Initial Generator Fleet

To construct our 2015 generator fleet, we begin with generators located in ERCOT and operational in 2015 in the National Electric Energy Data System (NEEDS) Version 5.15 [1]. Because NEEDS lacks data required in our capacity expansion and unit commitment and economic dispatch models, we add carbon dioxide (CO_2) emission rates [2], variable operation and maintenance (O&M) costs [3], and unit commitment parameters (i.e., ramp rate, minimum down time, start cost, and minimum stable level) [4] to generators.

We obtain unit commitment parameters – minimum stable load (MSL), minimum down time, start-up costs, and ramp rates – for existing generators from PHORUM [4], a price-validated reduced form UCED model of PJM [5]. Unit commitment parameters vary by plant and fuel type and, in some cases in order to capture nonlinearities in unit commitment parameter values for some plant types, plant size. Table C.1 provides the unit commitment parameter values used in our model.

Table C.1: Unit commitment parameter values by plant and fuel type and plant size, if applicable, used in our model. Parameters for coal-fired and natural gas combined cycle generators pertain to coal-fired generators without and with CCS.

Unit Commitment Parameter	Plant and Fuel Type	Plant Size	Value
Minimum Stable Load (% of total capacity)	Oil-fired combustion and O/G steam turbine	All	25%
	Wind and solar PV	All	0%
	Nuclear	All	90%

	All other generators	All	40%
Ramp Rate (Up and Down) (% of total capacity)	Coal	>150 MW	0.3%/min.
	Coal	<150 MW	0.6%/min.
	Natural gas combined cycle	>100 MW	0.5%/min.
	Natural gas combined cycle	<100 MW	1.1%/min.
	Combustion turbine (natural gas and oil)	All	0.6%/min.
	O/G steam turbine (natural gas and oil)	All	0.4%/min.
	Landfill gas, biomass, non-fossil waste, wind, and solar PV	All	1.7%/min.
	Nuclear	All	0.1%/min.
Startup Costs ($\$_{2012}$, as multiple of nameplate capacity)	Coal	All	100x
	Natural gas combined cycle	All	100x
	Combustion turbine (natural gas and oil)	All	25x
	Wind and solar PV	All	0
	Non-fossil waste	All	100x
	Landfill gas	All	50x
	Biomass	All	100x
	Nuclear	All	500x
	O/G Steam (natural gas and oil)	All	100x
Minimum Down Time (hours)	Coal	>150 MW	12
	Coal	<150 MW	6
	Nuclear	All	20
	Natural gas combined cycle	All	4
	Combustion turbine (natural gas and oil)	<60 MW	1
	Combustion turbine (natural gas and oil)	60-140 MW	2
	Combustion turbine (natural gas and oil)	>140 MW	3
	Landfill gas	All	4
	Biomass	All	4
	Non-fossil waste	All	4
	Wind and solar PV	All	0
	O/G Steam (natural gas and oil)	All	7

We assign variable operation and maintenance (VOM) costs to generators in the initial fleet using plant-type-specific values from the Annual Energy Outlook (AEO) (Table C.2) [6]. We assume O/G steam generators have the same VOM cost as coal steam generators and that landfill gas and non-fossil waste generators have the same VOM cost as municipal solid waste generators.

Table C.2: VOM costs by plant type.

Plant Type	Capacity-weighted VOM Cost ($\$_{2012}$/MWh)
Coal Steam	4.5
Wind	0
Solar PV	0
NGCC	3.6
Non-Fossil Waste	5.3
Nuclear	2.1
Landfill Gas	8.8
Biomass	5.3
O/G Steam	4.5
CT	15.5

C.1.2: Hydropower Operations

Given the small installed capacity of hydropower (0.5 GW) in our generator fleet and the significant computational requirements to model hydro-thermal coordination, we subtract hourly hydropower generation from demand, then remove hydropower generators from the initial generator fleet. To calculate hourly hydropower generation, we determine average monthly generation for each hydropower plant from 2011 to 2014 [7] and assume each generator operates at a constant capacity factor across hours in each month [8].

C.1.3: Fleet Compression

After removing hydropower generators, we compress the initial generator fleet by aggregating small (<75 MW) generators into combined generators less than 300 MW in size. We aggregate generators based on two features. First, we aggregate generators within each of the following plant types: landfill gas, natural gas-fired combustion turbine (CT), oil-fired CT, natural gas-fired O/G steam turbine, oil-fired O/G steam turbine, and natural gas combined cycle. Second, in order to model age-based retirements of combined generators, we aggregate generators that came online in the same decade beginning with 1975 – 1985. Heat rates and CO_2

emission rates of combined generators equal the capacity-weighted heat rates and CO_2 emission rates of their constituent generators. We assign all other parameters to combined generators based on their plant and fuel types.

C.1.4: Summary Statistics for Initial Generator Fleet

Table C.3 provides key summary statistics by plant type of the initial generator fleet after compression. The fleet consists of 319 generators with a total capacity of 92.6 GW. Combustion turbines are 99.5% natural-gas-fired and 0.5% oil-fired by capacity.

Table C.3: Key summary statistics for initial generator fleet after compression. NGCC and CT stand for natural gas combined cycle and combustion turbine, respectively.

Plant Type	Total Installed Capacity (GW)	Number of Generators	Average Capacity (MW)	Capacity-weighted Heat Rate (Btu/kWh)	Capacity-weighted CO_2 Emissions Rate (lb/MMBtu)
Coal Steam	19	34	559	10,560	226
Wind	13.8	94	147	0	0
Solar PV	0.3	15	22	0	0
NGCC	33.2	99	335	7,520	118
Non-Fossil Waste	0.1	8	14	11,770	213
Nuclear	5	4	1240	10,460	0
Landfill Gas	0.1	3	32	13,770	118
Biomass	0.2	2	106	14,530	0
O/G Steam	15.1	40	377	12,170	119
CT	5.8	20	291	12,290	118

C.2: FUEL PRICES

Table C.4 provides fuel prices used in our analysis. We obtain uranium prices from the AEO 2015 reference case [9]; landfill gas and non-fossil waste prices from the U.S.

Environmental Protection Agency's Integrated Planning Model documentation [10]; and all other prices from the AEO 2016 reference case [3].

Table C.4: Fuel prices by year used in our analysis.

Fuel Prices ($\$_{2012}$/MMBtu)	**2015**	**2025**	**2035**	**2045**
Coal	2.1	2.2	2.2	2.3
Natural gas	3.2	5.2	5.2	5.2
Oil	14.6	20.6	25.6	28.5
Uranium	0.8	0.9	1.0	1.0
Landfill gas	0.0	0.0	0.0	0.0
Non-fossil waste	0.0	0.0	0.0	0.0
Biomass	1.8	1.8	1.8	1.8

C.3: ANALYSIS OF REPRESENTATIVENESS OF 2015 DEMAND PROFILE

Since we ground our analysis in 2015, we use 2015 hourly demand for ERCOT in our analysis. This section compares ERCOT hourly demand in 2013 [11], 2014 [12], and 2015 [13] to understand how representative 2015 demand is of demand in other years. Table C.5 provides annual total and peak hourly demand for each year. Total and peak demand are less than 5% greater in 2015 than in 2013 and 2014, respectively. Figure C.1 provides monthly total demand for each year. Monthly demand in 2014 and 2015 differs by at most 4% in all months except July, when 2015 demand exceeds that in 2014 by 7%. Monthly demand in 2013 tends to be lower than 2014 and 2015, such that total demand in January and July are 13% and 10% lower, respectively, in 2013 than 2015.

Comparing hourly data, Figure C.2 provides average demand by hour of day for each year. Average hourly demand profiles share a similar shape between years, indicating daily demand patterns do not significantly differ between years. Hourly demand in 2015 is also highly

correlated with that in 2013 (0.79) and 2014 (0.80). Overall, aggregate and hourly demand is similar between 2013, 2014, and 2015, indicating that 2015 demand is broadly representative of demand in other years.

Table C.5: Annual total and hourly peak electricity demand in ERCOT in 2013, 2014, and 2015.

Year	Annual Total Demand (thousand GWh)	Annual Peak Hourly Demand (GWh)
2013	331.7	67.3
2014	340.1	66.5
2015	347.5	69.6

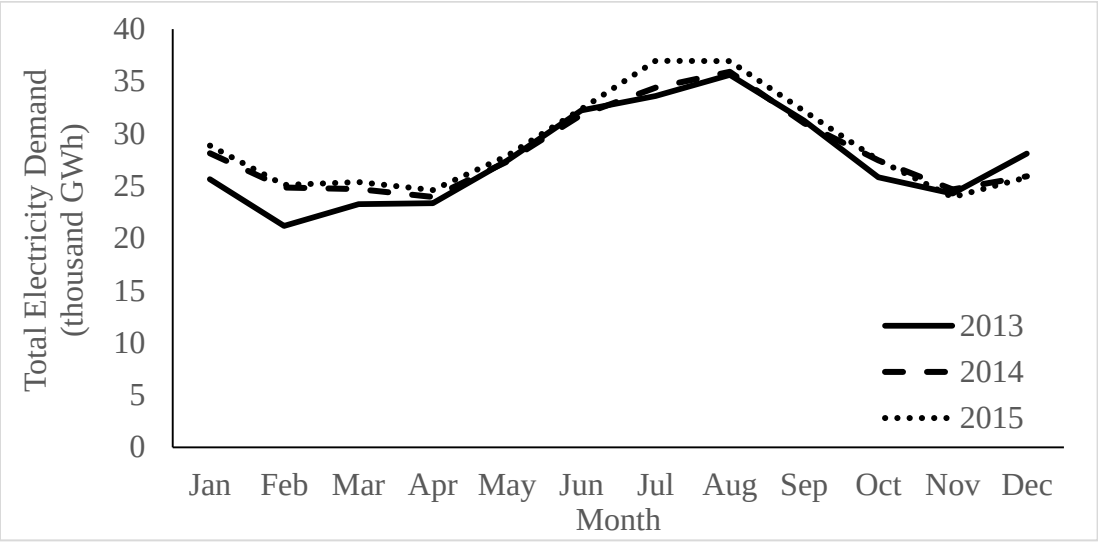

Figure C.1: Total electricity demand by month in 2013, 2014, and 2015 in ERCOT.

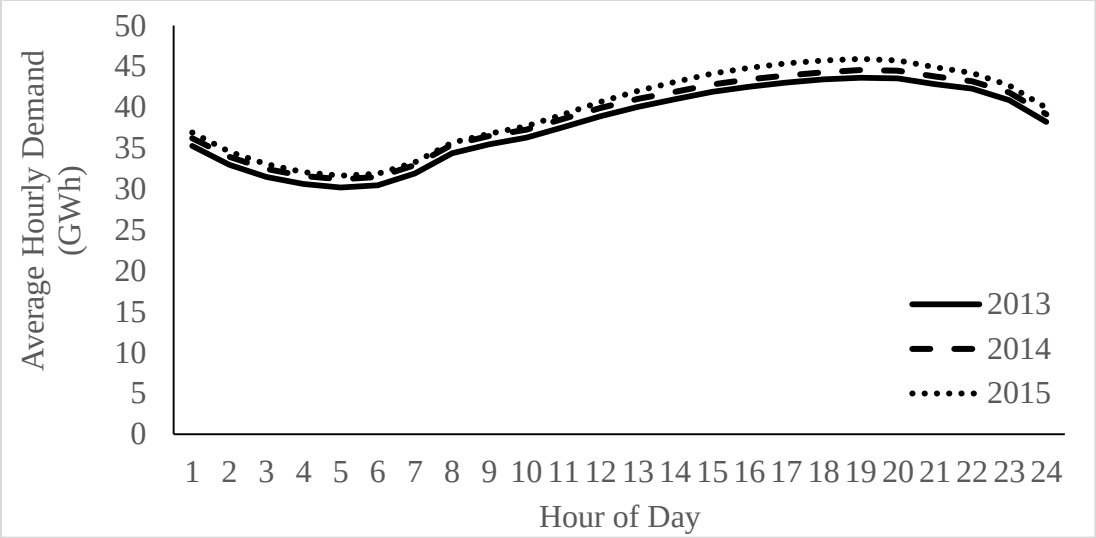

Figure C.2: Average demand by hour of day for the entire year in 2013, 2014, and 2015. For instance, in 2015, average demand at noon across all days equaled roughly 42 GWh.

C.4: CAPACITY EXPANSION (CE) MODEL FORMULATION

In order to account for variable wind and solar generation in generator addition decisions, our CE model includes unit commitment constraints using a grouped integer approach [14]. Additionally, since we set regulation and flexibility reserve requirements based on wind and solar generation, the CE model includes regulation and flexibility reserve requirements as variables.

Table C.6: Variables, parameters, and sets used in CE formulation.

Variable	Definition
n_c	Number of new generators built of plant type c
$g_{c,t}$	Electricity generation above minimum stable load by all new generators of plant type c at time t (MWh)
$g_{i,t}$	Electricity generation above minimum stable load by generator i at time t (MWh)
$p_{c,t}$	Electricity generation by all new generators of plant type c at time t (MWh)
$p_{i,t}$	Electricity generation by generator i at time t (MWh)
$r_{c,t}^{CNT}$	Contingency reserves provided by all new generators of plant type c at time t (MWh)

$r_{c,t}^{CNT}$	Contingency reserves provided by generator i at time t (MWh)
$r_{c,t}^{FLX}$	Flexibility reserves provided by all new generators of plant type c at time t (MWh)
$r_{c,t}^{FLX}$	Flexibility reserves provided by generator i at time t
$r_{c,t}^{REG}$	Regulation up reserves provided by all new generators of plant type c at time t (MWh)
$r_{i,t}^{REG}$	Regulation up reserves provided by generator i at time t (MWh)
rr_t^{CNT}	Required contingency reserves at time t (MWh)
rr_t^{FLX}	Required flexibility reserves at time t (MWh)
rr_t^{REG}	Required regulation up reserves at time t (MWh)
$u_{c,t}$	Number of new generators of plant type c that are on at time t
$u_{i,t}$	Binary variable indicating on/off state of generator i at time t, where 1 indicates on {0,1}
$v_{c,t}$	Number of new generators of plant type c that turn on at time t
$v_{i,t}$	Binary variable indicating generator i turns on at time t {0,1}
$w_{c,t}$	Number of new generators of plant type c that turn off at time t
$w_{i,t}$	Binary variable indicating generator i turns off at time t {0,1}

Parameter	**Definition**
$CF_{c_r,t}$	Capacity factor of renewable plant type c_r at time t
CRF_c	Capital recovery factor of plant type c
D_c	Lifetime of plant type c (year)
$E_{CO_2}^{MAX}$	Annual CO_2 emission cap (tons)
$ER_c^{CO_2}$	CO_2 emission rate of plant type c (ton/MMBtu)
$ER_i^{CO_2}$	CO_2 emission rate for generator i (ton/MMBtu)
FC_c	Fuel cost of plant type c ($/MMBtu)
FC_i	Fuel cost for generator i ($/MMBtu)
FOM_c	Annual fixed operation and maintenance costs of plant type c ($/MW)
HR_c	Heat rate of plant type c (MMBtu/MWh)
HR_i	Heat rate for generator i (MMBtu/MWh)
M	Planning reserve margin as fraction of demand
N_c^{MAX}	Maximum number of new generators that can be built of plant type c
OC_c	Operating cost of plant type c ($/MWh)
OC_i	Operating cost of generator i ($/MWh)
OCC_c	Overnight capital cost of plant type c ($/MW)
P_t^D	Electricity demand at time t (MWh)
P_c^{MAX}	Maximum electricity generation capacity of plant type c (MWh)
P_i^{MAX}	Maximum electricity generation capacity of generator i (MWh)
$P_t^{MAX,SOLAR}$	Maximum electricity generation by all existing solar generators at time t (MWh)
$P_t^{MAX,WIND}$	Maximum electricity generation by all existing wind generators at time t (MWh)
P_c^{MIN}	Minimum stable load of plant type c (MWh)
P_i^{MIN}	Minimum stable load of generator i (MWh)
Q	Discount rate

R_t^{FLX}	Required flexibility reserves at time t without additional wind or solar capacity (MWh)
R_t^{REG}	Required regulation up reserves at time t without additional wind or solar capacity (MWh)
RE_c^{CNT}	Plant type c eligible (1) or not (0) to provide contingency reserves
RE_i^{CNT}	Generator i eligible (1) or not (0) to provide contingency reserves
RE_c^{FLX}	Plant type c eligible (1) or not (0) to provide flexibility reserves
RE_i^{FLX}	Generator i eligible (1) or not (0) to provide flexibility reserves
RE_c^{REG}	Plant type c eligible (1) or not (0) to provide regulation up reserves
RE_i^{REG}	Generator i eligible (1) or not (0) to provide regulation up reserves
$RI_t^{FLX,SOLAR}$	Incremental flexibility reserve requirement per MW of additional solar capacity (MWh/MW)
$RI_t^{FLX,WIND}$	Incremental flexibility reserve requirement per MW of additional wind capacity (MWh/MW)
$RI_t^{REG,SOLAR}$	Incremental regulation up reserve requirement per MW of additional solar capacity (MWh/MW)
$RI_t^{REG,WIND}$	Incremental regulation up reserve requirement per MW of additional wind capacity (MWh/MW)
RL_c	Hourly ramp limit of plant type c (MWh)
RL_i	Hourly ramp limit of generator i (MWh)
RR_t^{CNT}	Required contingency reserves at time t (MWh)
RS^{CNT}	Scalar that translates hourly ramp limit to ramp limit over contingency reserve timeframe
RS^{FLX}	Scalar that translates hourly ramp limit to ramp limit over flexibility reserve timeframe
RS^{REG}	Scalar that translates hourly ramp limit to ramp limit over regulation reserve timeframe
SU_c	Start-up cost for plant type c ($)
SU_i	Start-up cost for generator i ($)
$U_{i,b}$	Binary parameter indicating whether generator is on or off in hour preceding time block b
VOM_c	Variable operation and maintenance costs of plant type c ($/MWh)
VOM_i	Variable operation and maintenance costs of generator i ($/MWh)
W_b	Scaling factor from number of representative hours included in CE model for time block b to number of total hours in time block b

Set	**Definition**
b	Time blocks (peak net demand and ramp days plus four seasons); b∈B
c	Potential new plant types; c∈C
c_r	Potential new renewable plant types; subset of C
c_t	Potential new thermal plant types; subset of C
c_w	Potential new wind plant type; subset of C
c_s	Potential new solar plant type; subset of C
i	Existing generators in fleet; i ∈ I
i_o	Existing solar generators in fleet; subset of I
i_w	Existing wind generators in fleet; subset of I

t	Time indices in optimization horizon; t∈T
t_b	Time indices in time block b; subset of T
t_p	Time index of peak demand; subset of T

C.4.1: Objective Function

The CE model minimizes annual total cost (*TC* [$]), which equals fixed plus variable electricity generation and start-up costs:

$$TC = \sum_c n_c * P_c^{MAX} * (FOM_c + OCC_c * CRF_c) + \sum_b \left(W_b \sum_{t_b \in T_b} \left(\sum_c p_{c,t_b} * OC_c + v_{c,t_b} * SU_c + \sum_i p_{i,t_b} * OC_i + v_{i,t_b} * SU_i \right) \right) \qquad \forall\, b \in B, i \in I, c \in C \qquad (1)$$

where *c*, *b*, *t*, and *i* index potential new plant types, time blocks, time intervals, and existing generators, respectively; *n* = number of new generators built; P^{MAX} = maximum capacity [MW]; *FOM* = fixed operation and maintenance (O&M) costs [$/MW/year]; *OCC* = overnight capital cost [$/MW]; *CRF* = capital recovery factor; *W* = scaling factor from number of representative to total hours in time block; *p* = electricity generation [MWh]; *OC* = operational cost [$/MWh]; v_i = binary variable indicating generator turns on; v_c = number of generators that turn on; and *SU* = start-up cost [$]. *OC* is defined for new and existing generators as:

$$OC = VOM + HR * FC \qquad (2)$$

where *VOM* = variable O&M costs [$/MWh], *HR* = heat rate [MMBtu/MWh], and *FC* = fuel cost [$/MMBtu]. *CRF* is defined as:

$$CRF_c = \frac{Q}{1 - (\frac{1}{(1+Q)^{D_c}})} \qquad (3)$$

where Q = discount rate and D = plant lifetime.

C.4.2: System Build, Generation, Capacity, and Reserve Constraints

The number of new generators built of plant type c is limited to a maximum value (N^{MAX}):

$$n_c \leq N_c^{MAX} \qquad \forall c \in C \qquad (4)$$

Electricity generation must equal demand (P^D [MWh]):

$$P_t^D = \sum_i p_{i,t} + \sum_c p_{c,t} \qquad \forall\, t \in T, i \in I, c \in C \qquad (5)$$

Additionally, sufficient capacity must exist to meet the planning reserve margin:

$$(1+M) * P_t^D \leq \sum_{c_t \in C_t} P_{c_t}^{MAX} * n_{c_t} + \sum_{c_r \in C_r} P_{c_r}^{MAX} * n_{c_r} * CF_{c_r,t} + \sum_{i \in (I - I_w - I_o)} P_i^{MAX} + P_t^{MAX,SOLAR} + P_t^{MAX,WIND} \qquad \forall\, t = T_p \qquad (6)$$

where c_t and c_r index new thermal and renewable plant types, respectively; i_w and i_o index existing wind and solar generators, respectively; M = a fraction of peak demand; CF = capacity factor; $P^{MAX,SOLAR}$ = maximum aggregate generation by existing solar generators [MWh]; and $P^{MAX,\,WIND}$ = maximum aggregate generation by existing wind generators [MWh].

Provided regulation (r^{REG} [MWh]), flexibility (r^{FLX} [MWh]), and contingency (r^{CNT} [MWh]) reserves must equal or exceed system requirements for regulation (rr^{REG} [MWh]), flexibility (rr^{FLX} [MWh]), and contingency (RR^{CNT} [MWh]), respectively:

$$\sum_i r_{i,t}^{REG} + \sum_c r_{c,t}^{REG} \geq rr_t^{REG} \qquad \forall t \in T, i \in I, c \in C \qquad (7)$$

$$\sum_i r_{i,t}^{FLX} + \sum_c r_{c,t}^{FLX} \geq rr_t^{FLX} \qquad \forall t \in T, i \in I, c \in C \qquad (8)$$

$$\sum_i r_{i,t}^{CNT} + \sum_c r_{c,t}^{CNT} \geq RR_t^{CNT} \qquad \forall t \in T, i \in I, c \in C \qquad (9)$$

Regulation and flexibility reserve requirements vary with added wind and solar capacity:

$$rr_t^{REG} = RI_t^{REG,SOLAR} * n_{c_s} * P_{c_s}^{MAX} + RI_t^{REG,WIND} * n_{c_w} * P_{c_w}^{MAX} + R_t^{REG} \qquad \forall t \in T, c_w \in C_w, c_s \in C_s \qquad (10)$$

$$rr_t^{FLX} = RI_t^{FLX,SOLAR} * n_{c_s} * P_{c_s}^{MAX} + RI_t^{FLX,WIND} * n_{c_w} * P_{c_w}^{MAX} + R_t^{FLX} \qquad \forall t \in T, c_w \in C_w, c_s \in C_s \qquad (11)$$

where c_w and c_s index new wind and solar plant types; *RI* = incremental regulation or flexibility reserve requirement per MW of additional wind or solar capacity [MWh/MW]; and *R* = initial regulation or flexibility reserve requirement [MWh].

C.4.3: Annual CO_2 Emissions Cap

Total CO_2 emissions from new and existing generators cannot exceed the annual CO_2 emission cap ($E_{CO_2}^{MAX}$ [tons]):

$$E_{CO_2}^{MAX} \geq \sum_b \left(W_b \sum_{t \in T_b} \left(\sum_i p_{i,t} * HR_i * ER_i^{CO_2} + \sum_c p_{c,t} * HR_c * ER_c^{CO_2} \right) \right) \quad \forall\, b \in B, i \in I, c \in C \qquad (12)$$

where ER^{CO_2} = CO_2 emission rate [ton/MMBtu].

C.4.4: Generator-Specific Generation Constraints

For existing generators, electricity generation is represented by two variables, total electricity generation (p [MWh]) and electricity generation above minimum stable load (g [MWh]) [15]:

$$p_{i,t} = P_i^{MIN} * u_{i,t} + g_{i,t} \qquad \forall t \in T, i \in I \qquad (13)$$

$$g_{i,t} \leq (P_i^{MAX} - P_i^{MIN}) * u_{i,t} \qquad \forall t \in T, i \in I \qquad (14)$$

where P^{MIN} = minimum stable load [MWh] and u = binary variable indicating the generator is on. Combined electricity generation by existing wind and solar generators is limited to aggregate wind and solar generation profiles:

$$\sum_{i_w} p_{i_w,t} \leq P_t^{MAX,WIND} \qquad \forall\, t \in T, i_w \in I_w \qquad (15)$$

$$\sum_{i_o} p_{i_o,t} \leq P_t^{MAX,SOLAR} \qquad \forall\, t \in T, i_o \in I_o \qquad (16)$$

Existing generators' electricity generation plus provided regulation, flexibility, and contingency reserves cannot exceed their maximum capacity:

$$p_{i,t} + r_{i,t}^{REG} + r_{i,t}^{FLX} + r_{i,t}^{CNT} \leq P_i^{MAX} \qquad \forall t \in T, i \in I \qquad (17)$$

As with existing units, total electricity generation and electricity generation above minimum stable load represent electricity generation by new units. To implement a grouped integer unit commitment approach, combined electricity generation by all new generators of each plant type depends on the number of generators online (u):

$$p_{c,t} = P_c^{MIN} * u_{c,t} + g_{c,t} \qquad \forall t \in T, c \in C \qquad (18)$$

$$g_{c,t} \leq (P_c^{MAX} - P_c^{MIN}) * u_{c,t} \qquad \forall t \in T, c \in C \qquad (19)$$

Electricity generation by new renewable generators is constrained by capacity factors:

$$p_{c_r,t} \leq u_{c_r} * P_{c_r}^{MAX} * CF_{c_r,t} \qquad \forall\, t \in T, c_r \in C_r \qquad (20)$$

New generators' electricity generation plus provided regulation, flexibility, and contingency reserves cannot exceed the combined maximum capacity of online generators:

$$p_{c,t} + r_{c,t}^{REG} + r_{c,t}^{FLX} + r_{c,t}^{CNT} \leq P_c^{MAX} * u_{c,t} \qquad \forall t \in T, c \in C \qquad (21)$$

C.4.5: Generator-Specific Reserve Provision Constraints

Existing generators must be online and eligible to provide regulation, flexibility, or contingency reserves, and provided regulation, flexibility, and contingency reserves cannot exceed each generator's ramp limit over the reserve timeframe:

$$r_{i,t}^{REG} \leq RE_i^{REG} * RL_i * RS^{REG} * u_{i,t} \qquad \forall\, i \in I, t \in T \qquad (22)$$

$$r_{i,t}^{FLX} \leq RE_i^{FLX} * RL_i * RS^{FLX} * u_{i,t} \qquad \forall\, i \in I, t \in T \qquad (23)$$

$$r_{i,t}^{CNT} \leq RE_i^{CNT} * RL_i * RS^{CNT} * u_{i,t} \qquad \forall\, i \in I, t \in T \qquad (24)$$

where *RE* = binary parameter indicating the generator can provide regulation, flexibility, or contingency reserves; *RL* = hourly ramp limit [MWh]; and *RS* = scalar that translate hourly ramp limit to ramp limit over the timeframe for regulation, flexibility, or contingency reserves.

Reserve provision constraints for new generators are similar to those for existing generators:

$$r_{c,t}^{REG} \leq RE_c^{REG} * RL_i * RS^{REG} * u_{c,t} \qquad \forall\, c \in C, t \in T \qquad (25)$$

$$r_{c,t}^{FLX} \leq RE_c^{FLX} * RL_i * RS^{FLX} * u_{c,t} \qquad \forall\, c \in C, t \in T \qquad (26)$$

$$r_{c,t}^{CNT} \leq RE_c^{CNT} * RL_i * RS^{CNT} * u_{c,t} \qquad \forall\, c \in C, t \in T \qquad (27)$$

C.4.6: Ramp Constraints

Ramping constraints for new and existing generators are enforced between time periods within each time block *b*, but not between time blocks. For each existing generator, increases in electricity generation plus provided reserves cannot exceed the ramp limit:

$$\left(g_{i,t_b} + r_{i,t_b}^{REG} + r_{i,t_b}^{FLX} + r_{i,t_b}^{CNT}\right) - g_{i,t_b-1} \leq RL_i \qquad \forall t_b > 1, i \in I \qquad (28)$$

Decreases in electricity generation also cannot exceed the ramp limit:

$$g_{i,t_b-1} - g_{i,t_b} \leq RL_i \qquad \forall t_b > 1, i \in I \qquad (29)$$

For new generators, ramp up and down constraints account for the number of new generators that turn on (*v*) and off (*w*), respectively, and both account for the number of new generators online:

$$\left(g_{c,t_b} + r_{c,t_b}^{REG} + r_{c,t_b}^{FLX} + r_{c,t_b}^{CNT}\right) - g_{c,t_b-1} \leq RL_c * u_{c,t_b} + P_c^{MAX} * v_{c,t_b} \qquad \forall t_b > 1, c \in C \qquad (30)$$

$$g_{c,t_b-1} - g_{c,t_b} \leq RL_c * u_{c,t_b} + P_c^{MAX} * w_{c,t_b} \qquad \forall t_b > 1, c \in C \qquad (31)$$

C.4.7: Unit Commitment Constraints

As with ramping constraints, unit commitment constraints are enforced between periods in each time block *b*, but not between time blocks. The commitment state (*u*) of each generator must be the same in the first and last period of each time block. For existing generators, the commitment state is linked to turn on and off decisions:

$$u_{i,t_b} = u_{i,t_b-1} + v_{i,t_b} - w_{i,t_b} \qquad \forall t_b > 1, i \in I \qquad (32)$$

where *w* = binary variable indicating the generator turns off. For $t_b = 1$ in each time block, we set u_{t-1} equal to a fixed value (*U*) determined via a simple economic dispatch model that meets demand in that hour at least cost subject to generator-specific capacity constraints. This serves as a rough heuristic for whether generator i would be on or off at the beginning of each time block.

$$u_{i,t_b} = U_{i,b} + v_{i,t_b} - w_{i,t_b} \qquad \forall t_b = 1, i \in I \qquad (33)$$

In each time block, generators also cannot turn on until they reach their minimum down time (*MDT* [hours]):

$$1 - u_{i,t_b} \geq w_{i,t_b-(MDT_i-1)} + w_{i,t_b-(MDT_i-2)} + \cdots + w_{i,t_b} \qquad \forall t_b > MDT_i, i \in I \qquad (34)$$

For new generators, a similar unit commitment constraint applies, but with integer rather than binary commitment variables:

$$u_{c,t_b} = u_{c,t_b-1} + v_{c,t_b} - w_{c,t_b} \qquad \forall t_b > 1, c \in C \qquad (35)$$

Additionally, the number of new generators online cannot exceed the number of new generators built:

$$u_{c,t} \leq n_c \qquad \forall t \in T, c \in C \qquad (36)$$

Minimum down time constraints also apply to new generators:

$$1 - u_{c,t_b} \geq w_{c,t_b-(MDT_c-1)} + w_{c,t_b-(MDT_c-2)} + \cdots + w_{c,t_b} \qquad \forall t_b > MDT_c, c \in C \qquad (37)$$

C.5: PARAMETERS OF GENERATORS THAT CAN BE ADDED IN CE MODEL

The CE model determines generator additions of six plant types: coal steam with carbon capture and sequestration (CCS), natural gas combined cycle (NGCC), NGCC with CCS, nuclear, wind, and solar photovoltaic. Given New Source Performance Standards for CO_2 emissions that prohibit new construction of coal-fired generators without CCS [16], we do not allow for construction of new coal-fired generators without CCS in our model. Table C.*7* and Table C.8 detail the parameters of each plant type eligible for addition in the CE model below. We obtain overnight capital costs, CO_2 emission rates, fixed and variable operation and maintenance (O&M) costs, and heat rates from the National Renewable Energy Laboratory's Annual Technology Baseline (ATB) [17]. Given Texas's excellent wind resources [18], wind data used here corresponds to mid-range cost forecasts for onshore wind in techno-resource group 3. Solar PV used here corresponds to mid-range estimates for utility solar PV. Since capital expenditure and fixed O&M costs in the ATB decline over time to reflect declining costs of new technologies, we present 2025 and 2045 values as a range in Table C.7. To account for the Investment Tax Credit, we reduce ATB wind capital expenditures in 2020 by 21%, the

average credit available to large wind units from 2016 through 2019, and reduce ATB solar capital expenditures by 30% and 10% in and after 2020, respectively [19]. Wind and solar capital expenditure values in Table C.7 do not reflect these cost reductions.

Given greater emphasis on flexible operational capabilities for new builds relative to existing generators, we obtain new-build-specific ramp rate and minimum load values from Black & Veatch [20]. Generator capacities equal those used in the U.S. Energy Information Administration's AEO 2013 [6]. Finally, start cost & minimum down times are obtained from PHORUM [4], a price-validated reduced form UCED model of PJM [5].

Table C.7: Key parameters of new technologies that can be added to the generator fleet by the CE model. Provided ranges are for 2020 to 2045 values. Capital expenditure values do not reflect the Investment Tax Credit.

Plant Type	**Fuel Type**	**Capacity (MW)**	**Heat Rate (Btu/ kWh)**	**Capital Expenditure (thousand $_{2012}$/MW)**	**Fixed O&M (thousand $_{2012}$/MW/ year)**	**Variable O&M ($_{2012}$/MWh)**
Coal Steam CCS	Coal	650	8,060	7,040 - 6,000	72	8.7
NGCC	Natural Gas	400	6,370	1,000 - 900	14	2.9
NGCC CCS	Natural Gas	340	7,270	2,040 - 1,660	31	6.8
Nuclear	Uranium	1117	10,170	6,180 - 5,420	92	1.9
Wind	Wind	100	0	1,650 - 1,550	49 - 46	0
Solar PV	Solar	20	0	1,410 - 870	8	0

Table C.8: Additional key parameters of new technologies that can be added to the generator fleet by the CE model.

Plant Type	CO_2 Emissions Rate (lb/MMBtu)	Minimum down time (hours)	Ramp rate (MW/hour)	Minimum load (MW)	Start cost (thousand $\$_{2012}$)
Coal Steam CCS	20.5	12	780	260	66
NGCC	119	4	1200	200	41
NGCC CCS	11.9	4	1020	170	35
Nuclear	0	20	3350	560	57
Wind	0	0	100	0	0
Solar PV	0	0	20	0	0

Since the CE model runs for a single year, we annualize capital expenditures prior to input to the CE model using a capital recovery factor (CRF) for each plant type. We calculate the CRF as:

$$CRF_c = \frac{r * (1+r)^{n_c}}{(1+r)^{n_c} - 1}$$

where c indexes plant type; r = discount rate (7%) [21]; and n_c = plant lifetime (years).

C.6: GENERATOR RETIREMENTS IN THE CE MODEL

In order to account for generator retirements, we use two heuristics. First, we retire generators based on age before each CE run. Second, we retire generators based on economic performance before and after each CE run [22]. Age-based retirements occur when a generator's age exceeds its lifetime. Table C.9 below provides lifetime by plant type for new and existing generators [23]. Since pre-existing transmission interconnections and other infrastructure would reduce development costs, we immediately replace wind, solar, geothermal, biomass, and hydropower units that retire with identical units [22]. Given the recent wave of coal-plant retirements driven by challenging economics [24] and the need to balance fixed costs with

operating profits, economic-based retirements occur only for coal-fired generators [22]. After each CE run, coal-fired generators retire when their capacity factor in the CE run is less than 0.3 and the remaining fleet capacity would exceed the planning margin. This retirement threshold reflects that nearly 90% of coal-fired generators in ERCOT had capacity factors above 0.5 in 2014 [2]. If a coal-fired generator should retire but doing so would prevent the system from maintaining the planning margin, that generator retires immediately prior to the next CE run.

Table C.9: Lifetimes of new and existing generators by plant type.

Plant Type	Lifetime (years)
Coal Steam	65
Coal Steam CCS	65
Combined Cycle	55
Combined Cycle CCS	55
Combustion Turbine	20
Nuclear	60
Biomass	40
Wind	30
Solar PV	20
Non-Fossil Waste	40
O/G Steam	55
Landfill Gas	20

C.7: SOLAR AND WIND ELECTRICITY GENERATION

In order to capture spatial and temporal variability in output among wind and solar farms, we match wind and solar power plants to simulated wind and solar generation profiles from the U.S. National Renewable Energy Laboratory (NREL) [25], [26]. These wind and solar generation databases provide simulated generation profiles for hypothetical plants in Texas at 10- and 5-minute increments, respectively, for 2004-2006 and 2006, respectively. Given that the minimum, average, and maximum of average annual CFs across wind plants are similar in 2004 (0.41, 0.44, and 0.47, respectively), 2005 (0.40, 0.44, and 0.47, respectively), and 2006 (0.39,

0.44, and 0.48, respectively), we use 2005 wind generation data. We aggregate generation data to hourly increments by calculating the average generation values for all time steps in each hour [27]. After excluding several solar plants with no generation data, hourly capacity factors for hypothetical wind and solar plants in Texas in the NREL dataset range from 41-46% and 15-23%, respectively.

For existing wind units in the CE and UCED models, we calculate the installed capacity of wind in our base fleet, and add wind farms from the NREL dataset to our fleet in order of decreasing capacity factor. Note that existing wind units in each CE and UCED model run include wind units added in previous CE runs. For instance, a wind unit added in the 2020 CE run is considered an existing wind unit in the 2025 CE and UCED runs. We perform the same process for existing solar units, which also include solar units added in CE runs prior to each CE and UCED run. Since we do not account for transmission in our CE and UCED models, each existing wind and solar unit varies only by capacity and hourly generation profile. As such, in order to improve the computational efficiency of both models, we combine existing wind and solar units into a single wind and solar unit by summing their capacities and hourly generation profiles.

In order to maintain computational tractability, rather than inputting numerous potential new wind and solar units with unique generation profiles to the CE model, we instead determine capacity additions for one representative wind unit and one representative solar unit in the CE model. These representative units each have an hourly generation profile. To determine these generation profiles, we estimate capacity-weighted generation profiles for assumed capacities of wind and solar incremental to the existing capacities of wind and solar. We set these assumed capacities equal to 3 GW in order to balance two competing factors: first, the generation profile

should represent marginal investment in wind and solar, i.e. the next MW of additional wind and solar, but second, the CE model runs in 5-year intervals, so wind and solar investment in each period will be on the order of gigawatts. To calculate the generation profiles for 3 GW of incremental wind and solar capacities, we temporarily remove wind and solar farms from the NREL datasets with a combined capacity equal to the existing fleet capacity in order of decreasing capacity factor. From the remaining wind and solar farms in the NREL datasets, we obtain hourly generation profiles for 3 GW of wind and solar in order of decreasing capacity factor, then calculate the capacity-weighted average hourly generation profile for those generators. As discussed above, once wind or solar capacity is added by a CE model run, that wind and solar capacity is treated as "existing" capacity in future CE and UCED model runs. Consequently, that added wind and solar capacity is assigned a generation profile in future CE and UCED model runs per the prior paragraph.

Note that in several scenarios, installed wind and/or solar capacities ultimately exceed total capacity in the NREL databases. In those cases, we cannot obtain generation profiles for additional wind and/or solar capacity for the CE model from the NREL databases, as no wind and/or solar capacities incremental to existing wind and solar capacities exists in the NREL databases. Consequently, we instead estimate generation profiles for additional wind and/or solar capacities as the capacity-weighted generation profiles of existing wind and/or solar units. Essentially, once total installed wind and/or solar capacities equal those in the NREL databases, we assume all future wind and/or solar investments will have the same generation profile as the capacity-weighted generation profile of all installed wind and solar.

C.8: CALCULATING RESERVE REQUIREMENTS

To accommodate variable generation from wind and solar, the CE and UCED models include two reserve types, regulation and flexibility, that vary hourly based on wind and solar generation. Since the CE model optimizes for wind and solar additions, it considers regulation and flexibility reserve requirements as variables that depend on added wind and solar capacity. In the UCED model, when wind and solar capacity are fixed, regulation and flexibility reserve requirements are treated as parameters. To account for generator and transmission outages, the CE model also procures contingency reserves that vary with hourly load.

To calculate hourly regulation, contingency, and flexibility reserve requirements used in our CE and UCED models, we follow the framework put forth in NREL's Western Wind and Solar Integration Study (WWSIS) (Table C.10) [28]. The remainder of this section specifies how we calculate the wind and solar components in regulation and flexibility reserve requirements. The key inputs to the analyses are generation profiles for wind and solar based on NREL data, which differ between existing and new generators (see Section C.7).

Since we input generation profiles for new and existing wind and solar generators into the CE model (but only for existing wind and solar generators into the UCED model), we use the same analytical framework described below to determine reserve requirements for existing and new generators. However, the form of reserve requirements differs between existing and new generators. For existing generators in the UCED and CE models, since installed capacity is fixed, the analytic framework below outputs total hourly reserve requirements for all existing wind and solar generators. For new generators, the CE model optimizes how much new wind and solar should be built. Consequently, reserve requirements output by the analytic framework below must accommodate a to-be-determined capacity of new wind and solar. To that end, we calculate

reserve requirements per unit of added wind and solar using the analytic framework below. Specifically, per Section C.7, in the CE model we calculate hourly reserve requirements for an assumed 3 GW of added wind and solar capacity using the below analytic framework, then divide those hourly reserve requirements by the assumed added capacity value of 3 GW.

Table C.10: Formula and time scale of data used to calculate hourly reserve requirement for each reserve type included in the CE and UCED models. *SR* and *WR* indicate solar and wind components, whereas *r* and *f* index regulation and flexibility reserves. NA indicates not applicable.

Type	Formula to Calculate Reserve Requirement	Demand Time Scale	Wind Generation Time Scale	Solar Generation Time Scale
Regulation	$\sqrt{(1\%\ demand)^2 + SR_r^2 + WR_r^2}$	Hourly	10-minute	5-minute
Flexibility	$\sqrt{SR_f^2 + WR_f^2}$	NA	Hourly	Hourly
Contingency	$3\%\ demand$	Hourly	NA	NA

C.8.1: Wind Reserve Components

To calculate the wind component in hourly regulation reserve requirements (WR_r), we estimate the 2.5th percentile of wind power output forecast errors (hereafter "wind forecast errors") as a function of wind power output. To estimate wind forecast error, we assume a persistence forecast [29], i.e. that wind power output will not change from one time period to the next [28]. With this assumption, wind forecast error equals the change in wind power output from one 10-minute period to the next. We pair each wind forecast error with total wind power output at the latter time period (e.g., we pair the wind forecast error from t=3 to t=4 with total wind power output at t=4). Doing so reveals that wind forecast error varies significantly with wind power output (Figure C.3). To account for the dependence of wind forecast error on wind

power output, we sort wind forecast error by wind power output, then segment the dataset into 10 groups with equal numbers of wind forecast errors. For each group, we calculate the average power output and the 2.5^{th} percentile of wind forecast error. (Note that regulation up must account for over-forecasts of wind power. Here, we define wind forecast error as the change in wind power output from one period to the next. Thus, over-forecasts equal negative error values in our calculation, so regulation up reserves correspond to the 2.5^{th}, not 97.5^{th}, percentile.) For each 10-minute wind power output value, we then interpolate between average power output values to obtain a power-output-specific estimate of the 2.5^{th} percentile of wind forecast error. Since we interpolate between average values, many wind power output values are less than the minimum of the 10 average power output values we calculate. Similarly, many wind power output values are greater than the maximum of the 10 average power output values we calculate. In these cases, we cannot interpolate between average power output values to determine a power-output-specific estimate of the 2.5^{th} percentile of wind forecast error. Instead, we use the 2.5^{th} percentile of wind forecast error for the closest average power output value. For instance, for wind power output values smaller than the minimum average power output value, we use the 2.5^{th} percentile of wind forecast error estimate for the minimum average power output value. Finally, we set hourly regulation reserve requirements equal to the absolute value of the minimum 2.5^{th} percentile value in each hour. We use the same process as above to set the wind component in hourly flexibility reserve requirements (WR_f), but use hourly wind power output data and the 15^{th} percentile of wind forecast error.

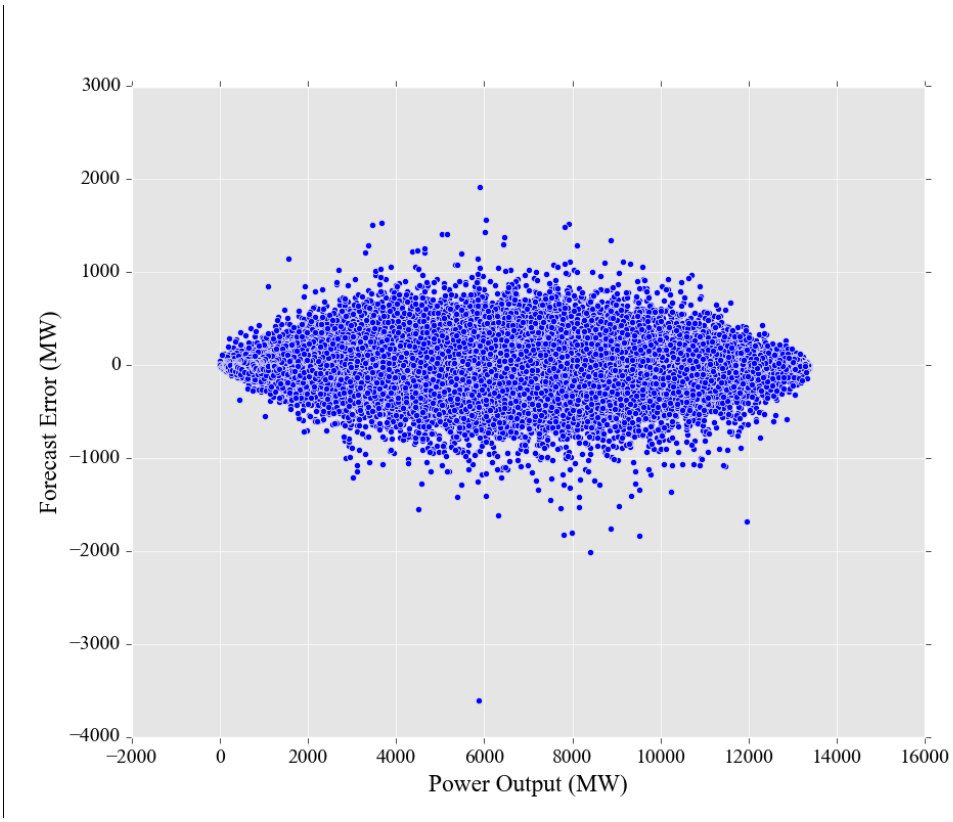

Figure C.3: Wind power output forecast errors for a year of 10-minute wind power output data for 13.8 GW of wind capacity. Assuming a persistence forecast, we estimate wind forecast errors as the change in power output from one time period to the next.

C.8.2: Solar Reserve Components

To calculate the solar component in hourly regulation reserve requirements (SR_r), we estimate the 2.5th percentile of solar power output forecast errors (hereafter "solar forecast errors") as a function of relative time of day. To estimate solar forecast error, we assume a persistence forecast, so solar forecast error equals the change in solar power output from one 5-minute period to the next. To account for predictable daily changes in solar generation (e.g., around sunrise and sunset) (Figure C.4), we exclude forecast errors overnight and around sunrise and sunset from further analysis. To do so, we divide our data into pairs of months, set sunrise and sunset as the earliest and latest times at which solar power output occurs in each month pair,

and exclude the 5 and 8 5-minute time periods succeeding and preceding sunrise and sunset, respectively. Given disparate trends in solar forecast errors pre- and post-midday (Figure C.4), we split the remaining errors in each month pair by whether they occur pre- or post-midday. For pre- and post-midday errors in each month pair, we estimate the 2.5^{th} percentile of solar forecast error. We then set regulation reserve requirements for each hour equal to the absolute value of the 2.5^{th} percentile of solar forecast error corresponding to the hour's month and whether it falls pre- or post-midday. For hours straddling midday, we set the regulation reserve requirement equal to the greater regulation reserve requirement. We use the same process as above to set the solar component in hourly flexibility reserve requirements (SR_f), but use hourly solar power output data; exclude 1 and 2 time periods succeeding and preceding sunrise and sunset, respectively; and use the 15^{th} percentile of solar forecast error.

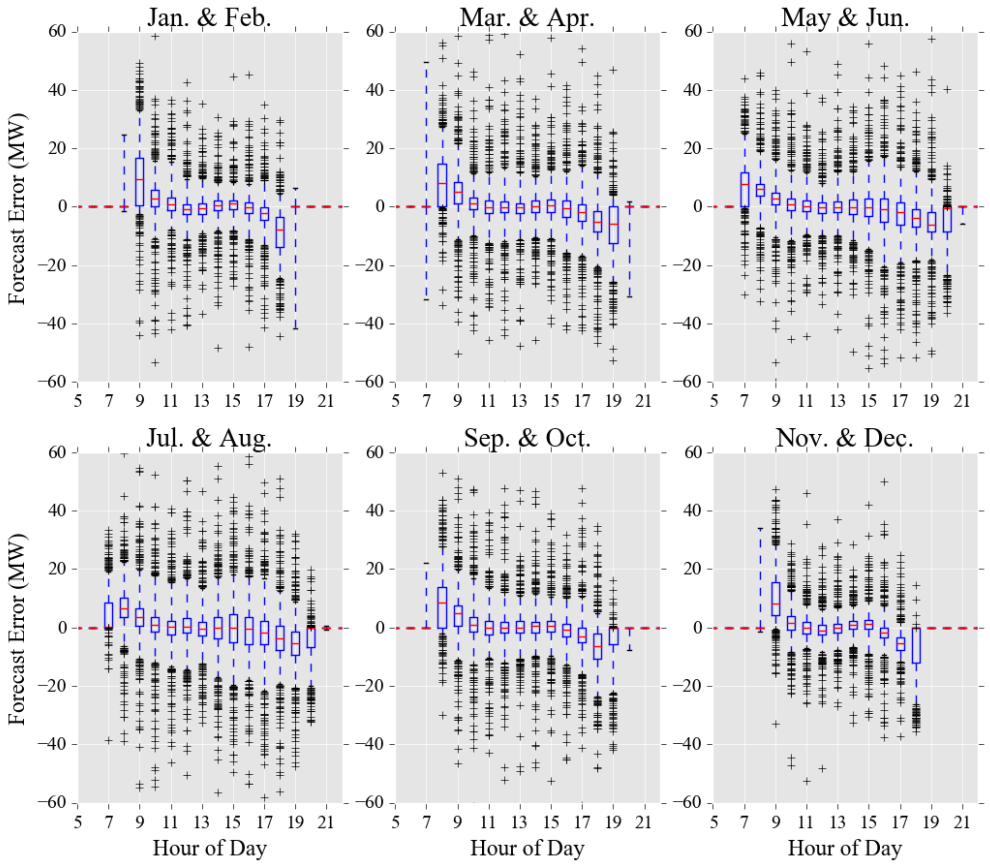

Figure C.4: Solar power output forecast errors for 326 MW solar for a year of 5-minute solar power output data by hour of day and grouped in pairs of months. Assuming a persistence forecast, we estimate solar forecast errors as the change in power output from one time period to the next. Boxes indicate 25th and 75th percentiles and whiskers indicate 0.5th and 99.5th percentile errors.

C.8.3: Time Series of Wind and Solar Generation and Reserve Requirements

Figure C.5 and Figure C.6 provide a sample time series of the wind and solar components of regulation and flexibility reserves, respectively, adjacent to wind and solar generation profiles. The solar component of both reserves assumes two values over the course of the day for pre- and post-midday hours. The solar component is greater post-midday than pre-midday because solar power output declines through sunset, leading to more over-forecasts of solar power output. The

solar component of both reserves equals zero overnight. The wind component of regulation and flexibility reserves varies with total wind power output, and is greatest at moderate wind power output values when forecast error is greatest (Figure C.3). Finally, Figure C.7 overlays regulation, flexibility, and contingency reserves. Over the illustrated period, contingency reserves tend to exceed flexibility reserves, which in turn exceed regulation reserves.

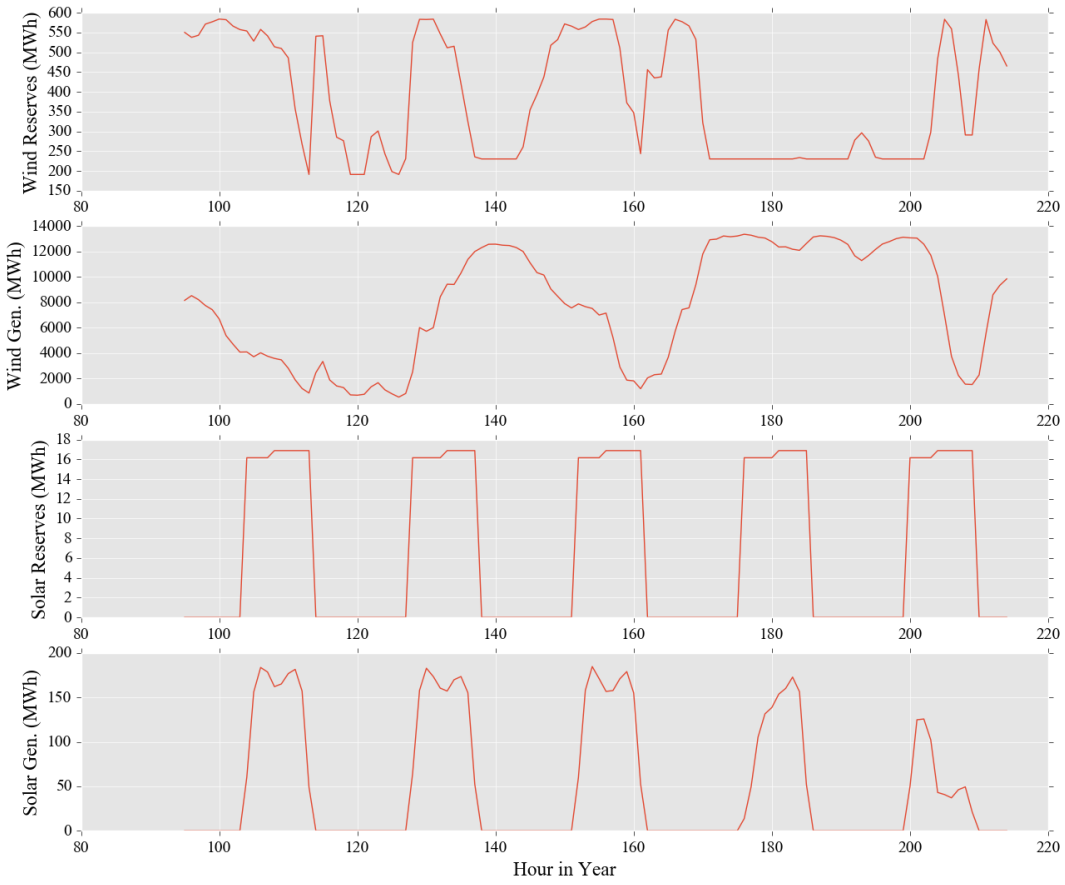

Figure C.5: Time series of wind component of regulation reserve requirement (top), wind generation (second from top), solar component of regulation reserve requirement (second from bottom), and solar generation (bottom). Time series is for January 5th to 10th.

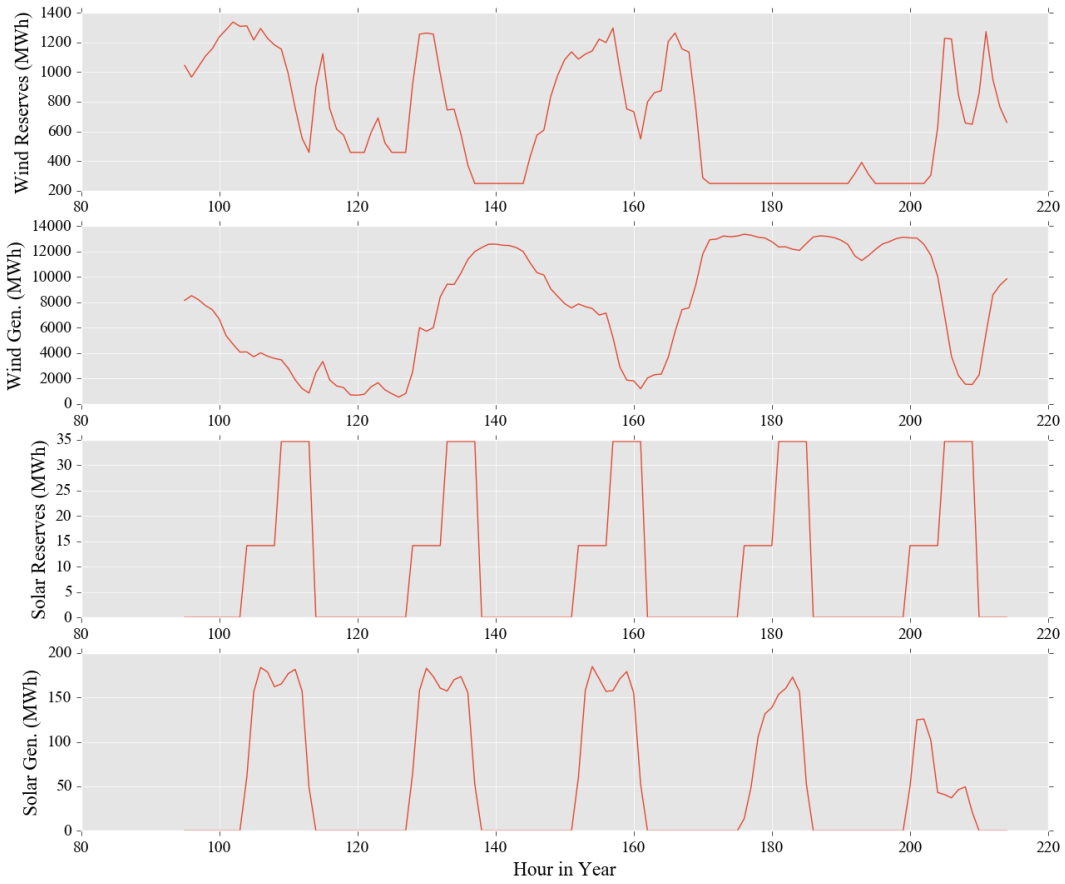

Figure C.6: Time series of wind component of flexibility reserve requirement (top), wind generation (second from top), solar component of flexibility reserve requirement (second from bottom), and solar generation (bottom). Time series is for January 5th to 10th.

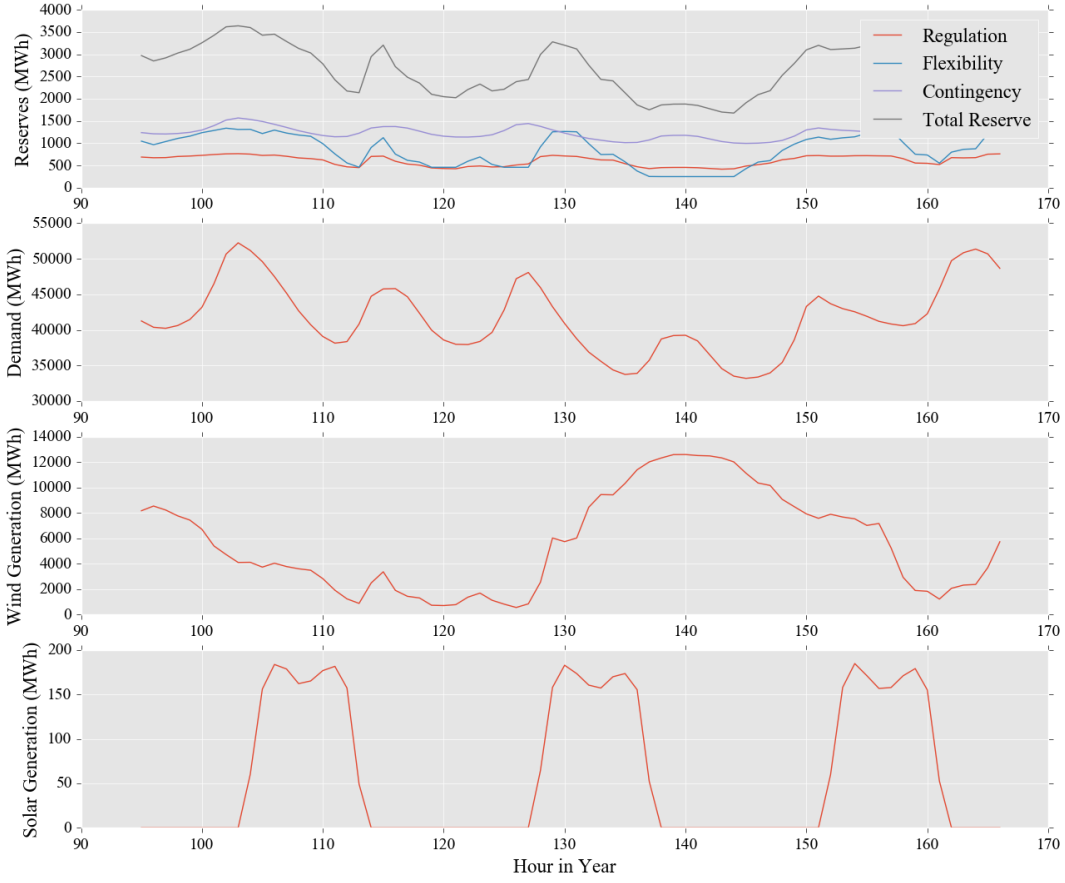

Figure C.7: Time series of hourly regulation, flexibility, contingency, and total reserve requirements (top); hourly electricity demand (2nd from top); hourly wind generation (3rd from top); and hourly solar generation (bottom).

C.9: SELECTION OF REPRESENTATIVE DAYS PER SEASON INCLUDED IN CE MODEL

For computational tractability, we run the CE model in hourly intervals for two representative contiguous days per season, the day with peak annual net demand, and the day with the peak annual change in hourly net demand, where net demand equals demand minus solar and wind generation. By using net rather than total demand, we implicitly value the time-

varying capacity of wind and solar units and the need for investment in flexible generation [30]. To select the representative days per season included in our CE model, we first divide the year into four seasons: winter (December - February), spring (March - May), summer (June - August), and fall (September - November). Since we already include peak annual demand and ramp days in the CE model, we remove them from the relevant season(s). For each season, we then determine the net load duration curve (NLDC) for the entire season and for each pair of contiguous days using wind and solar generation profiles. The pair of contiguous days with the lowest RMSE between their NLDC and the season's NLDC [31], [32] serve as the representative days for that season in the CE model. Normalized RMSEs for all seasons and scenarios in our analysis range from 2-5%. To scale costs and emissions in the CE model to annual values, we multiply costs and emissions on each pair of representative days by the quotient of total demand over the representative days and the season [23].

C.10: UNIT COMMITMENT AND ECONOMIC DISPATCH (UCED) FORMULATION

Here, we provide the UCED formulation including storage units. For UCED runs without storage, storage sets, parameters, and constraints are eliminated. Like our CE model, our UCED model includes three reserve types (regulation, flexibility, and contingency). Our UCED model co-optimizes for regulation reserves.

Table C.11: Variables, parameters, and sets used in UCED formulation.

Variable	Definition
$f_{i_s,t}$	Energy inflows at storage unit i_s at time t (MWh)
$g_{i,t}$	Electricity generation above minimum stable load by generator i at time t (MWh)
nse_t	Non-served energy at time t (MWh)
$p_{i,t}$	Electricity generation by generator i at time t (MWh)

$r_{i,t}^{CNT}$	Contingency reserves provided by generator i at time t (MWh)
$r_{i,t}^{FLX}$	Flexibility reserves provided by generator i at time t (MWh)
$r_{i,t}^{REG}$	Regulation up reserves provided by generator i at time t (MWh)
$u_{i,t}$	Binary variable indicating on/off state of generator i at time t, where 1 indicates on {0,1}
$v_{i,t}$	Binary variable indicating generator i turns on at time t {0,1}
$w_{i,t}$	Binary variable indicating generator i turns off at time t {0,1}
$x_{i_s,t}$	State of charge of storage unit i_s at time t (MWh)

Parameter	**Definition**
CNSE	Cost of non-served energy ($/MWh)
$ER_i^{CO_2}$	CO_2 emission rate for generator i (ton/MMBtu)
EC^{CO_2}	CO_2 emission cost ($/ton)
$F_{i_s}^{MAX}$	Maximum energy inflow capacity of storage unit i_s (MWh)
FC_i	Fuel cost for generator i ($/MMBtu)
G_i	Electricity generation above minimum stable load by generator i in last hour of prior optimization period (MWh)
HR_i	Heat rate for generator i (MMBtu/MWh)
K	Number of hours before which a generator can turn on in the current optimization horizon, based on when it shut off in the last optimization period and its MDT
MDT_i	Minimum down time for generator i, which indicates the number of hours that must elapse before a generator can turn on once it shuts off (hours)
OC_i	Operating cost of generator i ($/MWh)
P_i	Electricity generation by generator i in the last period of the prior optimization horizon (MWh)
P_t^D	Electricity demand at time t (MWh)
P_i^{MAX}	Maximum electricity generation capacity of generator i (MWh)
$P_t^{MAX,SOLAR}$	Maximum electricity generation by all solar generators at time t (MWh)
$P_t^{MAX,WIND}$	Maximum electricity generation by all wind generators at time t (MWh)
P_i^{MIN}	Minimum stable load of generator i (MWh)
R_t^{CNT}	Required contingency reserves at time t (MWh)
R_t^{FLX}	Required flexibility reserves at time t (MWh)
R_t^{REG}	Required regulation up reserves at time t (MWh)
RC_i	Regulation up provision cost for generator i ($/MWh)
RE_i^{CNT}	Generator i eligible (1) or not (0) to provide contingency reserves
RE_i^{FLX}	Generator i eligible (1) or not (0) to provide flexibility reserves
RE_i^{REG}	Generator i eligible (1) or not (0) to provide regulation up reserves
RL_i	Hourly ramp limit of generator i (MWh)
RS^{CNT}	Scalar that translates hourly ramp limit to ramp limit over contingency reserve timeframe
RS^{FLX}	Scalar that translates hourly ramp limit to ramp limit over flexibility reserve timeframe
RS^{REG}	Scalar that translates hourly ramp limit to ramp limit over regulation reserve timeframe
SU_i	Start-up cost for generator i ($)

U_i	On/off state of generator i in the last period of the prior optimization horizon {0,1}
VOM_i	Variable operation and maintenance cost of generator i ($/MWh)
X_{i_s}	State of charge of storage unit i_s in the last period of the prior optimization horizon (MWh)
$X_{i_s}^{MAX}$	Max state of charge, i.e. electricity storage capacity, of storage unit i_s (MWh)
$X_{i_s}^{MIN}$	Minimum state of charge of storage unit i_s (MWh)
η_{i_s}	Round-trip efficiency of storage unit i_s

Set	**Definition**
i	Generators in fleet; i∈I
i_o	Solar generators in fleet; subset of I
i_n	Non-storage generators in fleet; subset of I
i_s	Storage generators in fleet; subset of I
i_w	Wind generators in fleet; subset of I
t	Time indices in optimization horizon; t∈T

C.10.1: Objective Function

The UCED model minimizes total operational costs (*TC*), or the sum of electricity generation, reserve, start-up, and non-served energy costs:

$$TC = \sum_{i,t} p_{i,t} * OC_i + v_{i,t} * SU_i + r_{i,t}^{REG} * RC_i + \sum_t nse_t * CNSE \qquad \forall t \in T, i \in I \qquad (1)$$

where *i* and *t* index generators and time, respectively; *p* = electricity generation [MWh]; *OC* = operating cost [$/MWh]; *v* = binary variable indicating the generator turns on; *SU* = start-up cost [$]; r^{REG} = provided regulation up reserves [MWh]; *RC* = regulation up reserve cost [$/MWh]; *nse* = non-served energy [MWh]; and *CNSE* = cost of non-served energy [$/MWh]. Operating costs (*OC*) equal:

$$OC_i = HR_i * \left(FC_i + ER_i^{CO_2} * EC^{CO_2}\right) + VOM_i \qquad (2)$$

where *HR* = heat rate [MMBtu/MWh]; *FC* = fuel cost [$/MMBtu]; ER^{CO_2} = CO_2 emission rate [ton/MMBtu]; EC^{CO_2}= CO_2 emission cost [$/ton]; and *VOM* = variable operation and maintenance costs [$/MWh].

C.10.2: System-wide Electricity Demand and Reserve Requirement Constraints

Electricity generation plus non-served energy must equal system-wide demand (P^D [MWh]) plus energy inflows to storage units (f [MWh]) in each time period:

$$\sum_{i \in I} p_{i,t} + nse_t = P_t^D + \sum_{i_s \in I_s} f_{i_s,t} \qquad \forall t \in T \qquad (3)$$

Provided regulation, flexibility (r^{FLX} [MWh]), and contingency (r^{CNT} [MWh]) reserves must equal or exceed required regulation (R^{REG} [MWh]), flexibility (R^{FLX} [MWh]), and contingency (R^{CNT} [MWh]) reserves, respectively, in each time period:

$$\sum_i r_{i,t}^{REG} \geq R_t^{REG} \qquad \forall t \in T, i \in I \qquad (4)$$

$$\sum_i r_{i,t}^{FLX} \geq R_t^{FLX} \qquad \forall t \in T, i \in I \qquad (5)$$

$$\sum_i r_{i,t}^{CNT} \geq R_t^{CNT} \qquad \forall t \in T, i \in I \qquad (6)$$

C.10.3: Generator-Specific Generation Constraints

Electricity generation is represented by two variables, total generation (p [MWh]) and generation above minimum stable load (g [MWh]) [15]:

$$p_{i,t} = P_i^{MIN} * u_{i,t} + g_{i,t} \qquad \forall t \in T, i \in I \qquad (7)$$

$$g_{i,t} \leq (P_i^{MAX} - P_i^{MIN}) * u_{i,t} \qquad \forall t \in T, i \in I \qquad (8)$$

where P^{MIN} = minimum stable load [MWh] and u = binary variable indicating the generator is on (1) or off (0). Combined electricity generation by wind (I_w) and solar (I_o) generators is limited to aggregate wind ($P^{MAX,WIND}$ [MWh]) and solar ($P^{MAX,SOLAR}$ [MWh]) generation profiles:

$$\sum_{i_w} p_{i_w,t} \leq P_t^{MAX,WIND} \qquad \forall\, i_w \in I_w, t \in T \qquad (9)$$

$$\sum_{i_o} p_{i_o,t} \leq P_t^{MAX,SOLAR} \qquad \forall i_o \in I_o, t \in T \qquad (10)$$

For each generator, electricity generation plus regulation, flexibility, and contingency reserve provision cannot exceed maximum capacity:

$$p_{i,t} + r_{i,t}^{REG} + r_{i,t}^{FLX} + r_{i,t}^{CNT} \leq P_i^{MAX} \qquad \forall t \in T, i \in I \qquad (11)$$

C.10.4: Generator-Specific Reserve Provision Constraints for Non-Storage Units

Non-storage generators must be online and eligible to provide regulation, flexibility, or contingency reserves, and cannot provide reserves in excess of their ramp limit over the reserve timeframe:

$$r_{i_n,t}^{REG} \leq RE_{i_n}^{REG} * RL_{i_n} * RS^{REG} * u_{i_n,t} \qquad \forall\, i_n \in I_n, t \in T \qquad (12)$$

$$r_{i_n,t}^{FLX} \leq RE_{i_n}^{FLX} * RL_{i_n} * RS^{FLX} * u_{i_n,t} \qquad \forall\, i_n \in I_n, t \in T \qquad (13)$$

$$r_{i_n,t}^{CNT} \leq RE_{i_n}^{CNT} * RL_{i_n} * RS^{CNT} * u_{i_n,t} \qquad \forall\, i_n \in I_n, t \in T \qquad (14)$$

where *RE* = binary parameter indicating a generator can provide regulation, flexibility, or contingency reserves; *RL* = hourly ramp limit [MWh]; and *RS* = scalar that translates an hourly ramp limit to a ramp limit over the timeframe of regulation, flexibility, or contingency reserves.

C.10.5: Ramp Constraints

Up and down ramp constraints limit changes in electricity generation above minimum stable load plus provided regulation, flexibility, and contingency reserves:

$$\left(g_{i,t} + r_{i,t}^{REG} + r_{i,t}^{FLX} + r_{i,t}^{CNT}\right) - g_{i,t-1} \leq RL_i \qquad \forall t > 1, i \in I \qquad (15)$$

$$g_{i,t-1} - g_{i,t} \leq RL_i \qquad \forall t > 1, i \in I \qquad (16)$$

In the first time period, electricity generation above minimum stable load in the prior period equals generation above minimum stable load from the final hour of the last optimization horizon (*G* [MWh]):

$$\left(g_{i,t} + r_{i,t}^{REG} + r_{i,t}^{FLX} + r_{i,t}^{CNT}\right) - G_i \leq RL_i \qquad \forall t = 1, i \in I \qquad (17)$$

$$G_i - g_{i,t} \leq RL_i \qquad \forall t = 1, i \in I \qquad (18)$$

In the first UC run, G_i equals zero for all generators.

C.10.6: Unit Commitment Constraints

Whether a generator is on or off depends on turn on and turn off decisions:

$$u_{i,t} = u_{i,t-1} + v_{i,t} - w_{i,t} \qquad \forall t > 1, i \in I \qquad (19)$$

where *w* = binary variable indicating the generator turns off. In the first period, the commitment state in the prior period equals the commitment state in the last period of the prior UC run (*U*):

$$u_{i,t} = U_{i,t} + v_{i,t} - w_{i,t} \qquad \forall t = 1, i \in I \qquad (20)$$

In the first UC run, $U_{i,t}$ equals zero for all generators. Generators also cannot turn on until they reach their minimum down time (*MDT* [hours]):

$$1 - u_{i,t} \geq w_{i,t-(MDT_i-1)} + w_{i,t-(MDT_i-2)} + \cdots + w_{i,t} \qquad \forall t > K_i, i \in I \qquad (21)$$

To account for shut downs in the prior optimization window, carried hours of minimum down time from the prior UC run (*K*) are enforced:

$$u_{i,t} \leq 0 \qquad \forall t \leq K_i, i \in I \qquad (22)$$

C.10.7: Storage Constraints

For storage units (I_s), state of charge (*x* [MWh]) depends on the prior period's state of charge, electricity discharge (*p* [MWh]), and energy inflow times round-trip efficiency (η):

$$x_{i_s,t} = x_{i_s,t-1} - p_{i_s,t} + \eta * f_{i_s,t} \qquad \forall\, i_s \in I_s, t > 1 \qquad (23)$$

In hour 1, the state of charge in the prior period equals the state of charge in the final period of the prior UC run (X [MWh]):

$$x_{i_s,t} = X_{i_s} - p_{i_s,t} + \eta * f_{i_s,t} \qquad \forall\, i_s \in I_s, t = 1 \qquad (24)$$

In the first UC run, X equals half of each unit's maximum state of charge. The state of charge can vary between maximum (X^{MAX} [MWh]) and minimum (X^{MIN} [MWh]) values:

$$x_{i_s,t} \leq X_{i_s}^{MAX} \qquad \forall\, i_s \in I_s, t \in T \qquad (25)$$

$$x_{i_s,t} \geq X_{i_s}^{MIN} \qquad \forall\, i_s \in I_s, t \in T \qquad (26)$$

Energy inflows cannot exceed maximum values (F^{MAX} [MWh]), and can only occur when the storage unit is not generating electricity:

$$f_{i_s,t} \leq F_{i_s}^{MAX} * (1 - u_{i_s,t}) \qquad \forall\, i_s \in I_s, t \in T \qquad (27)$$

For each storage unit, energy inflow capacity equals electricity generation capacity.

Electricity discharge plus regulation, flexibility, and contingency reserve provision cannot exceed the state of charge:

$$p_{i_s,t} + r_{i_s,t}^{REG} + r_{i_s,t}^{FLX} + r_{i_s,t}^{CNT} \leq x_{i_s,t} \qquad \forall\, i_s \in I_s, t \in T \qquad (28)$$

Like other units, reserve provision by storage units is limited by ramp limits over the reserve timeframe. However, unlike other units, storage units do not have to be online to provide reserves:

$$r_{i_s,t}^{REG} \leq RE_{i_s}^{REG} * RL_{i_s} * RS^{REG} \qquad \forall t \in T,\ i_s \in I_s \qquad (29)$$

$$r_{i_s,t}^{FLX} \leq RE_{i_s}^{FLX} * RL_{i_s} * RS^{FLX} \qquad \forall t \in T,\ i_s \in I_s \qquad (30)$$

$$r_{i_s,t}^{CNT} \leq RE_{i_s}^{CNT} * RL_{i_s} * RS^{CNT} \qquad \forall t \in T,\ i_s \in I_s \qquad (31)$$

Rather, storage units can provide reserves while charging and discharging electricity. Specifically, provided reserves cannot exceed energy inflows plus spare electricity discharge capacity:

$$r_{i_s,t}^{REG} + r_{i_s,t}^{FLX} + r_{i_s,t}^{CNT} \leq (u_{i_s,t} * P_{i_s,t}^{MAX} - p_{i_s,t}) + f_{i_s,t} \qquad \forall\, i_s \in I_s, t \in T \qquad (32)$$

C.11: ECONOMIC DISPATCH MODEL FOR CONVERTING CO_2 CAP TO CO_2 PRICE

In order to account for carbon constraints in the UCED model, we use a simple economic dispatch (ED) model to convert each year's CO_2 emission limit to a shadow CO_2 price input to the UCED model [8]. Specifically, the ED model determines the shadow CO_2 price at which annual CO_2 emissions comply with the relevant annual CO_2 emission limit. The ED model minimizes total energy costs subject to the constraints that supply equals demand and each generator's electricity generation varies between zero and its maximum capacity [8], [33]. Total energy costs are defined as:

$$TC = \sum_{i,t} p_{i,t} * OC_i$$

where *i* and *t* index generators and time; *p* = electricity generation [MWh]; and *OC* = operating cost [$/MWh], which accounts for fuel, variable operations and maintenance, and CO_2 emission costs. We determine hourly wind and solar generation using the same hourly capacity factors from the National Renewable Energy Laboratory as used in the UCED model [25], [26], and remove wind and solar generation from demand prior to running the ED model.

C.12: SCENARIO DETAILS

Table C.12 provides the annual CO_2 emission limit imposed in the CE model in each year under the moderate and strong decarbonization targets.

Table C.12: Annual CO_2 emission limit (in million tons) imposed under each decarbonization target by year in the CE model. No CO_2 emission limit is enforced in 2015.

Decarbonization Target	**2020**	**2025**	**2030**	**2035**	**2040**	**2045**
Moderate	162.9	150.4	137.8	125.3	112.8	100.2
Strong	157.9	140.3	122.8	105.3	87.7	70.2

For the low natural gas scenario, Table C.13 provides the natural gas prices used in our analysis, which we obtain from AEO 2016's high oil and gas scenario [3].

Table C.13: Natural gas prices in the low natural gas price scenario.

Year	2020	2025	2030	2035	2040	2045
Natural Gas Price ($\$_{2012}$/MMBtu)	3.4	3.5	3.8	3.5	3.1	3.1

For the high storage capacity scenario, in which we deploy 1.5 GW storage rather than 0.5 GW storage, we assume the storage unit has the same power to energy ratio as in the 0.5 GW scenarios. Consequently, when participating only in the energy market, we assume an 81% efficient 1.5 GW / 12 GWh storage unit. When participating in only reserve markets and in both energy and reserve markets, we assume an 81% efficient 1.5 GW / 6 GWh storage unit.

C.13: SHADOW CO_2 PRICES ENFORCED IN AND ANNUAL CO_2 EMISSIONS OUTPUT BY UCED MODEL

Table C.14 provides the shadow CO_2 prices enforced in the UCED model for each year. Since we enforce no CO_2 emission limit in 2015, shadow CO_2 prices in that year equal zero. Under the moderate decarbonization target, shadow CO_2 prices decrease over time as wind, solar, and natural gas combined cycle (NGCC) capacities increase. Under the strong decarbonization target, though, the shadow CO_2 price increases despite growth in wind, solar, and NGCC capacities in order to meet the tight CO_2 emission limit. Since we determine shadow CO_2 prices by running the UCED model without storage, they do not change based on whether storage is included in the fleet or based on which market storage participates in.

Table C.14: Shadow CO_2 price (in $/ton) enforced in the UCED model in each year and decarbonization target in order to comply with the annual CO_2 emission limit.

Decarbonization Target	2015	2025	2035	2045
Moderate	0	13	12	11
Strong	0	16	17	43

Table C.15 provides annual CO_2 emissions output by the UCED model without storage for each year and decarbonization target. Annual CO_2 emissions output by the UCED model exceed the relevant CO_2 emission limit (see Table C.12) in 2025 and 2045 under the moderate decarbonization target and in 2045 under the strong decarbonization target by 1%, 2%, and 4%, respectively. In all other years, annual CO_2 emissions from the UCED model meet the annual CO_2 emission limit.

Table C.15: Annual CO_2 emissions (in million tons) output by the UCED model without storage in each year and decarbonization target.

Decarbonization Target	2015	2025	2035	2045
Moderate	175.6	153.7	124.8	103.9
Strong	175.6	138.8	99.3	70.8

C.14: GENERATOR FLEET COMPOSITION OVER TIME

Figure C.8 provides the generator fleet composition over time optimized by the CE model under each decarbonization target. While we run the CE model every five years, we provide the fleet composition here in the years that we run the UCED model, or every ten years. In both decarbonization targets, installed NGCC and renewable capacity increases at the expense of coal-fired capacity. No new construction of generators equipped with carbon capture and sequestration or nuclear generators occurs under either decarbonization target.

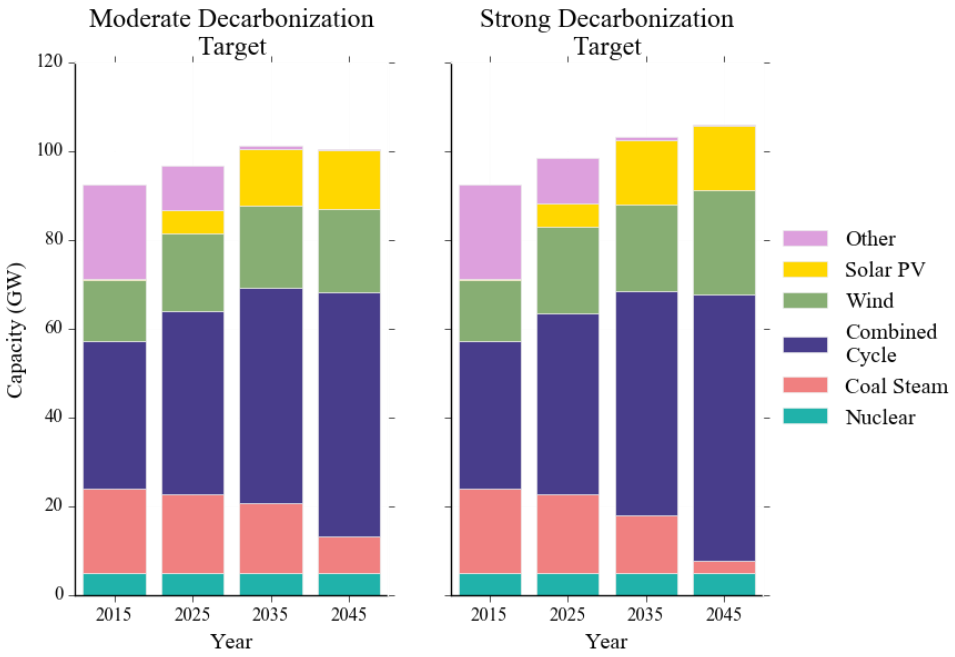

Figure C.8: Installed capacity by generator type output by our CE model each decade under the moderate (left) and strong (right) decarbonization targets.

C.15: RESERVE PROVISION BY GENERATOR TYPE WITHOUT STORAGE

Figure C.9 and Figure C.10 detail provided reserves by fuel type under the moderate and strong decarbonization targets, respectively, without storage in the generator fleet. Note that we do not allow reserve provision by wind and solar generators. Across years and decarbonization targets, only coal-fired and NGCC generators provide reserves. Regulation and flexibility reserve requirements, which vary with wind and solar generation, increase from 2015 through 2045 as wind and solar generation grows. Contingency reserve requirements, which vary with hourly demand, do not increase over time because we assume demand does not change across years.

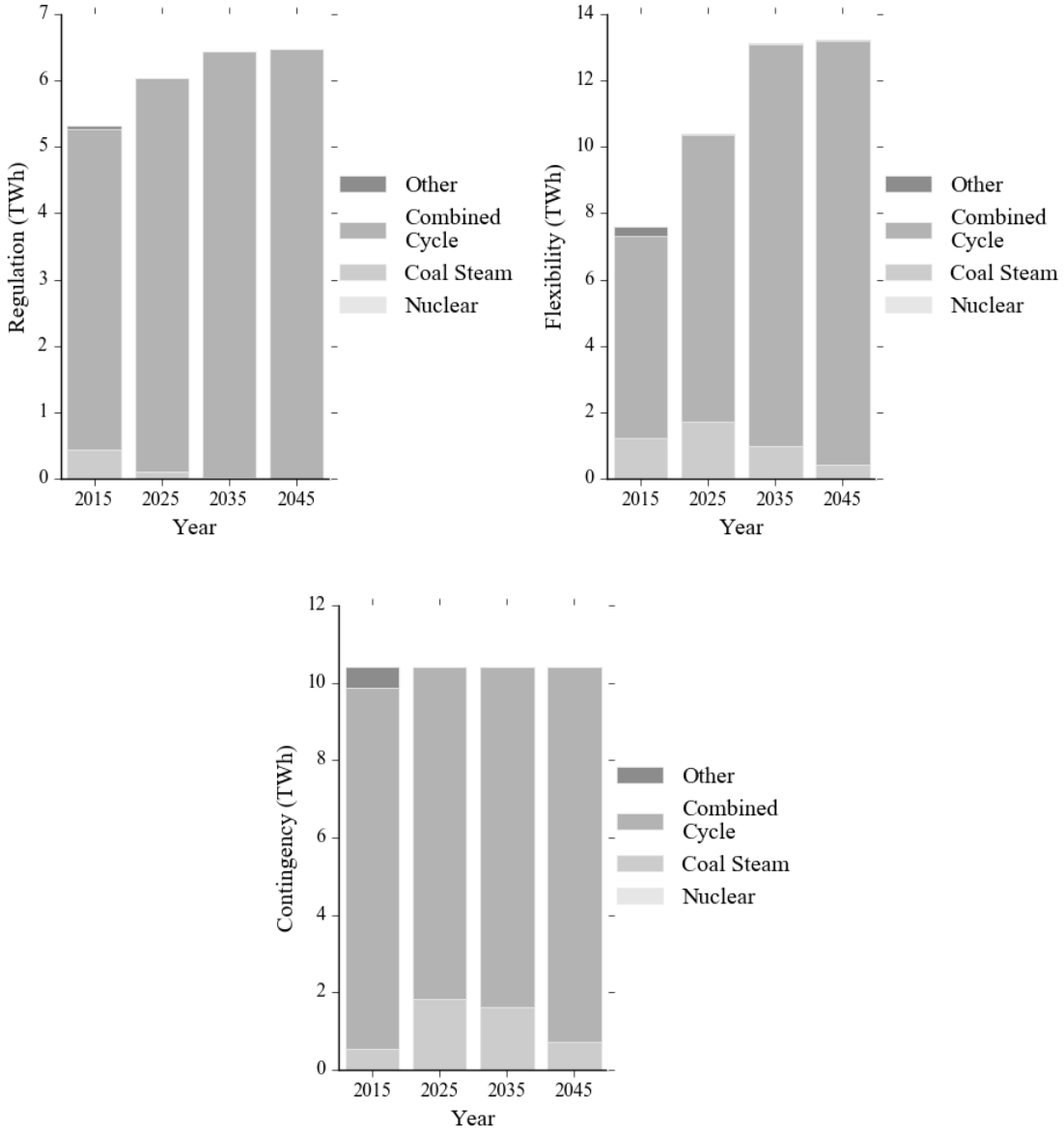

Figure C.9: Provided regulation, flexibility, and contingency reserves by fuel type and year under the moderate decarbonization target without storage in the generator fleet.

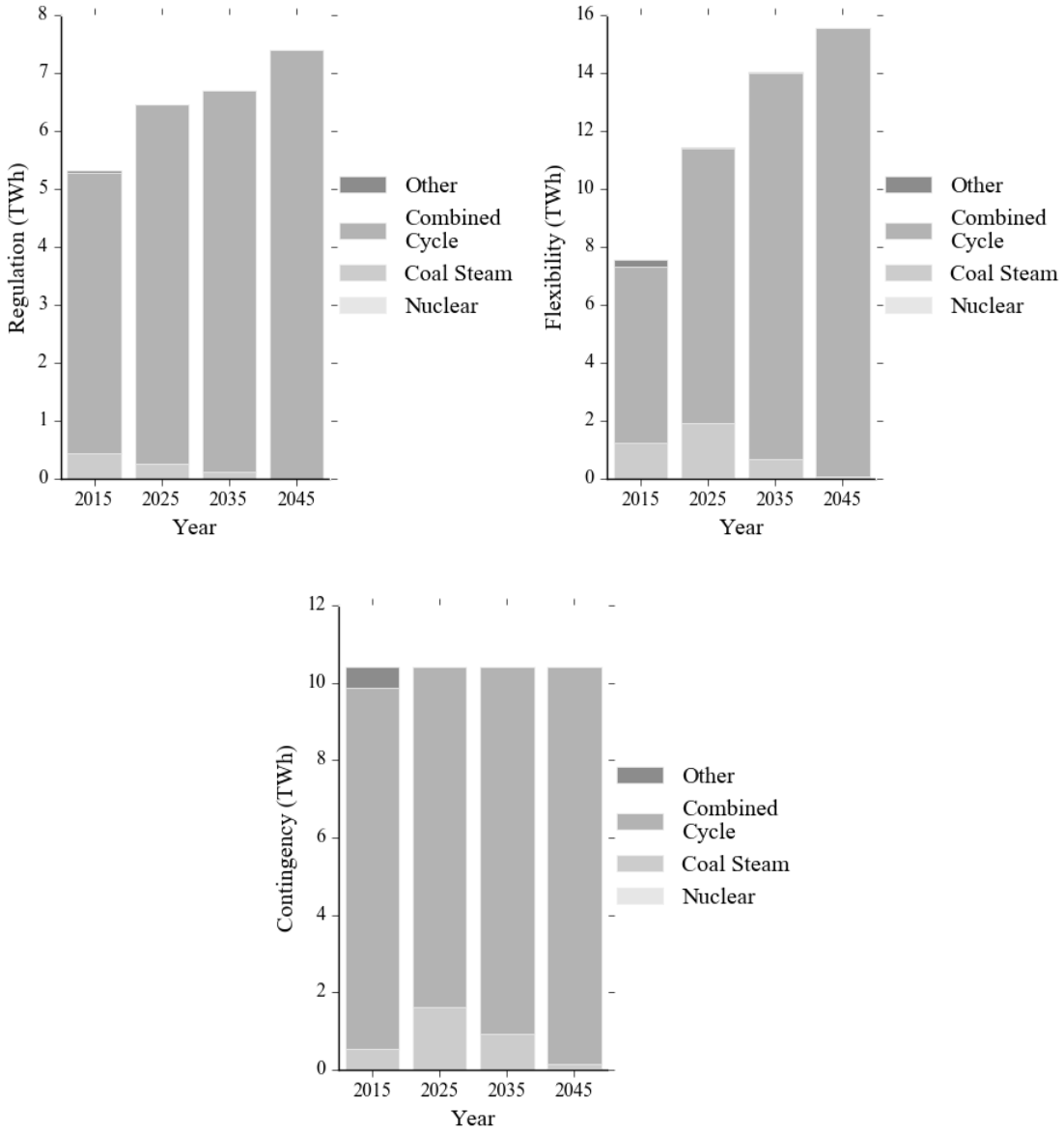

Figure C.10: Provided regulation, flexibility, and contingency reserves by fuel type and year under the strong decarbonization target without storage in the generator fleet.

C.16: EQUATION USED TO CALCULATE EFFECT OF STORAGE ON SYSTEM CO_2 EMISSIONS

To calculate how storage affects system CO_2 emissions, we use the following equation:

$$\Delta E^{CO_2} = \sum_{i,t} \Delta p_{i,t} * HR_i * ER_i^{CO_2}$$

where i and t index generators and time, respectively; ΔE^{CO_2} = change in annual system CO_2 emissions with storage relative to without storage [tons]; Δp = change in electricity generation with storage relative to without storage [MWh]; HR = heat rate [MMBtu/MWh]; and ER^{CO_2} = CO_2 emissions rate [ton/MMBtu]. Note that we use the UCED model to determine electricity generation by each generator in the fleet with and without storage. Sections C.1 and C.5 provide information on generator heat rates and CO_2 emission rates.

C.17: RE-DISPATCHING AMONG GAS-FIRED GENERATORS DUE TO STORAGE

Figure C.11 provides the change in cumulative generation by NGCC generators with versus without storage against the NGCC generators' CO_2 emission rates under the strong decarbonization target in 2045. Storage shifts generation from high to low-CO_2-emitting NGCC generators.

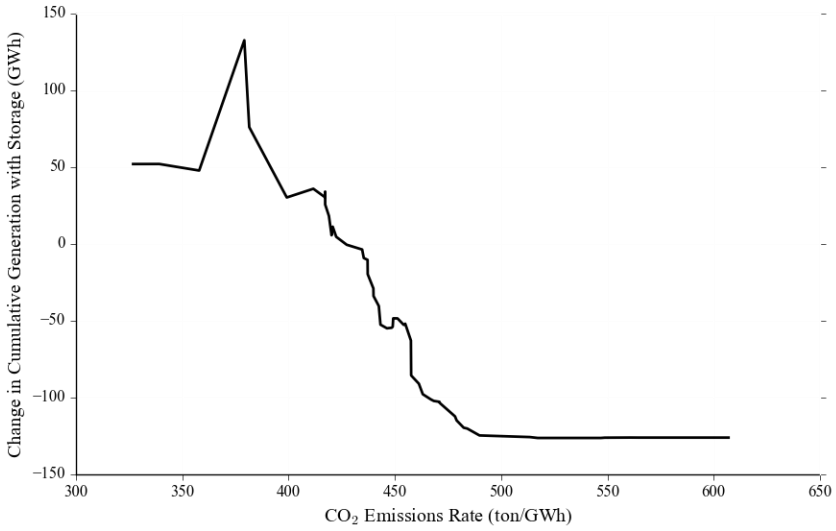
Change in Cumulative Generation with Storage (GWh)
150
100
50
0
−50
−100
−150
300
350
400
450
500
550
600
650
CO_2 Emissions Rate (ton/GWh)

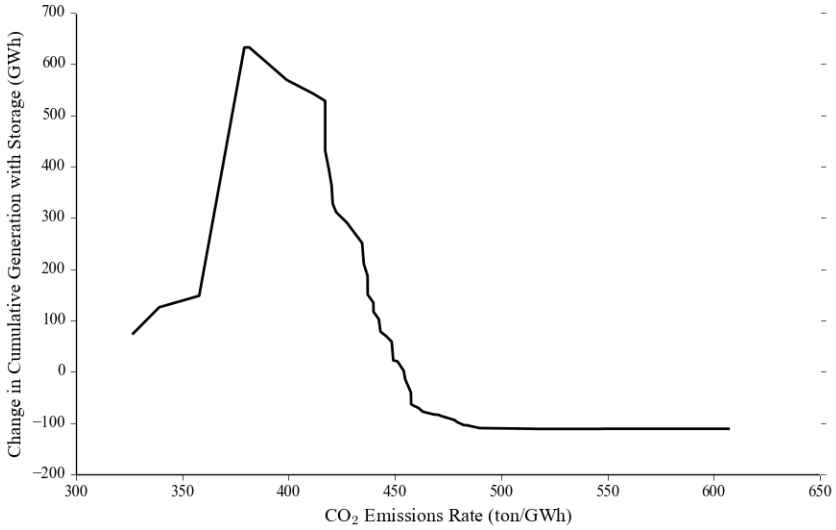
Change in Cumulative Generation with Storage (GWh)
700
600
500
400
300
200
100
0
−100
−200
300
350
400
450
500
550
600
650
CO_2 Emissions Rate (ton/GWh)

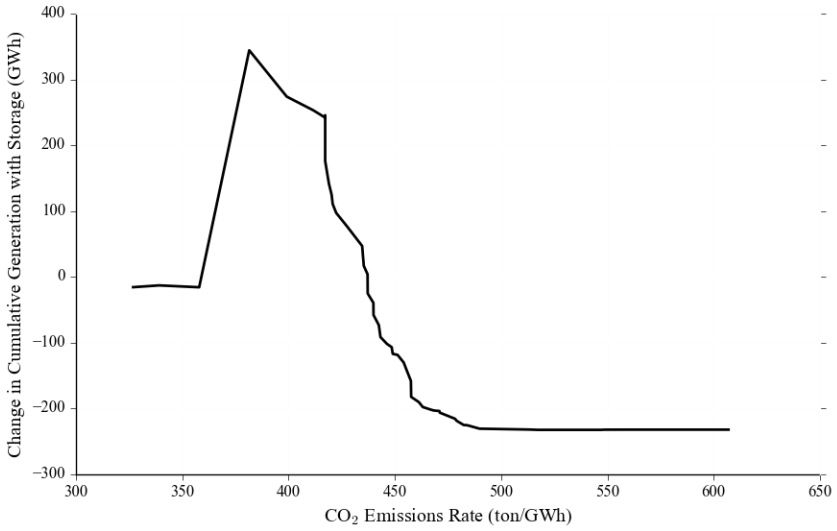

Figure C.11: Change in cumulative generation by NGCC generators with versus without storage against each generator's CO_2 emission rate under the strong decarbonization target in 2045 when storage participates in only energy (top), only reserve (middle), or energy and reserve (bottom) markets.

C.18: ESTIMATING SYSTEM CO_2 EMISSIONS DUE TO DISPATCHING OF REGULATION RESERVES PROVIDED BY STORAGE

Here, we provide a first-order estimate of CO_2 emissions due to the dispatch of regulation reserves provided by storage. In the absence of public data on the dispatch of regulation reserves in ERCOT, we assume an energy neutral regulation signal each hour, such that the integral of dispatched regulation up and down reserves equals zero each hour, as in PJM [34], [35]. Under an energy neutral regulation signal, dispatching regulation reserves provided by a storage unit reduces the unit's state of charge due to its round-trip efficiency penalty. To make up for lost energy, additional electricity must be generated to charge the storage device, which incurs CO_2 emissions when such additional electricity is not provided by a zero-emissions generator. Note that under an energy neutral regulation signal, dispatching reserves provided by thermal units does not change hourly CO_2 emissions of that thermal unit, as the sum of the change in

electricity generation (and therefore CO_2 emissions) equals zero over the hour. Thus, we only estimate emissions from dispatching reserves provided by storage here.

Using one year of regulation signal data from PJM, Fisher and Apt [34] estimate that roughly 13% of committed regulation up reserves are dispatched on an average hourly basis. Thus, if a storage unit commits 100 MW of regulation reserves in an hour, roughly 13 MWh would be dispatched. At 81% efficiency, dispatching 13 MWh would yield losses of roughly 2.47 MWh. Consequently, the storage unit's state of charge would decline by 2.47 over the hour.

With the value from Fisher and Apt [34], we estimate annual additional electricity generation needed to make up for state of charge losses at storage units due to the dispatch of regulation reserves. We then provide a first-order approximation of CO_2 emissions from that additional electricity generation by assuming all additional electricity is generated by a coal-fired or NGCC generator. The coal-fired generator represents a worst-case estimate, whereas the NGCC generator represents an optimistic but not lower-bound estimate, as zero-carbon electricity generators could provide some of the additional electricity. Based on average CO_2 emission rates of our initial generator fleet, we assign CO_2 emission rates of 1.2 and 0.5 ton per MWh to the coal-fired and natural gas fired generators, respectively.

Under the moderate decarbonization target, storage provides at most roughly 4.3 TWh of regulation reserves across years when participating in only reserve or both energy and reserve markets. Given the above assumptions and an 81% round-trip storage efficiency, annual energy losses by storage from dispatched regulation reserves equal 106 GWh. Assuming the hypothetical coal-fired or NGCC generator compensates for those losses, total annual CO_2 emissions equal 0.13 or 0.05 million tons per year, respectively. Under the moderate decarbonization target, these emissions would negate roughly 6-33% of emission reductions due

to storage when participating in only reserve or both energy and reserve markets from 2025 through 2045. Thus, from 2025 through 2045 under the moderate decarbonization scenario, storage would still reduce CO_2 emissions when participating in only reserve or both energy and reserve markets even when accounting for emissions associated with the dispatching of reserves.

Similarly, from 2025 through 2045 under the strong decarbonization target, emissions associated with dispatching reserves provided by storage would negate roughly 6-51% of emission reductions due to storage when participating in only reserve or both energy and reserve markets. Since coal-fired generation is nearly eliminated from the generator fleet in 2045 under the strong decarbonization target, we only use emissions associated with the hypothetical NGCC generator (0.05 million tons) in that year. Thus, even when accounting for emissions due to dispatching reserves provided by storage, storage still reduces CO_2 emissions when participating in only reserve or both energy and reserve markets under the strong decarbonization target, as under the moderate target.

C.19: SENSITIVITY ANALYSIS RESULTS

Figure C.12 and Figure C.13 provide the effect of storage on system CO_2 emissions for each of our sensitivity analyses under the moderate and strong decarbonization targets, respectively.

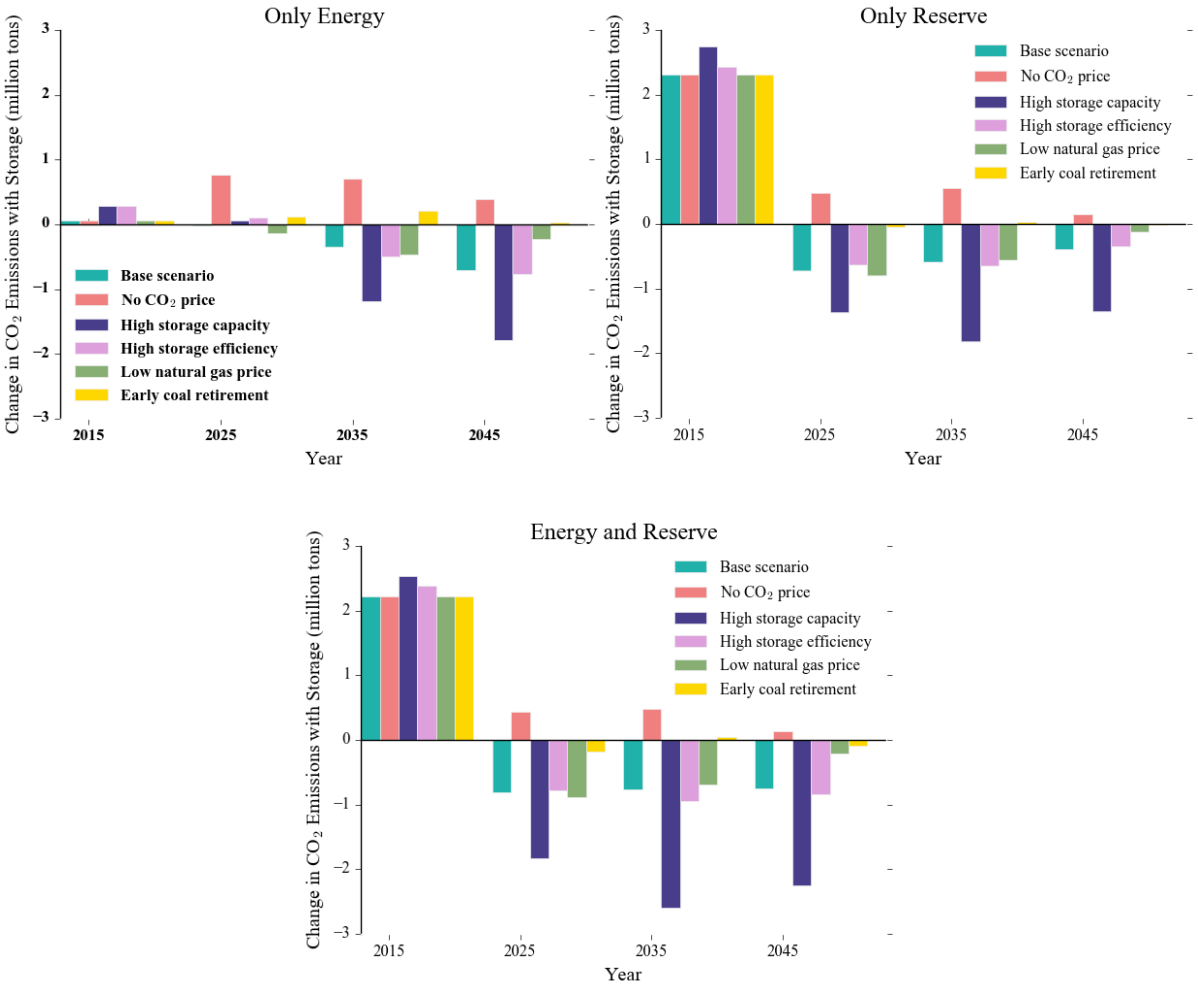

Figure C.12: Change in system CO_2 emissions with storage versus without storage when storage participates in only energy (top left), only reserve (top right), and energy and reserve (bottom) markets for each sensitivity analysis under the moderate decarbonization target. "Base scenario" refers to the base moderate decarbonization scenario. Positive values indicate storage increases system CO_2 emissions.

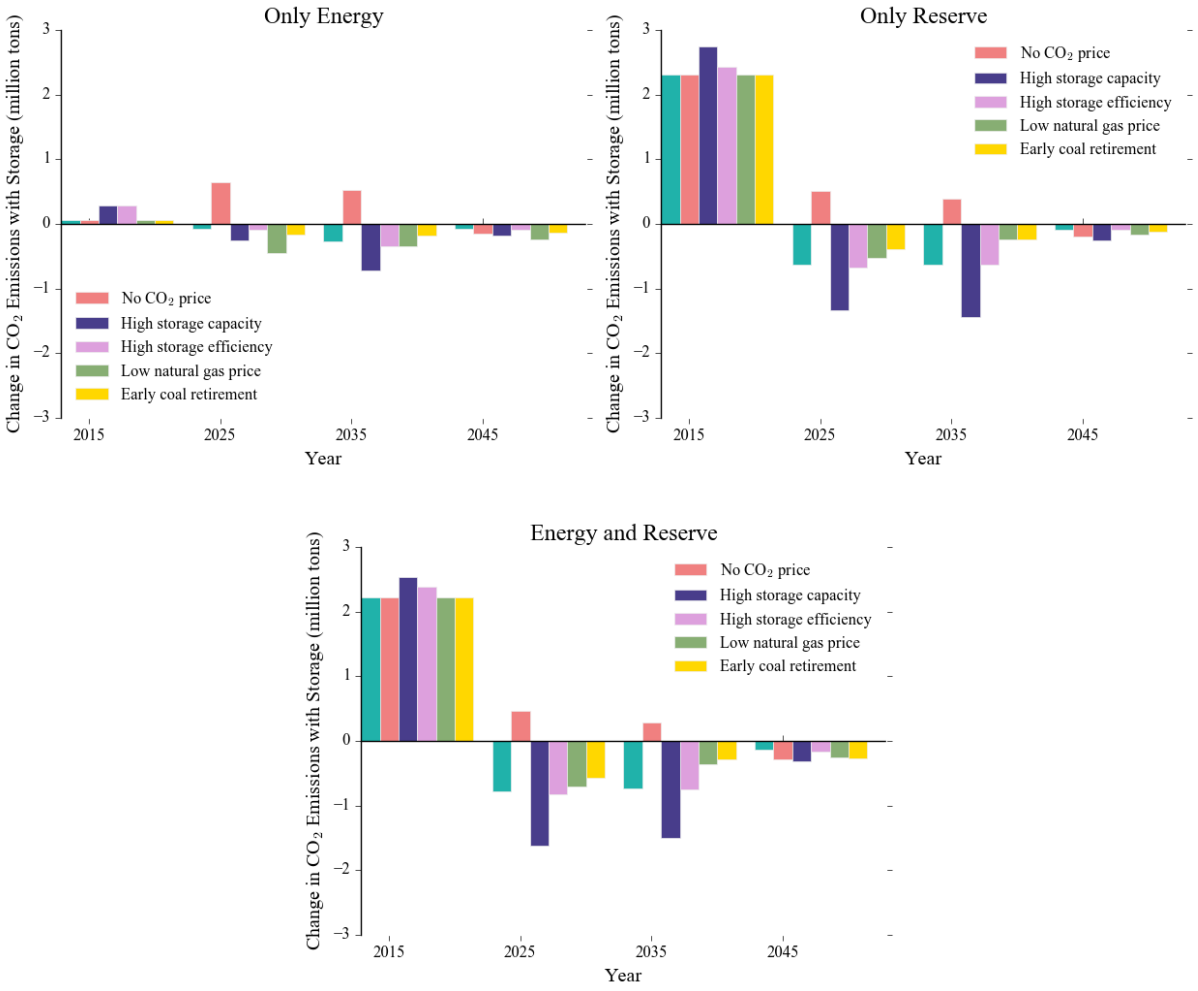

Figure C.13: Change in system CO_2 emissions with storage versus without storage when storage participates in only energy (top left), only reserve (top right), and energy and reserve (bottom) markets for each sensitivity analysis under the strong decarbonization target. "Base scenario" refers to the base strong decarbonization scenario. Positive values indicate storage increases system CO_2 emissions.

C.20: REFERENCES

[1] U.S. Environmental Protection Agency, "National Electric Energy Data System (Version 5.15)." 2015.

[2] U.S. Environmental Protection Agency, "Emissions & Generation Resource Integrated Database (eGRID)," 2017.

[3] U.S. Energy Information Administration, "Annual Energy Outlook 2016," 2016.

[4] R. Lueken, "PJM Hourly Open-source Reduced-form Unit Commitment Model (PHORUM)," 2013. [Online]. Available: https://github.com/rlueken/PHORUM. [Accessed: 12-Mar-2015].

[5] R. Lueken, "Reducing Carbon Intensity in Restructured Markets: Challenges and Potential Solutions," Carnegie Mellon University, 2014.

[6] U.S. Energy Information Administration, "Updated capital cost estimates for utility scale electricity generating plants," 2013.

[7] U.S. Energy Information Administration, "Form EIA-923," 2015.

[8] M. Craig, P. Jaramillo, H. Zhai, and K. Klima, "The economic merits of flexible carbon capture and sequestration as a compliance strategy with the Clean Power Plan," *Environ. Sci. Technol.*, vol. 51, pp. 1102–1109, 2017.

[9] U.S. Energy Information Administration, "Annual Energy Outlook 2015," 2015.

[10] U.S. Environmental Protection Agency, "Documentation for EPA Base Case v.5.13 Using the Integrated Planning Model," 2013.

[11] ERCOT, "2013 ERCOT hourly load data," 2015. [Online]. Available: http://www.ercot.com/gridinfo/load/load_hist/.

[12] ERCOT, "2014 ERCOT hourly load data," 2015. [Online]. Available: http://www.ercot.com/gridinfo/load/load_hist/.

[13] ERCOT, "2015 ERCOT hourly load data," 2016. [Online]. Available: http://www.ercot.com/gridinfo/load/load_hist/.

[14] B. Palmintier and M. Webster, "Impact of unit commitment constraints on generation expansion planning with renewables," *2011 IEEE Power Energy Soc. Gen. Meet.*, pp. 1–7, Jul. 2011.

[15] G. Morales-españa, S. Member, J. M. Latorre, and A. Ramos, "Tight and compact MILP formulation of start-up and shut-down ramping in unit commitment," *IEEE Trans. Power Syst.*, vol. 28, no. 2, pp. 1288–1296, 2013.

[16] U.S. Environmental Protection Agency, "Standards of performance for greenhouse gas emissions from new, modified, and reconstructed stationary sources: Electric utility generating units. Federal Register Vol. 80: 64510-64660," 2015.

[17] U.S. National Renewable Energy Laboratory, "Annual Technology Baseline 2016," 2016.

[18] U.S. National Renewable Energy Laboratory, "Wind Research: Wind Resource Assessment," 2015. [Online]. Available: http://www.nrel.gov/wind/resource_assessment.html. [Accessed: 08-Oct-2015].

[19] U.S. Department of Energy, "Business Energy Investment Tax Credit (ITC)," *Energy.gov*, 2017. [Online]. Available: https://energy.gov/savings/business-energy-investment-tax-credit-itc. [Accessed: 28-Mar-2017].

[20] Black & Veatch, "Cost and performance data for power generation technologies," 2012.

[21] The White House Office of Management and Budget, "Guidelines and discount rates for benefit-cost analysis of federal programs. Circular No. A-94 Revised.," 1992.

[22] W. Short, P. Sullivan, T. Mai, M. Mowers, C. Uriarte, N. Blair, D. Heimiller, and A. Martinez, "Regional energy deployment system (ReEDS)," *U.S. National Renewable Energy Laboratory*, 2011. .

[23] J. Johnston, A. Mileva, J. H. Nelson, and D. M. Kammen, "SWITCH-WECC: Data, assumptions, and model formulation," 2013.

[24] M. Parker and N. S. Malik, "Coal confronting bigger threat than Obama's rules for clean air," *Bloomberg*, 09-Jun-2015.

[25] U.S. National Renewable Energy Laboratory, "Transmission Grid Integration: Eastern Wind Dataset," 2012.

[26] U.S. National Renewable Energy Laboratory, "Transmission Grid Integration: Solar Power Data for Integration Studies Dataset," 2010.

[27] D. L. Oates and P. Jaramillo, "Production cost and air emissions impacts of coal cycling in power systems with large-scale wind penetration," *Environ. Res. Lett.*, vol. 8, no. 2, p. 24022, Jun. 2013.

[28] D. Lew, G. Brinkman, E. Ibanez, A. Florita, M. Heaney, B. Hodge, M. Hummon, and J. King, "The Western Wind and Solar Integration Study Phase 2," *U.S. National Renewable Energy Laboratory*, 2013. .

[29] M. Diagne, M. David, P. Lauret, J. Boland, and N. Schmutz, "Review of solar irradiance forecasting methods and a proposition for small-scale insular grids," *Renew. Sustain. Energy Rev.*, vol. 27, pp. 65–76, 2013.

[30] M. Hogan, F. Weston, and M. Gottstein, "Power Market Operations and System Reliability in the Transition to a Low-Carbon Power System," 2015.

[31] F. J. De Sisternes and M. D. Webster, "Optimal selection of sample weeks for approximating the net load in generation planning problems," 2013–3, 2013.

[32] M. Craig, E. McDonald-Buller, and M. Webster, "Technology adoption under time-differentiated market-based instruments for pollution control," *Energy Econ.*, vol. 60, pp. 23–34, 2016.

[33] D. L. Oates and P. Jaramillo, "State cooperation under the EPA's proposed clean power plan," *Electr. J.*, vol. 28, no. 3, pp. 26–40, 2015.

[34] M. J. Fisher and J. Apt, “Emissions and economics of behind-the-meter electricity storage,” *Environ. Sci. Technol.*, vol. 51, no. 3, pp. 1094–1101, 2017.

[35] Y. Lin, J. X. Johnson, and J. L. Mathieu, “Emissions impacts of using energy storage for power system reserves,” *Appl. Energy*, vol. 168, no. 784, pp. 444–456, 2016.

APPENDIX D:
SUPPLEMENTAL INFORMATION FOR CHAPTER 5

D.1: HISTOGRAMS OF PV SYSTEM AZIMUTHS AND TILTS IN NEM DATASET

Figure D.1 provides histograms of azimuths and tilts for fixed array PV systems interconnected through 2015, the end of our period of analysis, in the NEM dataset. Many (more than 11,000) PV systems in PGE have an azimuth and tilt of 0 degrees in the NEM dataset, which we attribute to spurious data collection or entry so do not include them in the histograms below. In each utility (PGE, SCE, and SDGE), the azimuth mode is 180 degrees, around which azimuths roughly follow a normal distribution. However, azimuths of 90 and 270 degrees are also common in all three utilities. With respect to tilt, most PV systems have tilts of 15-25 degrees across utilities.

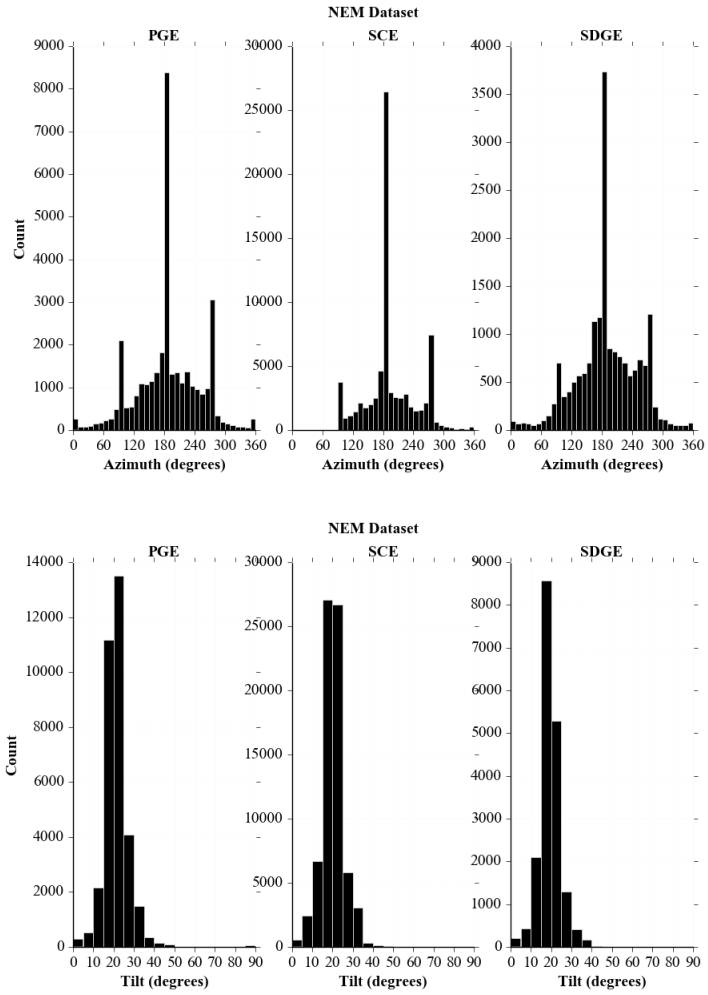

Figure D.1: Histograms of azimuths (top) and tilts (bottom) for fixed array PV systems interconnected through 2015 in the NEM dataset by IOU.

D.2: SUPPLEMENTAL DESCRIPTION OF METERED GENERATION AND PV SYSTEMS IN THE CSI DATASET

D.2.1: Histogram of PV System Azimuths and Tilts in CSI Dataset

Figure D.2 provides histograms of azimuths and tilts of the 492 PV systems with metered generation in the CSI dataset. Of these 492 PV systems, 20% and 13% have non-numerical azimuths and tilts, respectively, because of missing data and systems that use either tracking or

multiple orientations. Like in the NEM dataset (Figure D.1), in PGE, SCE, and SDGE the azimuth mode is 180 degrees, around which most azimuths extend from roughly 90 to 290 degrees. The high occurrence of azimuths of 90 and 270 degrees in the NEM dataset is not reflected in the CSI dataset.

Tilts in PGE and SCE are most common between 15 and 25 degrees (Figure D.2), as in the NEM dataset (Figure D.1). However, in SDGE, tilts between 30 and 35 degrees are most common in the CSI dataset versus between 15 and 25 degrees in the NEM dataset.

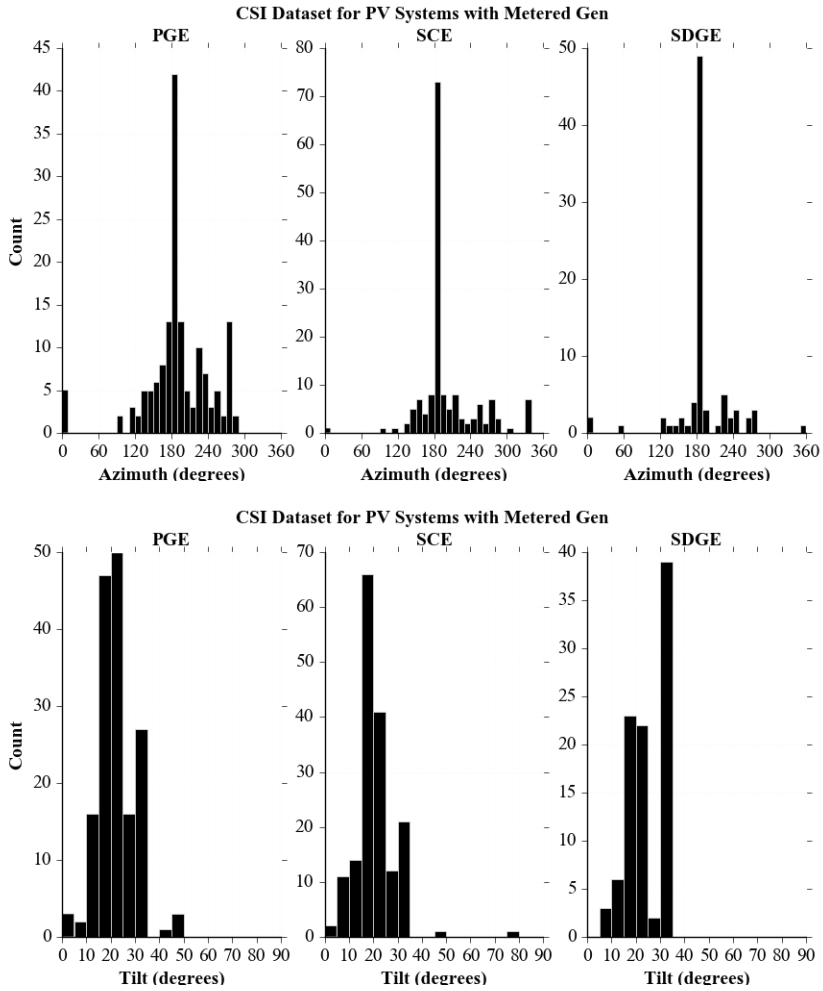

Figure D.2: Histograms of azimuths (top) and tilts (bottom) for PV systems in the CSI dataset with metered generation by IOU.

D.2.2: Time Series of Metered Generation Availability

Figure D.3 provides time series indicating availability of hourly metered generation in the CSI dataset from 2013 through 2015, our period of analysis. On average, each PV system lacks 25% of hourly metered generation over our study period.

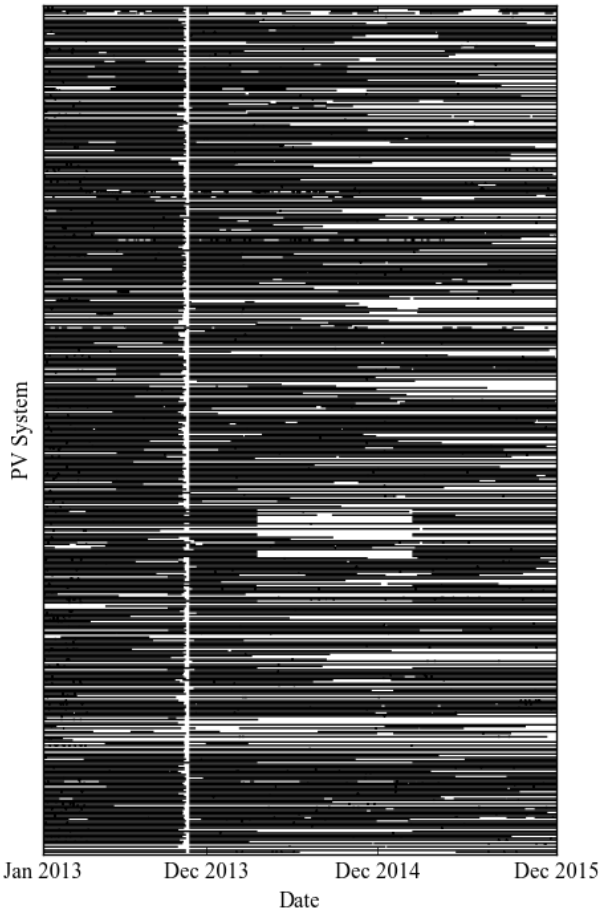

Figure D.3: Time series indicating availability of metered generation for each PV system in the CSI dataset from 2013 through 2015. Each line indicates data availability for one PV system.

D.3: DETAILS AND SENSITIVITY ANALYSIS ON SCALE UP METERED GENERATION METHOD

D.3.1: Method Details

Here, we further detail the scale up method for estimating distributed PV generation. Figure D.4 provides a flowchart of the method.

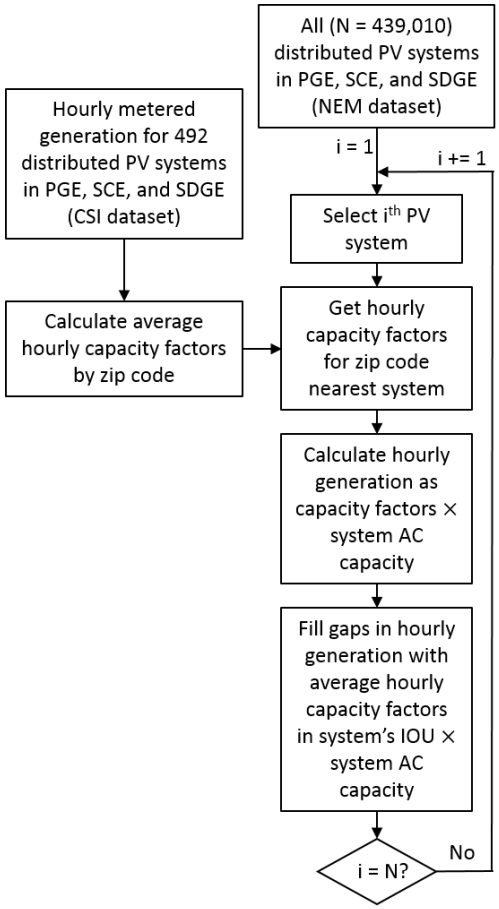

Figure D.4: Schematic for estimating hourly generation by each PV system in the NEM dataset from 2013 through 2015 by scaling up metered generation in the CSI dataset.

Among PV systems in the NEM dataset, roughly 44% are located in zip codes with average hourly capacity factors (CFs) calculated with metered generation in the CSI dataset. For

the remaining 56% of PV systems, we estimate their generation using CFs in the nearest zip code with metered generation in the CSI dataset. To calculate distances between zip codes, we obtain a central latitude and longitude for each zip code from Google's Geocoding API and calculate the distance between each pair of zip codes using the Haversine formula:

$$d = 2 * R * \text{asin}\left(\sqrt{\sin^2\left(\frac{lat_1 - lat_2}{2}\right) + \cos(lat_1) * \cos(lat_2) * \sin^2\left(\frac{lon_1 - lon_2}{2}\right)}\right) \quad (1)$$

where d = distance [km]; R = Earth's radius, or 6,371 km; lat_1 and lat_2 = latitude of points 1 and 2, respectively; and lon_1 and lon_2 = longitude of points 1 and 2, respectively.

To fill gaps in zip-code level average hourly CFs, we use average CFs by IOU. In SDGE, no IOU-level average CFs exist from November 4-10, 2013, so we instead use IOU-level average CFs for the same hours in the following year.

Figure D.5 provides a histogram of the distance between each PV system in the NEM dataset and the zip code from which we obtain metered generation to estimate the PV system's generation in the scale up method. Most (57%) of PV systems are within 5 km of the corresponding zip code, but many (14%) of PV systems are further than 20 km away from the corresponding zip code. Klima and Apt [1] find that correlation between hourly generation of solar plants in Gujarat, India, decreases from 0.8-0.9 at less than 5 km between plants to roughly 0.6 at roughly 20 km between plants. Long and Ackerman [2] find better correlation between 30-minute generation of solar plants in Wisconsin of 0.95 at roughly 20 km between plants. Based on these studies and distances between PV systems and corresponding zip codes in the scale up method (Figure D.5), we expect a high correlation between each PV system's actual historic generation and the generation profile we use to estimate its historic generation in the scale up method. Thus, using the scale up method is appropriate for most PV systems in our dataset.

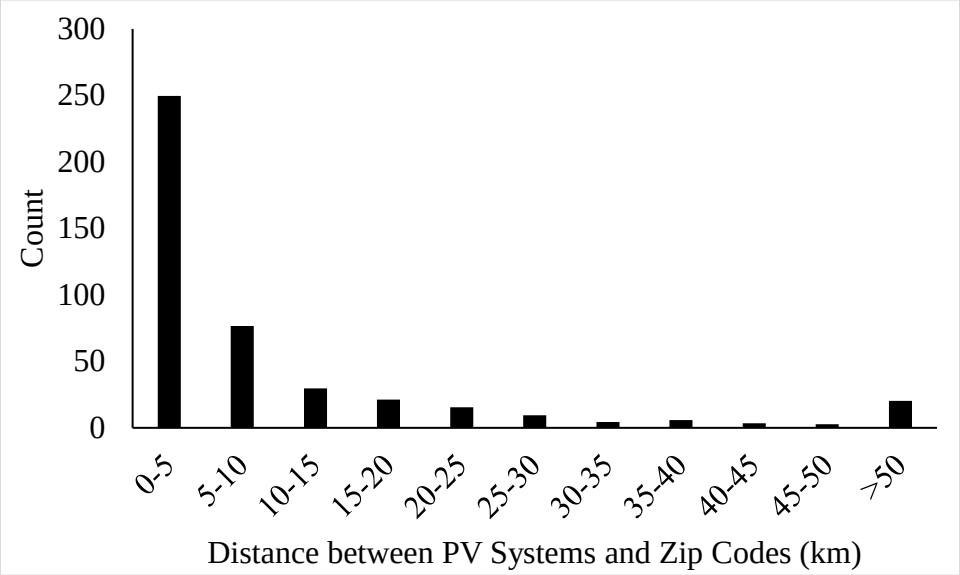

Figure D.5: Histogram of distance between PV systems in the NEM dataset and the zip code from which we obtain metered generation for each PV system in the scale up method.

D.3.2: Sensitivity of Scale Up Method to Distance

Here, we test the sensitivity of the scale up method to utilizing CFs from zip codes at increasing distances from each PV system. For this sensitivity analysis, we use the same data as during validation, i.e. metered generation from 2010 through 2016 for 205 distributed PV systems in PGE, SCE, and SDGE. To test the effect of increasing distance, we use the scale up method to estimate generation when we use CFs from the 1st, 2nd, 3rd, 6th, and 10th nearest zip codes to each PV system excluding the PV system's own zip code. In each scenario, we then calculate the error between estimated generation and metered generation.

For each scenario, Figure D.6 provides distances between PV systems and the zip codes from which we obtain CFs. From the 1st to 10th nearest zip code scenarios, median distances increase from 6.4 to 26.2 km in PGE, 5.5 to 17.7 km in SDGE, and 5.6 to 25.1 km in SCE.

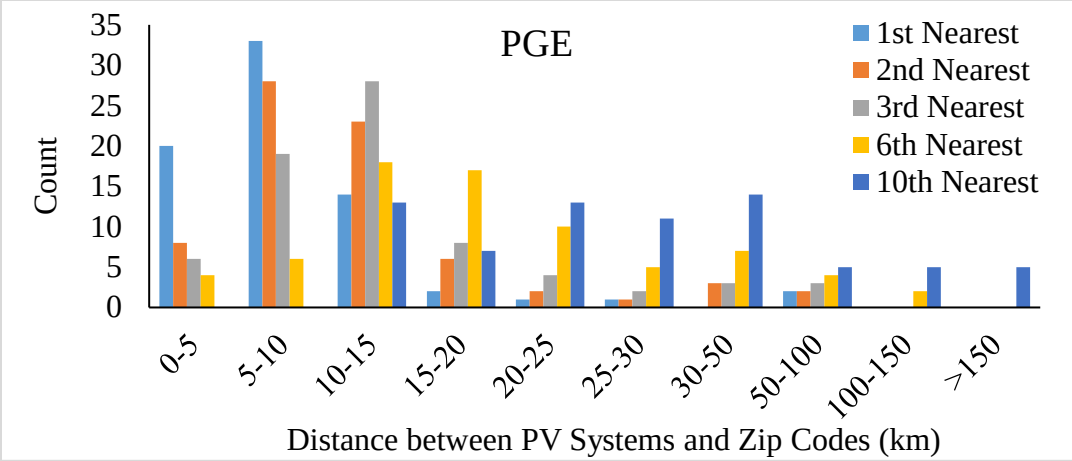

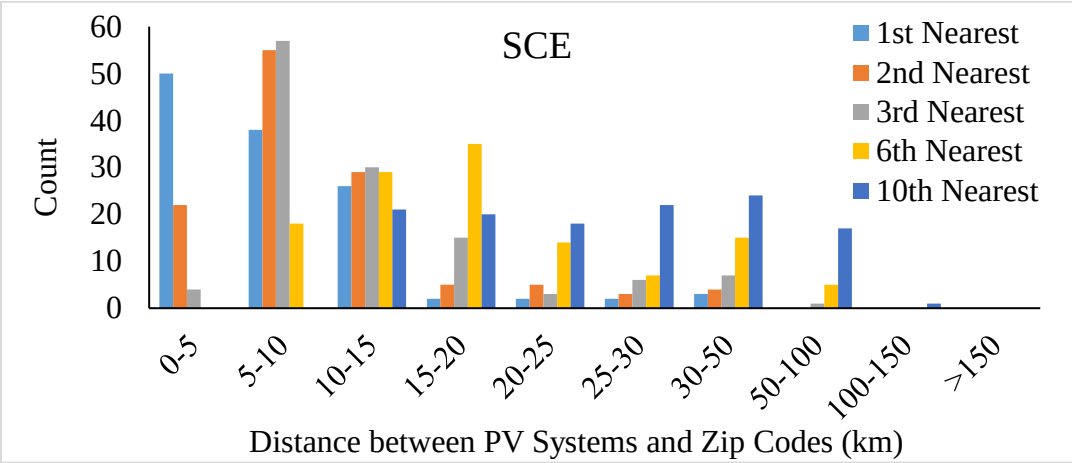

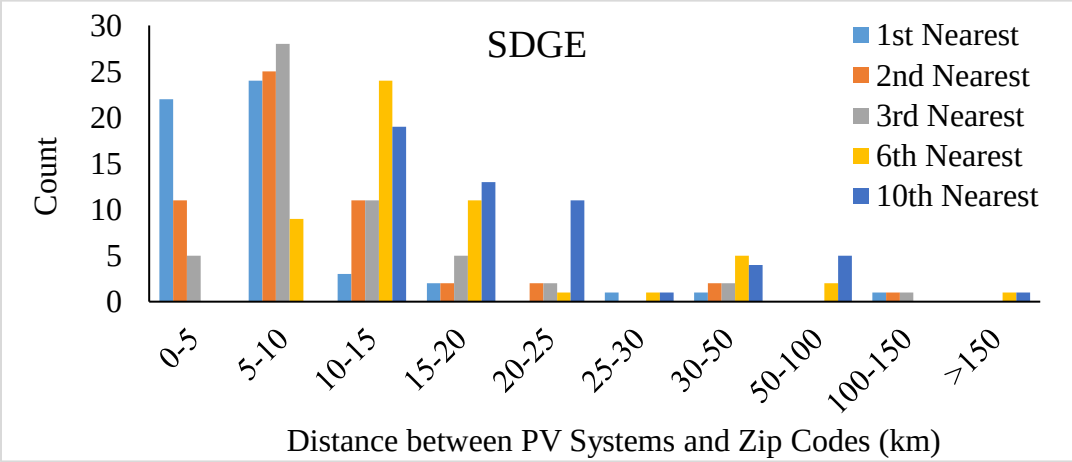

Figure D.6: Histograms of distances between PV systems and zip codes from which we obtain CFs in PGE (top), SCE (middle), and SDGE (bottom) when using CFs from the 1st, 2nd, 3rd, 6th, and 10th nearest zip code to each PV system (excluding each PV system's own zip code).

Figure D.7 provides the normalized root mean square error (NRMSE) for each scenario in PGE, SCE, and SDGE. NRMSEs do not monotonically increase as we use CFs from increasingly distant zip codes. For instance, NRMSEs in PGE and SDGE decrease from the 1st to 2nd nearest zip code scenarios, and in SCE decrease from the 6th to 10th nearest zip code scenarios. This suggests that errors between metered and estimated generation due to differences in uncontrolled PV system parameters in the scale up method, such as orientation, panel efficiency, and shading, outweigh errors due to differences in meteorology and solar irradiance between PV systems' locations and the zip codes from which we obtain CFs.

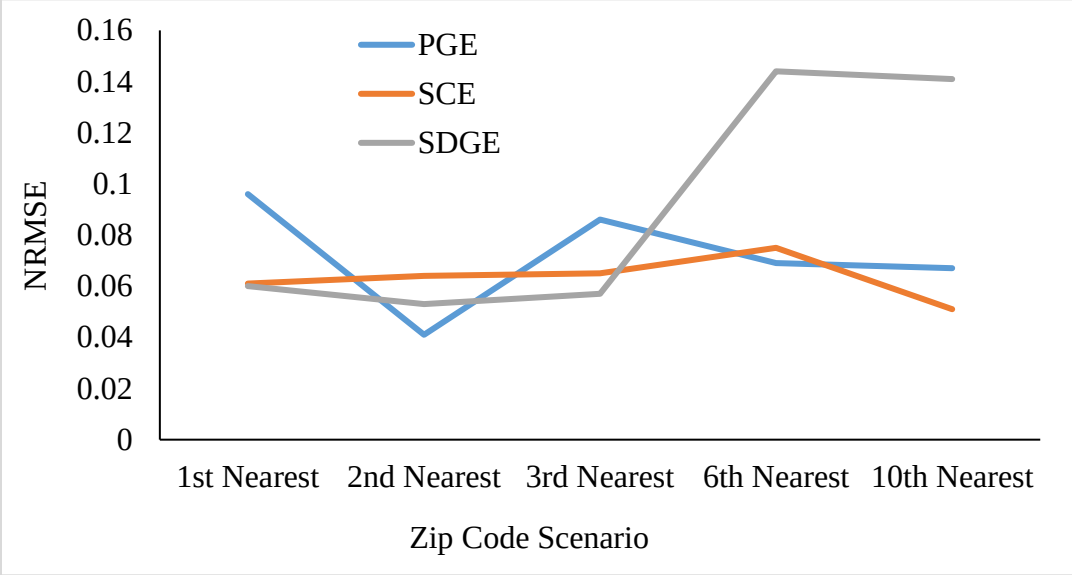

Figure D.7: NRMSEs in PGE, SCE, and SDGE when using CFs from the 1st, 2nd, 3rd, 6th, and 10th nearest zip codes to each PV system.

D.4: SUMMARY STATISTICS OF METEOROLOGY AND SOLAR IRRADIANCE DATA FROM THE NSRDB

Table D.1 provides summary statistics for meteorological and solar irradiance variables we download from the NSRDB [3] and input into PVLib in order to estimate distributed PV

generation using the specific, generic, and adjusted generic configuration methods. Since we download NSRDB data for each zip code with PV systems, we provide summary statistics across zip codes and years included in our analysis.

Table D.1: Summary statistics for meteorology and solar irradiance variables obtained from the National Solar Radiation Database across zip codes from 2013 through 2015.

Variable	Average	Standard deviation	Maximum	Minimum
Global horizontal irradiance (W/m^2)	224.68	10.66	1130.00	0.00
Diffuse horizontal irradiance (W/m^2)	53.88	5.60	578.00	0.00
Direct normal irradiance (W/m^2)	289.73	14.92	1100.00	0.00
Wind speed (m/s)	1.98	0.32	13.00	0.01
Air temperature (degrees C)	17.14	1.77	52.72	-29.18

D.5: CROSS-VALIDATION OF HOUR-OF-DAY CORRECTION FACTORS FOR ADJUSTED GENERIC CONFIGURATION METHOD

To ensure hour-of-day correction factors used in the adjusted generic configuration method do not result in over-fitting, we use 10-fold cross validation to test the out-of-sample accuracy of the generic configuration method with versus without correction factors on our validation data. Table D.2 provides the cross validation results, which indicate that the generic configuration method with correction factors better estimates (i.e., has lower out-of-sample root mean square error (RMSE) relative to) metered generation than the generic configuration method without correction factors.

Table D.2: Root mean square errors (RMSEs) between hourly metered generation and estimated generation using the generic configuration method without and with correction factors. RMSEs are average RMSEs across out-of-sample folds during 10-fold cross validation (CV).

IOU	10-fold CV RMSE for Generic Configuration Method without Correction Factors [kWh]	10-fold CV RMSE for Generic Configuration Method with Correction Factors [kWh]
PGE	3.64	3.39
SCE	2.49	2.16
SDGE	1.62	1.58

D.6: SUPPLEMENTAL REGRESSION INFORMATION

D.6.1: Regression Formulation without Year Dummy Variables

In order to account for temporal trends in power system operations in Regressions 1 and 2, we include dummy variables for hour of day, day of week, month, and year. In our analysis, we do not use our regressions to predict future prices, e.g. by training on 2013 through 2015 data then predicting 2016 prices. However, such prediction capabilities may be desired in future research. As such, here we consider an alternative formulation of Regressions 1 and 2 without year dummy variables. Table D.3 provides regression coefficients for Regressions 1 and 2 without year dummy variables. R-squared values for Regressions 1 and 2 without year dummy variables (0.77 and 0.79, respectively) are similar to those for Regressions 1 and 2 with year dummy variables (0.77 and 0.79, respectively), meaning including year dummy variables does not improve model fit over our period of analysis. Additionally, similar model fits with and without year dummy variables indicate that all variables included in Regressions 1 and 2 are stationary over our period of analysis, as also indicated by Augmented Dickey-Fuller tests (see main text).

To demonstrate the price prediction capabilities of Regressions 1 and 2 without year dummy variables, we train (fit) them on data from 2013 and 2014, then use the fitted regressions to predict 2015 prices. RMSEs for Regressions 1 and 2 between predicted and actual prices in 2015 (5.11 and 5.92 in NP15 and SP15, respectively) are only 3-6% larger than those between predicted and actual prices in 2013 and 2014 (4.94 and 5.58 in NP15 and SP15, respectively). Thus, Regressions 1 and 2 without year dummy variables may be useful for predicting future prices in future applications.

Table D.3: Coefficients and standard errors for Regressions 1 and 2 without year fixed effects using Newey-West standard errors with a maximum time lag of $4(T/100)^{2/9}$, where T = the number of observations in our dataset (26,280) [4]. For clarity, we provide regression results for data standardized as $(X/(X^{MAX} - X^{MIN}))$, where X^{MAX} and X^{MIN} equal the maximum and minimum variable value, respectively, and for dependent variables (LMPs) scaled to $/GWh. **Bold** values indicate statistical significance at p-value < 0.01.

	Regression 1		**Regression 2**	
Variable: definition	**Coeff.**	**Std. Error**	**Coeff.**	**Std. Error**
W_t^{NP15}: Hourly forecasted wind generation in NP15	**-22.08**	3.07	**-12.77**	3.41
S_t^{NP15}: Hourly forecasted solar generation in NP15	0.08	4.70	**-15.45**	5.02
W_t^{SP15}: Hourly forecasted wind generation in SP15	**-10.10**	2.57	**-37.20**	3.20
S_t^{SP15}: Hourly forecasted solar generation in SP15	**-23.15**	3.19	**-80.27**	3.83
D_t^{NP15}: Hourly forecasted net demand in PGE	**308.42**	32.32	**229.10**	24.63
D_t^{SP15}: Hourly forecasted net demand in SCE + SDGE	**57.79**	16.24	**189.28**	16.20
C_t: Daily generation by Diablo Canyon	**-26.84**	3.34	**-32.72**	3.04
V_t: Daily generation by Palo Verde	**-20.71**	3.51	**-16.13**	3.50
NG_t: Daily natural gas Henry Hub price	**228.33**	9.86	**227.72**	9.42
HI_t: Daily CA hydro index	**-31.82**	6.89	9.32	6.77
KR_t: Hourly Klamath river flow	-3.23	8.37	**-24.60**	8.02
SR_t: Hourly Sacramento river flow	**-23.08**	3.31	**-23.25**	3.80

D.6.2: Descriptions of and Descriptive Statistics for Regression Variables

In order to represent generation by major fuel types in CAISO, we include several generation-related variables in Regressions 1 and 2. Since natural gas provided roughly 60% of in-state electricity generation in CA from 2013 through 2015 [5], we include a term for natural

gas prices. Due to high generation levels and near-zero marginal costs, utility-scale wind and solar, nuclear, and hydroelectric generators also likely affect LMPs, so we include terms for each. To capture hourly hydroelectric generation, we use three proxy variables. Stream flows for lower segments of the Klamath and Sacramento rivers, the two largest rivers in CA by average discharge, approximate generation by upstream dams. In addition, the daily weighted average index of stream flows across CA provides a broader indicator of available water for hydroelectric generation.

We obtain all non-dummy variables except nuclear generation and natural gas prices at hourly intervals. Assuming constant values across days and weekends, we up-sample natural gas prices and nuclear generation from daily to hourly. Table D.4 provides descriptive statistics for each non-dummy variable used in Regressions 1 and 2. To check for stationarity in outcome and explanatory variables, we run an Augmented Dickey-Fuller (ADF) test [6] with drift on each variable at two time lags, or the number of lagged dependent variables we include in Regressions 1 and 2. We reject the null hypothesis of the ADF test for each variable (p-value < 0.014), which indicates all variables are stationary over our study period (2013-2015) and our coefficient estimates obtained through linear regression are consistent.

Table D.4: Descriptive statistics for non-dummy variables used in Regressions 1 and 2, where *t* indexes hour and *SP15* and *NP15* index CAISO zones. We determine stationarity with the Augmented Dickey-Fuller test at two time lags [6].

Variable	Definition	Stationary at $\alpha = 0.02$?	Average	Median	Standard Deviation	Maximum	Minimum
LMP_t^{NP15}	Average hourly DAM LMP for NP15 [$$_{2015}$/MWh]	Yes	37.8	36.6	9.91	171.6	0.0
LMP_t^{SP15}	Average hourly DAM LMP for SP15 [$$_{2015}$/MWh]	Yes	38.4	37.0	11.4	167.9	-2.6
D_t^{NP15}	Hourly forecasted load in NP15, i.e. PGE [MWh]	Yes	12028.9	11850.1	2073.5	23170.0	8288.3
D_t^{SP15}	Hourly forecasted load in SP15, i.e. SCE and SDGE [MWh]	Yes	14496.3	14126.1	2948.4	28753.0	9548.8
W_t^{NP15}	Hourly forecasted utility-scale wind generation in NP15 [MWh]	Yes	403.4	332.6	301.9	1204.0	0.0
S_t^{NP15}	Hourly forecasted utility-scale solar generation in NP15 [MWh]	Yes	172.3	6.2	240.0	1107.1	0.0
W_t^{SP15}	Hourly forecasted utility-scale wind generation in SP15 [MWh]	Yes	769.9	643.3	583.7	2558.7	0.0
S_t^{SP15}	Hourly forecasted utility-scale solar generation in SP15 [MWh]	Yes	716.2	21.8	1089.9	3935.1	0.0
NG_t	Daily natural gas Henry Hub prices [$$_{2015}$/MMBtu]	Yes	3.4	3.4	0.7	7.3	1.6
C_t	Daily Diablo Canyon nuclear station generation [MWh]	Yes	2020.9	2240.0	430.4	2240.0	279.5
V_t	Daily Palo Verde nuclear station generation [MWh]	Yes	3634.6	3937.0	567.6	3937.0	1312.0
KR_t	Flow on a lower segment of Klamath River [ft/s^3]	Yes	9283.9	5017.5	11936.0	171250.0	1990.0
SR_t	Flow on a lower segment of Sacramento River [ft/s^3]	Yes	11016.1	11250.0	7909.7	55325.0	-5970.0
HI_t	Daily weighted average index of CA stream flows	Yes	3.5	3.5	0.5	5.0	2.7

D.6.3: Autocorrelation and Partial Autocorrelation Plots of Residuals

Residuals of Regressions 1 and 2 exhibit autocorrelation, as evidenced by Durbin-Watson test statistics of 0.3 and autocorrelation and partial autocorrelation function plots (Figure D.8). Specifically, significant intra- and inter-day autocorrelation exists in the residuals, reflecting temporal trends in power system operations. For instance, prices usually follow diurnal patterns of low prices from midnight through the early morning, rising prices through the day, peak prices in early evening, and then falling prices through midnight.

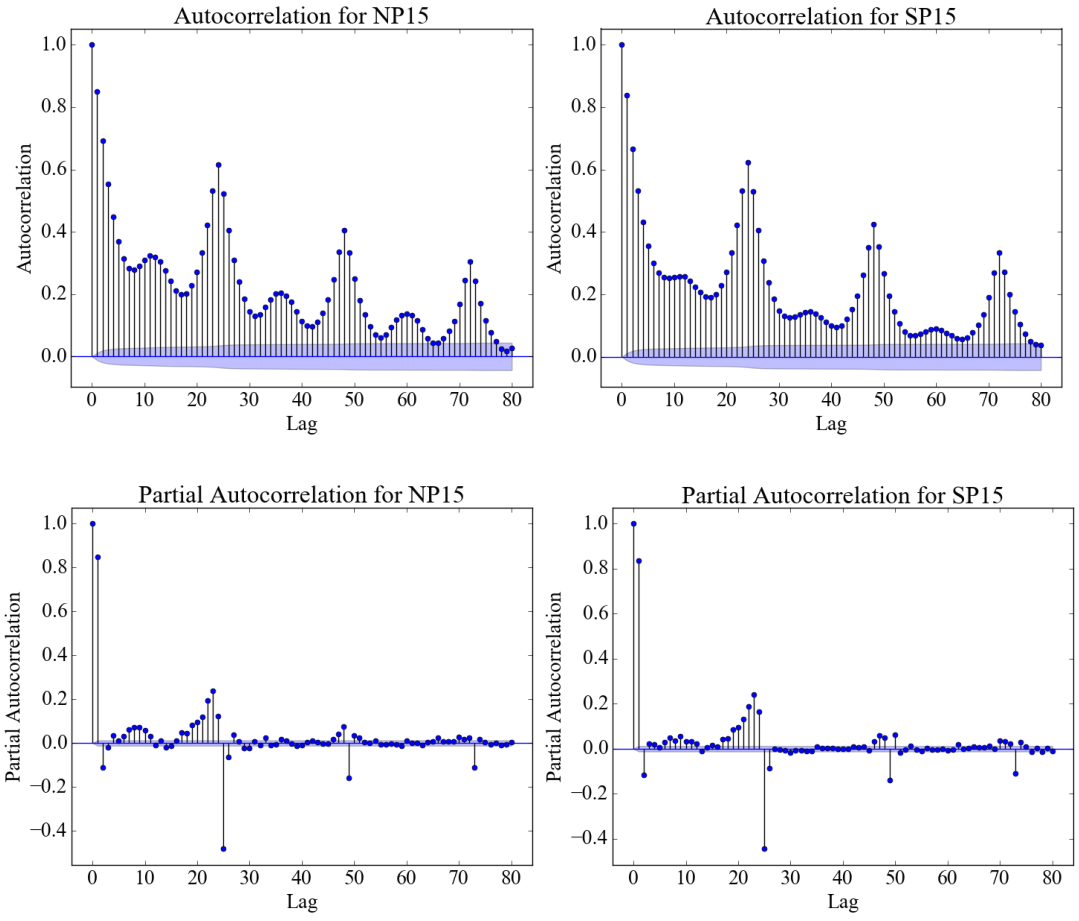

Figure D.8: Autocorrelation (top) and partial autocorrelation (bottom) function plots of residuals from Regressions 1 (left) and 2 (right).

D.6.4: Bootstrapped Standard Errors

Table D.5 provides bootstrapped (N=250) standard errors for non-dummy variables in Regressions 1 and 2. In order to maintain some structure of our original time series, we conduct block bootstrapping by sampling from 3-day periods. Bootstrapped standard errors are 13-90% larger than Newey-West standard errors. However, statistically significant coefficients per Newey-West standard errors have [2.5%,97.5%] bootstrapped confidence intervals that don't overlap with zero except for *KR* in Regressions 1 and 2 and S^{NP15} in Regression 2.

Table D.5: Coefficients and 3-day block bootstrapped (N=250) standard errors for Regressions 1 and 2. For clarity, we provide regression results for data standardized as $(X/(X^{MAX} - X^{MIN}))$, where X^{MAX} and X^{MIN} equal the maximum and minimum variable value, respectively, and for dependent variables (LMPs) scaled to $\$_{2015}$/GWh. A **bold** value indicates the (2.5%,97.5%) bootstrapped confidence interval for a coefficient does not overlap with zero.

	Regression 1		**Regression 2**	
Variable: definition	**Coeff.**	**Std. Error**	**Coeff.**	**Std. Error**
W_t^{NP15}: Hourly forecasted wind generation in NP15	**-20.92**	3.5	**-12.7**	4.0
S_t^{NP15}: Hourly forecasted solar generation in NP15	-5.22	5.0	-12.9	6.9
W_t^{SP15}: Hourly forecasted wind generation in SP15	**-13.21**	3.1	**-37.2**	4.7
S_t^{SP15}: Hourly forecasted solar generation in SP15	**-34.59**	3.1	**-81.0**	5.2
D_t^{NP15}: Hourly forecasted net demand in PGE	**317.23**	45.0	**227.9**	30.1
D_t^{SP15}: Hourly forecasted net demand in SCE + SDGE	**56.58**	23.0	**189.9**	19.9
C_t: Daily generation by Diablo Canyon	**-26.12**	5.4	**-33.5**	5.0
V_t: Daily generation by Palo Verde	**-26.06**	6.3	**-15.5**	6.0
NG_t: Daily natural gas Henry Hub price	**244.96**	30.3	**235.3**	28.0
HI_t: Daily CA hydro index	-5.28	12.8	9.6	12.6
KR_t: Hourly Klamath river flow	-29.37	19.6	-23.9	16.2
SR_t: Hourly Sacramento river flow	**-18.85**	5.9	**-22.7**	6.4

D.6.5: Coefficients and Standard Errors on Dummy Variables

Table D.6 provides coefficients and Newey-West standard errors [7] for intercepts and time dummy variables used in Regressions 1 and 2.

Table D.6: Coefficients and standard errors for intercepts and time dummy variables in Regressions 1 and 2 using Newey-West standard errors with a maximum time lag of $4(T/100)^{2/9}$, where T = the number of observations in our dataset (26,280) [4]. For clarity, we provide regression results for data standardized as $(X/(X^{MAX} - X^{MIN}))$, where X^{MAX} and X^{MIN} equal the maximum and minimum variable value, respectively, and for dependent variables (LMPs) scaled to $\$_{2015}$/GWh. **Bold** and *italics* values indicate statistical significance at p-values less than 0.01 and 0.05, respectively.

	Regression 1		**Regression 2**	
Variable	**Coefficient**	**Std. Error**	**Coefficient**	**Std. Error**
Intercept	**-127.44**	24.74	**-156.37**	21.73
February dummy	**15.22**	2.83	**11.62**	2.87
March dummy	**5.89**	2.19	*5.28*	2.54
April dummy	**6.58**	2.50	**9.29**	3.22
May dummy	-1.96	2.66	-5.31	2.85
June dummy	**-28.29**	3.33	**-25.04**	3.36
July dummy	**-38.39**	3.29	**-39.53**	3.64
August dummy	**-31.21**	3.39	**-36.33**	3.52
September dummy	**-18.70**	3.18	**-26.47**	3.53
October dummy	**-12.78**	3.01	**-15.84**	3.06
November dummy	**8.19**	2.76	*6.00*	2.81
December dummy	**21.84**	3.71	**14.08**	3.64
Tuesday dummy	*-3.87*	1.71	**-4.98**	1.79
Wednesday dummy	**-6.08**	1.59	**-6.86**	1.78
Thursday dummy	-3.64	2.05	-3.18	2.10
Friday dummy	-2.61	1.56	-1.66	1.82
Saturday dummy	**8.06**	1.60	**8.59**	1.72
Sunday dummy	**11.84**	1.74	**12.95**	1.76
Hour 2 dummy	**-3.20**	0.55	**-2.53**	0.49
Hour 3 dummy	**-3.83**	0.79	**-3.37**	0.71
Hour 4 dummy	**-2.34**	0.76	*-1.78*	0.72
Hour 5 dummy	**2.89**	0.60	**3.44**	0.65
Hour 6 dummy	**8.67**	1.03	**7.72**	0.94
Hour 7 dummy	**5.32**	1.98	**7.29**	1.62
Hour 8 dummy	-3.45	2.63	2.07	2.20
Hour 9 dummy	**-11.80**	2.95	-3.30	2.65
Hour 10 dummy	**-14.24**	3.14	-2.25	3.00
Hour 11 dummy	**-15.19**	3.20	0.20	3.17
Hour 12 dummy	**-15.24**	3.11	2.39	3.20
Hour 13 dummy	**-17.52**	3.06	0.53	3.14
Hour 14 dummy	**-17.83**	2.97	0.05	3.03
Hour 15 dummy	**-16.96**	2.85	-0.84	2.84

Hour 16 dummy	**-10.89**	2.92	1.42	2.70
Hour 17 dummy	-4.54	3.31	2.11	2.76
Hour 18 dummy	4.88	4.15	**10.88**	3.26
Hour 19 dummy	7.88	4.58	**13.33**	3.68
Hour 20 dummy	-5.16	4.59	2.07	3.69
Hour 21 dummy	**-13.11**	4.11	**-9.10**	3.23
Hour 22 dummy	**-14.16**	3.06	**-11.52**	2.40
Hour 23 dummy	**-5.49**	1.84	**-4.16**	1.48
Hour 24 dummy	-0.70	0.90	0.15	0.79
2014 dummy	**10.29**	1.49	-1.47	1.62
2015 dummy	**15.57**	3.55	1.58	3.45

D.6.6: Time Series of Actual versus Predicted Prices of Regressions

Figure D.9 and Figure D.10 provide four 30-day time series comparing actual and predicted LMPs using Regressions 1 and 2, respectively. Time series were selected to include peak LMPs in NP15 and SP15 over our study period (2013 through 2015) and prices in the winter, spring, and summer. Across time series, both regressions accurately predict most LMPs, but underestimate prices during the highest price periods.

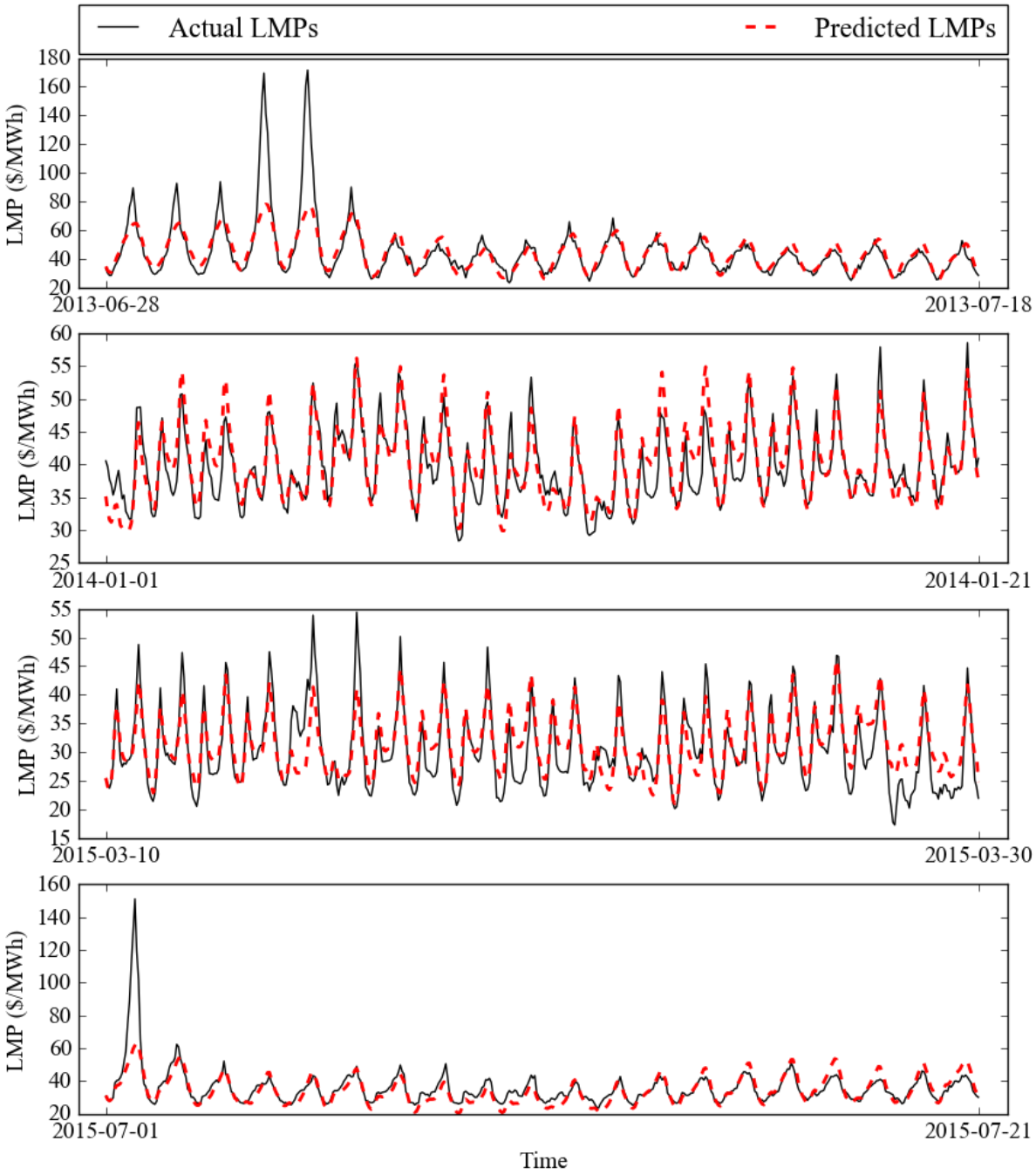

Figure D.9: Time series of actual (solid line) and predicted (red dashed line) LMPs in NP15 using Regression 1. Each subplot compares hourly LMPs over 20 days.

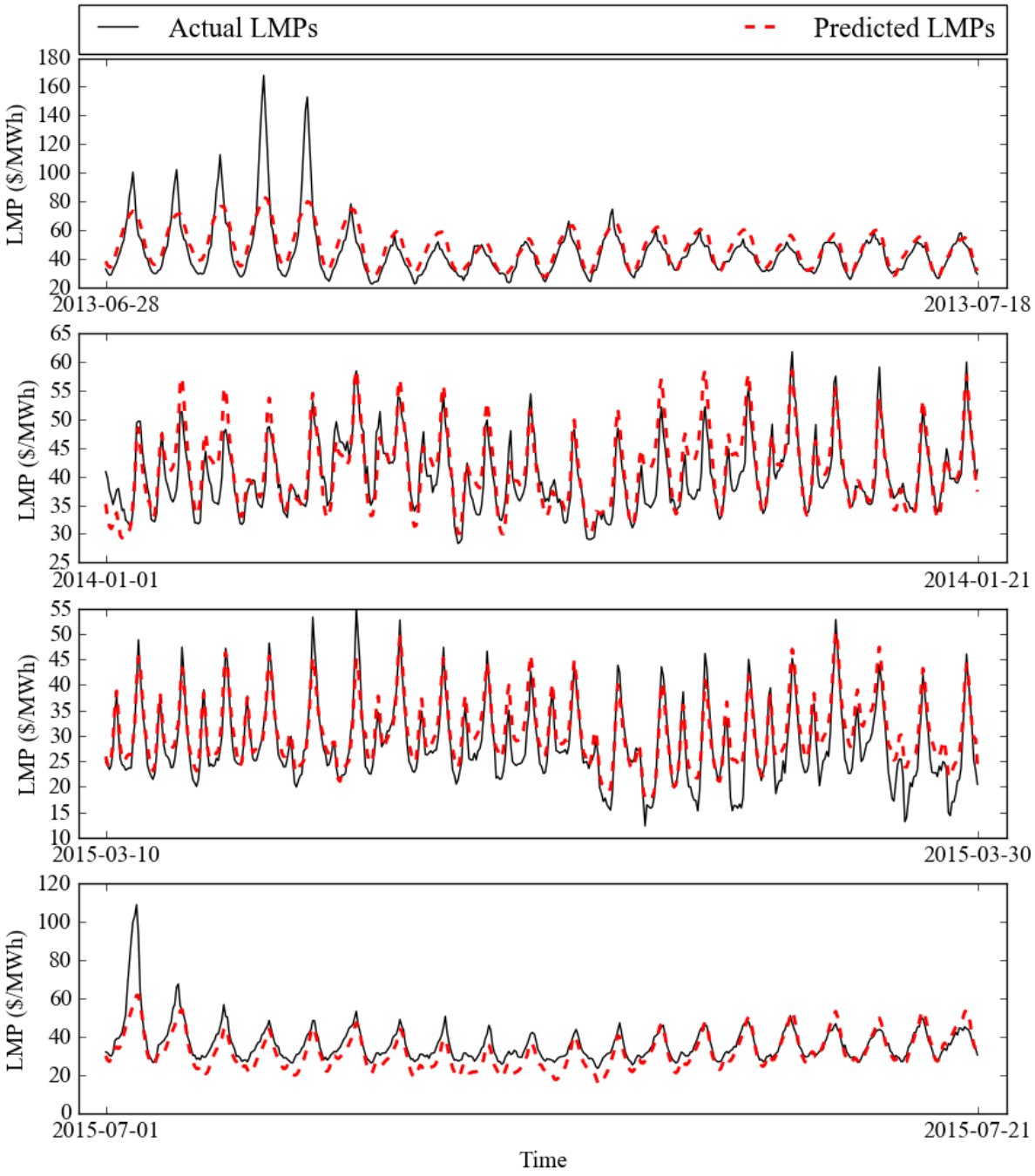

Figure D.10: Time series of actual (solid line) and predicted (red dashed line) LMPs in SP15 using Regression 2. Each subplot compares hourly LMPs over 20 days.

D.7: COMPARISON OF ACTUAL AND ESTIMATED MAX HOURLY AND TOTAL GENERATION BY PV SYSTEMS DURING VALIDATION

To check for systematic biases in PV generation estimates using the specific configuration, generic configuration, adjusted generic configuration, and scale up methods, Figure D.11 compares maximum hourly and total metered versus estimated generation for all PV systems in our validation analysis. Total generation equals the sum of hourly generation over our validation period (2010-2016). The specific configuration and scale up methods estimate maximum generation with less bias than the generic configuration and adjusted generation configuration methods, which tend to underestimate max generation. The adjusted generic configuration has less of a downward bias than the generic configuration method due to hour-of-day correction factors that increase generation during max generation periods. Conversely, the generic and adjusted generic configuration methods estimate total generation with less bias than the specific and scale up methods, which tend to over- and under-estimate total generation, respectively. These total generation biases are reflected in the mean bias errors (MBEs) given in the main text, which are positive and negative for the specific configuration and scale up methods, respectively.

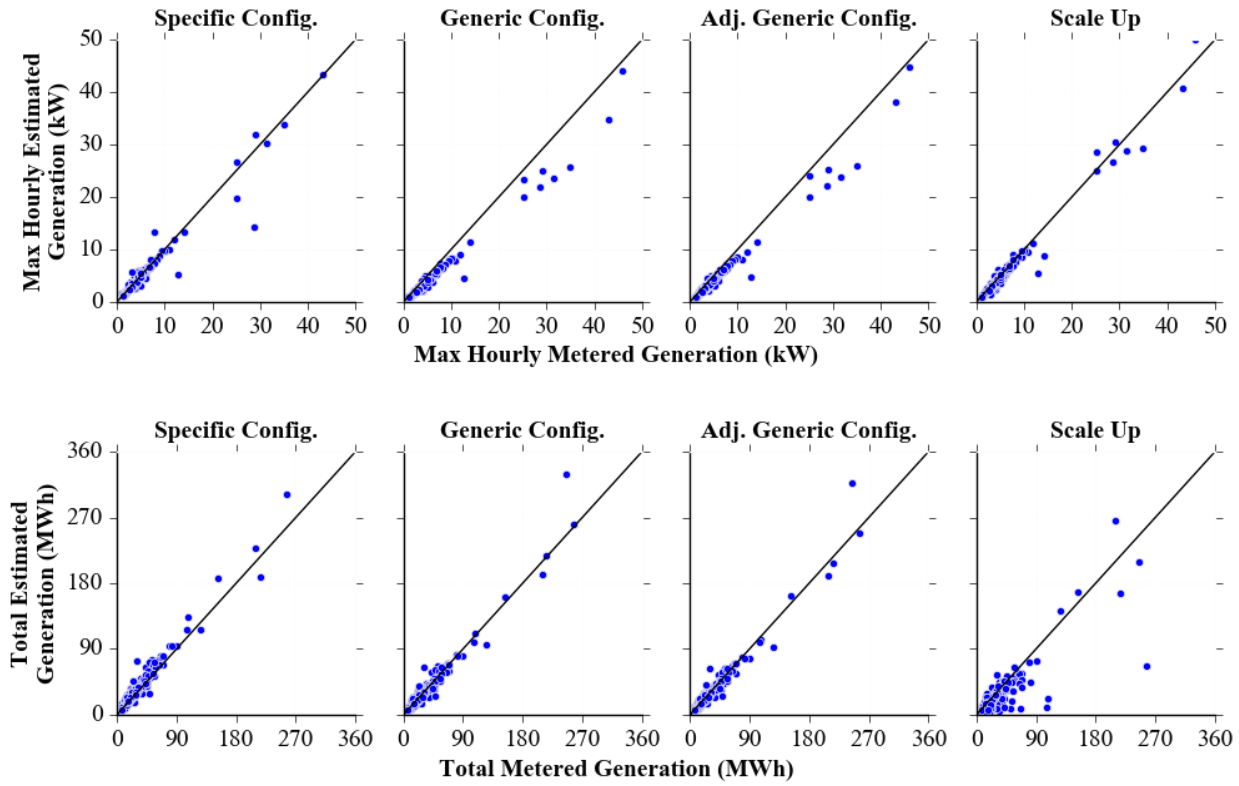

Figure D.11: Maximum hourly (top row) and total (bottom row) estimated versus metered generation for all PV systems in our validation analysis by method for estimating PV generation. Total generation equals generation summed across validation period (2010-2016). For reference, plotted lines indicate where estimated generation equals metered generation, i.e. y=x.

D.8: SUPPLEMENTAL RESULTS FOR ESTIMATES OF DISTRIBUTED PV GENERATION

D.8.1: Distributed PV Generation by Season

Figure D.12 and Figure D.13 provide box plots of distributed PV generation by hour of day in June and December, respectively, in 2013, 2014, and 2015. Distributed PV generation extends from 6 a.m. to 6 p.m. PST (7 a.m. to 7 p.m. PDT) in June, but only from 8 a.m. to 5 p.m. PST in December, reflecting longer days in the summer. Additionally, distributed PV generation tends to be higher in June than December, reflecting higher solar irradiance. In any given hour of

the day, significant variability exists in distributed PV generation. For instance, from 12 to 1 p.m. PST (1 to 2 p.m. PDT) in June, the first and third quartiles of distributed PV generation in PGE equal roughly 0.7 and 1.1 GWh, respectively, using the generic configuration method. Furthermore, hours with significantly less distributed PV generation than median generation values are more common in PGE than SCE and SDGE, potentially indicating cloudier conditions in PGE's footprint than in SCE's or SDGE's.

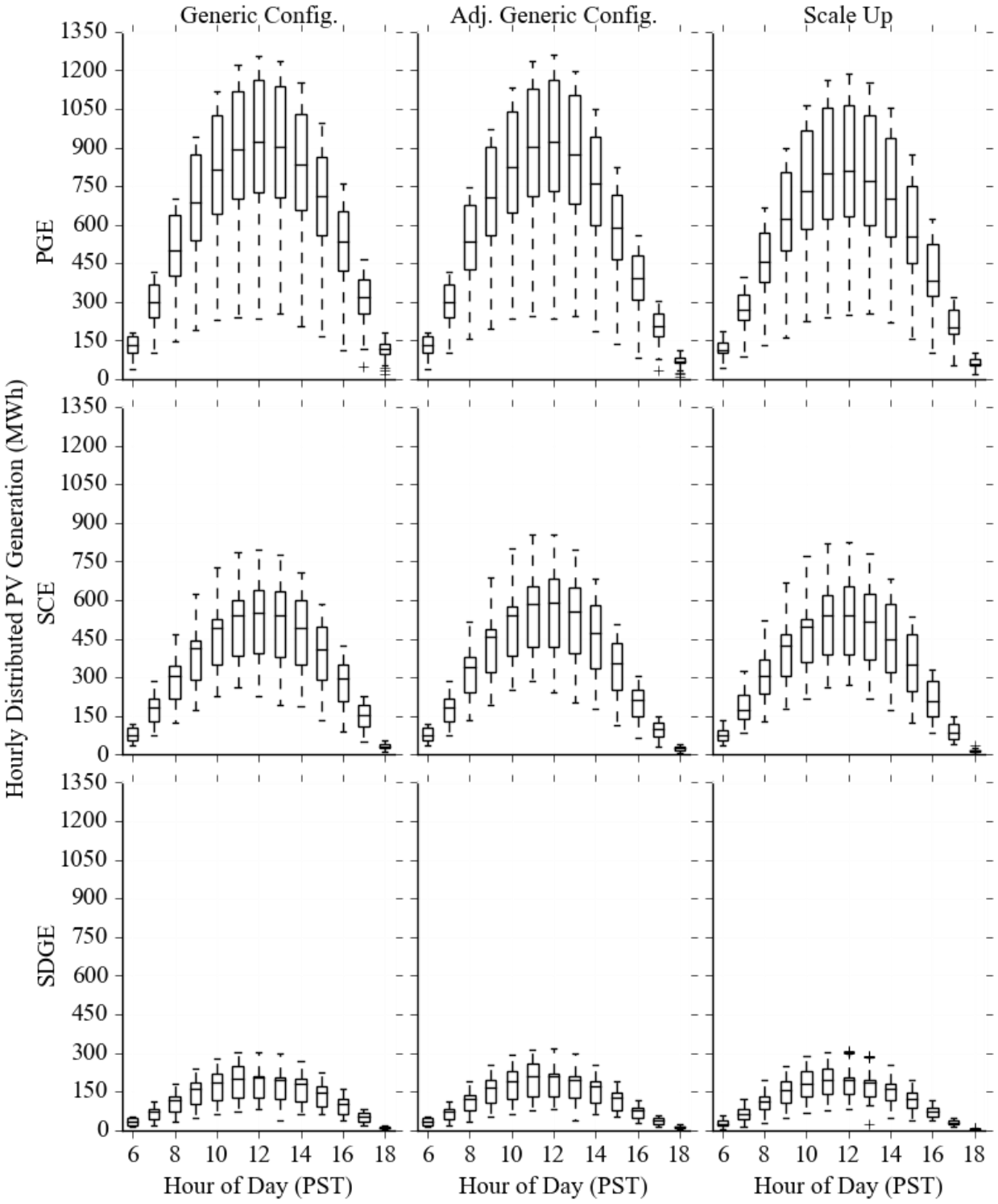

Figure D.12: Distributed PV generation in June of 2013, 2014, and 2015 by hour of day in PGE, SCE, and SDGE by method used to estimate generation. Boxes indicate the first, second, and third quartiles, while whiskers extend to 1.5 times the first and third quartiles.

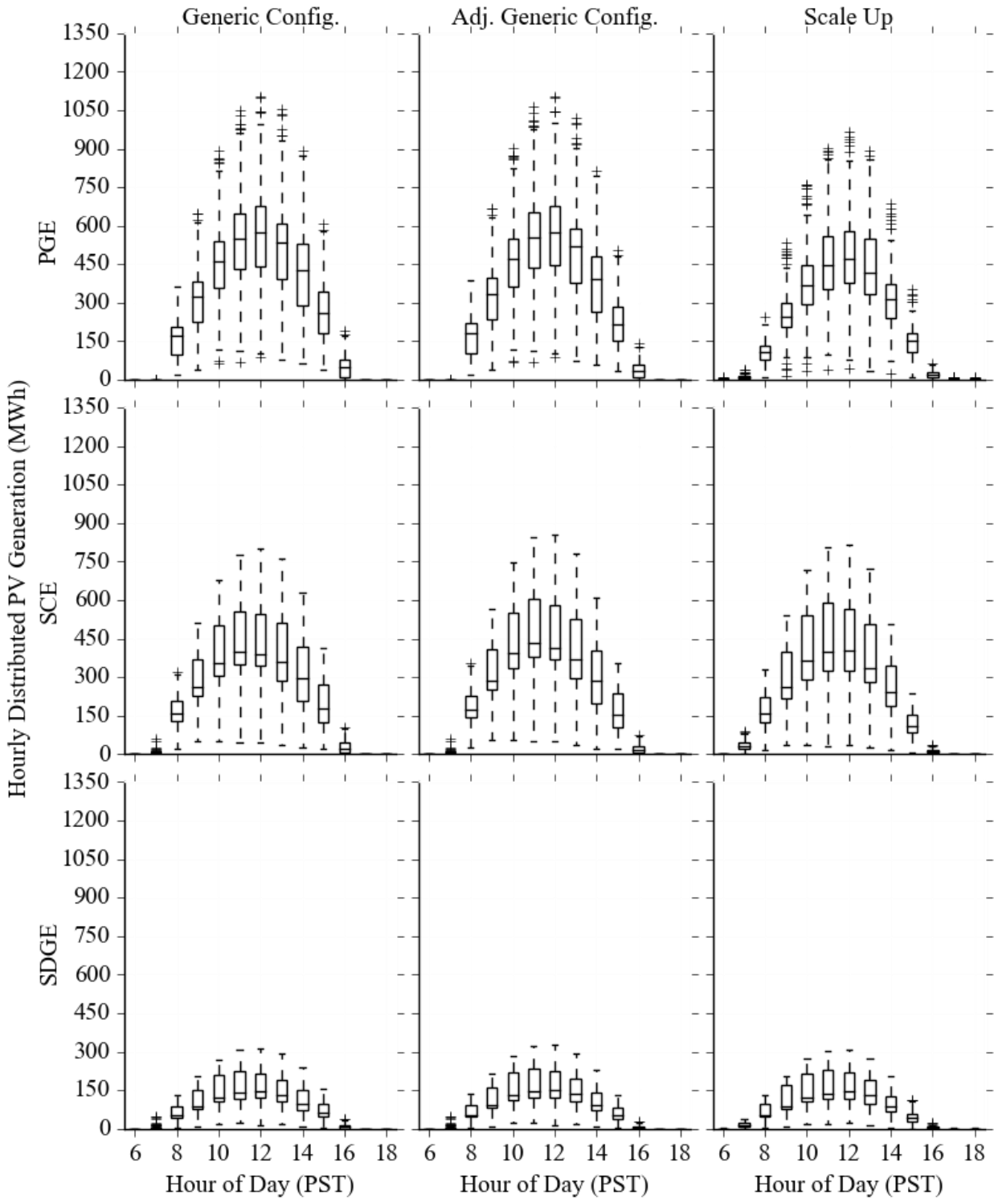

Figure D.13: Distributed PV generation in December of 2013, 2014, and 2015 by hour of day in PGE, SCE, and SDGE by method used to estimate generation. Boxes indicate the first, second, and third quartiles, while whiskers extend to 1.5 times the first and third quartiles.

D.8.2: Distributed PV Generation versus Demand

Figure D.14 and Figure D.15 overlay distributed PV generation estimated using each method on net demand for four 10-day time series in each season of 2015. Data are divided by CAISO zone, where NP15 corresponds to PGE and SP15 corresponds to SCE and SDGE. In all seasons, distributed PV generation tends to coincide with increasing demand from the morning through early evening. In January and April in both zones, net demand tends to have two daily peaks, one that usually coincides with peak distributed PV generation and another after distributed PV generation ends.

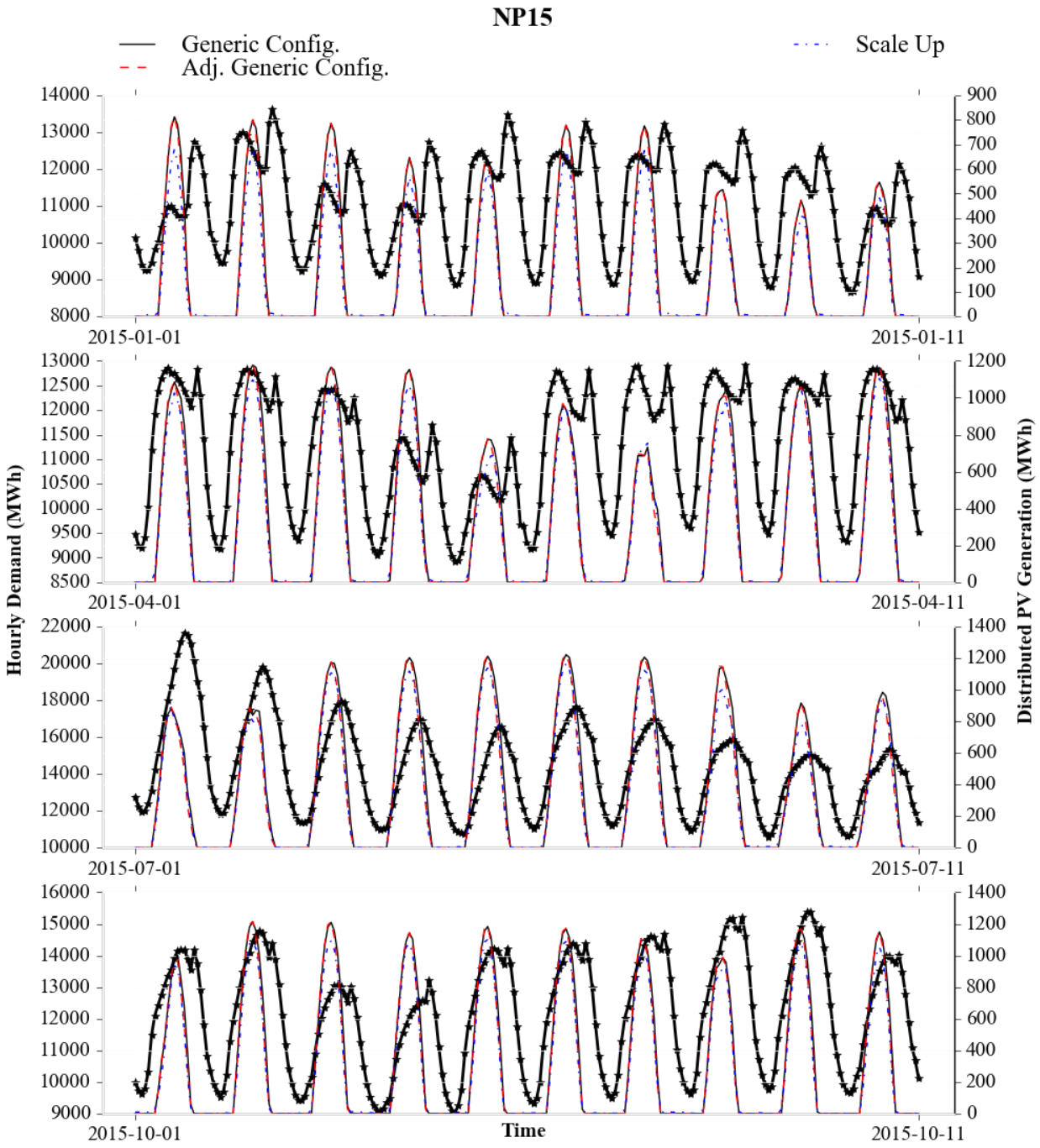

Figure D.14: Four 10-day time series in each season of net demand (solid line with star markers) and distributed PV generation in NP15 by method used to estimate generation. Note that y-axes differ between and within subplots.

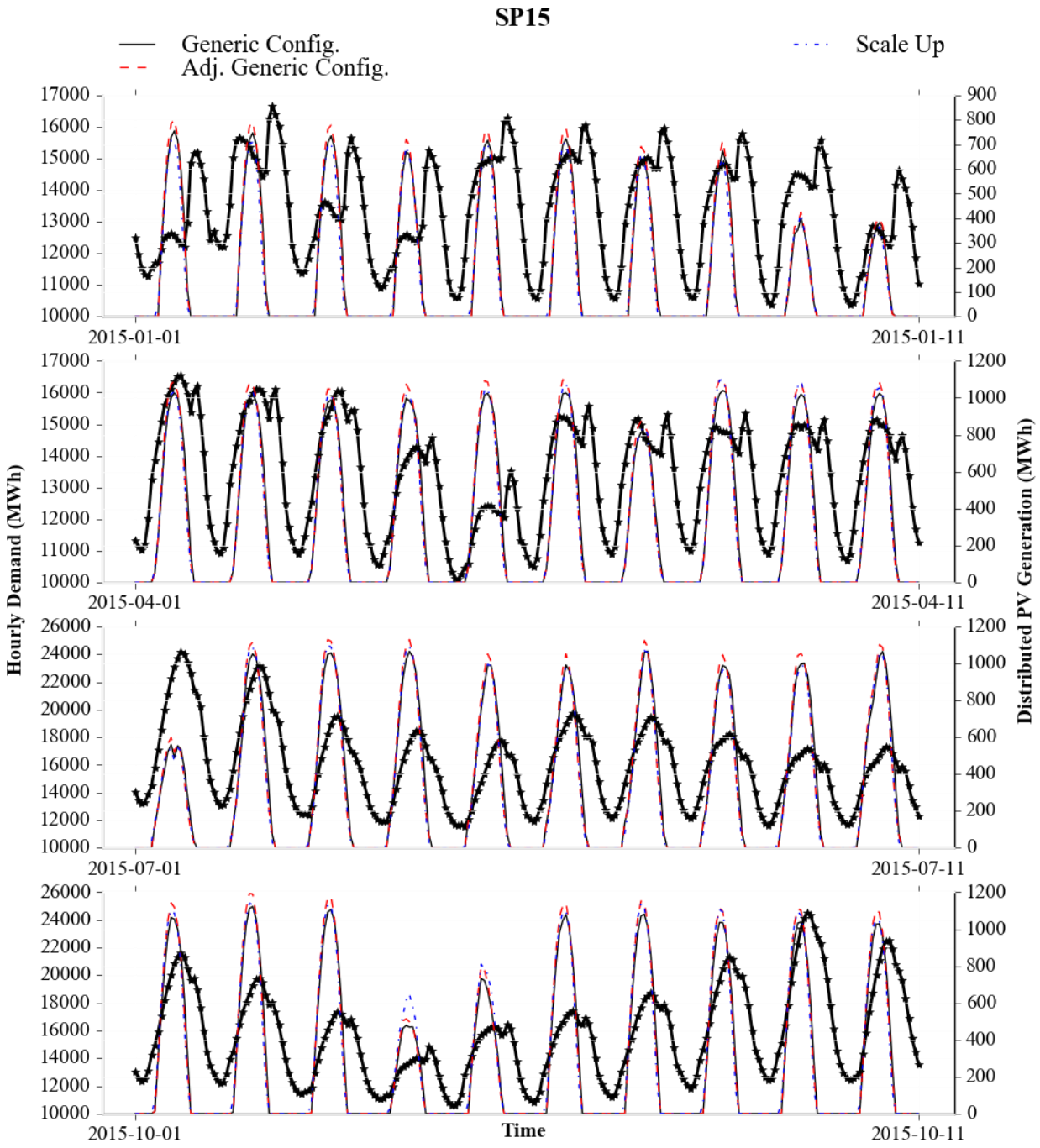

Figure D.15: Four 10-day time series in each season of net demand (solid line with star markers) and distributed PV generation in SP15 by method used to estimate generation. Note that y-axes differ between and within subplots.

D.9: SUPPLEMENTAL RESULTS FOR MARKET PRICE RESPONSE TO DISTRIBUTED PV GENERATION

To contextualize our estimates of LMP reductions from distributed PV generation, Figure D.16 provides distributions of LMPs by hour of day in NP15 and SP15 from 2013 through 2015. Median LMPs range from $30-50/MWh and $30-55/MWh in NP15 and SP15, respectively. In many hours, LMPs reach significantly higher values, ranging as high as $180/MWh over our study period. LMPs tend to increase from the morning through 7 p.m. PST, then decrease through the night. Notably, median LMPs are largely flat during the main hours in which median distributed PV generation occurs (10 a.m. through 4 p.m. PST) (increasing by only 8 and 10% in NP15 and SP15, respectively (Figure D.16).

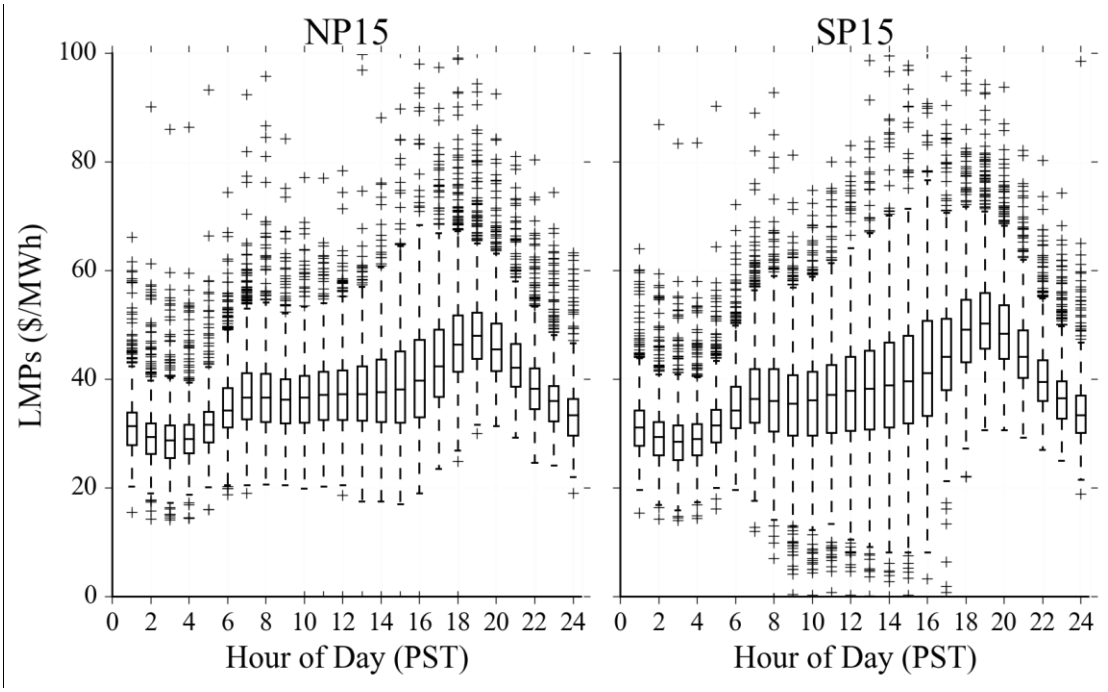

Figure D.16: Boxplots of historic LMPs ($_{2015}$/MWh) from 2013 through 2015 in NP15 (left) and SP15 (right) by hour of day. Boxes indicate the first, second, and third quartiles, while whiskers extend to 1.5 times the first and third quartiles.

Figure D.17 and Figure D.18 provide the distribution of changes in LMPs due to distributed PV generation in June and December, respectively, from 2013 through 2015. Due to greater distributed PV generation in the summer (June) than winter (December) (Figure D.12 and Figure D.13), distributed PV generation reduces LMPs more in June than December in both zones. For instance, given distributed PV generation estimated with the generic configuration method, median NP15 and SP15 LMP reductions from 12-1 p.m. PST equal roughly $0.9/MWh in June and $0.6-0.7/MWh in December. Due to longer daily distributed PV generation profiles in June than December, distributed PV also reduces LMPs over more of the day in June than in December.

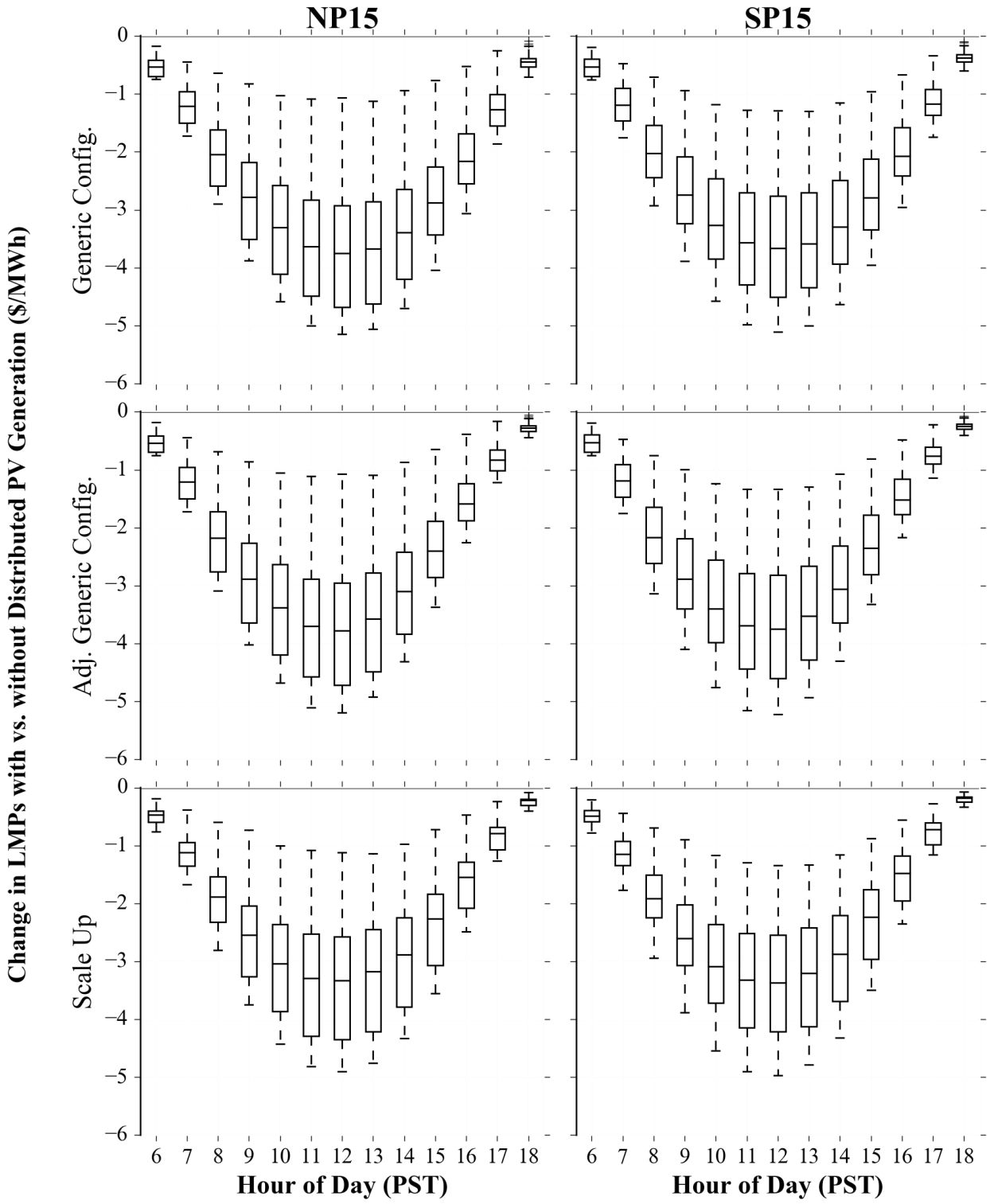

Figure D.17: Boxplots of changes in LMPs ($\$_{2015}$/MWh) with versus without distributed generation by hour of day in June 2013, 2014, and 2015 in NP15 (left) and SP15 (right) by method used to estimate distributed PV generation. Boxes indicate the first, second, and third quartiles, while whiskers extend to 1.5 times the first and third quartiles.

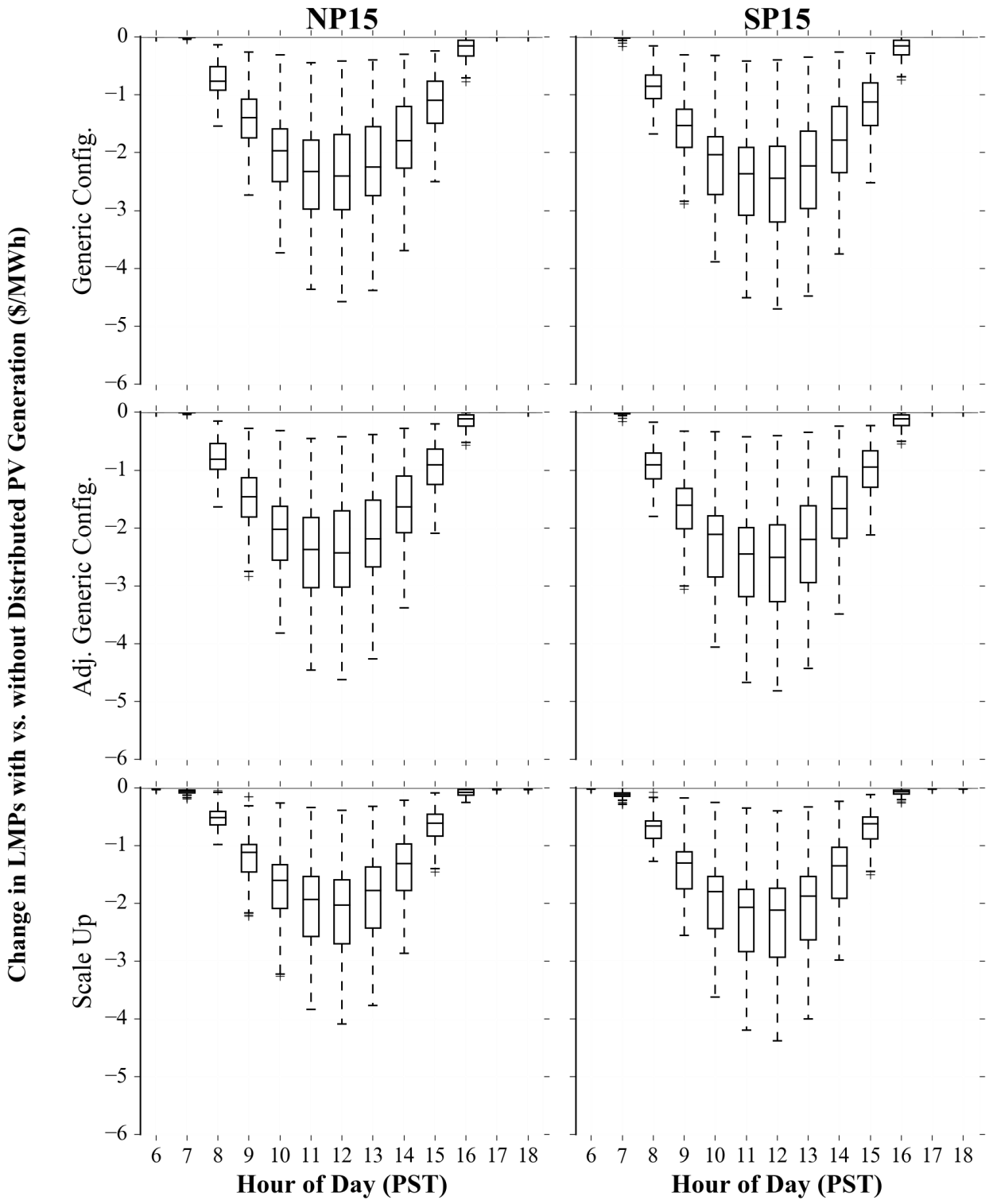

Figure D.18: Boxplots of changes in LMPs ($_{2015}$/MWh) with versus without distributed generation by hour of day in December 2013, 2014, and 2015 in NP15 (left) and SP15 (right) by method used to estimate distributed PV generation. Boxes indicate the first, second, and third quartiles, while whiskers extend to 1.5 times the first and third quartiles.

D.10: ESTIMATING AVOIDED COSTS ON PER-GENERATION AND PER-CAPACITY BASES

To estimate avoided costs per unit of distributed PV generation, we simply divide total avoided costs from 2013 through 2015 by total distributed PV generation from 2013 through 2015 for each method used to estimate distributed PV generation (Table D.7).

Table D.7: Avoided costs per distributed PV generation from 2013 through 2015 for each method used to estimate distributed PV generation.

Method Used to Estimate Distributed PV Generation	Total Distributed PV Generation (TWh)	Total Avoided Cost due to Market Price Response (million $2015)	Total Avoided Cost per Distributed PV Generation (cents2015/kWh)
Generic Configuration	11.5	730	6
Adjusted Generic Configuration	11.3	700	6
Scale Up	10.5	650	6

To calculate avoided costs per unit of distributed PV capacity, we account for varying interconnection times by determining connected distributed PV capacity in each hour from 2013 through 2015. We then sum distributed PV capacity across hours and divide that value by 8760 hours per year to yield an estimate of the combined annual capacity of distributed PV. Finally, we divide total avoided costs from 2013 through 2015 by that combined annual capacity. Mathematically, we calculate avoided costs per unit of distributed PV capacity as:

$$ACC = \frac{TAC}{TC} \qquad (1)$$

$$TAC = \sum_{y=2013}^{2015} AC_y \qquad (2)$$

$$TC = \frac{\sum_{y=2013}^{2015} \sum_{h=1}^{8760} P_{y,h}^{MAX}}{8760} \qquad (3)$$

where *y* and *h* index year and hour, respectively; *ACC* = avoided costs per unit of distributed PV capacity [$/kW]; *TAC* = total avoided costs from 2013 through 2015 [$_{2015}$]; *TC* = total distributed PV capacity from 2013 through 2015 [kW]; *AC* = annual avoided costs [$_{2015}$]; and P^{MAX} = hourly distributed PV capacity accounting for varying interconnection times.

D.11: RESULTS FOR SENSITIVITY ANALYSIS ON EFFICIENCY DEGRADATION AND HIGHER INVERTER LOAD

We test the sensitivity of our results using the generic configuration method to two PV system parameters: 0.5% (versus no) annual efficiency degradation and a 1.3 (versus 1.16) inverter loading ratio, or the ratio between the combined AC capacity of PV panels to the DC capacity of the inverter. Table D.8 provides total distributed PV generation from 2013 through 2015 by utility using the generic configuration method without efficiency degradation and with a standard inverter load of 1.16; with annual efficiency degradation of 0.5% and a standard inverter load of 1.16; and without efficiency degradation and with a higher inverter load of 1.30. Since PV systems in the NEM dataset have a median interconnection date of April 2014, accounting for PV system efficiency degradation of 0.5% per year only reduces total distributed PV generation by 1-2% across utilities relative to the generic configuration method. A higher inverter loading ratio of 1.3, by increasing clipping, also reduces distributed PV generation relative to the generic configuration method, but only marginally in PGE and by 3-5% in SCE and SDGE, indicating more clipping occurs in SCE and SDGE than PGE at a higher inverter loading ratio. .

Table D.8: Total distributed PV generation from 2013 through 2015 in PGE, SCE, and SDGE by method used to estimate generation.

Method Used to Estimate Distributed PV Generation	Total Distributed PV Generation (TWh)		
	PGE	SCE	SDGE
Generic Configuration	6.21	3.92	1.40
Generic Configuration with Efficiency Degradation	6.10	3.87	1.38
Generic Configuration with High Inverter Load	6.20	3.73	1.36

Total avoided costs from 2013 through 2015 in NP15 and SP15 equal 728, 718, and 716 million ($\$_{2015}$) in the base, efficiency degradation, and high inverter load scenarios, respectively (Table D.9). Thus, each sensitivity only reduces total avoided costs by roughly 2% relative to the generic configuration, in line with the reduction in distributed PV generation in each sensitivity.

Table D.9: Avoided costs from 2013 through 2015 by zone due to LMP reductions from, i.e. the market price response to, distributed PV generation. Avoided costs equal the sum of hourly LMP reductions due to distributed PV generation multiplied by historic hourly net demand.

Method Used to Estimate Distributed PV Generation	Avoided Cost due to Market Price Response in NP15 (million $\$_{2015}$)	Avoided Cost due to Market Price Response in SP15 (million $\$_{2015}$)
Generic Configuration	327	401
Generic Configuration with Efficiency Degradation	324	394
Generic Configuration with High Inverter Load	321	395

D.12 REFERENCES

[1] K. Klima and J. Apt, "Geographic smoothing of solar PV: Results from Gujarat," *Environ. Res. Lett.*, vol. 10, no. 10, 2015.

[2] C. N. Long and T. P. Ackerman, "Surface measurements of solar irradiance: A study of the spatial correlation between simultaneous measurements at separated sites," *Journal of Applied Meteorology*, vol. 34, no. 5. pp. 1039–1046, 1995.

[3] U.S. National Renewable Energy Laboratory, “National Solar Radiation Database (NSRDB),” *NREL.gov*, 2017. [Online]. Available: https://nsrdb.nrel.gov/. [Accessed: 08-Oct-2017].

[4] W. K. Newey and K. D. West, “Automatic lag selection in covariance matrix estimation,” *Rev. Econ. Stud.*, vol. 61, pp. 631–653, 1994.

[5] California Energy Commission, “Total system electric generation, 2013-2015,” *Electricity Data*, 2016. [Online]. Available: http://www.energy.ca.gov/almanac/electricity_data/system_power/2015_total_system_power.html. [Accessed: 29-Sep-2017].

[6] D. A. Dickey and W. A. Fuller, “Distribution of the estimators for autoregressive time series with a unit root,” *J. Am. Stat. Assoc.*, vol. 74, no. 366, pp. 427–431, 1979.

[7] W. K. Newey and K. D. West, “A simple, positive semi-definite, heteroskedasticity and autocorrelation consistent covariance matrix,” *Econometrica*, vol. 55, pp. 703–708, 1987.